

SEMMELWEIS EGYETEM
DOKTORI ISKOLA

Ph.D. értekezések

2503.

ACHIM LANGENBUCHER

Szemészet

című program

Programvezető: Dr. Nagy Zoltán Zsolt, egyetemi tanár

Témavezető: Dr. Szentmáry Nóra, klinikai kutatóprofesszor

OCULAR MAGNIFICATION IN PHAKIC AND PSEUDOPAKIC EYES AND IN EYES WITH KERATOPROSTHESES

Ph.D thesis

Dr. Achim Langenbacher

Clinical Medicine Doctoral School

Semmelweis University



Supervisor: Nóra Szentmáry, MD, Ph.D

Official reviewers: György Barcsay, MD, Ph.D

Péter Vámosi, MD, Ph.D

Head of the Complex Examination Committee:

László Schmeller, MD, D.Sc.

Members of the Complex Examination Committee:

Ágnes Kerényi, MD, Ph.D

Miklós Resch, MD, Ph.D

Budapest

2020

Table of Contents

Abbreviation List.....	2
1. Introduction	4
1.1. Definitions and context of ocular magnification and aniseikonia	4
1.2. Options for addressing aniseikonia	7
2. Objectives.....	10
3. Results	11
3.1. Application of our calculation strategy in cataract patients	12
3.1.1. Overall ocular magnification in the phakic and pseudophakic eye	12
3.1.2. Meridional ocular magnification in the phakic and pseudophakic eye.....	17
3.2. Change in overall and meridional magnification due to corneal surgery.....	22
3.3. Ocular magnification and visual angle in keratoprotheses	27
4. Discussion	31
4.1. Magnification and problems caused by magnification disparities	31
4.2. Handling with magnification disparities	32
4.3. Options for calculating ocular magnification	33
4.4. Application of a calculation strategy to clinical data	34
4.5. Our most relevant results.....	36
5. Conclusions.....	40
6. Summary	41
7. References	42
8. Bibliography of the candidate’s thesis related publications.....	46
9. Acknowledgements	47

Abbreviation List

ACD	External anterior chamber depth in mm
AL	Axial length in mm
Aniseikonia	Situation with disparity of ocular magnification, either comparing both eyes (binocular aniseikonia) or between meridians of one eye (meridional aniseikonia)
Anisometropia	Condition where measures of both eyes such as distances, curvatures of refractive surfaces or refractive indices do not match
Anisophoria	Situation with dynamic magnification disparity due to variation of viewing angle
AQD	Aqueous depth (internal anterior chamber depth) in mm
AST	Corneal astigmatism at front surface in dpt
Astigmatic	Condition of an optical system where surfaces show a variation in refractive properties for different meridians
Binocular aniseikonia	Image size (magnification) disparity between both eyes
CCT	Central corneal thickness in mm
Change in meridional OM	Ratio of major to minor principal meridian when transforming preoperative to postoperative meridional OM in %
Cylinder	Astigmatic power of spectacle correction in dpt
D	Diameter of the optics cylinder of a keratoprosthesis in mm
Diopter, dpt	Refractive power of an optical system or surface with focal length of 1 m
DMOM	Disparity of meridional magnification in %
Eikonic	Situation without ocular magnification disparity
Equivalent power	Average power of an optical system in dpt
Gain in OM	Ratio of postoperative to preoperative OM in %
IOLP	(Average) Power of the replacement lens in dpt
IOLPA	Orientation of astigmatism in a toric replacement lens in °
IOLPAST	Astigmatism of a toric replacement lens in dpt
L	Length of the optics cylinder of a keratoprosthesis in mm
LT	Lens thickness
Meridional aniseikonia	Variation of magnification in different meridians
Meridional OM	Meridional ocular magnification, ratio of OM in the magnification meridian to magnification axis in %

n_A	Refractive index of aqueous humour
n_C	Refractive index of cornea
n_K	Keratometer index, fictitious index for conversion of corneal radius to power
n_L	Refractive index of the lens
n_S	Refractive index of spectacle correction
n_V	Refractive index of vitreous
Ocular magnification	Ratio of lateral image size to object size (for objects at finite distances) or to incident ray slope (for objects at infinity)
OM	Ocular magnification (in this thesis it refers to the ratio of retinal image size to incident ray slope angle) in 1/mm. By literature convention, dimension is ignored
PAST	Corneal astigmatism at back surface in dpt
PR1 / PR2	Flat / steep radius of the corneal back surface in mm
PRA	Orientation of the flat axis of corneal back surface in $^\circ$
PR_{mean}	Average of PR1 and PR2 in mm
P_S	Refractive power of a spectacle correction in dpt
P_{Sf}	Front surface power of a spectacle correction in dpt
q	Ratio of lens front to back surface power
R1 / R2	Flat / steep radius of the corneal front surface in mm
RA	Orientation of the flat axis of corneal front surface in $^\circ$
R_f, R_b	Front and back surface of the optics cylinder of a keratoprosthesis
R_{mean}	Average of R1 and R2 in mm
SEQ	Spherical equivalent, average power of spectacle correction in dpt
Spectacle magnification	Ratio of magnification with glasses vs. situation without glasses in %
Sphere	Sphere or base curve of the spectacle correction in dpt
Stigmatic:	Condition of a centred optical system with rotationally symmetric surfaces only which form a symmetric spot image
Toric lens	Intraocular replacement lens with astigmatic correction
TR	Target refraction, intended refraction after surgery in dpt
VD	Vertex distance, distance between back surfaces of glasses and cornea in mm
VFA	Visual (half) field angle in $^\circ$

1. Introduction

1.1. Definitions and context of ocular magnification and aniseikonia

Human vision covers an optical portion, where the human eye images objects at an arbitrary object plane or space to the retina, which refers to the image plane, as well as a neural component. On the optical pathway from the object to the image, we find several optical elements such as spectacle correction, contact lenses, the cornea, aqueous humour, the natural lens or a replacement lens, and the vitreous. All of these elements are characterized by surfaces and a respective refractive index [17], which could be constant in the simplest case or could show some gradient such as the crystalline lens. If rays pass through refractive surfaces, the direction of the rays change, as described by the Snellius refraction law [18], and within a homogeneous refractive medium, rays are travelling linearly. The refractive index of an optical medium refers to the ratio of speed of light in vacuum to the speed of light in the medium. Optical media could cause some amount of absorption and scattering, which reduces the light intensity and the image contrast [53], but human vision is not restricted to optical imaging, the retinal image is processed first in the retina and later on the visual impression is interpreted in the brain [53].

Visual acuity is not the only quality criterion for visual performance. There are several parameters such as contrast transfer, blended vision, modulation transfer, defocus properties or the state of stereopsis which affect visual performance [40].

From the definition, optical magnification in general refers to the ratio of image to object size [3]. Lateral magnification in the eye is based on two different definitions, one for objects at infinity and one for objects at finite distances [40]. For objects at infinity, object size is not defined and therefore, magnification refers to the ratio of retinal image size to the visual angle of an object in radians. For objects at finite distances, the classical definition of magnification as the ratio of retinal image size to object size is valid. If we restrict to an eye as a centred optical system with rotational symmetric surfaces we call it *stigmatic* [40]. If the optical system is not centred or there is at least one element with some variation of curvature for different meridians we call it *astigmatic*. In the stigmatic case, lateral magnification is isometric, which means that for all meridians the object to image magnification is the same [33]. For an astigmatic eye, lateral magnification varies and the object to image transfer is no longer isometric, we have some image distortion [22,23].



Figure 1.1.: *Binocular aniseikonia refers to difference in the overall magnification between the left and right eye (upper row), astigmatic surfaces cause blur if uncorrected, or image distortion (meridional aniseikonia) if corrected.*

Two eyes are called isometric, if all dimensions match. In special, it means that all distances such as the axial length of the eye, corneal thickness, aqueous thickness, lens thickness and vitreous depth are identical, and all curvatures of refractive surfaces such as corneal front and back surfaces as well as lens front and back surfaces match. As a consequence, the refraction of both eyes matches. In reality, a complete match between two eyes of an individual is unrealistic, that means we have some amount of anisometropia. Anisometropia itself does not cause complain to the patient, it is not even noticed [40].

From the classical definition, aniseikonia refers to the binocular refraction status, where the lateral magnification of both eyes shows some disparity. In contrast to anisometropia, aniseikonia refers to the lateral magnification disparity. In ophthalmology, the classical understanding of aniseikonia in general is related to a difference in the overall object to image magnification comparing both eyes of one individual, which is also described as binocular aniseikonia [30]. This condition is shown in the upper row of **Figure 1.1**. If we have any astigmatic optical element in the eye, lateral magnification varies in different meridians. If astigmatism remains uncorrected we notice some blur in the image (**Figure 1.1** lower row in the middle), and if astigmatism is fully corrected (e.g. with spectacle glasses) we get a sharp image, but some image distortion (**Figure 1.1**, lower row right image). Such an image distortion due to a variation of ocular magnification in different meridians is called meridional aniseikonia. **Figure 1.2** shows the condition with image distortion in a corrected optical system with astigmatic surfaces [38].

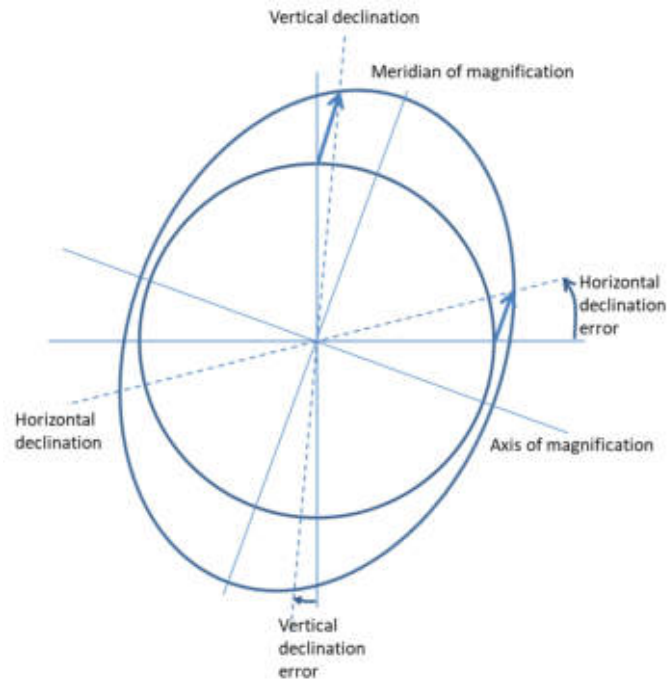


Figure 1.2: Meridional magnification in a corrected astigmatic optical system refers to a circle at object space transferred to an ellipse at image space. The meridian / axis of magnification refer to the meridian with the largest / smallest magnification, horizontal / vertical lines are slanted as shown with the horizontal / vertical declination error.

A circular object traced through the optical system yields an elliptical image defined by a long (with the highest magnification) and the short axis (with the lowest magnification) alongside with the 2 cardinal meridians (meridian of magnification and axis of magnification, **Figure 1.2**) [27-29]. Meridional magnification refers to the ratio of the long to short axis. Each point at the circle (at object plane) corresponds to a point at the ellipse (at image plane) [35,38]. Horizontal and vertical lines are inclined as referred with the horizontal and vertical declination error [22,23]. Meridional aniseikonia could take place isolated, if the overall magnification of both eyes is identical, or in combination with binocular aniseikonia, if the overall magnification of both eyes does not match [27-29]. Eyes are called eikonic if the overall magnification of both eyes is identical and we do not have variations on meridional magnification [6,7]. Aniseikonia is always a consequence of anisometropia, but not all cases of anisometropia cause aniseikonia. In some cases, differences in biometric measures could counterbalance each other so that the resulting binocular or meridional lateral magnification is identical [40].

In addition, we differentiate between static and dynamic aniseikonia. In case of static aniseikonia, we have constant, but different lateral magnifications for variation of viewing directions. In case of dynamic aniseikonia, we observe different lateral magnifications for different viewing angles due to a prismatic effect. This type of aniseikonia is called induced

anisophoria. A typical situation for anisophoria is, if the patient looks through different areas of anisometric refraction correcting glasses [30]. In addition to anisophoria, ocular magnification could also change dynamically with accommodation, which was not systematically investigated in the past. If translation lenses are used to maintain pseudophakic pseudo-accommodation after cataract surgery, changes in magnification can be analysed systematically [34,42].

The incidence of aniseikonia is mostly underestimated or even ignored in clinical routine, as in most cases, symptoms are not obvious or measurable [40]. In the normal adult population, with an age more than 20 years, prevalence of aniseikonia due to an anisometropia of 1 diopter (dpt) or more is estimated to 10% [2,13]. In contrast, especially after cataract surgery with implantation of an artificial lens (IOL), after corneorefractive surgery such as PRK or LASIK or other types of corneal (e.g. penetrating keratoplasty) or posterior eye segment (e.g. cerclage) procedures, prevalence of aniseikonia seems to be significantly increased up to 40% [30]. However, many cases of aniseikonia remain undiagnosed in clinical routine [40] and its high prevalence should sensitize ophthalmologists to the general problems of ocular magnification and aniseikonia.

Sensitivity to magnification disparity shows a large variation in the population. Some patients are already impaired with an overall magnification difference of around 1% between the left and the right eye, and others tolerate magnification differences between both eyes of 3 or 5 % without any interference of vision [2,10,11]. In contrast to binocular aniseikonia, the tolerance or acceptance to meridional aniseikonia is not studied systematically in the literature [40]. Some researchers report, that in case of meridional in combination with binocular aniseikonia, a correction of binocular aniseikonia is sufficient for the patient and the variation in meridional magnification is tolerated. Others report that especially meridional variation of magnification is less tolerated due to image distortion and causes in some cases severe complains to the patients such as headaches, fusion problems or asthenopic complains [2,10,11,31,33].

1.2. Options for addressing aniseikonia

In ophthalmology, the classical way of addressing aniseikonia is a correction using eikonic glasses [1,2]. With variations of the front and back (basic curvature) surface shape, thickness and refractive index of the glass as well as vertex distance, the individual spectacle magnification and subsequently the magnification of the entire eye can be varied [14]. For patients where a cataract surgery with implantation of an IOL is intended, aniseikonia can be directly addressed with an individual shape of the implant: for correction of binocular

aniseikonia the curvature of both surfaces, central thickness and the refractive index of the lens material could be adapted, and for correction of meridional aniseikonia central thickness, refractive index, and both surfaces have to be shaped individually with a bitoric eikonic design in order to compensate image distortion due to meridional variations in magnification [25,37,44,48]. If the variation in shape alone is not sufficient to compensate for binocular and/or meridional aniseikonia, combinations of a lens implant and an appropriate spectacle correction could help, but in those cases we are limited in planning the refractive outcome of the cataract surgery and the patient should be aware, that postoperative emmetropia is no longer possible. We have to keep in mind, that calculation and manufacturing of such (bitoric) eikonic IOLs is challenging and requires sophisticated tools, manufacturing strategies, and know-how [37]. Another option for correction of binocular or meridional aniseikonia is the implantation of additional lenses in the eye [38]. In the phakic eye, such lenses are called phakic lenses or intraocular contact lenses (ICL), and they are mostly used for correction of large spherical and/or astigmatic refraction errors in young adults, where the physiological accommodation of the eye should be maintained and corneorefractive surgery such as LASIK, LASEK or PRK fail. Today, such ICLs are implanted into the sulcus ciliaris, in front of the crystalline lens. In a progressed age where physiological accommodation is significantly reduced and first clinical signs of an opacification in the crystalline lens capsule, cortex, or nucleus are present, the cataract is typically re-scheduled to an earlier time point (so called ‘clear cataract extraction’) and a normal capsular bag lens is implanted [37]. As outlined above, such capsular bag lenses can be potentially used for an eikonic correction [25]. In situations, where aniseikonia is not tolerated by the patient after cataract surgery, we have the option of implanting an additional lens in front of the capsular bag lens (a so called add-on lens or piggy-bag lens). The shape of such add-on lenses can be customized to correct for aniseikonia, either for binocular or for meridional one [38].

Spectacle glasses show the largest effect on ocular magnification [1,2,36]. Due to the large distance from the eye’s image-sided principal plane, a spectacle correction for ametropia always affects ocular magnification much more than e.g. a contact lens correction. Minus corrections for myopic eyes minify the retinal image size, whereas plus corrections magnify the retinal image size [5]. That also has to be taken into consideration, if we measure the visual performance of the eye, in terms of visual acuity. With acuity tests, letters are projected with standard sizes (e.g. Landolt ring (EN ISO 8596) with an opening of 1 arc second for testing for visual acuity of 1.0), and with myopic / hyperopic spectacles the visual field angle of the letter is smaller / larger which implies a reduced / increased visual acuity by artefact. The same

occurs in measuring the defocus curve: the more plus is used for fogging the larger the retinal image! If the spectacle is simplified by a thin lens model, which means that the typical meniscus shape of the spectacle glass (with a front and back surface curvature, central thickness, and characteristic refractive index) is described by a refractive power only, the angular magnification indicating ratio of retinal image size with and without spectacle correction is described in **Figure 1.3**, where P_S refers to the refractive power of the spectacle and VD to the vertex distance (distance between the spectacle correction and the cornea) [2].

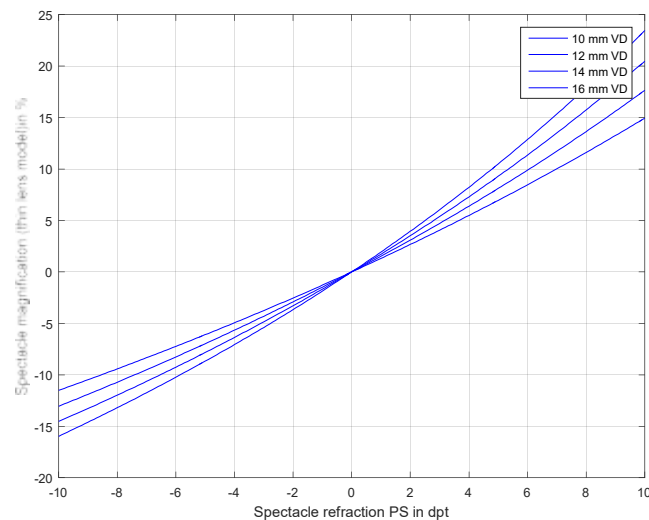


Figure 1.3: Spectacle magnification (thin lens model) as a function of spectacle refraction.

If we consider the spectacle correction as a thick lens with a front surface power P_{Sf} and a back vertex power P_S , a central thickness d_S , and a refractive index n_S , spectacle magnification is split into a factor related to power (as described for the thin lens simplification) and a factor related to shape. **Figure 1.4** shows the effect of spectacle magnification exemplarily for glasses with a central thickness of $d_S=3$ mm, a refractive index of $n_S=1.5$ and a vertex distance of $VD=12$ mm.

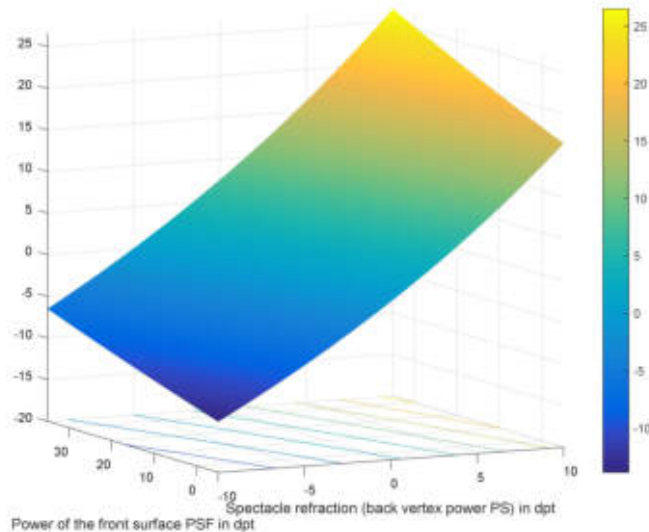


Figure 1.4: Spectacle magnification (thick lens model) for $VD=12$ mm. Magnification depends on spectacle refraction and front surface power

Hyperopic corrections with a large surface power at the front surface show the largest magnification effect, and myopic corrections with a low or negative front surface power show the largest minification effect [2]. In contrast to spectacle magnification, correction of refraction errors with contact lenses changes the ocular magnification much less, typically in a range of $\pm 2\text{-}3\%$.

2. Objectives

The purpose of this PhD thesis is

- to present mathematical strategies for determination of ocular magnification in the (spectacle-)corrected and uncorrected eye before and after cataract surgery with implantation of standard lenses and toric implants,
- to show how ocular magnification is changed in different clinical situations such as corneal surgery (e.g. LASIK, LASEK, PRK or keratoplasty), cataract surgery with implantation of a standard or toric capsular bag lens,
- to show how the optics part of keratoprotheses can be designed to realize intended magnification, visual field angle, and target refraction, and
- to give ideas how aniseikonia as a disparity between ocular magnification between both eyes or magnification between different meridians could be addressed in clinical routine to get an eikonic imaging.

3. Results

In all parts of the Results section we present clinical examples to get some insight into and to show the applicability of our calculation strategy to clinical data. In addition, we analyse a large master dataset including $N=8998$ eyes with biometric measurements (IOLMaster 700, Carl-Zeiss-Meditec, Jena, Germany) and refraction data before and after cataract surgery alongside with the respective data of the implanted lens. For simplicity, we restricted to objects located at infinity, which means that ocular magnification (OM) refers to the ratio of retinal image size to the slope angle of the incident rays in radians. Gain in ocular magnification refers to the change from preoperative to postoperative magnification in %. Meridional magnification refers to the ratio of meridional magnifications in the magnification meridian and the magnification axis (with respect to an elliptical image distortion as shown in **Figure 1.2**) in %. For evaluation of change in meridional magnification, a circular object at object space (at infinity) is considered, and change in meridional magnification refers to the ratio of magnification change comparing the magnification meridian and the magnification axis by transforming the preoperative to the postoperative retinal image. If not stated otherwise, vertex distance VD was considered 14 mm, keratometer index for a thin lens model of the cornea was $n_K=1.332$ and for the refractive indices of air, cornea (n_C), aqueous humour (n_A), crystalline lens (n_L) and vitreous (n_V) we used 1.000, 1.376, 1.336, 1.41, 1.336, as used in the Gullstrand schematic model eye [17].

The dataset included axial length measurement (AL), central corneal thickness (CCT), aqueous depth (AQD), anterior chamber depth (ACD) as a sum of CCT and AQD, phakic or pseudophakic lens thickness (LT), corneal front surface curvature in the flat (R1) and the steep (R2) meridian with orientation of the flat meridian (RA), corneal back surface curvature in the flat (PR1) and the steep (PR2) meridian with orientation of the flat meridian (PRA), spectacle refraction with sphere (Sphere), cylinder (Cylinder) and axis (Axis), the power of the implanted IOL (IOLP for rotational symmetric lenses and IOLP as equivalent power, IOLPAST as lens toricity and implantation axis IOLPA for toric lenses) alongside with the refractive index n_{IOL} and the ratio of average lens back surface to front surface power (q). Mean corneal front (R_{mean}) and back (PR_{mean}) surface radius was derived as average from R1 and R2 or PR1 and PR2, respectively, and spherical equivalent of refraction (SEQ, Sphere + $0.5 \cdot$ Cylinder). Astigmatism of the corneal front (AST) and back (PAST) surface was derived using $AST=(n_C-1)(1/R2-1/R1)$ and $PAST=(n_V-n_C)(1/PR2-1/PR1)$.

Out of the dataset with $N=8998$, 1119 cases show a corneal astigmatism more than 2 diopters and were treated with toric lenses. This subset of data was used to present results on ocular

overall and meridional magnification in astigmatic eyes. For presentation of the results of change in overall and meridional ocular magnification after corneal surgery, the dataset of $N=8998$ cases was filtered for those cases where the spherical equivalent was $|\text{SEQ}| > 1.5$ dpt or refractive cylinder was $\text{Cylinder} < -1.5$ dpt to mimic realistic conditions where corneorefractive surgery is typically performed. Finally, $N=5017$ clinical cases were considered. The dataset of $N=8998$ cases was also used for a simulations of ocular magnification, target refraction, and visual field angle (VFA) in keratoprotheses.

Results for the respective dataset are shown with descriptive statistics and a Monte-Carlo simulation with a focus in trend analysis to extract the effect sizes and fitting (multivariate) linear models. For that purpose we setup a Monte-Carlo simulation.

3.1. Application of our calculation strategy in cataract patients

3.1.1. Overall ocular magnification in the phakic and pseudophakic eye

Clinical case

In this example I would like to show a situation of a patient, who received cataract surgery with implantation of a standard IOL in both eyes (left eye: SN 60, Alcon, Fort Worth, USA, right eye: Vivinex XC1, Hoya, Tokio, Japan). The left eye was treated first and 6 weeks later the right eye received cataract surgery. We selected this patient as a normal case with average biometric measures, and the biometric and refraction data before and after cataract surgery are shown in **Table 3.1**. As phakometry is difficult and unreliable, we back-calculated the crystalline lens power from biometric measures and refraction [43].

Table 3.1: Preoperative and postoperative biometric and refraction data of the left (OS) and right (OD) eye alongside with resulting magnification. For the phakic eye we assumed a ratio of back to front surface power of 10/6, for the IOL we took the data from the data sheet.

	Axial length AL in mm	Anterior chamber depth ACD in mm	Lens thickness LT in mm	Lens shape factor q / n_{IOL}	Mean corneal radius R_{mean} in mm	Spherical equivalent SEQ in dpt	Ocular magnification OM x1000
OS preop	23.70	3.50	4.30	0.6 / 1.41	7.6	-1.50	15.8473
OS postop	23.70	5.20	0.81	0.7 / 1.55	7.6	-0.25	16.4365
OD preop	23.60	3.60	4.20	0.6 / 1.41	7.8	-0.50	15.9540
OD postop	23.60	5.30	0.80	1.3 / 1.56	7.8	0.00	16.3069

Preoperatively, the ratio of OM left/right eye was -0.67% and postoperatively 0.79%, the gain in OM from preoperative situation to the postoperative situation was 3.72% in the left and 2.21% in the right eye. In the time interval between both surgeries the pseudophakic left eye shows a larger OM (0.0164365) compared to the untreated right eye (0.0159540) by 3.02%.

This image size disparity caused some fusion and diplopia problems and the patient forced the treatment at the second eye.

Descriptive statistics of our clinical dataset

The descriptive data of our large consecutive dataset of N=8998 clinical cases before and after cataract surgery is displayed in **Table 3.2** with mean, standard deviation, median, minimum and maximum and 95% confidence interval. **Table 3.2** is restricted to a selection of the most relevant data for calculation of overall ocular magnification in the preoperative and postoperative situation.

Table 3.2: Descriptive statistics of the most relevant parameters for calculation of overall ocular magnification. SD refers to standard deviation, AL to axial length, ACD to anterior chamber depth (CCT+AOD), LT to lens thickness, and SEQ to the spherical equivalent in refraction.

	AL in mm	ACD preop in mm	ACD postop in mm	LT preop in mm	LT postop in mm	R _{mean} in mm	SEQ preop in dpt	SEQ postop in dpt
Mean	23.8510	3.2185	4.5972	4.5057	0.7941	7.7349	-0.5053	-0.1711
SD	1.3999	0.4560	0.3481	0.6048	0.1063	0.2775	3.2659	0.2635
Median	23.6765	3.2056	4.5918	4.5955	0.7951	7.7266	0.0	-0.1250
Minimum	18.7129	1.5305	3.3596	1.0066	0.3768	6.2948	-22.3750	-1.7500
Maximum	32.2087	5.5347	6.1917	8.6412	1.1988	9.5788	12.5000	0.6250
2.5% quantile	21.5167	2.3556	3.9289	3.2784	0.5823	7.2366	-8.2500	-1.0000
97.5% quantile	27.1137	4.0849	5.3042	5.4966	0.9966	8.3247	4.6250	0.2500

Table 3.2 presents the OM for the phakic eye before cataract surgery and the pseudophakic eye after cataract surgery alongside with the gain in OM from preoperative to postoperative situation.

Table 3.2: Descriptive statistics of ocular magnification (OM) and gain in ocular magnification from the preoperative to the postoperative situation.

	OM preoperatively x1000	OM postoperatively x1000	Gain in OM in %
Mean	16.2700	16.7128	2.6767
Standard deviation	0.5215	1.1189	5.1252
Median	16.2494	16.5667	1.9081
Minimum	14.2371	12.6524	-16.6503
Maximum	19.2368	24.0111	37.7394
2.5% quantile	15.3243	14.8520	-5.5938
97.5% quantile	17.3993	19.2687	14.1937

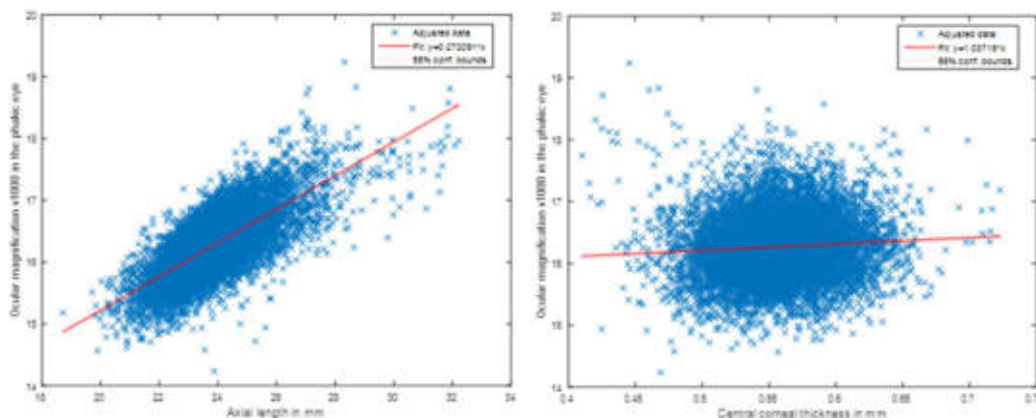
Overall, OM gains due to cataract surgery by 2.7% on average, and there is large individual scatter depending on several effect sizes, which is demonstrated in the following section. The 95% confidence interval ranges in between -5.6 and 14.2%.

Monte-Carlo simulation in our clinical dataset

For this Monte-Carlo simulation, we considered the cornea as a thick meniscus lens with R_{mean} , PR_{mean} , and CCT to study the effect sizes. Therefore ACD as a potential effect size was replaced by CCT and AQD. The linear multivariate prediction model for ocular magnification in the phakic and pseudophakic eye with the effect sizes AL, CCT, AQD, LT, R_{mean} , PR_{mean} , and SEQ read

- $OM = 0.41208 + 0.85444 \cdot AL - 0.28442 \cdot CCT - 0.2331 \cdot AQD - 0.173 \cdot LT - 0.21044 \cdot R_{\text{mean}} - 0.17223 \cdot PR_{\text{mean}} + 0.26351 \cdot SEQ$ (phakic eye)
- $OM = 0.057259 + 0.89048 \cdot AL - 0.27063 \cdot CCT - 206.08 \cdot AQD - 0.173 \cdot LT - 0.26 \cdot R_{\text{mean}} - 0.16754 \cdot PR_{\text{mean}} + 0.26673 \cdot SEQ$ (pseudophakic eye)

The root mean squared error of this prediction model for the phakic/pseudophakic situation is 0.0408 / 0.0253 and $R^2 = 0.994 / 0.999$. All effect sizes are highly significant with $p < 0.0001$. The multivariate model for the phakic eye including all 7 effect sizes shows a very good performance (**Figure 3.1** lower row right column), whereas the effect sizes in a univariate linear model yield a much lower performance as shown in **Figure 3.1**. Mostly AL, R_{mean} , PR_{mean} , and SEQ seem to have a strong impact on OM.



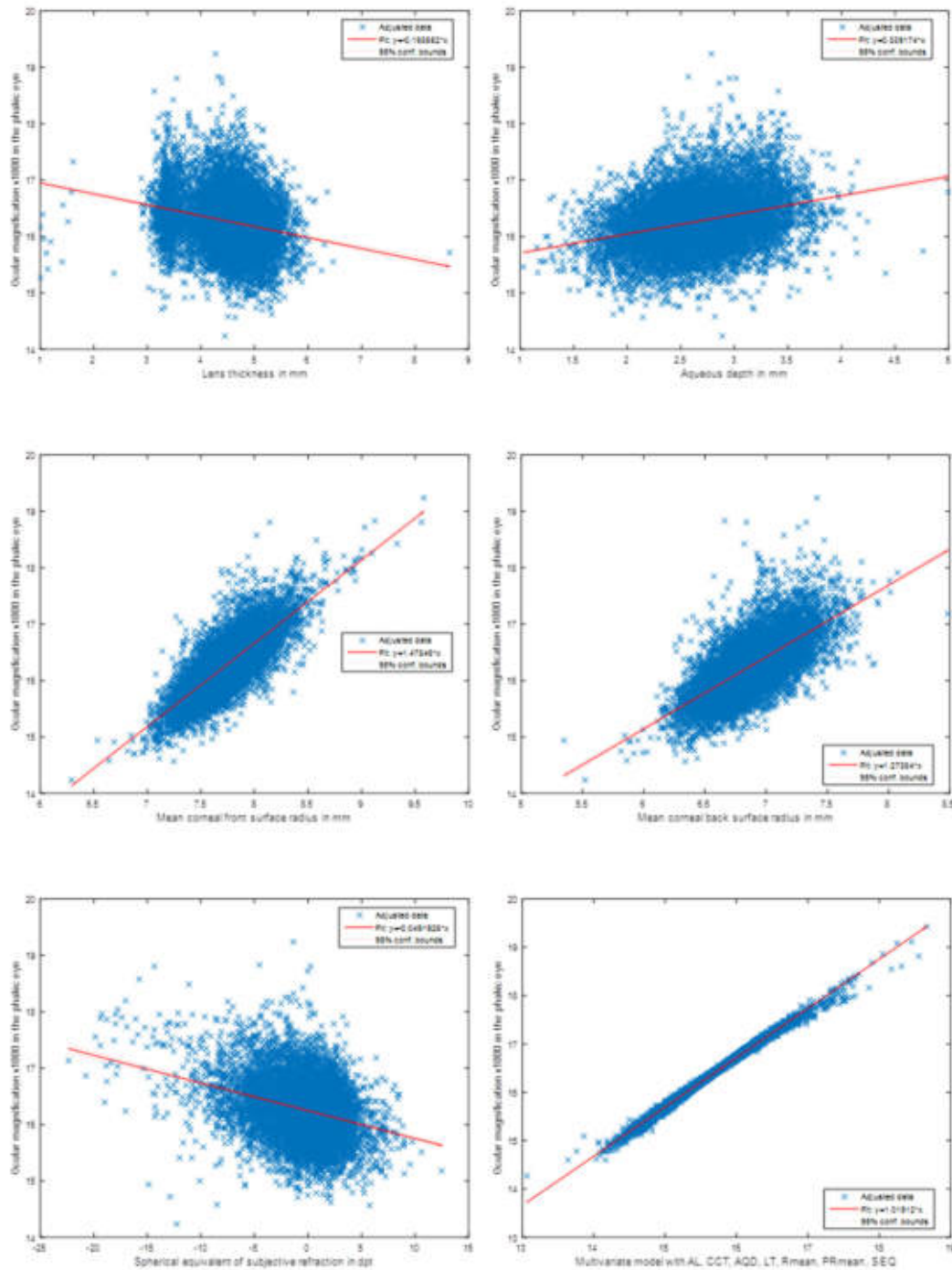
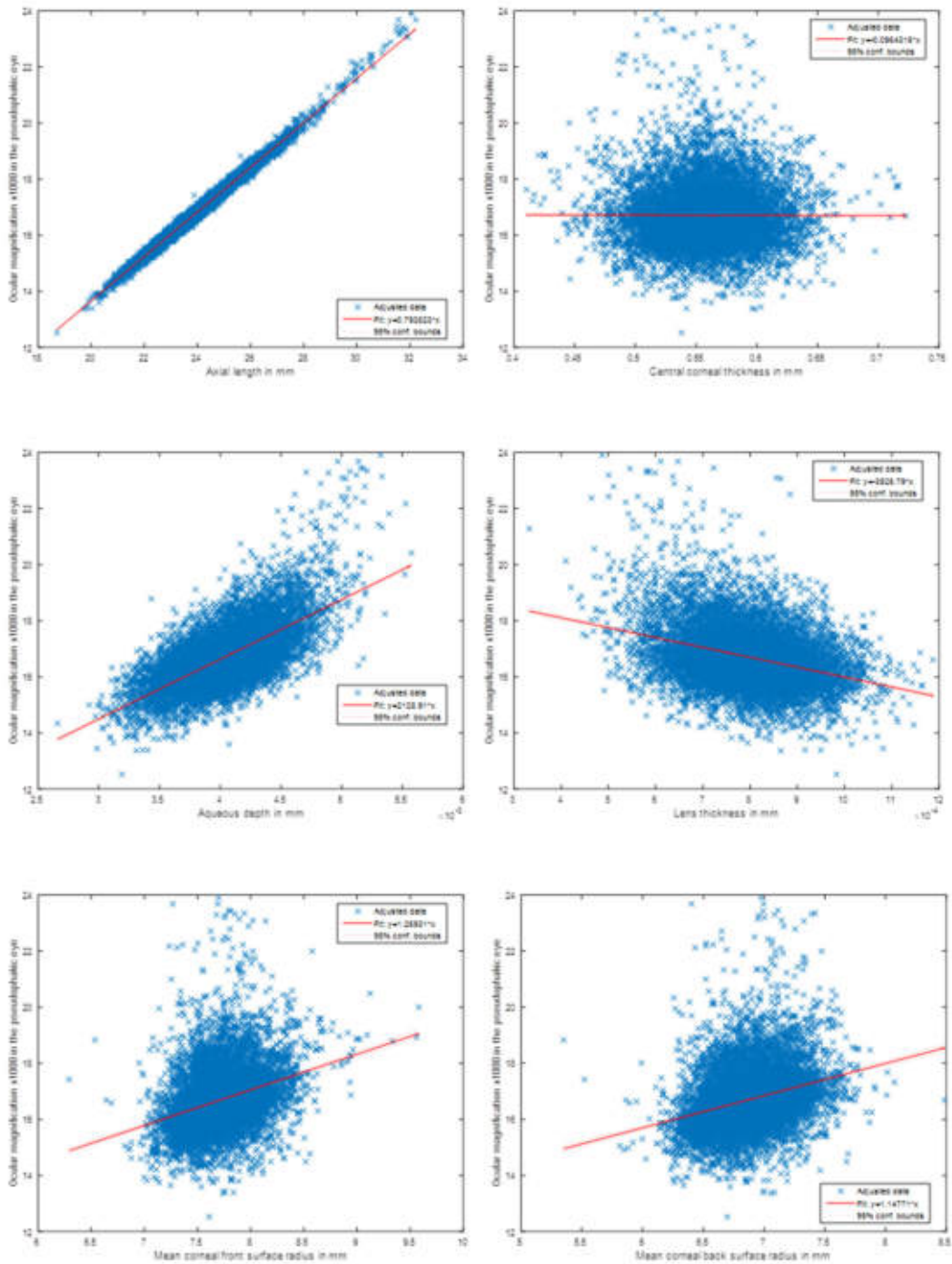


Figure 3.1: Phakic eye: univariate linear models to analyse the predictability of axial length (AL), central corneal thickness (CCT), aqueous depth (AQD), lens thickness (LT), mean curvature of the corneal front and back surface (R_{mean} , PR_{mean}), and spherical equivalent (SEQ) alongside with the performance plot for the multivariate model (lower right).

For the pseudophakic eye, the respective graphs for the 7 univariate and the multivariate linear models are shown in **Figure 3.2**. Due to the lower variation in refraction error in the pseudophakic eye, the performance of the prediction models is even better, compared to the phakic eye. In the univariate linear model AL seems to have a high and AQD and LT as well as

SEQ a moderate impact on OM. The multivariate model, as shown on the lower row right column implies, that pseudophakic OM could be predicted with a very low prediction error.



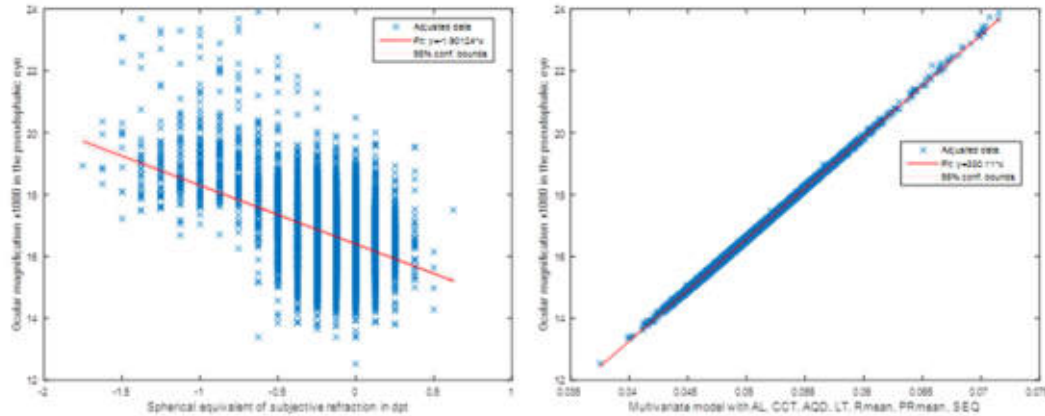


Figure 3.2: Pseudophakic eye: univariate linear models to analyse the predictability of axial length (AL), central corneal thickness (CCT), aqueous depth (AQD), lens thickness (LT), mean curvature of the corneal front and back surface (R_{mean} , PR_{mean}), and spherical equivalent (SEQ) alongside with the performance plot for the multivariate model (lower right).

3.1.2. Meridional ocular magnification in the phakic and pseudophakic eye

Clinical case

In this example I would like to present the situation of a patient, who underwent cataract surgery with implantation of a toric lens implant IOL in both eyes (both eyes: Vivinex XY1 toric, Hoya, Tokio, Japan). The right eye was treated first, and 2 weeks later the left eye underwent surgery. The biometric and refraction data before and after cataract surgery are shown in **Table 3.3**. Again, as phakometry is difficult and unreliable, we determined the crystalline lens power from biometric measures and refraction and the shape factor (ratio of front to back surface radius 10/6, $q=0.6$) and average refractive index ($n=1.41$), derived from the Gullstrand schematic model eye [17]. The shape factor for the IOL, as well as the refractive index was provided by the lens manufacturer.

Table 3.3: Preoperative and postoperative biometric and refraction data of the left (OS) and right (OD) eye alongside with resulting overall magnification and meridional magnification disparity. AL, CCT, AQD, LT refer to axial length, central corneal thickness, aqueous depth, lens thickness, R1 / R2 and PR1 / PR2 to the corneal front and back surface radius of curvature in the flat / steep meridian, corrected / uncorrected OM to the mean ocular magnification and disparity of meridional ocular magnification with/without spectacle correction.

	AL / CCT / AQD / LT in mm	R1 / R2 in mm	PR1 / PR2 in mm	Refraction SEQ / Cylinder	Corrected OM overall x1000 / meridional OM in %	Uncorrected OM overall x1000 / meridional OM in %
OS preop	25.50 / 0.54 / 2.84 / 4.13	8.05 / 7.45	6.85 / 6.60	-6.25 / -4.5	15.96 / 6.15	17.63 / 1.06
OS postop	25.50 / 0.54 / 4.62 / 0.73	8.05 / 7.45	6.85 / 6.60	-0.375 / - 0.25	18.07 / 1.99	18.15 / 1.99

OD preop	24.60 / 0.55 2.80 / 4.25	7.90 / 7.40	6.90 / 6.70	-2.50 / -3.0	15.88 / 3.76	16.95 / 1.15
OD postop	24.60 / 0.55 / 4.72 / 0.75	7.95 / 7.40	6.90 / 6.70	-0.25 / -0.5	17.25 / 1.05	17.34 / 1.91

Preoperatively, the difference in overall OM between left and right eye was 0.50% and postoperatively 4.75%, the gain in OM from preoperative situation to the postoperative situation was 13.22% in the left and 8.62% in the right eye. For the uncorrected eye (with blur), the preoperative ratio of overall OM left/right eye was 4.01% and postoperatively 4.67%, the gain in OM from preoperative situation to the postoperative situation was 2.94% in the left and 2.30% in the right eye.

Image distortion due to meridional OM for the spectacle corrected eye was 6.15% / 3.76% preoperatively and could be reduced by implantation of the toric lens to 1.99 / 1.05% for the left / right eye. For the uncorrected eye (with blur), the respective values were 1.06 / 1.15% preoperatively and 1.99 / 1.91% postoperatively.

In the time interval between both surgeries, the pseudophakic right eye shows larger overall magnification (0.01725) compared to the untreated left eye (0.01596) by 8.08%. Meridional image size disparity was in this time interval 1.05% in the right eye and 6.15% in the left eye, which again caused some fusion problems. The patient forced the treatment at the second eye.

Descriptive statistics of our clinical dataset

From the N=8998 clinical cases, we selected those cases which received a toric lens implant (N=1119). The biometric data and refraction data before and after cataract surgery are displayed in **Table 3.4** with mean, standard deviation, median, minimum and maximum, and 95% confidence interval. **Table 3.4** is restricted to a selection of the most relevant data for calculation of overall and meridional ocular magnification in the preoperative and postoperative situation.

Table 3.4: *Descriptive statistics of the most relevant parameters for calculation of overall ocular magnification. SD refers to standard deviation, AL to axial length, CCT to central corneal thickness, AQD to aqueous depth, LT to lens thickness, R_{mean} and PR_{mean} to mean corneal front and back surface radius, AST and PAST to corneal front and back surface astigmatism, and SEQ and Cylinder to spherical equivalent and refractive cylinder.*

	AL / CCT in mm	AQD preop / postop in mm	LT preop / postop in mm	R_{mean} / PR_{mean} in mm	AST / PAST in dpt	SEQ / Cylinder preop in dpt	SEQ / Cylinder postop in dpt
Mean	23.96 / 0.56	2.64 / 4.06	4.50 / 0.77	7.71 / 6.86	2.64 / 0.37	-1.57 / - 2.14	-0.16 / - 0.64

SD	1.64 / 0.04	0.47 / 0.38	0.63 / 0.11	0.29 / 0.30	0.94 / 0.22	4.10 / 0.76	0.23 / 0.24
Median	23.85 / 0.56	2.60 / 4.05	4.61 / 0.77	7.69 / 6.86	2.34 / 0.39	-1.00 / - 2.00	-0.12 / - 0.50
Minimum	18.71 / 0.43	1.15 / 2.96	3.13 / 0.44	6.29 / 5.34	1.50 / 0.02	-20.75 / - 7.25	-1.25 / -2- 25
Maximum	31.72 / 0.72	4.16 / 5.29	6.45 / 1.09	8.63 / 8.48	8.41 / 1.32	12.50 / - 1.00	0.50 / - 0.25
2.5% quantile	21.09 / 0.48	1.81 / 3.34	3.27 / 0.57	7.15 / 6.32	1.68 / 0.05	-11.06 / - 4.00	-0.62 / - 1.25
97.5% quantile	27.71 / 0.63	3.51 / 4.83	5.57 / 0.99	8.37 / 7.48	5.27 / 0.85	5.75 / - 1.25	0.25 / - 0.25

Table 3.5 presents the overall OM as well as the meridional OM disparity for the phakic eye before cataract surgery and the pseudophakic eye after cataract surgery.

Table 3.5: Descriptive statistics of overall ocular magnification (OM) and gain in ocular magnification from the preoperative to the postoperative situation.

	Overall OM x1000 preoperatively	Meridional magnification disparity preop. in %	Overall OM x1000 postoperatively	Meridional magnification disparity postop. in %
Mean	16.0606	2.7501	16.9501	0.4198
SD	0.5381	1.0309	1.3782	0.2884
Median	16.0634	2.5116	16.7817	0.3570
Minimum	13.9398	0.9029	12.4182	0.0134
Maximum	18.1613	7.8461	23.8516	2.4558
2.5% quantile	14.9934	1.4244	14.5012	0.0599
97.5% quantile	17.1305	5.4324	20.0408	1.1572

Overall, OM gains due to cataract surgery by 5.51%, on average. Image distortion due to meridional disparity in OM decreases from 2.75% preoperatively, to 0.42% postoperatively.

Monte-Carlo simulation in our clinical dataset

In this Monte-Carlo simulation, we considered N=1119 cases out of N=8998 eyes where a toric IOL was implanted during cataract surgery. The cornea was considered as a thick meniscus lens with front surface and back surface curvature (mean radius R_{mean} and PR_{mean}) and astigmatism (AST and PAST), with the respective orientation RA and PRA (not shown in this evaluation). From biometry, we extracted AL, CCT, and AQD pre- and postoperatively. From refraction, we used preoperative and postoperative SEQ and Cylinder. For the multivariate linear regression models, we used AL, CCT, AQD, R_{mean} , PR_{mean} , AST, PAST, SEQ and

Cylinder as potential effect sizes. The prediction model for disparity of meridional OM (DMOM) for the spectacle corrected phakic and pseudophakic eye read

- $DMOM = -0.20773 + 0.0027107 \cdot AL + 0.23983 \cdot CCT - 0.042348 \cdot AQD - 0.064563 \cdot LT - 0.10661 \cdot R_{mean} - 0.4588 \cdot AST + 0.1717 \cdot PR_{mean} + 0.78936 \cdot PAST + 0.067986 \cdot SEQ - 1.791 \cdot Cylinder$ (phakic eye)
- $DMOM = 0.35003 + 0.014072 \cdot AL + 0.12806 \cdot CCT - 0.0049123 \cdot AQD + 0.0022863 \cdot LT - 0.018822 \cdot R_{mean} - 0.019815 \cdot AST - 0.071684 \cdot PR_{mean} - 0.015104 \cdot PAST - 0.045766 \cdot SEQ - 0.40752 \cdot Cylinder$ (pseudophakic eye)

The root mean squared error of this prediction models for the phakic / pseudophakic situation is 0.131 / 0.263 and $R^2 = 0.984 / 0.178$. For the phakic model, all effect sizes except AL and intercept were statistically significant ($p < 0.05$), but for the pseudophakic model, the performance was much worse. Only Cylinder could be validated, as an effect size ($p < 0.05$).

Figure 3.3 shows the multivariate model for the phakic eye (left side) and the pseudophakic eye (left side) including all 10 effect sizes. The prediction model for disparity of meridional magnification shows a very good performance for the phakic eye in contrast to the prediction model for the pseudophakic eye.

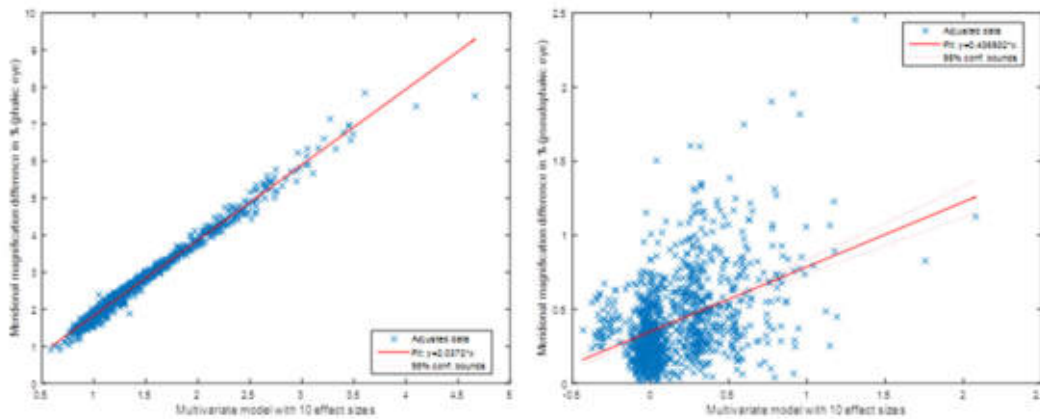
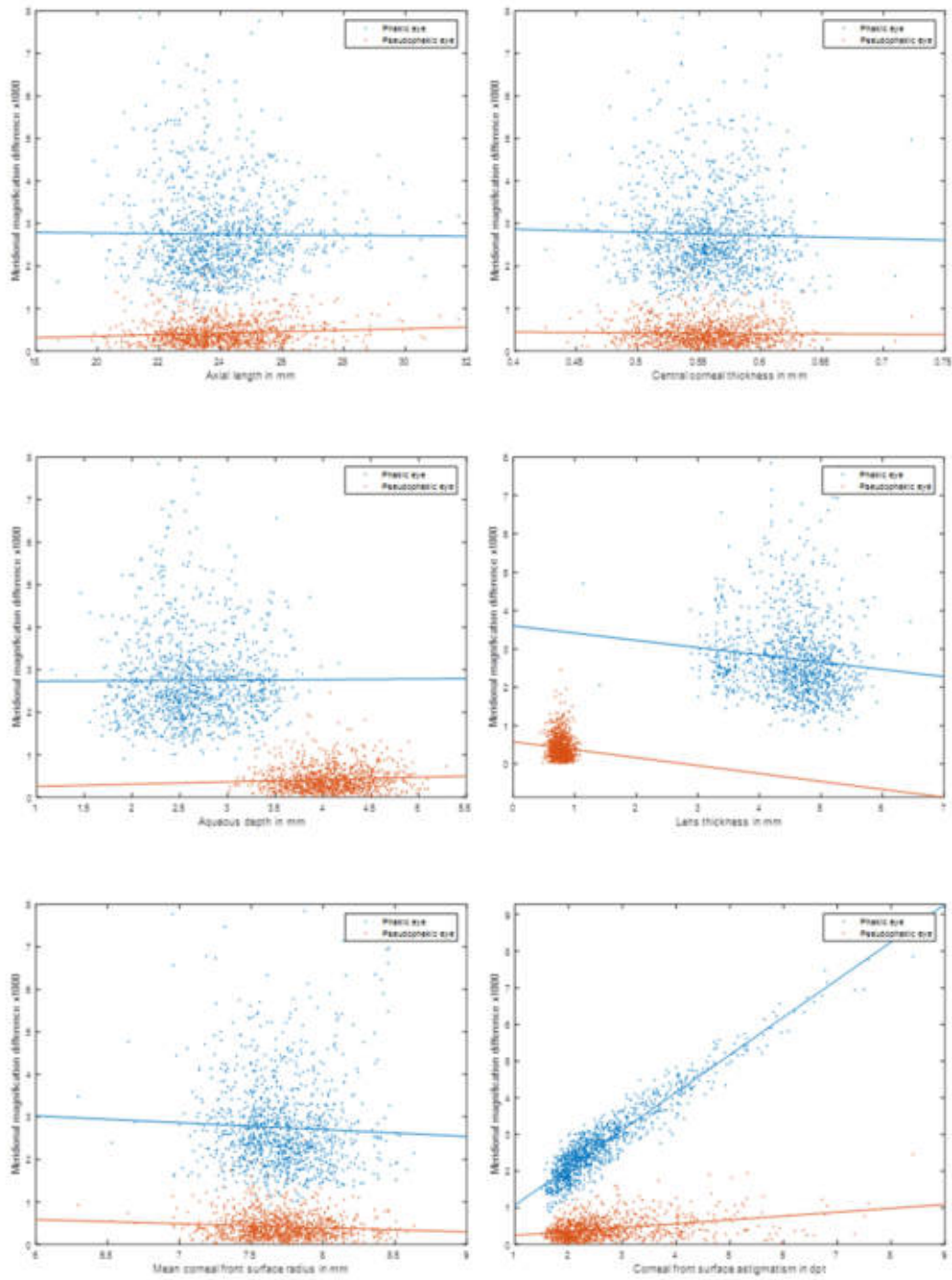


Figure 3.3: Multivariate linear prediction model disparity of meridional magnification (DMOM in the phakic (left) and the pseudophakic eye. As potential effect sizes were considered: axial length AL, central corneal thickness CCT, aqueous depth AQD, lens thickness LT, mean corneal front and back surface radius R_{mean} , and PR_{mean} , corneal front and back surface astigmatism AST and PAST, spherical equivalent SEQ and refractive cylinder Cylinder.

Figure 3.4 displays the graphs for the 10 potential effect sizes (AL, CCT, AQD, LT, R_{mean} , PR_{mean} , AST, PAST, SEQ, and Cylinder) analysed in a univariate linear model for the phakic and pseudophakic eyes. Axial length AL, central corneal thickness CCT, and aqueous depth AQD show almost no effect on disparity of meridional OM, whereas lens thickness presents some inverse effect. In the univariate model for disparity of meridional OM in the phakic eye,

AST and PAST as well as Cylinder show some impact. SEQ and Cylinder seem to have an inverse effect on disparity of meridional OM in the phakic and pseudophakic prediction model.



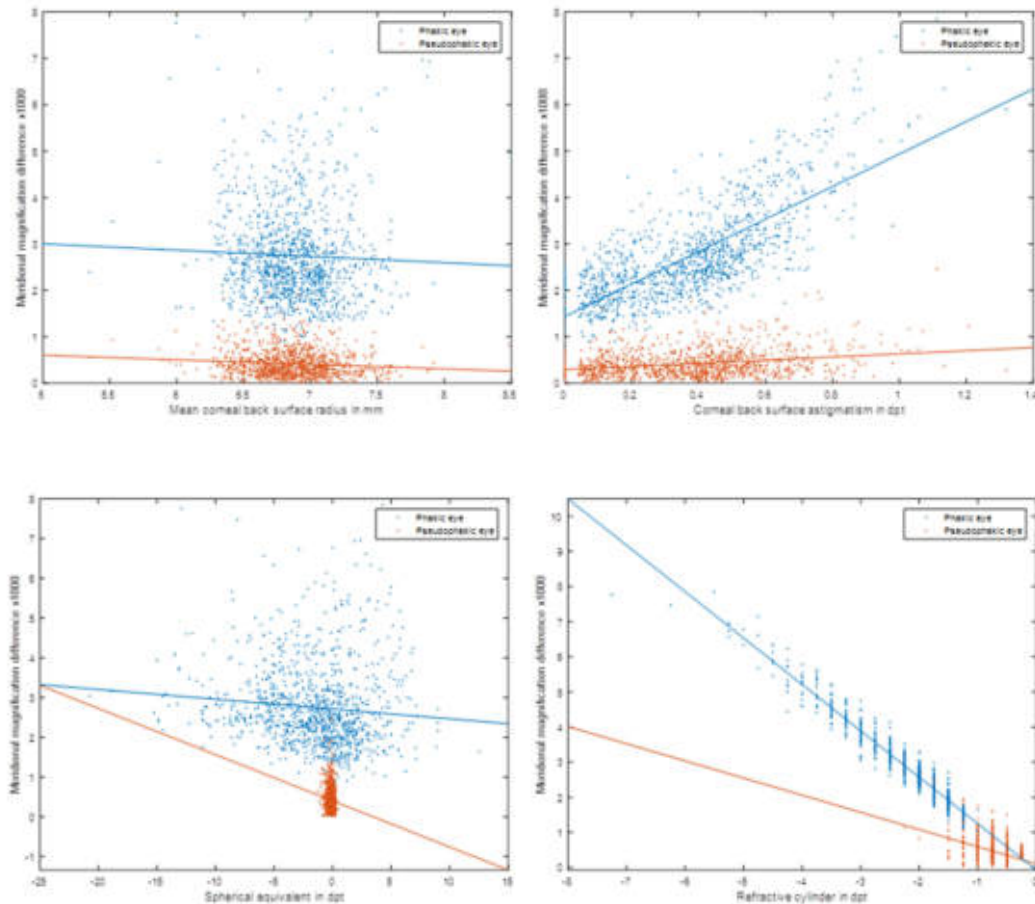


Figure 3.4: Meridional magnification before (phakic eye) and after (pseudophakic eye) cataract surgery with implantation of a toric lens described with univariate linear models for all 10 effect sizes axial length AL , central corneal thickness CCT , aqueous depth AQD , lens thickness LT , mean corneal front and back surface radius R_{mean} , and PR_{mean} , corneal front and back surface astigmatism AST and $PAST$, spherical equivalent SEQ and refractive cylinder $Cylinder$.

3.2. Change in overall and meridional magnification due to corneal surgery

Corneal curvature is one of the major effect sizes, which determine OM. The dominant portion of ocular astigmatism refers to the corneal front surface shape. Especially in keratoplasty or corneorefractive surgery such as LASIK, LASEK, or PRK, the correction with spectacles is shifted in part or completely to the corneal plane, which affects overall OM, and in case of corneal astigmatism also meridional OM. In this section, we address the change in OM due to change of corneal curvature [35,37]. The cornea is considered as a thick lens. We provide 2 clinical examples and present descriptive data and results of a Monte-Carlo simulation based on our clinical dataset where the change in OM is predicted for a potential population for corneorefractive surgery (target refraction was assumed to be plano) from biometric data and the change in corneal curvature. For the descriptive data and the Monte-Carlo simulation we extracted from the dataset of $N=8998$ all clinical cases with $|SEQ| > 1.5$ dpt or $Cylinder < -1.5$ dpt ($N=5017$), to mimic realistic situations for corneorefractive surgery.

Clinical case

In the first example we consider a clinical situation before and after LASIK. Preoperatively, R1/R2/RA and PR1/PR2/PRA are 7.80 mm / 7.50 mm / 10° and 6.80 mm / 6.60 mm / 5°, and spectacle refraction is -7.5 dpt -2.5 dpt / 5°. Postoperative refraction is intended to be 0 dpt – 0.25 dpt / 90° to support reading ability. The change in corneal front surface curvature was derived from the intended change in refraction and yielded 9.11 mm / 9.00 mm / 70°. Central corneal thickness prior to ablation was assumed to be 550 µm, and postoperatively it was reduced to 480 µm due to corneal ablation. Corneal back surface curvature and aqueous depth (3.5 mm) are assumed to be unchanged during surgery.

Due to corneal flattening overall OM gains by 12.05%, and expressed in the principal meridians [4] it gains by 13.99% in 90° (magnification meridian) and by 10.11% in 0° (magnification axis).

In the second example, we consider a clinical situation before and after penetrating keratoplasty. Preoperatively, R1/R2/RA and PR1/PR2/PRA are 8.00 mm / 7.30 mm / 25° and 6.90 mm / 6.40 mm / 35°, and spectacle refraction is 2.5 dpt -4.0 dpt / 30°. Postoperatively, R1/R2/RA and PR1/PR2/PRA are 7.90 mm / 7.20 mm / 95° and 6.80 mm / 6.50 mm / 100°, and spectacle refraction is 2.0 dpt -4.0 dpt / 100°. CCT and AQD preoperatively / postoperatively are 630 µm / 610 µm and 3.3 mm / 3.2 mm.

Due to the change in corneal shape (front and back surface), CCT and AQD, overall OM gains by 2.83%, and expressed in the principal meridians, it shows a gain of 12.06% in 91° (magnification meridian) and a loss of 6.40% in 1° (magnification axis).

Descriptive statistics of our clinical dataset

From the N=8998 clinical cases, we selected those situations with |SEQ|>1.5 dpt or Cylinder < -1.5 dpt (N=5017). The biometric data and refraction data and the simulated corneal front surface and thickness data after ‘simulated’ corneorefractive surgery are displayed in **Table 3.6** with mean, standard deviation, median, minimum and maximum, and 95% confidence interval. **Table 3.6** is restricted to a selection of the most relevant data, for calculation of overall and meridional OM in the preoperative and ‘simulated postoperative’ situation.

Table 3.6: Descriptive statistics of the most relevant (preoperative) parameters for calculation of overall and meridional ocular magnification. SD refers to standard deviation, CCT to central corneal thickness, AQD to aqueous depth, R_{mean} and PR_{mean} to mean corneal front and back surface radius, AST and PAST to corneal front and back surface astigmatism, and SEQ and Cylinder to spherical equivalent and refractive cylinder. Postoperative R_{mean} , AST and CCT were back-calculated to achieve postoperative plano refraction.

	CCT	preop	AQD	in	R_{mean}	/	AST / PAST	SEQ	preop	in	Cylinder
--	-----	-------	-----	----	------------	---	------------	-----	-------	----	----------

	in mm	mm	PR _{mean} in mm	in dpt	dpt	preop in dpt
Mean	0.5586	2.65	7.72 / 6.87	1.20 / 0.28	-0.99	-0.98
SD	0.0362	0.50	0.28 / 0.28	0.96 / 0.15	4.23	0.79
Median	0.5584	2.60	7.72 / 6.86	0.94 / 0.26	-1.62	-0.75
Minimum	0.4248	1.04	6.29 / 5.35	0.00 / 0.00	-20.75	-7.25
Maximum	0.7227	4.99	9.12 / 8.48	8.41 / 1.32	12.50	0.00
2.5% quantile	0.4870	1.72	7.22 / 6.36	0.15 / 0.05	-9.75	-3.0
97.5% quantile	0.6305	3.60	8.34 / 7.44	3.82 / 0.65	5.62	0.0

Table 3.7 presents the change in overall OM as well as meridional OM disparity from the situation before, to the situation after corneorefractive surgery.

Table 3.7: Descriptive statistics of the change in ocular magnification due to corneorefractive surgery intending plano refraction postoperatively. SD refers to standard deviation, change in ocular magnification in the magnification meridian (maximum change) and the magnification axis (minimum change), DMOM to the disparity of meridional magnification. Positive values refer to a gain and negative values to a loss in ocular magnification.

	Minimum change in OM in %	Maximum change in OM in %	Change in overall OM in %	DMOM in %
Mean	0.5683	2.2261	1.3972	1.6430
SD	5.7864	6.1652	5.9308	1.5012
Median	1.1319	3.0321	2.2774	1.2111
Minimum	-18.3908	-16.5965	-17.4936	0.0014
Maximum	30.8895	32.4685	31.3247	13.8338
2.5% quantile	-8.7642	-7.2717	-7.8769	0.0578
97.5% quantile	12.5965	15.2244	13.6861	5.5840

Overall, OM gains due to corneorefractive surgery based on our dataset by -7.88% to 13.69% (95% confidence interval), and distortion in terms of difference between the meridian with the maximum and the minimum change ranges in between 0.06% and 5.58% (95% confidence interval).

Monte-Carlo simulation in our clinical dataset

In this Monte-Carlo simulation we considered N=5017 cases out of N=8998 eyes with a mean ametropia $|SEQ| > 1.5$ dpt or Cylinder < -1.5 dpt. A corneorefractive surgery was not performed in any of those patients. From the dataset we extracted the curvature data of the front and back surface, CCT, AQD, and refraction, which was quoted as 'preoperative refractive error'. By targeting to a plano refraction, we estimated corneal front surface curvature and central corneal thickness in the postoperative situation, by transforming preoperative refraction error from spectacle plane to a change in corneal front surface

curvature, while keeping corneal back surface curvature and AQD constant. Change in overall OM, as well as change in meridional OM was calculated, and a multivariate linear model was defined for prediction of overall and meridional OM change, with the effect sizes preoperative CCT, AQD, R_{mean} , AST, PR_{mean} , PAST, SEQ and Cylinder. The prediction model for the change in overall and meridional ocular magnification Δ read

- $\Delta\text{OM} = -0.028076 - 0.005936 \cdot \text{CCT} + 0.0058624 \cdot \text{AQD} - 0.0033889 \cdot R_{\text{mean}} + 0.0088816 \cdot \text{AST} + 0.0044042 \cdot PR_{\text{mean}} + 0.015244 \cdot \text{PAST} - 1.3997 \cdot \text{SEQ} - 0.0012854 \cdot \text{Cylinder}$ (overall change in OM)
- $\Delta\text{OM} = -0.83477 - 0.30987 \cdot \text{CCT} + 0.37092 \cdot \text{AQD} - 0.087154 \cdot R_{\text{mean}} + 0.60646 \cdot \text{AST} + 0.086664 \cdot PR_{\text{mean}} + 0.29782 \cdot \text{PAST} - 0.02179 \cdot \text{SEQ} - 0.9742 \cdot \text{Cylinder}$ (change in meridional OM)

The root mean squared error of this prediction models (change in overall/meridional OM) are 0.015 / 0.599 and $R^2 = 0.999 / 0.841$. In the prediction model for the change in overall OM, all effect sizes except CCT and Cylinder were statistically significant ($p < 0.05$), and for the prediction model for change in meridional OM beside the intercept, the effect sizes AQD, AST, PAST, SEQ and Cylinder were statistically significant ($p < 0.05$).

Figure 3.5 shows the multivariate model for prediction of change in overall (left) and meridional (right) OM due to corneorefractive surgery targeting for a plano postoperative refraction, including all 8 effect sizes. The performance of predicting the change in overall OM seems to be much better compared to the performance of the predicting the change in meridional OM due to corneorefractive surgery.

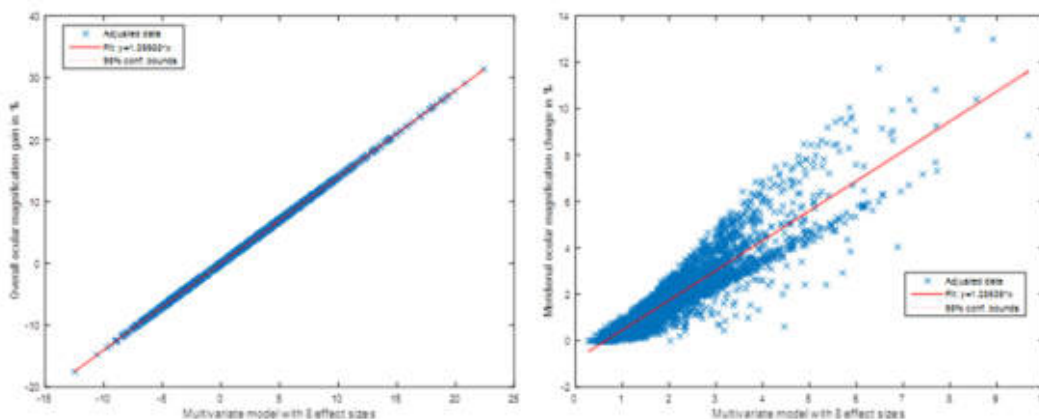
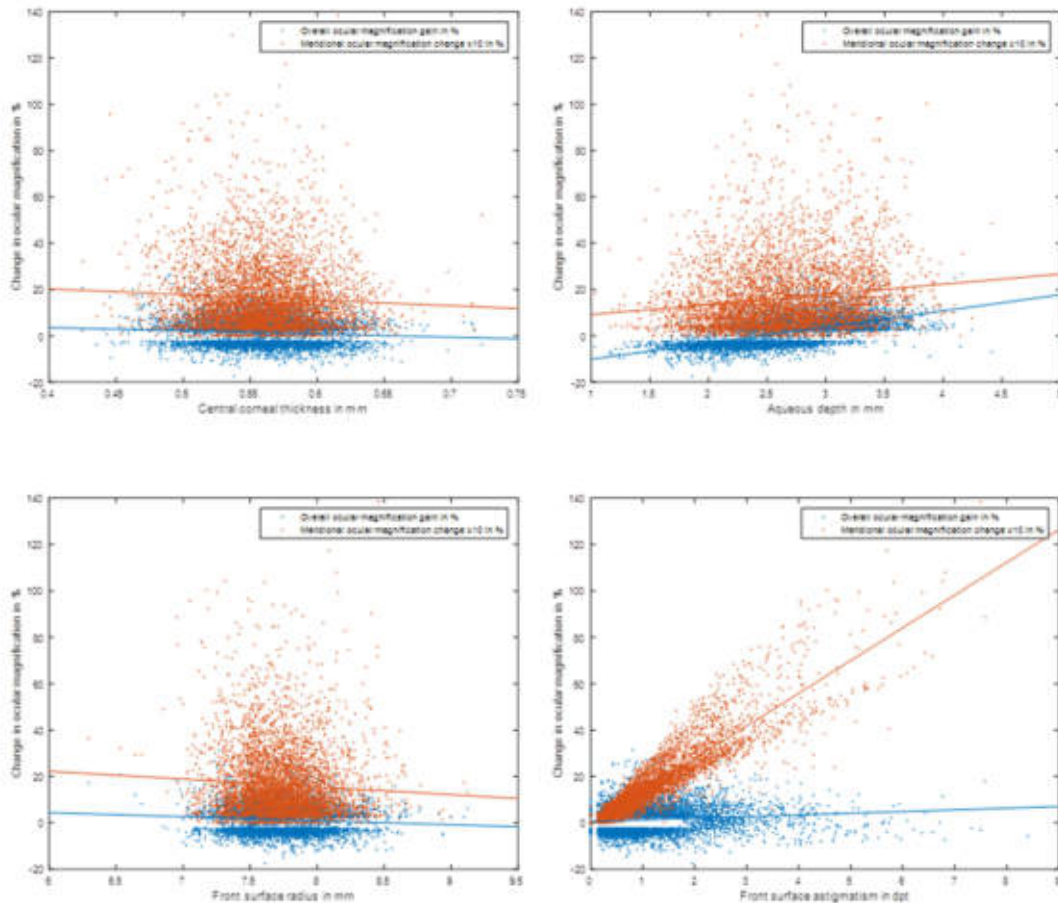


Figure 3.5: Multivariate linear prediction model for the change in overall ocular magnification (left) and in meridional ocular magnification (right) due to corneorefractive surgery. As potential effect sizes were considered: central corneal thickness CCT , aqueous depth AQD , lens thickness LT , mean curvature of the corneal front and back surface R_{mean} , and PR_{mean} , astigmatism of the corneal front and back surface AST and $PAST$, spherical equivalent SEQ and refractive cylinder $Cylinder$.

Figure 3.6 displays the graphs for the 8 potential effect sizes (CCT , AQD , R_{mean} , PR_{mean} , AST , $PAST$, SEQ and $Cylinder$) analysed in a univariate linear models for prediction of change in overall and change in meridional ocular magnification, due to corneorefractive surgery aiming for plano postoperative refraction. CCT seems to be no predictor, AQD and R_{mean} and PR_{mean} are weak predictors, AST , $PAST$, and $Cylinder$ seem to be strong predictors for change in meridional OM, and SEQ seems to be a strong predictor for estimating the change in overall OM.



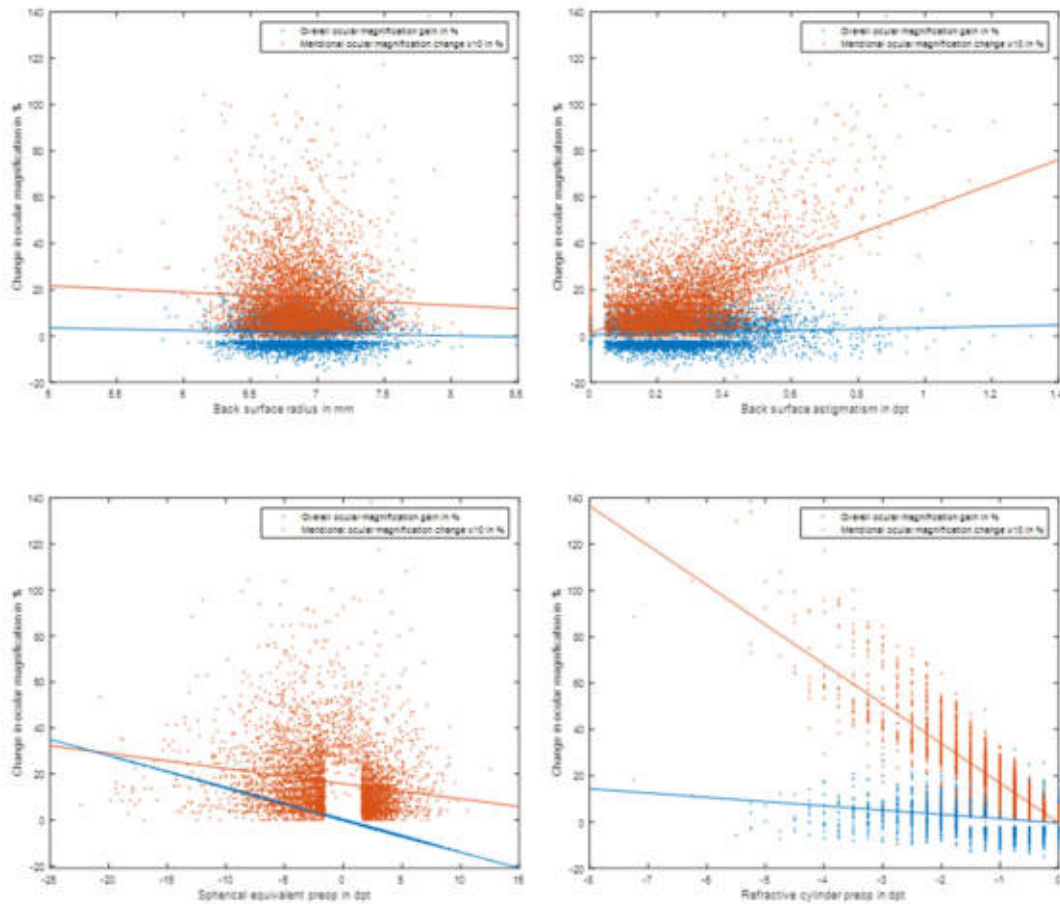


Figure 3.6: Univariate linear models for predicting the change in overall and meridional ocular magnification due to corneorefractive surgery. The change in corneal front surface curvature and thickness was estimated from the intended change in refraction. Please note that for integrating both target parameters into one plot, the change in meridional ocular magnification was multiplied by $\times 10$. Both target parameters were described with univariate linear models for all 8 effect sizes (CCT, AQD, R_{mean} , PR_{mean} , AST, PAST, SEQ, and Cylinder).

3.3. Ocular magnification and visual angle in keratoprotheses

Keratoprotheses are an artificial replacement of the cornea for clinical situations, where the prognosis of a standard keratoplasty procedure is poor. Keratoprotheses such as the Boston I or II are assembled from a central optics cylinder made from polymethylmethacrylate (PMMA) and a haptics part for fixation in the host cornea [9,12,19,45]. As the optics cylinder is intended to have a rotationally symmetric shape, it is defined with a surface curvature for the front (R_f) and back (R_b) surface, as well as a diameter (D) and length (L). The diameter and length characterize the visual (half) field angle (VFA) within the optics cylinder, whereas the refraction is defined by the thickness and the curvature of both refractive surfaces [39]. The optical model that we used consists of a spectacle correction (to mimic target refraction), the optics cylinder, which typically extends the cornea by around half a millimetre, and the focal distance as interspace between the optics cylinder and the retina (aqueous / vitreous).

Clinical case

If we consider for our clinical case $AL=23.5$ mm, a $VD=12$ mm, an optics cylinder of the keratoprosthesis with a diameter 2.8 mm and thickness of 3.5 mm, and a target refraction of $TR=-1.0$ dpt, we could analyse (exemplarily) 3 different scenarios by variation of the front surface curvature R_f :

- $R_f=6.0$ mm: $R_b=4.5$ mm, OM: 18.7077, equivalent power: 53.45 dpt, VFA: 34.8°
- $R_f=7.0$ mm: $R_b=8.9$ mm, OM: 18.0959, equivalent power: 55.26 dpt, VFA: 35.4°
- $R_f=8.0$ mm: $R_b=30.6$ mm, OM: 17.6626, equivalent power: 56.61 dpt, VFA: 35.9°

If we compare OM with the steep (6.0 mm) or the flat (8.0 mm) front surface curvature to the average of 7.0 mm, we read out a gain of 3.38% or a loss of 2.39% in OM. In contrast, if we vary the target refraction TR and keep front surface radius R_f constant at 7.0 mm, we get out:

- $TR=-3$ dpt: $R_b=10.6$ mm, OM: 17.5826, equivalent power: 56.87 dpt, VFA: 36.2°
- $TR=-1$ dpt: $R_b=8.9$ mm, OM: 18.0959, equivalent power: 55.26 dpt, VFA: 35.4°
- $TR=1$ dpt: $R_b=7.7$ mm, OM: 18.6400, equivalent power: 53.64 dpt, VFA: 34.7°

If we compare OM with the more myopic refraction (-3.0 dpt) or the more hyperopic refraction (1.0 dpt) to the average of -1.0 dpt, we read out a loss of 3.01% or a gain of 3.01% in OM.

Monte-Carlo simulation in our clinical dataset

In this Monte-Carlo simulation we consider $N=8998$ cases to resample the distribution of axial length in a clinical population. We varied target refraction TR, front surface radius of the optics cylinder R_f , as well as the diameter D and thickness L of the optics cylinder to analyse the effect sizes for OM and VFA. The back surface of the optics cylinder was adjusted to maintain the optical system balanced and to place the focus at the retina.

With some basics in optics [16] it is clear that from the potential effect sizes TR, AL, R_f , D and L the diameter of the optics cylinder does not affect magnification and AL does not affect the visual field angle, therefore, these components were omitted from the multivariate linear models. OM and VFA are described by:

- $OM = 0.0011146 + 0.00087566 \cdot AL + 0.00026564 \cdot TR - 0.00055671 \cdot R_f + 0.00025279 \cdot L$
- $VFA = 37.065 - 0.37185 \cdot TR + 0.55456 \cdot R_f + 10.676 \cdot D - 10.377 \cdot L$

Root mean squared fit error was 0.000483 / 0.408 and R^2 was 0.929 / 0.988 for prediction of OM and VFA, respectively.

Figure 3.7 shows the performance of the multivariate linear prediction model for ocular magnification (OM, left) and visual field angle (VFA, right), for variations of TR, AL, R_f , D and L.

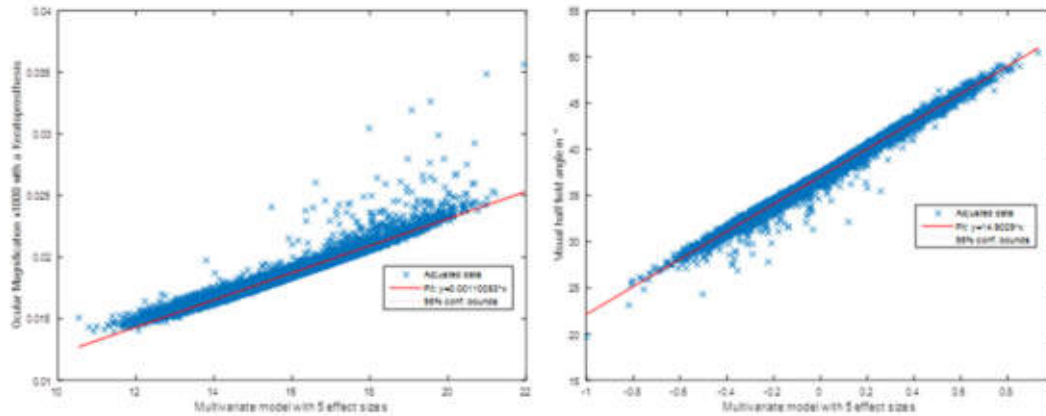


Figure 3.7: Performance of the multivariate prediction model for ocular magnification (OM) and visual (half) field angle (VFA).

Figure 3.8 presents the prediction of OM ($\times 1000$) and VFA as functions of AL, TR, R_f and D/L in univariate linear models. As D does not affect OM, in the lower right graph we condensed the effect of D and L on VFA.

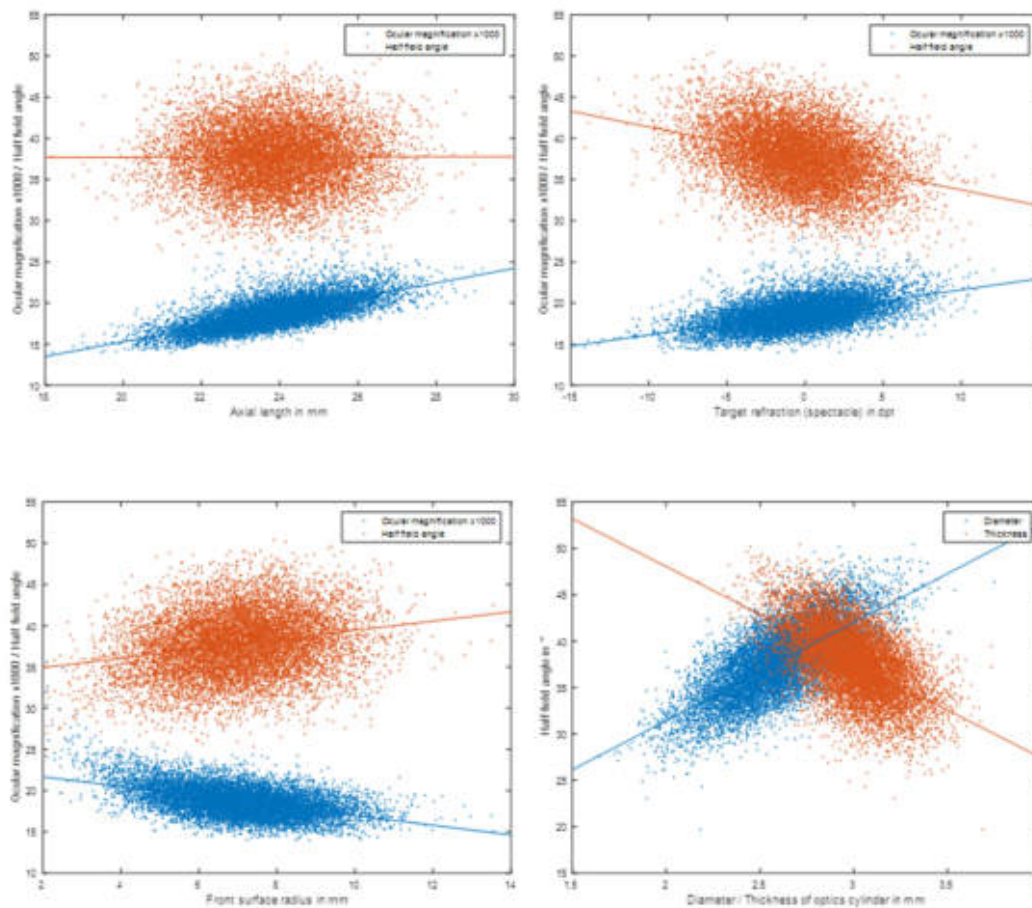


Figure 3.8: *Ocular magnification (OM) and visual (half) field angle (VFA) versus AL, TR, R_f and VFA versus D/L*

From the lower right graph we see that the aspect ratio D/L mostly determines VFA; and OM increases with larger AL, more hyperopic target refraction and steeper R_f.

4. Discussion

4.1. Magnification and problems caused by magnification disparities

In modern ophthalmic surgery, the major goal is to reach the intended refraction and to get out perfect image performance in terms of high visual acuity, high contrast sensitivity, negligible blur and halos [14]. The focus of today's research is mostly on reduction of optical aberration, chromatic errors and elimination of photic phenomena, and in this context classical problems such as magnification disparity, image fusion and stereopsis are mostly ignored [3,10,11,31,51,52]. Ocular magnification is determined by the entire optical system, which includes the spectacle refraction in addition with the shape of the glasses [1,2], contact lenses, corneal shape and thickness, lens shape and thickness [37] and the interspaces between cornea and lens, as well as between lens and retina. The refractive indices of cornea, aqueous and vitreous do not show large variations, but in the crystalline lens we have a complex structure of a gradient index which varies with the optical density of the cataract [18]. For spectacles, we have different options of optical materials from low refracting glasses to high refractive glasses, and for lens implants the material which are typically used by the IOL manufacturers show a range in refractive index between 1.46 (hydrophilic acrylate) to 1.57 (high index hydrophobic acrylic). In most of the textbooks, the disparity of retinal image size mostly refers to the overall magnification difference between both eyes [3,5]. For this classical perspective of aniseikonia, we have lots of clinical data about tolerance and problems of fusion, summation or suppression of images in the brain. As soon as we have at least one astigmatic surface in the optical system, we deal with a cylindrical telescope [33,35,38] and in best case, if all optical elements are centred and aligned, a circular structure at object space is distorted to an ellipse at the retina. That means that all structures show distortions, and meridional difference in ocular magnification refers to the ratio of the large to the short diameter of the ellipse (mostly provided in % of difference) [36,38]. With modern diagnostic techniques based on Scheimpflug imaging, optical coherence tomography (OCT) or confocal microscopy, we get a detailed insight into ocular structures, and lots of measures could be grabbed from those instruments. Today, we are mostly using optical biometers which provide information about the corneal front surface geometry, and all distances in the eye. In addition, some biometers provide the tomographic data of corneal front and back surface and a central OCT image of the para-foveal space. Anterior segment OCT gives some complementary information about the geometry of the chamber angle, the pupil outline, as well as the geometry of the crystalline or artificial lens' front and back surface in dedicated phakometry measurement modules.

Therefore, alongside with the refractive error of the eye, we have all relevant parameters to investigate ocular magnification [3,5,38].

4.2. Handling with magnification disparities

There are several strategies for addressing retinal image size disparity. Before going into detail, clinicians have to measure the tolerance of a patient to retinal image size disparities and image distortions due to variations in meridional magnification [10,11]. For that purpose, we have standard approaches such as eikonometers. But such instruments do not yield reliable data about the tolerance under realistic conditions, as most of the fusion problems typically arise in daily life and may be absent under ideal test conditions. If the tolerance levels are derived, the evaluation of the actual eikonic status should be mandatory, prior to any type of ocular surgery, where refractive surfaces or distance in the eye are systematically changed [5,10,11]. With that baseline of ocular magnification, we could use prediction models to estimate the effect of ocular surgery on the eikonic status of the patient [40].

In most cases of cataract surgery or corneorefractive surgery, both eyes show very similar measures (anisometropia is small), and if both eyes are treated with similar surgeries or implants, aniseikonia is not a major task. But if there is a larger time interval between treating the left and the right eye, the patient may complain about lack of stereopsis or fusion problems in this time interval. But even in case of isometric situations of both eyes, if only one eye is indicated for ocular surgery (e.g. for monovision), the preoperative situation should be analysed alongside with any prediction of the postoperative situation, to get some idea how much change in (overall or meridional) magnification could be expected after surgery [36]. In case of anisometric eyes, such an analysis of the baseline eikonic situation and a prediction of the postoperative situations are even more important to avoid severe eikonic problems after interventions [36].

The most popular surgical intervention which may change the eikonic status of the patient are cataract surgery, corneorefractive procedures such as LASIK, LASEK, PRK, refractive procedures at the lens [38] such as implantation of an artificial lens in a phakic or pseudophakic eye, or keratoplasty [36]. In cases where an implantation of a toric lens is scheduled or a corneorefractive procedure includes a correction of cylindrical refraction errors, the meridional magnification may change in addition to the overall magnification, and should be considered in the calculation concept.

4.3. Options for calculating ocular magnification

In this thesis we restricted to models based on linear Gaussian optics (paraxial optics), which can be applied to thick lens models as well as simplified thin lens models [4-7,20,21,27,28]. There are different strategies to deal with optical systems in linear optics: one option is to trace vergences [46] from the object to the image [18]. Such calculation strategies are step-by-step approaches, which can deal with rotational symmetric optical systems, where all optical elements are centred and aligned, but also with astigmatic systems where we use complementary notations such as the standard and Humphrey notation [20,21]. The standard notation is in general used if we trace through a homogeneous optical medium, and the Humphrey notation is used if we consider (rotational symmetric or spherocylindrical) optical surfaces. We can switch between both notations and vergences are described with both notations equivalently.

Alternatively, we could use matrices for analysing paraxial optical systems [43,49]. The benefit of the matrix notation is that the calculation is performed *en bloc*, instead of a step-by-step approach. Refractive surfaces are defined using refraction matrices, and interspaces with a homogeneous medium are represented by translation matrices [26-29,32]. A system matrix which represents the entire optical system is calculated by multiplying all matrices from the object to the image (in an inverse order) together [27,28]. Ocular magnification can be directly extracted from the system matrix of the entire system if it is fully corrected to image the object sharply to the retina. If we deal with rotationally symmetric optical systems, a simple 2x2 matrix strategy is sufficient [34,42,49], and if at least one refractive surface is astigmatic, an upgrade to 4x4 matrices is sufficient. In that case the system matrix is of dimension 4x4 and decomposes into 4 2x2 submatrices. One of those 2x2 submatrices describes the ocular magnification properties, and with a principal component analysis [4] we could derive the ocular magnification in both principal meridians (the major and the minor axis of the ellipse including orientation, if a circle is imaged to the retina). If the optical system is not fully corrected, we have to calculate the principal ray, which passes through the centre of the aperture stop, and magnification of such an uncorrected system is referenced to that principal ray [36].

In the general case if all refractive surfaces are well-defined with topographic data (corneal front and back surface, lens front and back surface and if available the design data of the spectacle correction) we could use full aperture raytracing instead of paraxial setting [41,47]. With raytracing, we trace a representative bundle of rays starting from the object through all optical surfaces and media to the retina. Instead of simplifications (linearization) of the Snellius

refraction law the sine of the angle between the surface normal and the incident ray characterizes the sine of the exiting ray. The benefit of full aperture raytracing is that we could deal adequately with image distortions, large numerical apertures or rays with a larger height, with respect to the optical axis [47]. However, raytracing strategies require a full set of surface data, which – up to my knowledge – are at the moment only available for the corneal front and back surface, but not for the lens [41]. In general, phakometry is difficult and in this thesis we back-calculated the refractive properties of the crystalline lens from biometric data of the cornea [18,44,46], all distances in the eye, refractive error, and an average refractive index ($n_L=1.41$) and curvature ratio of front and back surface (10 mm / 6 mm), derived from a schematic model eye [17].

Currently there are only few companies which manufacture dedicated individual eikonic implants [26,37] or glasses to reach a target ocular magnification [1]. The major problem is that such lenses are limited in thickness, and as the optical thickness between front and back surface is a critical parameter for the change of magnification, the variation of the shape of both surfaces necessary for achieving a target magnification could be dramatically [37]. But if we plan during surgery to vary e.g. the spectacle correction (target refraction) and the cornea (corneorefractive surgery, e.g. LASIK) or the spectacle correction and the IOL (lens power) to be implanted, we have a wide range of eikonic correction even with small or moderate modifications in the target refraction and the corneal shape or IOL power [33]. In contrast to using individual eikonic designs for the glasses or the IOL, we could deal with standard lenses and glasses, as the combination of both maintains the eikonic correction.

4.4. Application of a calculation strategy to clinical data

In this PhD thesis, we applied our calculation strategy for analysing and predicting overall and meridional magnification to the special condition of standard cataract surgery (with implantation of rotational symmetric IOL), to cataract surgery with implantation of a toric lenses, to situations of corneal surgery, as well as keratoprotheses implanted in the aphakic eye in situations with severe corneal pathologies. For all fields of application we provided clinical examples to give some idea about the change in ocular magnification. The calculation strategy for standard cataract surgery is very simple dealing with 2x2 matrices [32,40,42], and therefore it could be implemented and integrated easily in all IOL calculation concepts (even with an Excel spreadsheet). If the biometric data of both eyes of an individual together with the actual refraction and the target refraction after surgery is entered, we can read out the actual eikonic status as well as the estimated postoperative eikonic status and the situation if only one of both eyes is treated. The calculation concept for astigmatic systems which are treated with a

standard or toric lens implant is much more complex, as we have to deal with 4x4 matrices. As long as the principal meridians of all astigmatic surfaces are properly aligned, magnification can be simplified to a separate calculation, according to standard lenses for both principal meridians [33]. But in general, the principal meridians are not aligned and we consider astigmatic axes at random by using 4x4 matrix calculations [26-29]. As a result, we read out the average ocular magnification as well as the disparity in meridional magnification (comparing the meridional magnification in the magnification meridian and magnification axis) at image plane if a circle at object plane is traced through the optical system. Finally, we get out an ellipse for the left and for the right eye each for the preoperative and the postoperative situation, in total 4 ellipses. If comparing the ellipses of both eyes in the preoperative or in the postoperative situation, we could analyse the preoperative and the estimated postoperative eikonic situation of the patient. By comparing the preoperative and the postoperative situation for the left and the right eye, we calculate the gain or loss in overall or meridional magnification due to surgery. For the application of our concept to corneal surgery, we restricted to analysis of ocular magnification gain or loss and ignored absolute magnification values and a comparison of both eyes [36]. In those situations, the measurement of the posterior eye segment is not required for this analysis, and we are restricted to measurement of the anterior eye segment. In general cases, if we have no data whether the eye is fully corrected or not, we require the measurement of the anterior segment from the object to the aperture stop (pupillary plane) for calculation.

For the application of keratoprotheses, the situation is completely different. Keratoprotheses are implanted into aphakic eyes, and therefore, we have a very simple optical system with a spectacle correction and both surfaces of the optics cylinder of the prosthesis [8,9,12,19,24,39,45,50]. Designing such an optics cylinder we modulate the front and back surface curvature of the cylinder and the aspect ratio defined by the length and diameter. The diameter as an artificial aperture stop solely changes the amount of light entering the eye and the visual field which can be realized, but the length and both radii affect the refraction status, magnification properties as well as the visual field [39].

Beside some clinical cases, we setup a Monte-Carlo simulation, which shows the impact of the effect sizes on ocular magnification. The most crucial issue is the selection of a proper dataset for the Monte-Carlo simulation. This dataset should represent the typical clinical conditions. That mean, that the distributions of all effect sizes as well as the interaction between effect sizes should resample the real life situation. We used a large clinical dataset from a modern optical biometer, where data of the corneal front surface (keratometry and optical coherence

tomography data), from the corneal back surface (only optical coherence tomography data) as well as data on all distances in the eye are available. In this patient cohort, measurements were performed prior to and after cataract surgery, and alongside to the preoperative and postoperative biometry, we have data of subjective refraction (derived with trial glasses in a trial frame). These data are properly reflecting the standard cataract population. For our analysis of toric intraocular lenses, we restricted to those eyes where due to a moderate or high corneal astigmatism, toric lenses have been implanted. For both Monte-Carlo simulations (standard situation and toric lens implantation), we used an appropriate study population. In contrast, for the study where we presented the application of our calculation strategy to the change in overall and meridional magnification [36] due to corneorefractive surgery or to analysis of the situation with keratoprotheses [39], the study population might be inappropriate for a Monte-Carlo simulation. Corneorefractive surgery (e.g. LASIK) is typically performed in a young study population, where the proportions of the eye – especially the crystalline lens – are somehow different and we have a significant refraction error which should be corrected by corneal ablation procedure. Therefore, we decided to extract those patients from the dataset, where the mean refractive error is larger than 1.5 dpt or the refractive cylinder is more than 1.5 dpt. But even though, this is a typical cataract population where due to the growth of the crystalline lens, the anterior chamber is flattened and the lens thickness is increased. Lens thickness was not used for this Monte-Carlo simulation, but as the axial position of the aperture stop is defined at the front surface of the crystalline lens, there might be a small inaccuracy as the principal ray through the centre of the aperture is slightly incorrect. For the Monte-Carlo simulation on ocular magnification in situations of keratoprotheses implantation the age and cataract related changes of aqueous depth and lens thickness does not play a role as keratoprotheses are implanted in aphakic eyes. Therefore, we do not expect any potential inaccuracy of our Monte-Carlo simulation model.

4.5. Our most relevant results

Overall, from our dataset of N=8998 clinical cases, we learn that mean ocular magnification is 0.0162700 ± 0.0005215 with a 95% confidence interval ranging from 0.0153243 to 0.0173993. That means that e.g. the retinal image size of an object with an angular field of 1 arc minute (according to the opening of a Landolt ring for vision test with acuity of 1.0) is on average $4.733 \mu\text{m}$, which is about 2 diameters of a photoreceptor. After cataract surgery, retinal image size is on average gained to $4.862 \mu\text{m}$, which is about 3% more than preoperatively. But for the individual change in magnification we calculated a range (95% confidence interval) from -5.6%

to 14.2%, which could have a strong impact on image fusion, summation or suppression in the brain, if only 1 eye is treated.

In the phakic as well as in the pseudophakic eye axial length, mean corneal front and back surface radius seem to have the most impact on ocular magnification, whereas aqueous depth, lens thickness and spherical equivalent of refraction show a minor impact. Corneal thickness seems to have no systematic impact, which is mostly due to the small variation of some 10 microns. From mathematics, variation in corneal thickness affects ocular magnification, but this small effect is mostly dominated by other effect sizes with larger variations. In the pseudophakic eye, the high performance of our prediction model is mostly due to the axial length as predictor. Spherical equivalent after cataract surgery is typically small as clinicians intend more or less plano refraction during lens power calculation [15,44], and therefore, in the scatterplot in the lower left graph we observe some quantization effect as sphere and cylinder are given in steps of quarter diopters.

If we deal with astigmatism in the eye, we have an overlay of overall and meridional ocular magnification in the phakic as well as in the pseudophakic eye. This astigmatism in the optical system is mostly due to the corneal shape and especially in the corneal front surface with a large index step from air to cornea even small variation in curvature between meridians induces some astigmatism. For that purpose, we extracted those eyes from our dataset where a toric lens was implanted. Decades ago, ophthalmologists were more reluctant with indication for toric lenses [15], but today indication for toric lenses starts already with a corneal astigmatism of 1 diopter [35]. With implantation of multifocal lenses or additional lenses [38], correction of corneal astigmatism could be even indicated with a small corneal cylinder of half a dioptre and manufacturers of IOLs reacted on this trend and include a large toricity range for their IOLs. In our dataset, the portion of toric lenses was relatively high with 12.4%. For this study population, which received a toric lens implant, we analysed the ratio of the long to the short axis of the ellipse at retinal plane, if a circle was imaged at object plane. Preoperatively, we derived an image distortion due to astigmatism of 2.8% on average, with a range from 1.42% to 5.43% (95% confidence interval). If both eyes are anisometric or if the orientation of the magnification meridians is asymmetric, there might arise some problems of image fusion in the brain, and stereopsis or binocular vision might be lost [31]. Postoperatively, image distortion is much less and ranges between 0.06% and 1.16% (95% confidence interval). This reduction in meridional aniseikonia is obvious, because the refractive correction of corneal astigmatism is shifted from spectacle plane to lens plane, which is located much closer to the nodal point and principal point of the eye. That means, if patients with corneal astigmatism indicated for

cataract surgery show some image fusion problems, clinicians should think about a correction with toric lenses instead of standard lenses and a postoperative correction of the residual astigmatism with spectacles. The potential meridional magnification at baseline and the estimated meridional magnification after cataract surgery with implantation of a standard lens or a toric lens implant could be derived using our calculation strategy. From the scatterplots in **Figure 3.4** we learn that all distances in the eye such as axial length, central corneal thickness, aqueous depth and lens thickness as well as mean corneal front and back surface curvature have a negligible effect on meridional ocular magnification. In the phakic eye, corneal front and back surface astigmatism as well as refractive cylinder show a large impact in meridional magnification. Again in the pseudophakic eye, due to the small variation in meridional magnification and residual refractive cylinder with toric lens implantation, the effect sizes corneal front and back surface astigmatism as well as refractive cylinder show much less predictability compared to the preoperative situation.

For analysing the impact of corneal surgery on overall and meridional magnification changes of the eye, we restricted to a Monte-Carlo model focused on ‘simulated’ situations with corneorefractive surgery (e.g. LASIK) and a plano target refraction to keep the simulation model simple [36]. The change in corneal front surface curvature and the reduction in central corneal thickness due to tissue ablation were derived from the preoperative corneal front surface curvature, assuming that corneal back surface curvature keeps unchanged. From the patient cohort we selected those cases with a sufficient mean ametropia or refractive cylinder, where corneorefractive surgery procedure seems to be justified. The change in ocular magnification means, that if a circle at object plane is imaged to the retina both for the preoperative to the postoperative situation, we read out an elliptical image at image plane both for the preoperative and the postoperative situation. In general, both ellipses are defined by the long and short axes as well as the orientation, and what we calculated is the transform from the preoperative to the postoperative ellipse using a principal component analysis [4]. This transform again refers to an elliptical design, where we have a meridian with the lowest change in magnification and an orthogonal meridian, where we have the highest change in ocular magnification. In **Table 3.7** we present descriptive statistics on the meridians with the minimum and maximum change, the difference of both, as well as the average change in ocular magnification. In general, the meridional change ranges in between -8.76% and 15.22% (95% confidence interval), and the distortion due to surgery ranges in between 0.05% and 5.58% (95% confidence interval). On average, we observed a loss in ocular magnification up to 7.88%

(mostly hyperopic interventions) and a gain up to 13.69% (mostly myopic corrections)(95% confidence interval).

For keratoprotheses, we extracted from our data axial length and subjective refraction in terms of spherical equivalent and cylinder. As keratoprotheses are implanted in aphakic eyes [19,45,50], the only optics on the pathway between object and image is the target refraction (in terms of a spectacle correction) and the optics cylinder of the keratoprosthesis. The optics cylinder was designed in a way that the entire optical system including spectacle refraction was corrected to image an object at infinity sharply to the retina. As we have the option to split the required refractive power into front and back surface of the optics cylinder and to spectacle correction after surgery, we could aim for some target magnification. As we directly see from **Figure 3.8**, the more fraction of refractive power is given to the front surface (and the less to the back surface), the higher will be ocular magnification, but this gain of magnification is on cost of field angle. The same situation is observed with the target refraction: the more plus (patient will be hyperopic), the higher is ocular magnification, but on cost of field angle. The optics diameter is independent of ocular magnification, and the larger the diameter (and the shorter the optics cylinder,) the larger the field angle.

Overall, the multivariate linear models shown in this thesis could help to avoid complex calculations of ocular magnification, using matrix algebra or vergence transformation, especially in case of an astigmatic system. They could be used for the phakic eye or in the pseudophakic eye to estimate the eikonic status of the patient at baseline, and they can be utilized for an estimation of the situation after cataract surgery, with implantation of a standard or toric lens, for estimation of change in ocular magnification after corneal (especially corneorefractive) surgery, as well as for designing and customizing the shape of the optics cylinder for keratoprotheses. From our point of view, such an estimate of magnification at baseline and potential change due to surgery seems to be mandatory in the planning phase of cataract surgery and corneal surgery to avoid eikonic [52] problems, postoperatively.

5. Conclusions

In conclusion, we developed a calculation scheme for analysis of overall and meridional magnification of the eye. This calculation scheme is based in linear Gaussian optics and considers rotationally symmetric optical systems as well as astigmatic systems with cylinder axes at random. This algorithm has been applied to situations before and after cataract surgery in standard situations, as well as with implantation of toric intraocular lenses, to situations before and after corneal surgery, as well as to keratoprostheses. From a comparison of the left to the right eye, we read out overall and meridional magnification disparities in terms of aniseikonia for the preoperative and the postoperative situation. By comparing for both eyes, the preoperative with the estimated postoperative situation, we read out data on gain or loss in the overall or meridional magnification. The optics cylinder of keratoprostheses (Bostin I and II type) could be designed with this calculation strategy in order to realize a specific magnification, target refraction, and/or visual field angle. The applicability of this calculation scheme has been shown with clinical examples as well as on a large study population before and after cataract surgery. From this population we studied the potential effect sizes for overall and meridional magnification, of magnification disparities, as well as changes due to surgery, and we established multivariate linear prediction models in terms of a Monte-Carlo simulation. We strongly recommend integrating assessment of eikonic evaluation at baseline and estimation of postoperative eikonic situation into the routine preoperative cataract biometry and intraocular lens power calculation procedure as well as in the planning of corneorefractive surgery.

6. Summary

In modern ophthalmology, the main goal is to reach the target refraction, to optimize visual performance, and to avoid photic phenomena such as halos, glare, or starburst. Ocular magnification disparities with their clinical consequences of deterioration of image fusion, diplopia, binocular vision problems or rapid fatigue are almost overlooked in daily routine,

In this PhD thesis we addressed the impact of cataract surgery, corneal surgery, and implantation of keratoprotheses on ocular magnification properties. Therefore, we developed calculation strategies based on matrix optics (restricted to linear Gaussian optics in the paraxial space) to describe overall and meridional ocular magnification. For stigmatic optical systems we used 2x2 system matrices, and for astigmatic systems we described the optical system with 4x4 system matrices. Calculations are based on biometric and refraction data of the eye. Ocular magnification (disparity) was analysed at baseline and – if postoperative data are available - after surgery. For situations prior to ocular surgery, we developed mathematical methods to predict the change in overall and meridional ocular magnification due to surgery.

The calculation strategies were applied to clinical examples to give some insight, how to interpret the results. In addition, we applied our calculation schemes to a large dataset of clinical data. We could find out that in a cataract population overall, ocular magnification gained due to implantation of a standard replacement lens by $2.67 \pm 5.13\%$ (-5.59 to 14.19% (95% confidence interval)). In a sub-population with implantation of a toric lens we found out that meridional magnification disparity could be decreased from $2.75 \pm 1.03\%$ (95% confidence interval 1.42 to 5.43%) preoperatively to $0.42 \pm 0.29\%$ (95% confidence interval 0.06 to 1.16%) postoperatively. Due to ‘simulated’ corneorefractive surgery in a sub-population of our dataset we noticed a change in overall magnification by $1.40 \pm 5.93\%$ (95% confidence interval -7.88 to 13.68%) and a change in meridional magnification by $1.64 \pm 1.50\%$ (95% confidence interval 0.06 to 5.58%). Applying our algorithms to keratoprosthesis surgery we found out that with front and back surface curvature and aspect ratio of the optics cylinder, we could individually modulate target refraction, magnification and visual field angle.

Assuming an overall tolerance level of 3 to 5% of overall or meridional magnification disparity, a significant portion of cases in our dataset might be affected by fusion problems in the interval between treatment of both eyes, or in case surgery in one eye only. Ocular magnification evaluation at baseline as well as a sophisticated prediction of magnification change should be performed to escape from avoidable problems of stereopsis.

7. References

1. Achiron LR, Witkin N, Primo S, Broocker G. (1997) Contemporary management of aniseikonia. *Surv Ophthalmol* 41:321-330.
2. Achiron LR, Witkin NS, Ervin AM, Broocker G. (1998) The effect of relative spectacle magnification on aniseikonia. *J Am Optom Assoc* 69:591-599.
3. Amselem L, Diaz-Llopis M, Felipe A, Artigas JM, Navea A, García-Delpech S. (2008) Clinical magnification and residual refraction after implantation of a double intraocular lens system in patients with macular degeneration. *J Cataract Refract Surg* 34(9):1571-1577.
4. Arfken G. (1985) Eigenvectors, Eigenvalues. §4.7 in *Mathematical Methods for Physicists*, 3rd ed. Orlando, FL: Academic Press pp. 229-237.
5. Becken W, Alheimer H, Esser G, Müller W, Uttenweiler D. (2008) Optical magnification matrix: near objects in the paraxial case. *Optom Vis Sci* 85(7):581-592.
6. Bennett AG. (1986) Two simple calculation schemes for use in ophthalmic optics. - I: Tracing oblique rays through systems including astigmatic surfaces. *Ophthalmic Physiol Opt* 1986; 6:325-331.
7. Bennett AG. (1986) Two simple calculation schemes for use in ophthalmic optics. - II: Tracing axial pencils through systems including astigmatic surfaces at random axes. *Ophthalmic Physiol Opt* 6:419-429.
8. Chew HF, Ayres BD, Hammersmith KM, Rapuano CJ, Laibson PR, Myers JS, Jin YP, (2009) Cohen EJ. Boston keratoprosthesis outcomes and complications. *Cornea* 28(9):989-996.
9. Ciolino JB, Dohlman CH. (2009) Biologic keratoprosthesis materials. *Int Ophthalmol Clin* 49(1):1-9.
10. Crone RA, Leuridan OMA. (1973a) Tolerance for aniseikonia. I. Diplopia thresholds in the vertical and horizontal meridians of the visual field. *Albrecht v Graefes Archiv für Ophthalmologie*. 31:1-16.
11. Crone RA, Leuridan OMA. (1973b) Tolerance for aniseikonia. II. Determination based on the amplitude of cyclofusion. *Albrecht v Graefes Archiv für Ophthalmologie*. 31:17-22.
12. Doane MG, Dohlman CH, Bearse G. (1996) Fabrication of a keratoprosthesis. *Cornea* 15(2):179-184.

13. Dunne MC, Elawad ME, Barnes DA. (1994) A study of the axis of orientation of residual astigmatism. *Acta Ophthalmol (Copenh)* 72:483-489.
14. Dunne MC, Elawad ME, Barnes DA. (1997) Determination of the influence of effectivity upon residual astigmatism. *Acta Ophthalmol* 75:170-173.
15. Frohn A, Dick HB, Thiel HJ. (1999) Implantation of a toric poly(methyl methacrylate) intraocular lens to correct high astigmatism. *J Cataract Refract Surg* 25:1675-1685.
16. Gerrard A, Burch JM. (1975) *Introduction to matrix methods in optics*. Wiley (London), p. 287.
17. Gullstrand A. (1909) Anhang zu Teil 1. In: von Helmholtz H. *Physiologische Optik*, 3. Ausgabe, Band 1, Voss Hamburg pp. 350-358.
18. Haigis W. (1999) Strahldurchrechnung in Gaußscher Optik. In: Schott, Jacobi, Freyler (eds.): 4. DGII-Kongress, Springer pp. 233-246.
19. Harissi-Dagher M, Slim E. (2019) La kératoprothèse de Boston type 1 [Boston keratoprosthesis type 1]. *J Fr Ophtalmol* 42(3):295-302.
20. Harris WF. (1999) A unified paraxial approach to astigmatic optics. *Optom Vis Sci*. 76:480-499.
21. Harris WF. (2000) Interconverting the matrix and principal-meridional representations of dioptric power and reduced vergence. *Ophthal Physiol Opt* 20:494-500.
22. Harris WF. (2001) Magnification, blur, and ray state at the retina for the general eye with and without a general optical instrument in front of it. 1. Distant objects. *Optom Vis Sci* 78:888-900.
23. Harris WF. (2001) Magnification, blur, and ray state at the retina for the general eye with and without a general optical instrument in front of it. 2. Near objects. *Optom Vis Sci* 78:901-905.
24. Hicks CR, Fitton JH, Chirila TV, Crawford GJ, Constable IJ. (1997) Keratoprotheses: advancing toward a true artificial cornea. *Survey Ophthalmol* 42(2):175-189.
25. Jacobi KW, Nowak MR, Strobel J. (1990) Spezielle Intraokularlinsen [Special intraocular lenses]. *Fortschr Ophthalmol* 87(Suppl):29-32.
26. Keating MP. (1982) A matrix formulation of spectacle magnification. *Ophthalmic Physiol Opt* 2:145-158.
27. Keating PK. (1981) A system matrix for astigmatic optical systems: I. Introduction and dioptric power relations. *Am J Optom Physiol Opt* 58:810-819.
28. Keating PK. (1981) A system matrix for astigmatic optical systems: II. Corrected systems including an astigmatic eye. *Am J Optom Physiol Opt* 58:919-929.

29. Keating PK. (1980) An easier method to obtain the sphere, cylinder and axis from an off-axis dioptric power matrix. *Am J Optom Physiol Optics* 57:734-737.
30. Kramer PW, Lubkin V, Pavlica M, Covin R. (1999) Symptomatic aniseikonia in unilateral and bilateral pseudophakia. A projection space eikonometer study. *Binocul Vis Strabismus Q.* 14(3):183-90. Erratum in: Kramer PW, Lubkin V, Pavlica M, Covin R. (1999) *Binocul Vis Strabismus Q* 14(4):263.
31. Krzizok T, Kaufmann H, Schwerdtfeger G. (1996) Binocular problems caused by aniseikonia and anisophoria after cataract operation. *Klin Monatsbl Augenheilkd* 208:477-480.
32. Langenbacher A, Huber S, Nguyen NX, Seitz B, KÜchle M. (2003) Cardinal points and image-object magnification with an accommodative lens implant (1 CU). *Ophthalmic Physiol Opt* 23(1):61-70
33. Langenbacher A, Reese S, Huber S, Seitz B. (2005) Compensation of aniseikonia with toric intraocular lenses and spherocylindrical spectacles. *Ophthalmic Physiol Opt* 25:35-44.
34. Langenbacher A, Reese S, Jakob C, Seitz B. (2004) Pseudophakic accommodation with translation lenses--dual optic vs mono optic. *Ophthalmic Physiol Opt* 24(5):450-457.
35. Langenbacher A, Reese S, Sauer T, Seitz B. (2004) Matrix-based calculation scheme for toric intraocular lenses. *Ophthalmic Physiol Opt* 24:511-519.
36. Langenbacher A, Seitz B, Szentmáry N. (2007) Modeling of lateral magnification changes due to changes in corneal shape or refraction. *Vision Res* 47(18):2411-2417.
37. Langenbacher A, Seitz B. (2003) Calculation scheme for bitoric eikonic intraocular lenses. *Ophthalmic Physiol Opt* 23:213-220.
38. Langenbacher A, Szentmáry N, Seitz B. (2007) Magnification and accommodation with phakic intraocular lenses. *Ophthalmic Physiol Opt* 27(3):295-302.
39. Langenbacher A, Szentmáry N, Speck A, Seitz B, Eppig T. (2013) Calculation of power and field of view of keratoprostheses. *Ophthalmic Physiol Opt* 33(4):412-419.
40. Langenbacher A, Szentmáry N. (2008) Anisometropie und Aniseikonie—ungelöste Probleme der Kataraktchirurgie [Anisometropia and aniseikonia--unsolved problems of cataract surgery]. *Klin Monbl Augenheilkd* 225(9):763-769.
41. Langenbacher A, Viestenz A, Viestenz A, Brünner H, Seitz B. (2006) Ray tracing through a schematic eye containing second-order (quadric) surfaces using 4 x 4 matrix notation. *Ophthalmic Physiol Opt* 26:180-188.

42. Langenbucher A, Huber S, Nguyen NX, Seitz B, Kuchle M (2003) Cardinal points and object-image magnification with an accommodative lens implant (1 CU). *Ophthalmol Physiol Opt* 23:61-70.
43. Long WF. (1979) Matrix optics of catadioptric systems. *Am J Optom Physiol Opt* 55:760-764.
44. MacKenzie GE, Harris WF. (2003) The thick intraocular lens required for a given target refraction. *S Afr Optom* 62:66-71.
45. Magalhaes FP, de Sousa LB, de Oliveira LA. (2012) Boston type I keratoprosthesis. Review. *Arq Bras Oftalmol* 75(3):218-222
46. Naeser K. (1997) Intraocular lens power formula based on vergence calculation and lens design. *J Cataract Refract Surg* 23:1200-1207.
47. Preussner PR, Wahl J, Lahdo H. (2002) Raytracing for intraocular lens calculation. *J Cataract Refract Surg* 28:1412-1419.
48. Robbie SJ, Tabernero J, Artal P, Qureshi MA. (2018) Initial Clinical Results With a Novel Monofocal-Type Intraocular Lens for Extended Macular Vision in Patients With Macular Degeneration. *J Refract Surg* 34(11):718-725.
49. Rosenblum WM, Christensen JL. (1974) Optical matrix method: Optometric applications. *Am J Optom Physiol Optics* 51:961-868.
50. Saeed HN, Shanbhag S, Chodosh J. (2017) The Boston keratoprosthesis. *Curr Opin Ophthalmol* 28(4):390-396.
51. Scarpatetti A. (1983) Binocular vision after lens implantation. *Acta Ophthalmol Scand* 61:844-850.
52. Wang GJ, Pomerantzeff O. (1983) Iseikonia and accommodation in the fellow eye in monocular IOL implantation. *J Am Intraocul Implant Soc* 9(4):441-444.
53. Watkins RD. (1970) The optical systems of the eye. *Austr J Optom* 53(10):289-299.

8. Bibliography of the candidate's thesis related publications

Original articles

Langenbacher A, Szentmáry N, Speck A, Seitz B, Eppig T. (2013) Calculation of power and field of view of keratoprostheses. *Ophthalmic Physiol Opt* 33(4):412-419. **IF: 2.664**

Langenbacher A, Szentmáry N. (2008) Anisometropie und Aniseikonie—ungelöste Probleme der Kataraktchirurgie [Anisometropia and aniseikonia--unsolved problems of cataract surgery]. *Klin Monbl Augenheilkd* 225(9):763-769. **IF: 0.470**

Langenbacher A, Seitz B, Szentmáry N. (2007) Modeling of lateral magnification changes due to changes in corneal shape or refraction. *Vision Res* 47(18):2411-2417. **IF: 2.055**

Langenbacher A, Szentmáry N, Seitz B. (2007) Magnification and accommodation with phakic intraocular lenses. *Ophthalmic Physiol Opt* 27(3):295-302. **IF: 1.097**

Langenbacher A, Reese S, Huber S, Seitz B. (2005) Compensation of aniseikonia with toric intraocular lenses and spherocylindrical spectacles. *Ophthalmic Physiol Opt* 25(1):35-44. **IF: 1.074**

Langenbacher A, Seitz B. (2003) Computerized calculation scheme for bitoric eikonic intraocular lenses. *Ophthalmic Physiol Opt* 23(3):213-220. **IF: 1.016**

Langenbacher A, Huber S, Nguyen NX, Seitz B, Küchle M. (2003) Cardinal points and image-object magnification with an accommodative lens implant (1 CU). *Ophthalmic Physiol Opt* 23(1):61-70. **IF: 1.016**

Langenbacher A, Reese S, Jakob C, Seitz B. (2004) Pseudophakic accommodation with translation lenses--dual optic vs mono optic. *Ophthalmic Physiol Opt* 24(5):450-457. **IF: 0.925**

9. Acknowledgements

Foremost, I would like to thank my supervisor, Prof. Dr. Nóra Szentmáry for the continuous support and assistance during my doctoral study and research, for her patience, motivation, and enthusiasm.

Besides I would like to thank Prof. Dr. Zoltán Zsolt Nagy for his support and many fruitful discussions.

My sincere thanks also go to Priv.-Doz. Dr. Timo Eppig, for his support and friendship during the last 15 years at the Institute of Medical Physics in Erlangen and the Institute of Experimental Ophthalmology in Homburg/Saar.

I thank all my co-authors for their patience and plenty of hours of scientific discussions.

I would also like to thank for the support of all colleagues at the Department of Medical Physics, University of Erlangen-Nuremberg and at the Department of Experimental Ophthalmology, Saarland University, Germany.

Special thanks for the stimulating discussions with my “PhD-colleagues”, Dr. Milán Tamás Pluzsik and Dr. Orsolya Németh.

Finally, I would like to thank my family and my beloved son Marcell for his patience during this difficult, exciting and challenging period.



TECHNICAL NOTE

Calculation of power and field of view of keratoprosthesesAchim Langenbucher^{1,2}, Nóra Szentmáry³, Alexis Speck¹, Berthold Seitz³ and Timo Eppig¹¹Experimental Ophthalmology, Saarland University, Homburg/Saar, Germany, ²Erlangen Graduate School in Advanced Optical Technologies (SAOT), Erlangen, Germany, and ³Department of Ophthalmology and University Eye Clinic, Saarland University Medical Center, Homburg/Saar, Germany**Citation information:** Langenbucher A, Szentmáry N, Speck A, Seitz B & Eppig T. Calculation of power and field of view of keratoprostheses. *Ophthalmic Physiol Opt* 2013; **33**, 412–419. doi: 10.1111/oppo.12046**Keywords:** artificial cornea, field angle, keratoprosthesis, magnification, modelling, refractive power, vignettingCorrespondence: Achim Langenbucher
E-mail address: achim.langenbucher@uks.eu

Received: 26 November 2012; Accepted: 8 February 2013

Abstract**Purpose:** To demonstrate a mathematical algorithm for calculating the refractive power of keratoprostheses and to estimate vignetting effects.**Methods:** A paraxial calculation scheme based on vergence transformation is developed for determination of the front surface radius or front surface refractive power of a Boston type I or II keratoprosthesis based on the design data of the manufacturer. A concept for derivation of lateral magnification (ratio of image size to slope of the incident ray) is presented based on 2×2 matrix representation of the eye. For estimation of vignetting effects, numerical ray tracing was used and the maximum half field angle and half luminance half field angle was extracted.**Results:** Simulation calculations were performed in MATLAB. The front surface radius or refractive power is given in explicit form as a function of axial length, target refraction, as well as the principal design data of the keratoprosthesis such as posterior refractive power, length, or refractive index. With variation of the back surface radius it was shown that lateral magnification can be modulated e.g. to match the magnification of the fellow eye. The Boston type I does not restrict the field angle substantially, whereas type II shows significant vignetting effects.**Conclusion:** We present a strategy on the calculation of keratoprostheses and variation of the design (e.g. back surface curvature) to help to avoid aniseikonia in case of binocular vision (e.g. one phakic eye and one with keratoprosthesis).**Introduction**

The majority of patients suffering from visual impairment due to an opaque cornea can be successfully treated by corneal transplantation. For more than 100 years penetrating keratoplasty has been established in clinical routine for the treatment of keratoconus, endothelial decompensation, corneal scars, corneal dystrophies or others.¹ Anterior lamellar techniques have been used in situations of chemical burn, superficial scars or corneal dystrophies affecting the anterior part of the cornea. In general the optical outcome of anterior lamellar techniques is limited. During the past two decades, posterior lamellar keratoplast techniques such as DSAEK or DMEK have been proposed. Since then the portion of non-penetrating keratoplasty is rising due to

promising optical results, fast rehabilitation and the lower risk of infections.

Nevertheless, in situations of poor prognosis of keratoplasty due to chronic inflammations, one or more unsuccessful keratoplasties, limbal stem cell insufficiencies or severe chemical burn, where the success rate of keratoplasty is low, keratoprostheses may be the last chance to restore functional vision. Various forms of devices have been described for many years with varying degree of success.² Most of these devices are designed with a central optic part made of PMMA (polymethylmethacrylate) and include biological haptic combinations using tibia bone or teeth (osteo-odonto keratoplasty).^{3,4} The most used keratoprostheses today are the Boston types I and II: the Boston type I keratoprosthesis consists of a twin plate collar button-style

design that is used in eyes that have sufficient tear fluid production to maintain wetting of the anterior surface of the eye. Type II is of a similar design, with an additional anterior cylinder that protrudes through the permanently closed eyelid, which is preferred in severe forms of dry eye syndrome.⁸ Figure 1 shows the schematic layout of the two Boston type keratoprotheses.

In contrast to keratoplasty surgery using tissue to rehabilitate the cornea, where the eye is often left phakic to facilitate remaining accommodation, implantation of an artificial keratoprosthesis should usually be performed in the aphakic eye to avoid further surgery like cataract extraction.⁶⁻⁸ Up to now, the design of the keratoprosthesis optics is mostly limited to a cylinder with a curved anterior and a plane posterior surface. The curvature of the anterior surface could be adapted to the biometric properties of the patient, but today most surgeons use standard designs.

The purpose of our study is (1) to show a simple strategy how to determine an appropriate optic design for keratoprotheses such as the Boston I and II by modulating the anterior and posterior surface geometry for any target refraction, (2) to demonstrate the effect of vignetting for different optic designs, and (3) to present how lateral magnification of a (spectacle corrected) eye with keratoprosthesis could be calculated e.g. for estimation of aniseikonia effects.

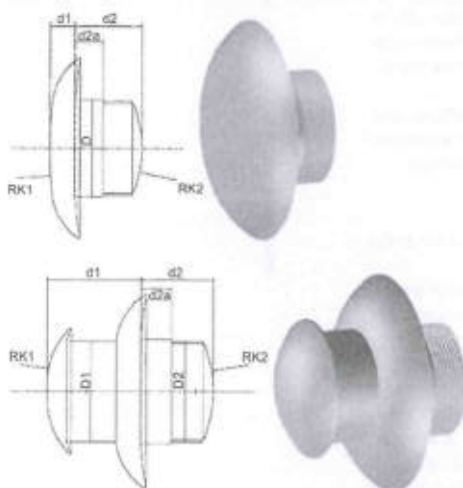


Figure 1. Technical drawing (left) and 3D rendered model (right) of the Boston type I (upper) and type II (lower) keratoprotheses. The parameters in the technical drawing refer to the parameters in the calculation section of the manuscript.

Methods

Optical model and calculation of surface radii of curvature
 For a simple calculation, we employ linear optics (Gaussian optics) in a paraxial space.⁹ The methods themselves are not new, they have been published in the context of intraocular lens calculation or spectacle correction. Also back surface modification has been shown for correction of aniseikonia and anisometropia. In the present paper we describe the adaptation to calculation of keratoprotheses. The vergence of a ray bundle V_1 starting at $z = -\infty$ at the front apex plane of a keratoprosthesis is given by the vergence transformation equation¹⁰

$$V_1 = \frac{P_5}{1 - \frac{(VD-d_1)}{n_v} P_5} \stackrel{n_v \neq 0}{=} \frac{1}{\frac{1}{P_5} - (VD - d_1)} \quad (1)$$

where P_5 denotes the target refraction (postoperatively intended refraction), VD the vertex distance (distance between the front apex of the keratoprosthesis and the spectacle correction) and d_1 the portion of the keratoprosthesis which extends the cornea anteriorly and $n_{air} = 1$ ($VD - d_1 > 0$). P_5 and VD are given in case of a slightly ametropic target refraction to enhance reading ability as it is usually done in cataract surgery.

The vergence V_1' behind the front apex plane of a keratoprosthesis is given by

$$V_1' = \frac{1}{\frac{1}{n_v} - PK_2 + \frac{d_1 + d_2}{n_c}} \quad (2)$$

where AL is the axial length of the aphakic eye, d_2 the portion of the keratoprosthesis behind the anterior corneal plane, PK_2 the refractive power of the posterior surface of the keratoprosthesis, and n_v / n_c the refractive indices of vitreous / the keratoprosthesis optics.

The vergence deficit $V_1' - V_1$ has to be obtained by the refraction of the anterior surface of the keratoprosthesis PK_1 :

$$PK_1 = \frac{1}{\frac{1}{n_v} - PK_2 + \frac{d_1 + d_2}{n_c}} - \frac{1}{\frac{1}{P_5} - (VD - d_1)} \quad (3)$$

or expressed in radius of curvature

$$RK_1 = \frac{n_c - 1}{\frac{1}{\frac{1}{n_v} - PK_2 + \frac{d_1 + d_2}{n_c}} - \frac{1}{\frac{1}{P_5} - (VD - d_1)}} \quad (4)$$

where RK_1 and RK_2 refer to the radius of curvature of the anterior and posterior surface of the keratoprosthesis, respectively.

Printed by Universitätsbibliothek Der Universität Des Saarlandes · 134.096.155.211 · AboVolltext 11110topo 120494 at 11/01/2020 11

Lateral magnification and optical field angle

The entire optical system from spectacle plane to focal plane can be represented with a 2 × 2 system matrix *S* consisting of a product of translation and refraction matrices¹¹:

$$S = \begin{bmatrix} 1 & 0 \\ \frac{AL-d_1}{n_v} & 1 \end{bmatrix} \cdot \begin{bmatrix} 1 & -PK_1 \\ 0 & 1 \end{bmatrix} \cdot \begin{bmatrix} 1 & 0 \\ \frac{d_1+d_2}{n_k} & 1 \end{bmatrix} \cdot \begin{bmatrix} 1 & -PK_2 \\ 0 & 1 \end{bmatrix} \cdot \begin{bmatrix} 1 & 0 \\ \frac{VD-d_1}{n_v} & 1 \end{bmatrix} \cdot \begin{bmatrix} 1 & -P_2 \\ 0 & 1 \end{bmatrix} \tag{5}$$

The lower left element of the system matrix describes the lateral magnification *M* as a proportion of the image size at focal plane to the slope of the incident ray.¹⁰ After multiplying all the matrices in equation 5 together, *M* reads:

$$M = \frac{AL - d_2}{n_v} + \frac{d_1 + d_2}{n_k} - PK_2 \frac{AL - d_2 d_1 + d_2}{n_v n_k} + (VD - d_1) \left[PK_1 \left(PK_2 \frac{AL - d_2 d_1 + d_2}{n_v n_k} - \frac{AL - d_2 - d_1 + d_2}{n_v} \right) + \left(1 - PK_2 \frac{AL - d_2}{n_v} \right) \right] \tag{6}$$

The equations to calculate the magnification of a phakic or pseudophakic fellow eye for estimating aniseikonia are given in the Appendix S1.

For estimation of vignetting effects, paraxial ray tracing is only an estimate as vignetting usually is accompanied with large angles of incidence. For demonstration of the principal effect of the optical field angle and vignetting of the incident ray, the graphical interface of a professional optical design software (OSLO Premium 6.6, www.lamdares.com) was used. Numerical calculation was performed in MATLAB (Release 7.11.1, www.mathworks.co.uk/products/matlab/). For both types of Boston keratoprostheses (types I and II), the power or radius of the front surface was determined using a vergence transformation as a function of axial length for five different target refractions (-4.0, -2.0, plano, 2.0, and 4.0 D) at spectacle plane and for a plano and 20.0 D back surface of the keratoprostheses. Both types of keratoprostheses were modelled with the data provided in Table 1. Figure 2 shows the vignetting effect in principle for the Boston I and Boston II keratoprostheses for three different angles of the incident rays: for a ray angle of 0° (rays plotted in green) all rays passing through the front part of the cylinder are also passing through the thread, for the ray angle plotted in blue approximately half of the rays passing through the front part of the cylinder are not passing through the thread indicating half luminance condition at the retina, and for the ray plotted in red only the extreme ray is passing through the thread indicating total vignetting or the maximum half field angle.¹²

Results

Figure 3 shows the radius of curvature of the front surface of the Boston type I (Figure 3 a,b) and Boston type II (Figure 3 c,d) keratoprostheses as a function of axial length for five different target refractions. The upper graph shows the data for a plano (0 D) back surface of the keratoprostheses, which has been established as a standard, and the lower graph shows the situation for a 20.0 D back surface.

Figure 4 provides the lateral magnification of the spectacle corrected eye after implantation of a Boston type I (Figure 4 a,b) and Boston type II (Figure 4 c,d) keratoprostheses as a function of axial length for five different target refractions. The upper graph shows the data for a plano (0 D) back surface of the keratoprostheses, and the lower graph shows the situation for a 20.0 D back surface. In each

subplot the lateral magnification phakic model eye (based on Gullstrand's schematic eye with variation of the axial length¹³) with spectacle correction for emmetropia is added as reference. This graph implies that lateral magnification can be matched within limits to the respective magnification of the fellow eye by modulating the back surface of the keratoprostheses.

Figure 5a displays the maximum field angle of the eye after implantation of a Boston type I and Boston type II keratoprostheses calculated for emmetropia as a function of axial length for a plano and 20.0 D back surface. This graph

Table 1. Specification of the optical model for representation of the Boston type I and II keratoprostheses

Distances in mm	Axial length	20.5–26.5 (0.01 steps)
	d1/d2/d2a Boston I	0.7 / 2.0 / 1.0
	d1/d2/d2a Boston II	2.7 / 2.0 / 1.0
	Vertex distance	12.0
Diameters in mm	Front optics	7.0
	Cylindrical part	3.3
	Thread inner diameter	2.8
Refractive power in D	Anterior surface of keratoprostheses	Customised
	Posterior surface of keratoprostheses	0.0 / 20.0
	Target refraction at spectacle plane	-4.0 / -2.0 / 0.0 / 2.0 / 4.0
Refractive indices (λ = 555 nm)	Vitreous / aqueous humour	1.336
	Keratoprostheses optics (PMMA)	1.4913

Funded by Universitätsklinikum Der Universität Des Saarlandes - 1341/096_153/2111 - 0404/2010_1111/14/05_1204/4 at 15/11/2020/9

DOI:10.14753/SE.2021.2503

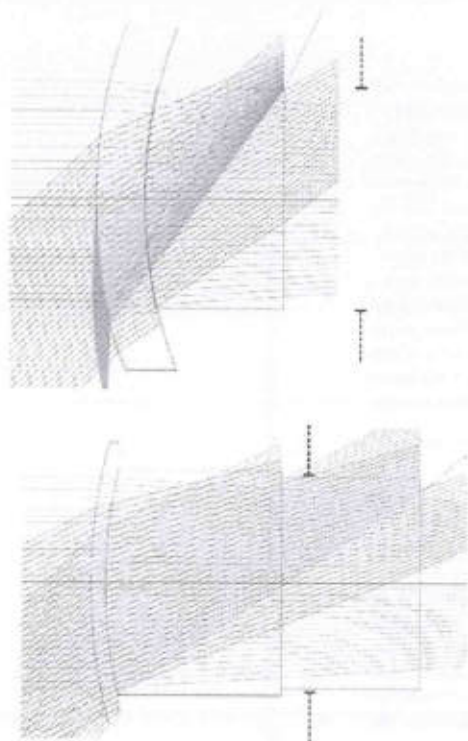


Figure 2. Schematic drawing of the effect of vignetting for the Boston type I (upper) and type II (lower) keratoprostheses. The green ray bundle refers to the on-axis condition, the blue bundle to the half luminance half field angle, and the red ray to the maximum half field angle. The approximate position of the iris is drawn with dashed lines.

proofs that the Boston type I keratoprosthesis yields a full field of view, whereas the field of view is significantly restricted by the Boston type II. In combination with the Boston I and a back surface power of 20.0 D, the maximum field angle is larger than 90° for all axial length and not plotted in the graph. Figure 5b shows the field angle with half luminance for the eye after implantation of a Boston type I and Boston type II keratoprosthesis calculated for emmetropia as a function of axial length for a plano and 20.0 D back surface. Again, the Boston II restricts the field of view significantly and causes severe vignetting of the viewing field.

Discussion

In the last few decades, keratoprostheses have become more and more popular in non-standard situations of patients

requiring penetrating keratoplasty, with a high risk for graft rejection. Such conditions have a history of one or more unsuccessful keratoplasties, stem cell deficiency, or immunologic problems.^{14–17} More than 6000 implantations of Boston keratoprostheses were reported by the Massachusetts Eye and Ear Infirmary between 2002 and autumn 2011.¹⁸ Usually, implantation of a keratoprosthesis is taken as ultimate ratio for monocular patients with bad prognosis. However, implantation could also be performed to restore basic binocular vision. Pineles *et al.* reported promising binocular results in patients with unilateral implantation of Boston type I keratoprostheses.¹⁹ In the hypothetical case that the keratoprosthesis is used to restore binocular vision (e.g. remaining healthy phakic eye and one with severe injury), the magnification difference (aniseikonia) of both eyes must be taken into account. There are some types of keratoprostheses available on the market, and the Boston type keratoprostheses are the most common ones according to many years' reported clinical experience.^{20–22} To our knowledge, no formulae have been published in the literature on the calculation of keratoprostheses, unlike that which has been available for intraocular lenses. In accordance to intraocular lens calculation formulae, which have been proven to yield clinically sufficient results with paraxial simplifications, we intended to provide a simple mathematical formula for calculation of the front surface curvature or front surface power based on the parameters known for IOL calculation. These are axial length, the general design data including the refractive index of the optics material, the back surface design, portion of the keratoprosthesis in front of corneal plane, as well as target refraction and back vertex distance of the spectacle correction. This formula is rather simple, as for the Boston keratoprosthesis of type I and II the crystalline lens usually has to be removed. Several studies, however, showed that it is possible to implant a keratoprosthesis in a phakic eye. Due to the massive medical substitution, the occurrence of cataract is very likely, therefore most surgeons suggest a lens extraction for implantation of a keratoprosthesis.^{6–8}

The second task was to show how lateral magnification of an aphakic eye with a Boston like keratoprosthesis can be derived using Gaussian optics. If representing the optical system with a 2×2 system matrix from the spectacle correction to the focal plane (retinal plane), lateral magnification can be calculated from the system matrix. In our metric this is expressed by the lower left element. Typically, lateral magnification of the eye is provided as a ratio of the image ray angle times refractive index to the incident ray angle. If lateral magnification is required for near distance objects, it is expressed as the ratio of image size to object size.

Optical elements with a high aspect ratio (ratio of axial size to diameter) are known to cause vignetting of the field.

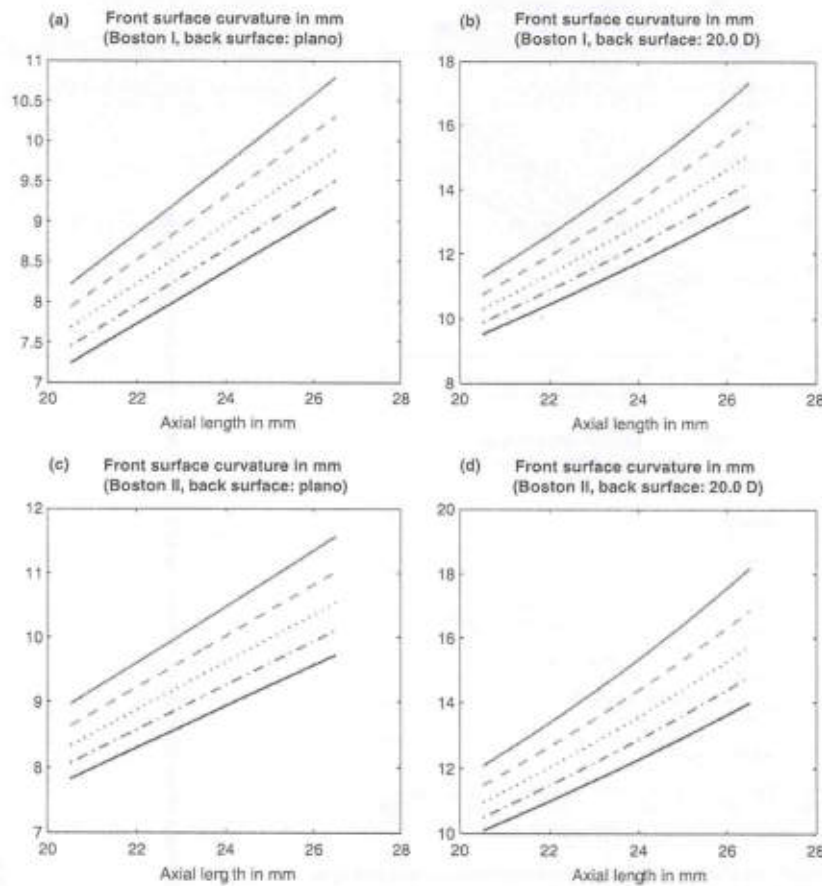
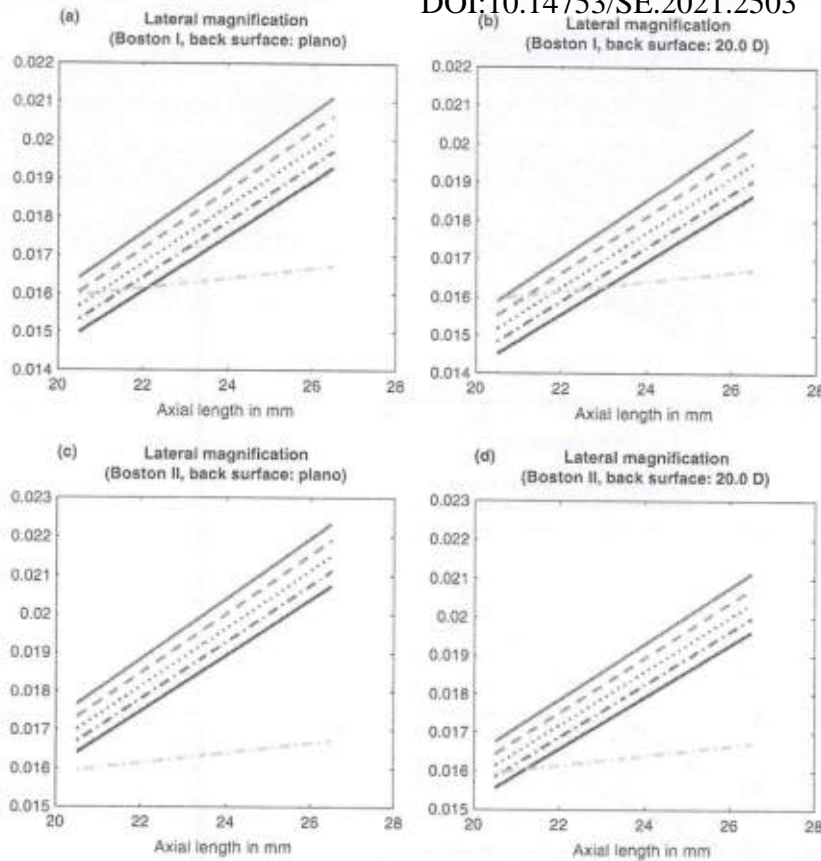


Figure 3. Front surface radius of the Boston keratoprosthesis for a plano back surface (left) and a 20.0 D back surface power (right). The radii are plotted as a function of axial length for five target refractions. -4.0 D = blue/solid, -2.0 D = green/dash-dot, plano = red/dotted, 2.0 D = cyan/dashed, 4.0 D = purple/solid (a, b): Boston type I keratoprosthesis, (c, d): Boston type II keratoprosthesis.

That means that the luminance is decaying from the centre to the periphery, impairing the patient with inhomogeneous brightness over the field of view and a deteriorated recognition of objects in the periphery. As the effect of field of view is typically associated with larger angles, simplifications of paraxial optics are only an approximation and rays have to be traced through the eye using the Snellius law and including side effects such as Fresnel reflection. In addition to analysing the eye model graphically in a professional ray tracing software (OSLO) we implemented such a ray tracing algorithm in MATLAB to estimate the effect of vignetting of the field of view. We calculated the maximum

angle of the field of view, which refers to the situation where only a marginal ray is passing through the optical system, as well as the half luminance field angle, where 50% of the rays are passing through the optical system, which is known to be the limit for comfortable vision. For the Boston type I keratoprosthesis, the vignetting effects are uncritical and the maximum half field angle for a back surface of 20.0 D and the plano back surface of the keratoprosthesis exceed 85°. For the Boston II vignetting of the field of view is an issue, and the maximum half field angle was determined to be between 45° and 55° depending on the curvature of the front surface of the keratoprosthesis, which is



Printed by Universitätsbibliothek Der Universität Des Saarlandes - 134/994, 135/211 - Abaq/2021, 11/10/2021 at 11:51:11 (2021)

Figure 4. Lateral magnification (ratio of image size to slope of the incident ray) of the eye with a Boston keratoprosthesis for a plano back surface (upper) and a 20.0 D back surface power (lower). Lateral magnifications are plotted as a function of axial length for five target refractions: -4.0 D = blue/solid, -2.0 D = green/dash-dot, plano = red/dotted, 2.0 D = cyan/dashed, 4.0 D = purple/solid. For reference, the lateral magnification of a spectacle corrected 3 surface Gullstrand-Emsley schematic model eye is displayed (dash/dotted line) with variations of axial length keeping all other parameters constant (a, b): Boston type I keratoprosthesis, (c, d): Boston type II keratoprosthesis.

determined by the axial length of the eye, and the curvature of the back surface. The half field angle for the half luminance condition with the Boston type II ranges in between 20° and 25°, which narrows the field of view visibly for the patient.

Our results show, that the power and radius of curvature can be explicitly calculated with a formula from the biometric data of the eye, the design data of the keratoprosthesis, and the target refraction. Up to now, the design of both types of Boston keratoprostheses have a plane back surface, which does not allow for matching the lateral magnification

of the eye to the fellow eye and therefore could cause aniseikonia. We showed in our results that by changing the back surface of the keratoprosthesis e.g. to a 20.0 D convex design, the lateral magnification could be reduced significantly (Figures 4a and b, lower half) to a value, which is similar to the lateral magnification of the fellow eye to avoid diplopia or headaches as a consequence of aniseikonia. If we restrict to a predefined design of the keratoprosthesis including back surface power (e.g. plano), no explicit calculation of the front surface radius is required and the curvature could be directly extracted from the plots shown

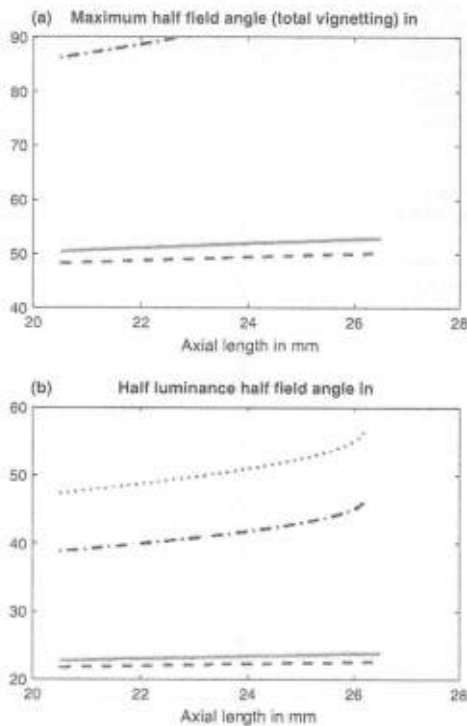


Figure 5. (a) Maximum field angle (indicating total vignetting, upper graph) and (b) half luminance field angle (50% of rays entering the keratoprosthesis are passing through the exit pupil, lower graph) for Boston type keratoprotheses I and II for plano refraction as a function of axial length. Boston type I with plano back surface = blue/dash-dot, Boston type I with 20.0 D back surface=green/dotted, Boston type II with plano back surface = red/dashed, Boston type II with 20.0 D back surface = cyan/solid. The maximum half angle for the Boston I with 20.0 D back surface is not displayed because the values exceed 90°.

in Figures 3a and b. If the general design is changed, the calculation formula given in equations three or four could be used.

The provided metric allows the ophthalmologist to calculate the optical parameters for different kinds of keratoprotheses. These could be used for Boston type keratoprotheses and others which may be manufactured by third party manufacturers. Similar to the procedure with toric intraocular lenses the ophthalmologist can cross check the optical parameters suggested by the prosthesis manufacturer or optimise its design to adjust magnification to the fellow eye. This may help to improve the outcome of visual rehabilitation with keratoprotheses.

In conclusion, to our knowledge, there is no study published about calculation of the refractive power of keratoprotheses. This study provides a simple calculation methodology for determining the front surface curvature of Boston type keratoprotheses and shows formulae to estimate lateral magnification. Estimation of the maximum field angle or half luminance field angle is more complex and requires numerical ray tracing, therefore we restricted it to a graphical presentation of the data. The calculation scheme will be implemented into a web application which will be available soon free of charge for scientific purposes.

Conflict of interest

The authors report no conflicts of interest and have no proprietary interest in any of the materials mentioned in this article.

References

- Seitz B, Langenbacher A & Naumann GOH. The penetrating keratoplasty. A 100-year success story. *Ophthalmologie* 2005; 102: 1128–1136.
- Dohlman CH & Harissi-Dagher M. The Boston keratoprosthesis: a new threadless design. *Digit J Ophthalmol* 2007; 13: <http://www.djo.harvard.edu/site.php?url=/physicians/oa/1055>, accessed on 23/11/12.
- Ciolino JB & Dohlman CH. Biologic keratoprosthesis materials. *Int Ophthalmol Clin* 2009; 49: 1–9.
- Hille K, Hille A & Ruprecht KW. Medium term results in keratoprotheses with biocompatible and biological haptic. *Graefes Arch Clin Exp Ophthalmol* 2006; 244: 696–704.
- Doane MG, Dohlman CH & Bearse G. Fabrication of a keratoprosthesis. *Cornea* 1996; 15: 179–184.
- Liu C, Hille K, Tan D, Hicks C & Herold J. Keratoprosthesis surgery. *Dev Ophthalmol* 2008; 41: 171–186.
- Harissi-Dagher M & Colby KA. Cataract extraction after implantation of a type I Boston keratoprosthesis. *Cornea* 2008; 27: 220–222.
- Utine CA, Tzu J, Dunlap K & Akpek EK. Visual and clinical outcomes of explantation versus preservation of the intraocular lens during keratoprosthesis implantation. *J Cataract Refract Surg* 2011; 37: 1613–1622.
- Langenbacher A, Huber S, Nguyen NX, Seitz B & Kuehle M. Cardinal points and image-object magnification with an accommodative lens implant (1 CU). *Ophthalmic Physiol Opt* 2003; 23: 61–70.
- Becken W, Altheimer H, Esser G, Müller W & Uttenweiler D. Optical magnification matrix: near objects in the paraxial case. *Optom Vis Sci* 2008; 85: 581–592.
- Rosenblum WM & Christensen JL. Optical matrix method: optometric applications. *Am J Optom Physiol Opt* 1974; 51: 961–968.

DOI:10.14753/SE.2021.2503

12. Sayegh RR, Avena Diaz L, Vargas-Martin F, Webb RH, Dohlman CH & Peli E. Optical functional properties of the Boston keratoprosthesis. *Invest Ophthalmol Vis Sci* 2010; 51: 857–863.
13. Watkins RD. The optical systems of the eye. *Asst J Optom* 1970; 53: 289–299.
14. Hicks CR, Fitton JH, Chirila TV, Crawford GI & Constable JJ. Keratoprotheses: advancing toward a true artificial cornea. *Surv Ophthalmol* 1997; 42: 175–189.
15. Colby KA & Koo EB. Expanding indications for the Boston keratoprosthesis. *Curr Opin Ophthalmol* 2011; 22: 267–273.
16. Koller B, Neuhann T & Neuhann L. Results with the Boston keratoprosthesis. *Ophthalmologe* 2012; 109: 454–461.
17. Magalhaes FP, de Sousa LB & de Oliveira LA. Boston type I keratoprosthesis. Review. *Arq Bras Oftalmol* 2012; 75: 218–222.
18. *Massachusetts Eye and Eye Infirmary*. Boston KPro news 2011; 8:3. <http://www.masseyeandear.org/for-professionals/physician-resources/keratoprosthesis/>, accessed 06/02/13.
19. Pincus SL, Ela-Daiman N, Rosenbium AL, Aldave AJ & Velez FG. Binocular visual function in patients with Boston type I keratoprotheses. *Cornea* 2010M; 29: 1397–1400.
20. Arment JD, Pineda R, Lawson B, Belau I & Dohlman CH. *The Boston keratoprosthesis: international protocol*, http://www.masseyeandear.org/gedownload/KPro%20International%20Protocol.pdf?item_id=5816015&version_id=5816016, accessed 23/11/12.
21. Chew HF, Ayres BD, Hammersmith KM et al. Boston keratoprosthesis outcomes and complications. *Cornea* 2009; 28: 989–996.
22. Aldave AJ, Sangwan VS, Basu S et al. International results with the Boston type I keratoprosthesis. *Ophthalmology* 2012; 119: 1530–1538.

Supporting Information

Additional Supporting Information may be found in the online version of this article:

Appendix S1. Formulae for calculating a phakic or pseudophakic fellow eye.

Anisometropie und Aniseikonie – ungelöste Probleme der Kataraktchirurgie

Anisometropia and Aniseikonia – Unsolved Problems of Cataract Surgery

Autoren

A. Langenbucher¹, N. Szentmáry²

Institute

¹ Institut für Medizinische Physik, Universität Erlangen-Nürnberg
² Augenklinik mit Poliklinik, Semmelweis Universität Budapest

Schlüsselwörter

- Physiologische Optik
- Katarakt
- Kornea

Key words

- cataract
- physiological optics
- cornea

eingereicht 4.2.2008
akzeptiert 6.6.2008

Bibliografie

DOI 10.1055/s-2008-1027601
 Klin Monatsbl Augenheilkd
 2008; 225: 763 – 769 © Georg
 Thieme Verlag KG Stuttgart ·
 New York · ISSN 0023-2165

Korrespondenzadresse

Prof. Achim Langenbucher
 Institut für Medizinische Physik,
 Universität Erlangen-Nürnberg
 Henkestr. 91
 91052 Erlangen
 Tel.: ++ 49/91 31/8 52 55 57
 Fax: ++ 49/91 31/8 52 28 24
 achim.langenbucher@imp.uni-
 erlangen.de

Zusammenfassung



Hintergrund und Zielsetzung: Aniseikonie ist eines der wichtigen bisher ungelösten Probleme der modernen Kataraktchirurgie. Es zeichnet verantwortlich für eingeschränktes Binokularesehen, Doppelbilder oder Kopfschmerzen. Ziel der vorliegenden Arbeit ist, dem Kliniker ein Verfahren an die Hand zu geben, mit dem der Abbildungsmaßstab abgeschätzt werden kann und Möglichkeiten aufgezeigt werden, wie bei der Kataraktchirurgie der Abbildungsmaßstab gezielt variiert werden kann.

Methoden: Auf der Basis eines zentrierten optischen Systems im paraxialen Raum wird das optische System Auge mit 2×2 Matrizen modelliert und der Abbildungsmaßstab extrahiert. Die Methodik wird auf das Modell einer „dünnen Linse“ sowie das Modell einer „dicken Linse“ angewandt und die Anwendung in Beispielen detailliert erläutert. Weiter wird aufgezeigt, wie durch eine geeignete Kombination aus Kunstlinse und Brillenkorrektur ein vorgegebener Abbildungsmaßstab realisiert werden kann.

Ergebnisse: In Beispiel 1 wird der Abbildungsmaßstab für ein bereits kataraktoperiertes Referenzauge ermittelt. Beispiel 2 schätzt ab, welcher Abbildungsmaßstab nach Kataraktoperation am OP-Auge zu erwarten ist, wenn der gleiche Linsentyp implantiert wird. Beispiel 3 soll eine Übersicht geben, wie der Abbildungsmaßstab variiert, wenn die Linsenposition, die Geometrie oder die Dicke der Linse moduliert wird. Beispiel 4 zeigt auf, wie eine Kombination einer Kunstlinse und einer Brillenkorrektur für eine eikonische Abbildung berechnet wird.

Schlussfolgerung: Die Studie soll den Ophthalmochirurgen sensibilisieren für die Problematik der Aniseikonie nach Kataraktoperationen und ein mathematisches Werkzeug an die Hand geben, wie mit einfachen Mitteln Abbildungsmaßstäbe

Abstract



Background and Purpose: Aniseikonia is one of the relevant unsolved problems of modern cataract surgery and may cause severe functional problems such as deteriorated binocular vision, diplopia or headaches. The aim of the present study is to assist the clinician as to how to estimate lateral magnification in a pseudophakic eye and how to reduce or eliminate aniseikonia.

Methods: Based on the characterisation of a centred optical system in the paraxial space, the optical system eye is modelled with 2×2 matrices and the lateral magnification is extracted. This method is applied on the “thin lens model” as well as the “thick lens model” and illustrated in detail with 4 working examples. Additionally, we demonstrate how a predefined lateral magnification (e.g., from the contralateral eye) can be realised during cataract surgery by calculating an appropriate combination of an IOL and a spectacle correction.

Working Examples: In example 1 the lateral magnification of the reference eye following cataract surgery is determined. In example 2 we estimate the lateral magnification behaviour that is expected after cataract surgery using the same IOL as in example 1. Example 3 gives an overview of how the magnification varies if the IOL position in the eye, the geometry of the lens or the central thickness is changed. Example 4 shows how to calculate an appropriate combination of an IOL and spectacle correction to realise an eikonic imaging of both eyes.

Conclusion: The present study should sensitise ophthalmic surgeons for the still unsolved problem of aniseikonia after cataract surgery and should give them a simple mathematical tool to help determine object-image magnification and show how to reduce or eliminate aniseikonia during cataract surgery.

abgeschätzt werden können und wie man bei der Kataraktchirurgie gezielt Aniseikonie reduzieren und eliminieren kann.

Hintergrund und Zielsetzung

Nach der klassischen Definition ist Aniseikonie ein binokularer Refraktionsstatus, bei dem der retinale laterale Abbildungsmaßstab der beiden Augen voneinander abweicht [10]. Dies meint nicht zwangsläufig, dass der globale Abbildungsmaßstab beider Augen unterschiedlich ist („globale Aniseikonie“), sondern kann auch durch einen unterschiedlichen meridionalen Abbildungsmaßstab aufgrund astigmatischer Grenzflächen im Auge verursacht sein („meridionale Aniseikonie“). Weiter unterscheidet man zwischen der statischen und der dynamischen Aniseikonie. Im Falle der statischen Aniseikonie liegen für verschiedene Blickrichtungen konstante, aber unterschiedliche Abbildungsmaßstäbe bei beiden Augen vor, wohingegen man bei der dynamischen Aniseikonie auch von der induzierten Anisophorie spricht. Hier treten für unterschiedliche Blickrichtungen aufgrund eines prismatischen Effekts unterschiedliche laterale Abbildungsmaßstäbe auf, da der Patient z. B. durch unterschiedliche Areale von 2 (anisometrischen) refraktionskorrigierenden Brillengläsern blickt. Die Inzidenz der Aniseikonie ist in der Klinik oft unterschätzt, da die Symptome meist nicht unmittelbar in Erscheinung treten oder direkt fassbar sind. Neben der nicht zu vernachlässigenden Gruppe an Patienten im Alter über 20 Jahren mit einer Prävalenz der Aniseikonie von bis zu 10% aufgrund einer Anisometropie größer als 1 Dioptrie unterliegen speziell Patienten nach einer Kataraktoperation oder einem refraktiv-chirurgischen Eingriff dem Risiko einer Aniseikonie. Kramer [10] bestätigte, dass rund 40% aller Patienten, die sich einer Kataraktoperation mit Implantation einer Kunstlinse unterzogen hatten, mehr oder weniger an einer Aniseikonie leiden. Schon aufgrund dieser beachtlichen Häufigkeit sollte das Problem der Aniseikonie in diesem Zusammenhang eingehend erörtert und in das Gedächtnis der Ophthalmochirurgen gerufen werden.

Die Sensitivität gegenüber Aniseikonie ist in der Bevölkerung individuell unterschiedlich: Während manche Patienten bereits den Ausgleich eines Bildgrößenunterschiedes von 1% zwischen beiden Augen als hilfreich empfinden ist das subjektive Empfinden anderer Patienten bei 3% Bildgrößenunterschied nicht im mindesten beeinträchtigt. Anders als bei der globalen Aniseikonie liegen für die Akzeptanz bzw. Toleranz der meridionalen Aniseikonie keine Literaturwerte vor. So ist für manche Patienten beschrieben, dass der Ausgleich der globalen Aniseikonie ausreicht und meridionale Bildgrößenunterschiede bis zu einem bestimmten Grad toleriert werden, wohingegen an anderer Stelle behauptet wird, dass gerade die meridionale Aniseikonie mit der Folge von Bildverzerrungen verantwortlich zeichnet für Kopfschmerzen und asthenopische Beschwerden [13].

Das klassische Verfahren der Aniseikoniekorrektur ist die Verwendung eikonischer Brillengläser. So kann die individuelle Brillenvergrößerung eines Brillenglases variiert werden durch die Basiskurve, die zentrale Dicke, den Brechungsindex des Materials sowie den Hornhautscheitelabstand. Für Patienten nach Kataraktextraktion mit Hinterkammerlinsenimplantation konnte als logische Antwort auf Aniseikonie in einer früheren Studie bereits gezeigt werden, wie mit bitorischen eikonischen Intraokularlinsen, bei denen die zentrale Dicke, der Brechungsindex sowie die beiden Sphären und Zylinderwerte (mit Orientierung

des Zylinders) der Linsenvorder- und Rückfläche justiert werden müssen, um eine eikonische Abbildung des Patienten (im Sinne einer Korrektur der globalen und meridionalen Aniseikonie) zu erzielen [12]. Allerdings ist die Herstellung und Berechnung derartiger individueller Linsenimplantate derzeit noch eine Herausforderung der innovativen Medizintechnikfirmen.

Das Ziel der vorliegenden Studie ist, ein Berechnungsmodell vorzustellen wie anhand der biometrischen Daten des phaken Auges präoperativ der Abbildungsmaßstab eines pseudophaken Auges postoperativ für eine beliebige Zielrefraktion auf der Basis der paraxialen Optik abgeschätzt werden kann und wie gezielt der Abbildungsmaßstab des Operationsauges auf die Gegebenheiten des Partnerauges angepasst werden kann. Falls vom Linsenhersteller ausschließlich die geschätzte Linsenposition (in Form einer ACD-Konstante) vorliegt, wird das Modell einer „dünnen Linse“ angesetzt, falls umfangreichere geometrische Daten vorliegen (geschätzte Linsenposition, Mittendicke, Brechungsindex und die Krümmung der Vorder- und Rückfläche) kann das Modell einer „dicken Linse“ angesetzt werden. Die meridionale Aniseikonie wird hierbei ausgeklammert und in einer separaten Arbeit adressiert werden.

Material und Methoden

Refraktions- und Translationsmatrizen sowie die Systemmatrix

Geht man von einem zentrierten optischen System aus, bei dem sphärische optische Grenzflächen homogene optische Medien trennen, so können die optischen Grenzflächen bzw. die Zwischenräume zwischen den Grenzflächen durch 2×2 Refraktionsmatrizen R bzw. Translationsmatrizen T beschrieben werden mit

$$R = \begin{bmatrix} 1 & -P \\ 0 & 1 \end{bmatrix} \quad T = \begin{bmatrix} 1 & 0 \\ \frac{d}{n} & 1 \end{bmatrix}, \quad (1)$$

wobei P der Flächenbrechkraft in Dioptrien, d dem geometrischen Abstand zwischen den Grenzflächen und n dem Brechungsindex des (homogenen) optischen Mediums entspricht [11, 20].

Das gesamte optische System für eine alternierende Anordnung von refraktiven Grenzflächen und optischen Zwischenräumen beginnend von links nach rechts mit der Indizierung 1... m ist charakterisiert durch eine Systemmatrix S , die aus dem Produkt der zugehörigen Refraktions- und Translationsmatrizen gebildet wird:

$$S = R_m \times T_{m-1,m} \times R_{m-1} \times T_{m-2,m-1} \times \dots \times R_2 \times T_{1,2} \times R_1. \quad (2)$$

Diese Systemmatrix beschreibt nun, wie ein Strahl einfallend an der Grenzfläche 1 (von links) charakterisiert durch die Strahlhöhe y_0 und den Einfallswinkel α_0 auf den Ausgang des Systems (Grenzfläche m , nach rechts) in eine Strahlhöhe y und einen Ausfallwinkel α übertragen wird.

$$\begin{pmatrix} \alpha \\ y \end{pmatrix} = S \times \begin{pmatrix} \alpha_0 \\ y_0 \end{pmatrix}. \quad (3)$$

Umgekehrt wird ein Strahl charakterisiert durch die Strahlhöhe y_0 und den Einfallswinkel α_0 , der von rechts auf das System trifft,

auf einen Strahl charakterisiert durch die Strahlhöhe y und den Einfallswinkel α (Grenzfläche 1, nach links) übersetzt durch

$$\begin{pmatrix} \alpha \\ y \end{pmatrix} = S^{-1} \times \begin{pmatrix} \alpha_0 \\ y_0 \end{pmatrix}. \tag{4}$$

Beschreibung eines pseudophaken Auges durch Matrizen, Abbildungsmaßstab

Das optische System „pseudophakes Auge“ in der einfachsten Form ist charakterisiert durch eine einflächige Brillenkorrektur (bei Emmetropie identisch null), einflächige Hornhaut, die Vorderkammer des Auges, eine dünne (einflächige) Kunstlinse sowie den Glaskörper. Die zugehörige Systemmatrix S beschreibt sich demnach zu

$$S = T_V \times R_{IOL} \times T_{VK} \times R_{HH} \times T_B \times R_B, \tag{5}$$

wobei T_V der (pseudophaken) Glaskörperstrecke entspricht, R_{IOL} der Kunstlinse, T_{VK} der (pseudophaken) Vorderkammertiefe, R_{HH} der Hornhaut, T_B dem Hornhautscheitelabstand und R_B dem Refraktionsausgleich auf Brillenebene.

Sofern die Position der Kunstlinse im Auge als bekannt vorausgesetzt werden kann (z.B. ACD-Konstanten, „lens haptic plane concept“ [15, 16, 18, 19]), so sind die Matrizen T_V , T_{VK} , R_{HH} und T_B bekannt, wohingegen im einfachsten Fall die Matrizen R_{IOL} und R_B oder genauer deren Elemente P verwendet werden, um den Abbildungsmaßstab zu justieren. Selbstverständlich können auch über spezielle Designs der Kunstlinse (z.B. unterschiedliche ACD-Konstanten) oder der Brillenfassung (anderer Hornhautscheitelabstand) die Werte der Matrizen T_V , T_{VK} und T_B verändert werden.

Der retinale Abbildungsmaßstab ist definiert als das Verhältnis der lateralen Ausdehnung des Netzhautbildes y zum Winkel α_0 des zugehörigen Objektes (unter dem es wahrgenommen wird), das im Unendlichen lokalisiert ist. Für den Fall, dass das optische System refraktiv korrigiert ist (d.h. die Brille die Fehlsichtigkeit des Auges ausgleicht), ist das Matrixelement (2,2) der Systemmatrix identisch null (d.h. ein parallel zur Achse einfallendes Strahlbündel wird stets auf die Netzhaut fokussiert) und der laterale Abbildungsmaßstab M lässt sich unmittelbar aus dem Matrixelement (2,1) aus der Systemmatrix ablesen:

$$\begin{pmatrix} \alpha \\ y \end{pmatrix} = \begin{bmatrix} \dots & \dots \\ M & 0 \end{bmatrix} \times \begin{pmatrix} \alpha_0 \\ y_0 \end{pmatrix}. \tag{6}$$

Geht man davon aus, dass der Abbildungsmaßstab ausschließlich durch Veränderung der Brechkkräfte der Kunstlinse und der Brillenrefraktion an den Referenzwert des Partnerauges angepasst werden soll, so kann mit der Definition eines Subsystems S_A

$$S_A = T_{VK} \times R_{HH} \times T_B = \begin{bmatrix} 1 - P_{HH} d_B & 0 \\ \frac{d_{VK}}{n_{VK}} (1 - P_{HH} d_B) + d_B & 1 \end{bmatrix} = \begin{bmatrix} s_{11} & s_{12} \\ s_{21} & s_{22} \end{bmatrix} \tag{7}$$

die Systemmatrix S vereinfachend geschrieben werden als

$$S = \begin{bmatrix} 1 & 0 \\ \frac{d_V}{n_V} & 1 \end{bmatrix} \times \begin{bmatrix} 1 - P_{IOL} & \\ 0 & 1 \end{bmatrix} \times \begin{bmatrix} s_{11} & s_{12} \\ s_{21} & s_{22} \end{bmatrix} \times \begin{bmatrix} 1 - P_B & \\ 0 & 1 \end{bmatrix} = \begin{bmatrix} 1 & -P_{IOL} \\ \frac{d_V}{n_V} - P_{IOL} \times \frac{d_V}{n_V} + 1 & \end{bmatrix} \times \begin{bmatrix} s_{11} & s_{12} \\ s_{21} & s_{22} \end{bmatrix} \times \begin{bmatrix} 1 - P_B & \\ 0 & 1 \end{bmatrix} \tag{8}$$

Multipliziert man die Beziehung (8) aus, so resultieren die beiden Elemente der zweiten Zeile der Systemmatrix zu

$$S = \left[\begin{array}{cc} \frac{d_V}{n_V} s_{11} + (-P_{IOL} \times \frac{d_V}{n_V} + 1) s_{21} & \frac{d_V}{n_V} (-P_B s_{11} + s_{12}) + \\ \dots & \dots \\ + (-P_{IOL} \times \frac{d_V}{n_V} + 1) (-P_B s_{21} + s_{22}) & \end{array} \right] \tag{9}$$

n_V bzw. n_{VK} bezeichnen hier den Brechungsindex von Glaskörper und Kammerwasser und P_{HH} , P_{IOL} bzw. P_B die Flächenbrechkkräfte der Hornhaut, der dünnen Kunstlinse bzw. der Brillenkorrektur und d_{VK} bzw. d_B die pseudophake Vorderkammertiefe bzw. den Hornhautscheitelabstand.

Aus Beziehung (9) erkennt man unmittelbar, dass in den retinalen Abbildungsmaßstab M (Element (2,1) der Matrix S) die Brillenrefraktion nicht einfließt, wenn das Brillenglas als „dünne Linse“ angenommen wird.

Somit ist die Bestimmung der Brechkraft der Kunstlinse und der Brillenkorrektur entkoppelt: In einem ersten Schritt wird der Abbildungsmaßstab M an den Abbildungsmaßstab des Partnerauges angepasst, indem eine geeignete Brechkraft für die Kunstlinse bestimmt wird:

$$M = \frac{d_V}{n_V} s_{11} + (-P_{IOL} \times \frac{d_V}{n_V} + 1) s_{21}$$

$$P_{IOL} = \frac{n_V}{d_V} \left(1 - \frac{M - \frac{d_V}{n_V} s_{11}}{s_{21}} \right) \tag{10}$$

Im zweiten Schritt wird nun unter Verwendung der mit Gleichung (10) bestimmten Kunstlinse eine geeignete Brillenkorrektur derart bestimmt, dass das gesamte optische System refraktiv auskorrigiert ist (d.h. das Element (2,2) der Systemmatrix identisch null ist):

$$\frac{d_V}{n_V} (-P_B s_{11} + s_{12}) + (-P_{IOL} \times \frac{d_V}{n_V} + 1) (-P_B s_{21} + s_{22}) = 0$$

$$P_B = \frac{P_{IOL} \frac{d_V}{n_V} s_{22} - \frac{d_V}{n_V} s_{12} - s_{22}}{P_{IOL} \frac{d_V}{n_V} s_{21} - \frac{d_V}{n_V} s_{11} - s_{21}} \tag{11}$$

Beispiele

Bei den hier vorgestellten Beispielen gehen wir davon aus, dass ein Auge (Referenzauge) bereits einer Kataraktoperation unterzogen wurde und von diesem Auge die biometrischen Daten (Tab. 1) sowie die Position und die Stärke der implantierten Linse bekannt sind. Vom Operationsauge sind ausschließlich die biometrischen Daten bekannt. Es soll nun eine Kunstlinse in Kombination mit einer Brillenkorrektur derart ausgewählt werden, dass der Abbildungsmaßstab des Referenzauges nachgebildet wird und das gesamte optische System inklusive Brillenkorrektur refraktiv auskorrigiert ist.

Beispiel 1: Berechnung des Abbildungsmaßstabs des Referenzauges

Implantiert wurde eine Kunstlinse mit der nominellen Brechkraft von 19,5 D. Gegenübergestellt werden hier die Ergebnisse des Ansatzes auf der Basis eines „Modells der dünnen Lin-

Tab. 1 Spalte 2 und 3: Biometrische Größen des pseudophaken Referenzzauges zusammen mit der Position, des Brechungsindex, der Äquivalentbrechkraft sowie den Flächenbrechkraften der Kunstlinse. Spalte 3: Angabe der biometrischen Daten für das OP-Auge, bei dem die Kunstlinse sowie die Brillenrefraktion verwendet wird, um den Abbildungsmaßstab des Referenzzauges nachzubilden.

	Referenzauge (pseudophak)		OP-Auge (phak)
	„dünne Linse“	„dicke Linse“	
Achslänge in mm	24,2	24,2	22,60
phake Linsenposition in mm	/	/	3,50
phake Linsendicke in mm	/	/	3,80
pseudophake Linsenposition in mm	5,20	4,80	
pseudophake Linsendicke in mm	0,00	0,80	
Vorderflächenbrechkraft der IOL in D	/	9,78	
Rückflächenbrechkraft der IOL in D	/	9,78	
Äquivalentbrechkraft der IOL in D	19,50	19,5	
Brechungsindex der IOL	/	1,46	
Hornhautbrechkraft P_{HH} in D	43,50	43,50	42,50
Refraktion auf Brillenebene (HSA 14 mm) in D	-1,00	-1,00	

se“, bei dem die Kunstlinse als ideal dünne einflächige Linse angenommen wurde sowie des „Modells einer dicken Linse“, bei dem davon ausgegangen wurde, dass die Kunstlinse identische Flächenbrechkraften der Vorder- und Rückfläche aufweist (equibikonvex). Damit lässt sich unmittelbar der Abbildungsmaßstab M für dieses Auge aus der Systemmatrix S ableiten. Setzt man für den Fall der dünnen Linse die Refraktionsmatrizen für die Brillenrefraktion und Hornhaut sowie die Translationsmatrizen für den Hornhautscheitelabstand, die pseudophake Vorderkammer und den Glaskörperraum nach Beziehung (1) an und multipliziert nach Gleichung (2) zu einer Systemmatrix S zusammen:

$$S = \begin{bmatrix} 0,0870 & -59,5887 \\ 0,0168 & 0,0000 \end{bmatrix}, \quad (12)$$

so erhält man direkt eine Äquivalentbrechkraft von 59,5887 D für das Auge bzw. eine Brechkraft von 19,5490 D für die dünne Linse. Der Abbildungsmaßstab wird aus der Systemmatrix abgelesen mit einem Wert von $M=0,0167817$.

Setzt man für den Fall der dicken Linse die Refraktionsmatrizen für die Brillenrefraktion und Hornhaut sowie die Translationsmatrizen für den Hornhautscheitelabstand, die pseudophake Vorderkammer, die Kunstlinse und den Glaskörperraum nach Beziehung (1) an und multipliziert nach Gleichung (2) zu einer Systemmatrix S zusammen unter der Voraussetzung, dass die beiden Flächenbrechkraften der Linse identisch sind (equibikonvex), so ergibt sich:

$$S = \begin{bmatrix} 0,0876 & -59,6804 \\ 0,0168 & 0,0000 \end{bmatrix}, \quad (13)$$

Die beiden Grenzflächen der Linsen besitzen eine Brechkraft von 9,8056 D und die Äquivalentbrechkraft berechnet sich zu 19,5585 D. Der Abbildungsmaßstab wird aus der Systemmatrix abgelesen mit einem Wert von $M=0,0167559$ und stimmt aufgrund der equibikonvexen Geometrie sehr gut mit dem Vergleichswert für das Modell der dünnen Linse überein.

Beispiel 2: Berechnung einer dünnen Linse für das OP-Auge
Zunächst soll mit den in **Tab. 1** aufgelisteten biometrischen Daten für das OP-Auge eine dünne und eine dicke equibikonvexe Kunstlinse berechnet werden, die das Auge für eine Zielrefraktion von $-1,0$ D auskorrigiert.

Für den Fall der dünnen Linse werden die Refraktionsmatrizen für die Brillenkorrektur und die Hornhaut sowie die Transla-

tionsmatrizen für den Hornhautscheitelabstand, die pseudophake Vorderkammer (5,2 mm) und die pseudophake Glaskörperstrecke (19 mm) nach (1) angesetzt.

Anschließend wird in Gleichung (9) Element (2,2) identisch null gesetzt und nach der Brechkraft der Kunstlinse aufgelöst. Die Brechkraft der Kunstlinse berechnet sich zu 27,5426 D. Wird nun die Refraktionsmatrix für die Kunstlinse nach Beziehung (1) angesetzt und die Systemmatrix S für das gesamte optische System einschließlich Brillenkorrektur berechnet, so kann man direkt ablesen, dass mit

$$S = \begin{bmatrix} -0,0248 & -65,4311 \\ 0,0153 & 0,0000 \end{bmatrix}, \quad (14)$$

das gesamte System refraktiv auskorrigiert ist (Element [2, 2] identisch null), die Äquivalentbrechkraft des Auges mit Korrektur 65,4311 D und der Abbildungsmaßstab $M=0,0152833$ beträgt. Damit ist die laterale Vergrößerung im Vergleich zum Partnerauge (Modell der dicken Linse) um 8,8% kleiner.

Für den Fall der dicken Linse mit einer Mittendicke von 0,8 mm und einem Brechungsindex von 1,46 entsprechend den Vergleichswerten des Referenzzauges werden die Refraktionsmatrizen für die Brillenkorrektur und die Hornhaut sowie die Translationsmatrizen für den Hornhautscheitelabstand, die pseudophake Vorderkammer (4,8 mm), die Kunstlinse (0,8 mm) und die pseudophake Glaskörperstrecke (17 mm) nach (1) angesetzt. Anschließend wird eine dicke Linse mit Gleichung (9) unter der Bedingung berechnet, dass die beiden Flächenbrechkraften der Linse identisch sind (equibikonvex). Daraus ergeben sich die Flächenbrechkraften bzw. die Äquivalentbrechkraft der Kunstlinse zu 13,7876 D bzw. 27,4710 D. Werden nun die Refraktionsmatrizen der beiden Kunstlinsenflächen nach Beziehung (1) angesetzt und die Systemmatrix S für das gesamte optische System einschließlich Brillenkorrektur berechnet, so kann man direkt ablesen, dass mit

$$S = \begin{bmatrix} -0,0226 & -65,4779 \\ 0,0153 & 0,0000 \end{bmatrix}, \quad (15)$$

das gesamte System refraktiv auskorrigiert ist (Element [2, 2] identisch null), die Äquivalentbrechkraft des Auges mit Korrektur 65,4779 D und der Abbildungsmaßstab $M=0,0152723$ beträgt. Damit ist die laterale Vergrößerung im Vergleich zum Partnerauge (Modell der dicken Linse) wieder um 8,8% kleiner.

Tab. 2 Variation der Linsenparameter unter der Bedingung eines refraktiv korrigierten Auges, um die Wirkung auf den lateralen Abbildungsmaßstab abzuschätzen. Angegeben wurden die beiden Flächenbrechkkräfte der Kunstlinse (anterior und posterior), die Äquivalentbrechkraft, der Abbildungsmaßstab sowie der relative Abbildungsmaßstab (als Verhältnis des Abbildungsmaßstabes zum Vergleichswert des Referenzauges). In Zeile 2 und 3 wurde die Kunstlinse aus Beispiel 2 jeweils um 0,5 mm nach vorne bzw. hinten verschoben, in Zeile 4 und 5 wurde das Design auf plan-konvex bzw. konvex-plan geändert, in Zeile 6 und 7 wurde die Dicke auf 1,2 mm bzw. 1,6 mm erhöht unter Beibehaltung der Äquatorebene (pseudophake Vorderkammertiefe dann 4,6 mm bzw. 4,4 mm).

	Fläche anterior in D	Fläche posterior in D	Äquivalentbrechkraft in D	Abbildungsmaßstab	relativer Abbildungsmaßstab
Position 4,3 mm	13,1561	13,1561	26,2174	0,0154264	0,9207
Position 5,3 mm	14,4665	14,4665	28,8183	0,0151125	0,9019
plan-konvex	0,0000	28,4566	28,4566	0,0151538	0,9044
konvex-plan	26,5527	0,0000	26,5527	0,0153838	0,9181
Dicke 1,2 mm	13,8622	13,8622	27,5664	0,0152503	0,9101
Dicke 1,6 mm	13,9350	13,9350	27,6573	0,0152294	0,9089

Beispiel 3: Variation der Linsenposition, der Geometrie sowie der Dicke der Linse

Hier soll die dicke Kunstlinse aus Beispiel 2 variiert werden in ihrer Position (4,3 mm und 5,3 mm anstatt 4,8 mm), ihrer Geometrie (plan-konvex, konvex-plan anstatt equibikonvex) und ihrer zentralen Dicke (1,2 mm und 1,6 mm anstatt 0,8 mm) um den Effekt dieser Einflussgrößen auf den lateralen Abbildungsmaßstab abzuschätzen. Die Ergebnisse sind in **Tab. 2** dargestellt. Die Übersicht zeigt, dass die Wirkung der Variation o.g. Parameter auf den Abbildungsmaßstab sehr gering ist und maximal im Bereich von 1 – 2% rangiert.

Beispiel 4: Eikonische Abbildung durch Kombination aus dünner Kunstlinse und Brille

In diesem Beispiel soll gezeigt werden, wie man durch eine geeignete Kombination aus Kunstlinse (zur Vereinfachung wird das Modell einer dünnen Linse verwendet) und Brillenkorrektur den Abbildungsmaßstab an den Vergleichswert des Referenzauges anpassen kann. Wir gehen wieder von den in **Tab. 1** dargestellten biometrischen Daten des OP-Auges und einer Position der dünnen Kunstlinse bei 5,2 mm (siehe Beispiel 2) aus und berechnen zunächst die 4 Elemente des Subsystems SA gemäß Beziehung (7). Weiter ermitteln wir mit Gleichung (10) die Brechkraft der Kunstlinse für die Anpassung des Abbildungsmaßstabes an das Referenzauge zu $P_{iOL} = 20,1831$ D. Mit Beziehung (11) wird abschließend die Brillenkorrektur zu $P_B = +3,7077$ D ermittelt, die das gesamte optische System Auge inklusive Brillenkorrektur refraktiv auskorrigiert. Multipliziert man nun zur Kontrolle alle Refraktionsmatrizen und Translationsmatrizen gemäß Gleichung (5) auf, so resultiert eine Systemmatrix

An dieser Systemmatrix kann unmittelbar abgelesen werden, dass die Äquivalentbrechkraft des Auges 59,6804 D beträgt und dass das System refraktiv auskorrigiert ist. Erweitert man die Dezimalstellen für den Abbildungsmaßstab (Element [2, 1] der Systemmatrix) so entspricht dieser dem Vergleichswert des Referenzauges mit $M = 0,0167817$ (vgl. Beispiel 1).

Diskussion

Vereinfacht versteht man unter Anisometropie einen Unterschied im Brechungsverhalten beider Augen, wohingegen Ani-

$$S = \begin{bmatrix} 0,0906 & -59,6804 \\ 0,0168 & 0,0000 \end{bmatrix}, \quad (16)$$

seikonie einen funktionellen binokularen Defekt bezeichnet, bei dem die Geometrie und/oder die Größe der beiden Netzhautbilder unterschiedlich sind. In einer Vielzahl von wissenschaftlichen Veröffentlichungen wurden retinale Bildgrößenunterschiede zwischen zwei Augen eines Individuums analysiert („globale Aniseikonie“), allerdings wurde in den wenigsten Fällen differenziert zwischen der globalen und der meridionalen Aniseikonie, bei der die Netzhautbilder aufgrund astigmatischer Grenzflächen im Auge unterschiedlich verzerrt sind [6, 7]. In dieser ersten Studie beschränken wir uns auf die Untersuchung der globalen Aniseikonie, in einer zweiten Arbeit wird im Detail auf die Analyse meridionaler Bildverzerrungen eingegangen werden.

In der Literatur finden sich für den retinalen Bildgrößenunterschied beider Augen Werte bis zu 5%, die vom Patienten akzeptiert und toleriert werden [1, 2, 21]. Höhere Werte der Aniseikonie führen zu Doppelbildern, Suppression oder auch zum Verlust der binokularen Addition. Aniseikonie ist nicht auf das optische System Auge beschränkt, sondern hat auch eine entscheidende neuronale Komponente, z.B. bedingt durch individuelle Unterschiede im Abstand der Fotorezeptoren. In einer Reihe von mehr oder weniger empirischen Arbeiten wurde in der Vergangenheit versucht, dieses Problem zu analysieren und zu charakterisieren. In dieser Studie haben wir uns bewusst auf die geometrisch-optische Abbildung eines Objektes auf die Netzhaut beschränkt und neuronale Einflussfaktoren außer Acht gelassen.

Das optische System Auge kann mit unterschiedlichen Formalismen beschrieben werden [4, 5]. Generell unterscheidet man zwischen numerischen Beschreibungen mittels Raytracing und der vereinfachten Darstellung mit paraxialer Näherung. Beim Raytracing wird ein repräsentatives Strahlenbündel (z.B. mehrere Tausend Strahlen) von einem Objekt ausgehend auf das Auge projiziert und sukzessive jeder einzelne Strahl unter Einhaltung des Snellius-Brechungsgesetzes bis auf die Netzhautebene verfolgt. Bei der paraxialen Näherung (lineare Gaußsche Optik) geht man davon aus, dass das optische System zentriert ist und ausschließlich sphärische Grenzflächen besitzt. Die Strahlen treffen so achsnah auf die refraktiven Grenzflächen, dass die paraxiale Näherung gilt und im Snellius-Brechungsgesetz der Sinus des Winkels des ein- und ausfallenden Strahles durch den Winkel im Bogenmaß ersetzt werden kann. Im Vergleich zum Raytracing liefert diese Vereinfachung geschlossene analytische Lösungen und ist mit geringem mathematischem Aufwand umzusetzen. Für klinische Anwendungen reicht die Genauigkeit dieser Näherung bei weitem aus, sodass der Mehraufwand bei

der Berechnung mit Raytracing nur in Ausnahmefällen gerechtfertigt erscheint.

In der vorliegenden Arbeit wurde für den paraxialen Ansatz ein matrixbasierter Formalismus gewählt, der eine sehr übersichtliche Darstellung des optischen Systems Auge zulässt. So werden alle refraktiven Grenzflächen durch 2×2 Refraktionsmatrizen dargestellt und die mit homogenem optischem Medium gefüllten Zwischenräume zwischen den Grenzflächen durch 2×2 Translationsmatrizen [8, 11, 14, 20]. Multipliziert man die Refraktions- und Translationsmatrizen gemäß Gleichung (2) zusammen, so kann das optische System ohne detaillierte Kenntnis als „Black Box“ vollständig durch die 2×2 Systemmatrix beschrieben werden, die charakterisiert, wie ein einfallender Strahl (definiert durch die Strahlhöhe und den Einfallswinkel) auf einen ausfallenden Strahl (definiert durch die Strahlhöhe und den Ausfallwinkel) übersetzt wird. Der hier vorgestellte Formalismus ist vielseitig verwendbar. Falls, wie im Falle eines pseudophaken Auges, die Positionen und Brechkraft aller refraktiven Flächen bekannt sind sowie die Refraktion und Position der besten Brillenkorrektur ermittelt ist, so kann sehr einfach wie in Beispiel 1 aufgezeigt die Äquivalentbrechkraft des Auges inklusive Brillenkorrektur sowie der Abbildungsmaßstab aus der Systemmatrix abgeleitet werden. Die fehlenden Brechungsindizes für Kammerwasser und Glaskörper variieren individuell nur sehr gering und können einem der klassischen Augenmodelle entnommen werden (z.B. [3, 9, 17]). Falls die biometrischen Daten und die implantierte Kunstlinse zur gemessenen Refraktion auf Brillenebene passt, so erwarten wir insgesamt ein refraktiv auskorrigiertes optisches System, bei dem ein parallel zur Achse einfallendes Strahlbündel ungeachtet der Einfallshöhe die optische Achse auf der Netzhautebene trifft und damit Element (2,2) der Systemmatrix identisch null ist. Kleine Abweichungen von der Null sind möglich aufgrund der Fertigungstoleranzen von Kunstlinsen und der Messungenauigkeit bei der Erhebung der biometrischen Daten.

Soll am Operationsauge der Abbildungsmaßstab des Partnerauges nachgebildet werden und das gesamte optische System refraktiv auskorrigiert sein, benötigt man zwei Freiheitsgrade. Dafür kommen mehrere Optionen in Betracht: Zum einen kann eine dicke eikonische Kunstlinse berechnet werden, bei der die Flächenbrechkraft der Vorder- und Rückfläche der Linse separat variiert werden können. Für den Fall eines astigmatischen Systems wurde die generelle Vorgehensweise in einer früheren Arbeit im Detail erläutert [12]. Allerdings zeigt Beispiel 3 (plan-konvex und konvex-plan) im Vergleich zur equibikonvexen Linse aus Beispiel 2 eindrucksvoll, dass aufgrund des geringen Abstandes der beiden Linsengrenzflächen die Variation des Abbildungsmaßstabes sehr gering ist und im Bereich von rund 1–2% liegt. Auch die Variation der Mittendicke der Linse sowie der Position im Auge über unterschiedliche Geometrien der Haptiken oder Positionierung im Sulkus anstatt im Kapselsack (siehe Beispiel 3) sind nur eingeschränkt geeignet, den Abbildungsmaßstab auf den Referenzwert des Partnerauges anzupassen. Zum anderen kann über eine geeignete Kombination aus Kunstlinse und Brillenkorrektur aufgrund des großen Abstandes voneinander sehr effizient der Abbildungsmaßstab verändert und somit Aniseikonie ausgeglichen werden, wie Beispiel 4 dokumentiert.

Vergleicht man die Ergebnisse der Beispiele 1 und 2 miteinander, so erkennt man selbst bei biometrischen Werten im „Normalbereich“ für das Referenz- und OP-Auge, dass der Abbildungsmaßstab bei Berechnung einer dünnen Linse durchaus

bis zu 10% unterschiedlich ausfallen kann. Da derartige Aniseikonien nur sehr schwer vom Patienten akzeptiert und toleriert werden, sollte man sich vor einer anstehenden Kataraktoperation die biometrischen Daten beider Augen sehr sorgfältig im Vergleich ansehen und ggf. für beide Augen eine Abschätzung des Abbildungsmaßstabes machen, wie er weiter oben in dieser Arbeit beschrieben ist. Dazu sind die Detaildaten der bereits implantierten bzw. der zu implantierenden Kunstlinse hilfreich (um ein Modell der dicken Linse anzusetzen), aber nicht zwingend erforderlich (Modell der dünnen Linse). Weiter ist in fraglichen Fällen zu evaluieren, welches Maß an Aniseikonie vom Patienten toleriert wird (z.B. mit einem Eikonometer), um zu entscheiden, ob eine Variation der Linsenposition und/oder ein geeignetes Linsendesign zur Abmilderung der Aniseikonie ausreichen oder ob gezielt eine Kombination aus Kunstlinse und Brillenkorrektur notwendig ist.

Generell gilt (für den klinisch relevanten Fall einer Kunstlinse mit positiver Brechkraft), dass der Abbildungsmaßstab größer wird, wenn

- ▶ Die Kunstlinse mehr anterior (kleinere ACD-Konstante) im Auge positioniert ist,
- ▶ die Flächenbrechkraft der Kunstlinse vorne erhöht und hinten reduziert wird (z.B. konvex-plan anstatt plan-konvex),
- ▶ bei stationärem Äquator der Kunstlinse die Mittendicke reduziert wird, und
- ▶ eine geringere brechende Kunstlinse mit einer geeigneten positiv brechenden Brillenkorrektur kombiniert wird (sehr effizient).

Zusammenfassend und schlussfolgernd ist die moderne Kataraktchirurgie so sicher, komplikationsarm und im funktionellen Ergebnis vorhersagbar, dass Risiken wie eine nicht tolerierte Aniseikonie in den Vordergrund treten. Ophthalmochirurgen sollen auf die Problematik der Aniseikonie nach Kataraktchirurgie sensibilisiert werden und bereits bei der Planung des Eingriffs anhand der biometrischen Daten beider Augen abschätzen, welche Bildgrößenunterschiede zu erwarten sind, ggf. die Akzeptanz und Toleranz des Patienten für Aniseikonie messen und durch geeignete Maßnahmen Bildgrößenunterschiede beider Augen reduzieren oder eliminieren. Die vorliegende Arbeit soll aufzeigen, welche Maßnahmen ergriffen werden können und, wie man die Effizienz dieser Maßnahmen einschätzen kann.

Interessenkonflikt: Nein

Literatur

- 1 Crone RA, Leuridan OMA. Tolerance for aniseikonia. I. Diplopia thresholds in the vertical and horizontal meridians of the visual field. *Albrecht v Graefes Archiv für Ophthalmologie* 1973; 31: 1–16
- 2 Crone RA, Leuridan OMA. Tolerance for aniseikonia. II. Determination based on the amplitude of cyclofusion. *Albrecht v Graefes Archiv für Ophthalmologie* 1973; 31: 17–22
- 3 Gullstrand A. Anhang zu Teil 1. In: von Helmholtz H (Hrsg). *Physiologische Optik*. Hamburg: Voss, 1909; 3. Ausgabe, Band 1: 350–358
- 4 Haigis W. Biometrie. In: Straub W, Kroll P, Küchle HJ (Hrsg). *Augenärztliche Untersuchungsmethoden*. Biermann, 1995: 255–304
- 5 Haigis W. Pseudophakic correction factors for optical biometry. *Graefes Arch Clin Exp Ophthalmol* 2001; 239: 589–598
- 6 Harris WF. Magnification, blur, and ray state at the retina for the general eye with and without a general optical instrument in front of it. 1. Distant objects. *Optom Vis Sci* 2001; 78: 888–900
- 7 Harris WF. Magnification, blur, and ray state at the retina for the general eye with and without a general optical instrument in front of it. 2. Near objects. *Optom Vis Sci* 2001; 78: 901–905
- 8 Harris WF, MacKenzie GE. The thin intraocular lens required for a given target refraction. *S Afr Optom* 2003; 62: 3–7

DOI:10.14753/SE.2021.2503

- 9 Kooijman AC. Light distribution on the retina of a wide-angle theoretical eye. *J Opt Soc Am* 1983; 73: 1544–1550
- 10 Kramer PW, Lubkin V, Pavlica M et al. Symptomatic aniseikonia in unilateral and bilateral pseudophakia. A projection space eikonometer study. *Binocul Vis Strabismus* 1999; Q 14: 183–190
- 11 Langenbacher A, Huber S, Nguyen NX et al. Cardinal points and object-image magnification with an accommodative lens implant (1 CU). *Ophthal Physiol Opt* 2003; 23: 61–70
- 12 Langenbacher A, Seitz B. Calculation scheme for bitoric eikonic intraocular lenses. *Ophthal Physiol Opt* 1999; 23: 213–220
- 13 Langenbacher A, Reese S, Huber S et al. Compensation of aniseikonia with toric intraocular lenses and spherocylindrical spectacles. *Ophthalmic Physiol Opt* 2005; 25: 35–44
- 14 MacKenzie GE, Harris WF. The thick intraocular lens required for a given target refraction. *S Afr Optom* 2003; 62: 66–71
- 15 Naeser K. Intraocular lens power formula based on vergence calculation and lens design. *J Cataract Refract Surg* 1997; 23: 1200–1207
- 16 Naeser K, Boberg-Ans J, Bargum R. Biometry of the posterior lens capsule: a new method to predict pseudophakic anterior chamber depth. *J Cataract Refract Surg* 1990; 16: 202–206
- 17 Navarro R, Santamaria J, Bescos J. Accommodation-dependent model of the human eye with aspherics. *J Opt Soc Am* 1985; 2: 1273–1281
- 18 Norrby NE, Koranyi G. Prediction of intraocular lens power using the lens haptic plane concept. *J Cataract Refract Surg* 1997; 23: 254–259
- 19 Olsen T, Corydon L, Gimbel H. Intraocular lens power calculation with an improved anterior chamber depth prediction algorithm. *J Cataract Refract Surg* 1995; 21: 313–319
- 20 Rosenblum WM, Christensen JL. Optical matrix method: Optometric applications. *Am J Optom Physiol Optics* 1974; 51: 961–968
- 21 Scarpatetti A. Binocular vision after lens implantation. *Acta Ophthalmol Scand* 1983; 61: 844–850

Modeling of lateral magnification changes due to changes in corneal shape or refraction [☆]

Achim Langenbucher ^{a,*}, Berthold Seitz ^b, Nóra Szentmáry ^c

^a Department of Medical Physics, Friedrich-Alexander-University Erlangen-Nürnberg, Henkestrasse 91, D-91052 Erlangen, Germany

^b Department of Ophthalmology, University of Saarland, Homburg (Saar), Germany

^c Department of Ophthalmology, Semmelweis University, Budapest, Hungary

Received 11 January 2007; received in revised form 23 May 2007

Abstract

Background and Purpose: Especially after corneal surgery the lateral magnification of the eye providing the retinal image size of an object is a crucial factor influencing visual acuity and binocularity. The purpose of this study is to describe a paraxial computing scheme calculating lateral magnification changes (ratio of the image sizes before and after surgery) due to variation in corneal shape and spectacle refraction.

Calculation strategy: From the 4×4 refraction and translation matrices the system matrix representing the entire 'optical system eye' and the pupil matrix describing the sub-system from the spectacle correction to the aperture stop were defined for the state before and after surgery. As the chief ray is assumed to pass through the centre of the aperture stop, the 2×2 matrix of the lateral magnification ratio from preoperative to postoperative is described by the 2×2 sub-matrices of the respective pupil matrices. The cardinal meridians can be extracted by calculating the eigenvalues and eigenvectors.

Working example: Vertex distance 14 mm, measured distance between corneal apex and aperture stop 3.6 mm, keratometry 39 D + 6 D/0° to 47 D + 3 D/30° and refraction 3.5 D – 5 – 5 D/5° to –4.0 D – 3.5 D/25° preoperatively to postoperatively. The matrix of magnification ratio from preop to postop yields (0.8960 – 0.0085; 0.0074 0.9371) and the eigenvalues decomposition provided a 10.7% minified image at 170.1° and a minified image of 6.1% at 78.7°, which both are clinically relevant.

Conclusion: We presented a straight-forward computer-based strategy for calculation of retinal image size changes using 4×4 matrix notation. With this model the meridional changes in lateral magnification from the preoperative to the postoperative stage or between follow-up stages can be estimated from keratometry, refraction, vertex distance and anterior chamber depth, which might be important for binocularity and vision tests in corneal surgery.

© 2007 Elsevier Ltd. All rights reserved.

Keywords: Lateral magnification; Corneal shape; Refractive change; Mathematical modeling; Matrix representation

1. Introduction

In an ophthalmological examination the visual function is normally evaluated as an isolated parameter beside other clinical parameters such as keratometry or refraction at

spectacle or corneal plane. But especially after corneal refractive surgery, corneal grafting or cataract surgery, the lateral magnification of the eye providing the retinal image size of an object is a crucial collateral factor influencing the potential visual acuity of an individual.

In case, when corneal shape is changed inducing a change in the refractive state and the refractive conditions of the posterior segment of the eye (lens, vitreous) remain unchanged, the exit pupil of the eye is not affected. In such situations, the change in lateral magnification of the entire 'optical system eye' can be determined in a simple

[☆] The authors have no proprietary interest in the development or marketing of this or any competing instrument or piece of equipment.

* Corresponding author. Fax: +49 9131 8522824.

E-mail address: achim.langenbucher@imp.uni-erlangen.de (A. Langenbucher).

calculation scheme considering the change in corneal architecture and (spectacle) refraction. That magnification change has to be taken into account in evaluating changes in visual outcome and to differentiate between an intrinsic and an extrinsic part.

In the last decades, raytracing strategies for evaluation of the optical properties of optical systems became more and more popular. A matrix based description of spherical optical systems in ophthalmologic applications has first been investigated by (Rosenblum & Christensen, 1974; Long, 1979) and later used by many other investigators. This formalism breaks down any spherical optical system into a product of 2×2 refraction and translation matrices and the resulting system matrix relates the slope and height of an incident ray to the respective slope and height of the exiting ray. Then, Keating (Harris, 1999, 2000; Keating, 1980, 1981a, 1981b) was the first to introduce a generalization of these 2×2 matrices to astigmatic systems described by 4×4 system matrices. In accordance with the spherical case, this generalized formulation of astigmatic optical systems breaks down into 4×4 refraction and translation matrices and the system matrix relates the impinging ray with slopes in x - and y -direction and intersection co-ordinates x and y at the first refractive surface to the respective slopes in x - and y -direction and the co-ordinates x and y of the exiting ray at the last refractive surface of the optical system (Langenbucher & Seitz, 2003). Without restriction to coaxiality, a spherical system may be described using 3×3 system matrices (Gerrard & Burch, 1975) and astigmatic optical systems containing decentred optical surfaces are consequently represented by 5×5 system matrices (Harris, 1994). In the present study, we restrict to a coaxial optical setup containing spherical and astigmatic surfaces.

The purpose of this paper was to describe a straight-forward mathematical matrix-based strategy for calculating lateral magnification changes (ratio of the image sizes before and after surgery) due to variation in corneal shape and spectacle refraction under the constriction, that other biometrical parameters of the eye remain unchanged. The applicability of this calculation scheme will be demonstrated in two working examples.

1.1. Refraction and translation matrices and the system matrix

In spherical optical systems, the refraction matrices R and translation matrices T can be written in the form

$$R = \begin{bmatrix} 1 & -P \\ 0 & 1 \end{bmatrix}, \quad T = \begin{bmatrix} 1 & 0 \\ \frac{d}{n} & 1 \end{bmatrix}, \quad (1)$$

where P refers to the dioptric power of a refractive surface, d is the interspace between surfaces and n is the refractive index of the medium (Rosenblum & Christensen, 1974; Langenbucher, Huber, Nguyen, Seitz, & Kühle, 2003; Long, 1979). An optical system consisting of m refractive surfaces (1 to m from left to right) with dioptric powers

P_1 to P_m , and interspaces $d_{1,2}$ to $d_{m-1,m}$ (refractive indices $n_{1,2}$ to $n_{m-1,m}$) the system matrix S reads

$$S = R_m \cdot T_{m-1,m} \cdot R_{m-1} \cdot T_{m-2,m-1} \cdots R_2 \cdot T_{1,2} \cdot R_1 \quad (2)$$

and any incident ray from the left (surface 1) with a slope angle α_0 and a height y_0 will exit the system at surface m with a slope angle α and a height y so that

$$\begin{pmatrix} \alpha \\ y \end{pmatrix} = S \cdot \begin{pmatrix} \alpha_0 \\ y_0 \end{pmatrix}. \quad (3)$$

In any astigmatic system, the respective refraction matrix R reads

$$R = \begin{bmatrix} 1 & 0 & X & Y \\ 0 & 1 & Y & Z \\ 0 & 0 & 1 & 0 \\ 0 & 0 & 0 & 1 \end{bmatrix} \quad (4)$$

and the translation matrix T is defined as

$$T = \begin{bmatrix} 1 & 0 & 0 & 0 \\ 0 & 1 & 0 & 0 \\ \frac{d}{n} & 0 & 1 & 0 \\ 0 & \frac{d}{n} & 0 & 1 \end{bmatrix}. \quad (5)$$

Elements X , Y and Z of the refraction matrix are given with

$$\begin{aligned} X &= -(\text{SPH} + \text{CYL} \cdot \sin^2(\varphi)), \\ Z &= -(\text{SPH} + \text{CYL} \cdot \cos^2(\varphi)), \\ Y &= \text{CYL} \cdot \sin(\varphi) \cdot \cos(\varphi), \end{aligned} \quad (6)$$

where the parameters SPH, CYL and φ refer to the spherical power, cylindrical power each in diopters and the orientation of the cylinder (in degrees) and d/n refers to the reduced optical distance in the translation matrix T as defined in the spherical case.

Analogue to the 2×2 spherical case Eq. (2), the system matrix of an optical system consisting of m spherocylindrical surfaces can be written as

$$S = R_m \cdot T_{m-1,m} \cdot R_{m-1} \cdot T_{m-2,m-1} \cdots R_2 \cdot T_{1,2} \cdot R_1 = \begin{pmatrix} A & B \\ C & D \end{pmatrix} \quad (7)$$

and any incident ray from the left (surface 1) with slope angles α_{0x} and α_{0y} in x and y direction and intersection coordinates x_0 and y_0 with surface 1 will exit the system at surface m with slope angles α_x and α_y at coordinates x and y so that

$$\begin{pmatrix} \alpha_x \\ \alpha_y \\ x \\ y \end{pmatrix} = S \cdot \begin{pmatrix} \alpha_{0x} \\ \alpha_{0y} \\ x_0 \\ y_0 \end{pmatrix}. \quad (8)$$

The 2×2 sub-matrices A , B , C and D refer to A : magnification, B : divergence or negative of the power matrix, C : disjucy, and D : dilation. The reverse calculation of the

elements SPH, CYL and φ from the sub-matrix A can easily be performed with the trace and the determinant if A is a symmetric matrix.

1.2. Definition of the 'optical system eye' before and after surgical intervention with matrices

The optical system of an eye containing spherocylindrical surfaces is characterized in the simplest form with a spherocylindrical spectacle correction, a single surface cornea, and a crystalline lens (MacKenzie & Harris, 2002). Thus, before surgical intervention the matrix representation of the entire system starting from the spectacle plane and ending at the retina is represented with a system matrix S with

$$S_{pr} = T_V \cdot R_{Lback} \cdot T_L \cdot R_{Lfront} \cdot T_{ACDpr} \cdot R_{Cpr} \cdot T_{Spr} \cdot R_{Spr}, \quad (9)$$

where T_V refers to the vitreous space, R_{Lback} and R_{Lfront} refer to the refraction matrices of the back and front surface of the crystalline lens, T_L to the central thickness of the lens, T_{ACDpr} refers to the phakic anterior chamber of the eye, R_{Cpr} to the corneal surface, T_{Spr} to the vertex distance from the cornea to the spectacle plane and R_{Spr} to the intended target refraction before cataract surgery at spectacle plane. The matrices T_{ACDpr} , R_{Cpr} , T_{Spr} and R_{Spr} are known from ultrasound or optical biometry, keratometry and refractometry and are potentially subject to change during intervention, whereas the other matrices can be assumed to be stable. The respective optical system after the surgical intervention reads

$$S_{po} = T_V \cdot R_{Lback} \cdot T_L \cdot R_{Lfront} \cdot T_{ACDpo} \cdot R_{Cpo} \cdot T_{Spo} \cdot R_{Spo}. \quad (10)$$

For simplicity of the formalism, we define for the preoperative and postoperative state a subsystem S_{PUPpr} and S_{PUPpo} which includes the part of the optical system from the spectacle correction to the aperture stop

$$\begin{aligned} S_{PUPpr} &= T_{ACDpr} \cdot R_{Cpr} \cdot T_{Spr} \cdot R_{Spr}, \\ S_{PUPpo} &= T_{ACDpo} \cdot R_{Cpo} \cdot T_{Spo} \cdot R_{Spo}. \end{aligned} \quad (11)$$

1.3. Determination of the relative lateral magnification

In case the spectacle correction fully compensates the spherocylindrical refraction error at spectacle plane, matrix C equals zero and the lateral magnification of the eye is characterized by the retinal image size divided by the angle of the incident ray. The respective magnification matrix is given by the lower right 2×2 matrix D of the system matrix S . As the respective matrices for the crystalline lens cannot be derived with common measurement techniques (in vivo phakometry), the absolute magnification of the eye cannot be extracted.

Instead, as the reference ray traced through the eye has to pass through the centre of the pupil and all dimensions and curvature data in the anterior segment of the eye from

the spectacle to the plane of the aperture stop (S_{PUPpr} and S_{PUPpo}) are known, the change in magnification due to the change of corneal shape or refraction can be derived in case the exit pupil does not change.

An arbitrary ray entering the optical system at the spectacle is passing through the pupil centre if x and y equal zero:

$$\begin{pmatrix} \alpha_x \\ \alpha_y \\ x \\ y \end{pmatrix} = S_{PUP} \cdot \begin{pmatrix} \alpha_{0x} \\ \alpha_{0y} \\ x_0 \\ y_0 \end{pmatrix} = \begin{pmatrix} A_{PUP} & B_{PUP} \\ C_{PUP} & D_{PUP} \end{pmatrix} \cdot \begin{pmatrix} \alpha_0 \\ y_0 \end{pmatrix} = \begin{pmatrix} \cdot \\ 0 \end{pmatrix}, \quad (12)$$

where α or y_0 refer to the 2×1 vector with the components α_x and α_y or the coordinates x and y . Eq. (12) can be written as

$$\begin{aligned} C_{PUP} \cdot \alpha_0 + D_{PUP} \cdot y_0 &= 0, \\ y_0 &= -D_{PUP}^{-1} \cdot C_{PUP} \cdot \alpha_0. \end{aligned} \quad (13)$$

Together with Eq. (13), the slope angle α at the aperture stop is related to the slope angle α_0 of a ray entering the optical system by

$$\begin{aligned} \alpha &= A_{PUP} \cdot \alpha_0 - B_{PUP} \cdot D_{PUP}^{-1} \cdot C_{PUP} \cdot \alpha_0, \\ &= (A_{PUP} - B_{PUP} \cdot D_{PUP}^{-1} \cdot C_{PUP}) \alpha_0. \end{aligned} \quad (14)$$

As the exit pupil is determined by the optical pathway between the aperture stop and the retina and is assumed to be unchanged due to the surgical intervention, the lateral magnification change (ratio of the image sizes before and after surgery) due to the intervention M_{rel} is calculated from the angle magnifications M_{PUPpr} and M_{PUPpo} preoperatively and postoperatively by

$$\begin{aligned} M_{relPUP} &= M_{PUPpo} \cdot M_{PUPpr}^{-1} \\ &= (A_{PUPpo} - B_{PUPpo} \cdot D_{PUPpo}^{-1} \cdot C_{PUPpo}) \\ &\quad \cdot (A_{PUPpr} - B_{PUPpr} \cdot D_{PUPpr}^{-1} \cdot C_{PUPpr})^{-1}. \end{aligned} \quad (15)$$

As we postulate, that the ray is passing through the centre of the aperture stop, the system is not necessarily fully corrected in refraction. If the system is not fully corrected by the spectacle lens, Eq. (15) gives the change in magnification of the blurred images due to the surgical intervention.

The cardinal meridians of magnification are extracted from the 2×2 matrix M_{relPUP} by deriving the eigenvectors and the eigenvalues (Arfken, 1985). Thus, the eigenvalues are directly related to the change in magnification and the respective eigenvectors provide information about the orientation of the cardinal meridians:

$$M_{relPUP} = H^{-1} \cdot I \cdot H, \quad (16)$$

where H is the 2×2 matrix containing the eigenvectors and I refers to the diagonal matrix containing the eigenvalues. From H we extract the orientation of the meridians φ_1 and φ_2 in the classical form to

$$H = \begin{pmatrix} h_{11} & h_{12} \\ h_{21} & h_{22} \end{pmatrix} \Rightarrow \varphi_1 = \arctan\left(\frac{h_{21}}{h_{11}}\right), \quad \varphi_2 = \arctan\left(\frac{h_{22}}{h_{12}}\right). \quad (17)$$

In the special case if the axes of the spectacle cylinder and the corneal astigmatism are aligned (or orthogonal), the cardinal meridians φ_1 and φ_2 are orthogonal, but in general H is not a symmetric matrix and both meridians are not orthogonal.

2. Working examples

2.1. Example 1

For the first example we assume a vertex distance of 14 mm preoperatively and postoperatively and a measured anterior chamber depth of 3.6 mm (from corneal apex to the anterior apex of the lens, which is assumed to coincide with the aperture stop plane). The keratometry changed from 41.5 D + 4.5 D/15° preoperatively to 44.0 D + 2.5 D/25° after the surgical intervention. Spectacle refraction changed from +1.0 D – 3.5 D/15° to –1.0 D – 1.0 D/115°. In this example, the orientation of the spectacle cylinder and the corneal astigmatism is aligned before and after the intervention. The refractive index of the aqueous humour is assumed to be 1.3374.

Using Eq. (4), the refraction matrices prior to and after surgical intervention read with a precision of four digits

$$R_{Spr} = \begin{bmatrix} 1 & 0 & -0.7655 & -0.8750 \\ 0 & 1 & -0.8750 & 2.2655 \\ 0 & 0 & 1 & 0 \\ 0 & 0 & 0 & 1 \end{bmatrix},$$

$$R_{Spo} = \begin{bmatrix} 1 & 0 & 1.8214 & 0.3830 \\ 0 & 1 & 0.3830 & 1.1786 \\ 0 & 0 & 1 & 0 \\ 0 & 0 & 0 & 1 \end{bmatrix},$$

$$R_{Cpr} = \begin{bmatrix} 1 & 0 & -41.8014 & 1.1250 \\ 0 & 1 & 1.1250 & -45.6986 \\ 0 & 0 & 1 & 0 \\ 0 & 0 & 0 & 1 \end{bmatrix},$$

$$R_{Cpo} = \begin{bmatrix} 1 & 0 & -44.4465 & 0.9576 \\ 0 & 1 & 0.9576 & -46.0535 \\ 0 & 0 & 1 & 0 \\ 0 & 0 & 0 & 1 \end{bmatrix},$$

and using Eq. (5) the translation matrices read

$$T_{Spr} = T_{Spo} = \begin{bmatrix} 1 & 0 & 0 & 0 \\ 0 & 1 & 0 & 0 \\ 0.0140 & 0 & 1 & 0 \\ 0 & 0.0140 & 0 & 1 \end{bmatrix},$$

$$T_{ACDpr} = T_{ACDpo} = \begin{bmatrix} 1 & 0 & 0 & 0 \\ 0 & 1 & 0 & 0 \\ 0.0027 & 0 & 1 & 0 \\ 0 & 0.0027 & 0 & 1 \end{bmatrix}.$$

Multiplying the refraction and translation matrices together using Eq. (11), the system-matrix characterizing

the sub-system from the spectacle to the aperture stop before and after surgical intervention read

$$S_{PUPpr} = \begin{bmatrix} 0.4148 & 0.0158 & -42.1328 & 0.7978 \\ 0.0158 & 0.3602 & 0.7978 & -44.8962 \\ 0.0151 & 0.0000 & 0.8759 & -0.0101 \\ 0.0000 & 0.0150 & -0.0101 & 0.9109 \end{bmatrix},$$

$$S_{PUPpo} = \begin{bmatrix} 0.3777 & 0.0134 & -43.7534 & 1.1180 \\ 0.0134 & 0.3553 & 1.1180 & -45.6296 \\ 0.0150 & 0.0000 & 0.9077 & 0.0084 \\ 0.0000 & 0.0150 & 0.0084 & 0.8937 \end{bmatrix}.$$

Using Eq. (15), the change in magnification is calculated to

$$M_{relPUP} = \begin{bmatrix} 0.9651 & -0.0205 \\ -0.0203 & 1.0194 \end{bmatrix}$$

and after extracting the eigenvectors and eigenvalues according to Eq. (16)

$$M_{relPUP} = \begin{bmatrix} -0.9489 & 0.3182 \\ -0.3156 & -0.9480 \end{bmatrix}^{-1} \cdot \begin{bmatrix} 0.9583 & 0 \\ 0 & 1.0263 \end{bmatrix} \cdot \begin{bmatrix} -0.9489 & 0.3182 \\ -0.3156 & -0.9480 \end{bmatrix}$$

and re-converted to standard notation using Eq. (17), we get a magnification change of 0.9583 in an axis of 18.4° and 1.0263 in an axis of 108.6°. This means clinically, that in an orientation of 18.4° the image is minified by 4.17% and in an orientation of 108.6° the image is magnified by 2.63% due to surgical intervention.

2.2. Example 2

For the second example we assume a vertex distance of 14 mm preoperatively and postoperatively and a measured anterior chamber depth of 3.6 mm (from corneal apex to the anterior apex of the lens, which is assumed to coincide with the aperture stop plane). The keratometry changed from 39.0 D + 6.0 D/0° preoperatively to 47.0 D + 3.0 D/30° after the surgical intervention. Spectacle refraction changed from +3.5 D – 5.5 D/5° to –4.0 D – 3.5 D/25°. In this example, the orientation of the spectacle cylinder and the corneal astigmatism is not aligned before and after the intervention. For calculation of the absolute object–image magnification, the axial length of the eye is 23.8 mm, the central thickness of the crystalline lens is 3.6 mm. The dioptric power of the front/back surface measured by phakometry is determined to be 8.26 D/14.0 D (radii of curvature: 10.0 and 6.0 mm). The refractive index of the aqueous humour/crystalline lens/vitreous is assumed to be 1.3374/1.4200/1.3360.

Using Eq. (4), the refraction matrices prior to and after surgical intervention read with a precision of four digits

$$R_{Spr} = \begin{bmatrix} 1 & 0 & -3.4582 & -0.4775 \\ 0 & 1 & -0.4775 & 1.9582 \\ 0 & 0 & 1 & 0 \\ 0 & 0 & 0 & 1 \end{bmatrix},$$

$$R_{Spo} = \begin{bmatrix} 1 & 0 & 4.6251 & -1.3406 \\ 0 & 1 & -1.3406 & 6.8749 \\ 0 & 0 & 1 & 0 \\ 0 & 0 & 0 & 1 \end{bmatrix},$$

$$R_{Cpr} = \begin{bmatrix} 1 & 0 & -39.0000 & 0.0000 \\ 0 & 1 & 0.0000 & -45.0000 \\ 0 & 0 & 1 & 0 \\ 0 & 0 & 0 & 1 \end{bmatrix},$$

$$R_{Cpo} = \begin{bmatrix} 1 & 0 & -47.7500 & 1.2990 \\ 0 & 1 & 1.2990 & -49.2500 \\ 0 & 0 & 1 & 0 \\ 0 & 0 & 0 & 1 \end{bmatrix},$$

$$R_{Lfront} = \begin{bmatrix} 1 & 0 & -8.2600 & 0.0000 \\ 0 & 1 & 0.0000 & -8.2600 \\ 0 & 0 & 1 & 0 \\ 0 & 0 & 0 & 1 \end{bmatrix},$$

$$R_{Lback} = \begin{bmatrix} 1 & 0 & -14.0000 & 0.0000 \\ 0 & 1 & 0.0000 & -14.0000 \\ 0 & 0 & 1 & 0 \\ 0 & 0 & 0 & 1 \end{bmatrix},$$

and using Eq. (5) the translation matrices read

$$T_{Spr} = T_{Spo} = \begin{bmatrix} 1 & 0 & 0 & 0 \\ 0 & 1 & 0 & 0 \\ 0.0140 & 0 & 1 & 0 \\ 0 & 0.0140 & 0 & 1 \end{bmatrix},$$

$$T_{ACDpr} = T_{ACDpo} = \begin{bmatrix} 1 & 0 & 0 & 0 \\ 0 & 1 & 0 & 0 \\ 0.0027 & 0 & 1 & 0 \\ 0 & 0.0027 & 0 & 1 \end{bmatrix},$$

$$T_L = \begin{bmatrix} 1 & 0 & 0 & 0 \\ 0 & 1 & 0 & 0 \\ 0.0025 & 0 & 1 & 0 \\ 0 & 0.0025 & 0 & 1 \end{bmatrix},$$

$$T_V = \begin{bmatrix} 1 & 0 & 0 & 0 \\ 0 & 1 & 0 & 0 \\ 0.0124 & 0 & 1 & 0 \\ 0 & 0.0124 & 0 & 1 \end{bmatrix},$$

Multiplying the refraction and translation matrices together using Eq. (11), the system-matrix characterizing the sub-system from the spectacle to the aperture stop before and after surgical intervention read

$$S_{PUPpr} = \begin{bmatrix} 0.4540 & 0.0000 & -40.5700 & -0.2168 \\ 0.0000 & 0.3700 & -0.1767 & -44.2755 \\ 0.0152 & 0.0000 & 0.8424 & -0.0073 \\ 0.0000 & 0.0150 & -0.0072 & 0.9082 \end{bmatrix},$$

$$S_{PUPpo} = \begin{bmatrix} 0.3315 & 0.0182 & -46.2412 & 0.9797 \\ 0.0182 & 0.3105 & 0.9669 & -47.1397 \\ 0.0149 & 0.0000 & 0.9403 & 0.0161 \\ 0.0000 & 0.0148 & -0.0162 & 0.9694 \end{bmatrix}.$$

Using Eq. (15), the change in magnification is calculated to

$$M_{relPUP} = \begin{bmatrix} 0.8960 & 0.0085 \\ 0.0074 & 0.9371 \end{bmatrix}$$

and after extracting the eigenvectors and eigenvalues according to Eq. (16)

$$M_{relPUP} = \begin{bmatrix} -0.9852 & -0.1957 \\ 0.1716 & -0.9807 \end{bmatrix}^{-1} \cdot \begin{bmatrix} 0.8945 & 0 \\ 0 & 0.9386 \end{bmatrix} \cdot \begin{bmatrix} -0.9852 & -0.1957 \\ 0.1716 & -0.9807 \end{bmatrix}$$

and re-converted to standard notation using Eq. (17), we get a magnification change of 0.8945 in an axis of 170.1° and 0.9386 in an axis of 78.7°. This means clinically, that in an orientation of 170.1° the image is minified by 10.7% and in an orientation of 78.7° the image is minified by 6.1% due to surgical intervention. If we multiply together the complete system matrix using Eqs. (9) and (10), we get

$$S_{pr} = \begin{bmatrix} 0.1035 & 0.0000 & -57.6345 & -0.0494 \\ 0.0000 & 0.0275 & -0.0131 & -62.6550 \\ 0.0173 & 0.0000 & 0.0058 & -0.0083 \\ 0.0000 & 0.0150 & -0.0076 & -0.0015 \end{bmatrix},$$

$$S_{po} = \begin{bmatrix} -0.0074 & 0.0165 & -65.2549 & 1.2992 \\ 0.0165 & -0.0264 & 1.2877 & -66.7603 \\ 0.0153 & 0.0003 & -0.0074 & 0.0028 \\ 0.0003 & 0.0150 & 0.0026 & 0.0000 \end{bmatrix}.$$

As the upper left 2×2 sub-matrix of the system matrix differs from the null matrix (Langenbacher, Reese, Huber, & Seitz, 2005), the complete system is not fully corrected and the image at the retina is blurred. If we postulate, that phakometry and keratometry as well as the distances measured by biometry are measured correctly, the refraction matrix for a fully correcting spectacle reads

$$\begin{bmatrix} 1 & 0 & -3.7909 & 0.0000 \\ 0 & 1 & 0.0000 & 2.0541 \\ 0 & 0 & 1 & 0 \\ 0 & 0 & 0 & 1 \end{bmatrix}$$

before surgery and

$$\begin{bmatrix} 1 & 0 & 5.1143 & -1.5255 \\ 0 & 1 & -1.5255 & 6.8757 \\ 0 & 0 & 1 & 0 \\ 0 & 0 & 0 & 1 \end{bmatrix}$$

after surgery. From these matrices, we derive a fully correcting spectacle refraction of $+3.7909 \text{ D} - 5.8450 \text{ D}/0^\circ$ before and $-4.2335 \text{ D} - 3.5229 \text{ D}/30^\circ$ after surgery. The absolute lateral magnification M relating the lateral size of an object on the retina to the slope of the incident ray in the case of a blurred image (Langenbucher et al., 2005; Harris, 2001a, 2001b) yields

$$x = C_{pr} \cdot \alpha_0 - D_{pr} \cdot D_{PUP}^{-1} \cdot C_{PUP} \cdot \alpha_0 = M_{pr} \cdot \alpha,$$

$$M_{pr} = \begin{bmatrix} 0.0172 & 0.0001 \\ 0.0001 & 0.0160 \end{bmatrix},$$

$$x = C_{po} \cdot \alpha_0 - D_{po} \cdot D_{PUP}^{-1} \cdot C_{PUP} \cdot \alpha_0 = M_{po} \cdot \alpha,$$

$$M_{po} = \begin{bmatrix} 0.0154 & 0.0003 \\ 0.0003 & 0.0150 \end{bmatrix}.$$

Calculating the relative change in magnification from the state before surgical intervention to the state after surgical intervention, we get

$$M_{rel} = M_{po} \cdot M_{pr}^{-1} = \begin{bmatrix} 0.8960 & 0.0085 \\ 0.0074 & 0.9371 \end{bmatrix},$$

which can be interpreted as a proof of concept for our mathematical strategy.

3. Discussion

A series of surgical interventions especially at the cornea change the corneal architecture significantly resulting in a shift of the sphere and/or of the astigmatism. Even if the net astigmatism is not changed, a rotation of the astigmatism axis refers to a change of the optical path. Many surgeons more or less ignore the effect of lateral magnification and focus on a full refractive correction of the eye. But an adequate correction of the eye i.e. using spherical or spherocylindrical glasses is not able to compensate for magnification disparities, because the corneal and the spectacle plane do not coincide. It is generally accepted, that minus lenses for correction of myopia minify the retinal image, whereas plus lenses for correction of hyperopia magnify the retinal image. This effect may for example in cataract surgery with posterior chamber lens implantation influence the potential visual acuity significantly, when the lens power is calculated inappropriately. If the power of the intraocular lens is too low and the resulting hyperopia is corrected with plus glasses, the magnification is increased and we expect an artificially increased visual acuity. The opposite can be observed, when the lens power is too high and the resulting myopia is corrected with minus lenses. Fusion of disparate images can be achieved if the difference in magnification between the two eyes does not exceed 5% (Kramer, Lubkin, Pavlica, & Covin, 1999;

Krzizok, Kaufmann, & Schwerdtfeger, 1996; Scarpatetti, 1983). In the astigmatic eye the difference in magnification should not exceed 5% in any meridian to preserve a proper fusion of the retinal images. In other words the spherocylindrical telescope including the spectacle correction and the cornea must present to the retina an image of approximately the same size as the image in the fellow eye for all meridians.

Thus, especially surgeons who are working on the anterior segment of the eye should consider beside a proper correction of ametropia with spectacles the lateral magnification of the eye and the change of magnification to surgery. If only the corneal architecture of the eye is changed during the intervention and all other relevant parameters in the optical systems such as the lens, the anterior chamber depth and the axial length remain stable, the calculation of the change in magnification of the eye is not very complex. However, for determination of the total magnification lacks if there are no data of the anterior chamber depth, the vitreous length and the lens geometry.

In the present paper we derived a matrix based methodology for determination of the change in lateral magnification of the eye (ratio of the image sizes before and after surgery) due to a change in corneal shape corrected by a spectacle lens. This concept is a straight-forward strategy of tracing a pencil of rays through the optical system eye restricting to a coaxial optical system in the Gaussian paraxial space.

The system matrix of the eye breaks down into a product of 4×4 refraction matrices representing the refracting surfaces in the optical system and 4×4 translation matrices representing the interspaces between surfaces. For the formulation of the refraction matrices, we follow the notation introduced by Keating (Keating, 1981a, 1981b) and Harris (Harris, 1999, 2000, 2001a, 2001b). The system matrix representing the entire optical system is therefore a product of the refraction and translation matrices. With the typical structure of the refraction and translation matrices as well as the system matrix, the 4×4 system matrix can be subdivided into 4 2×2 sub-matrices A , B , C and D . For example, a fully corrected system starting from the first refracting surface to the focal plane is characterized with the condition, that for a bundle of rays parallel to the optical axis entering the system from left is focussed to a single point irrespective the height of the ray at the first refracting surface. That means that the sub-matrix A equals the null matrix. The power of the matrix notation for characterizing the optical system eye or for determination of toric intraocular lenses could be demonstrated in a series of previous papers (Langenbucher, Reese, Sauer, & Seitz, 2004, 2005). The re-conversion of a sub-matrix to the standard notation can be realized by using the trace and the determinant of the matrix (Langenbucher et al., 2004) or by calculating the eigenvectors and the eigenvalues of the matrix. The first re-conversion technique is restricted to symmetric 2×2 matrices and fail, if the matrix is not symmetric.

In the present paper, the applicability of the mathematical formalism is demonstrated with two working examples

in a step-by-step approach. In example 1, the cylinder axis of the spectacle correction matches the axis of the corneal astigmatism perfectly before and after the surgical intervention. We assume, that we do not have data about the axial length, the geometry of the crystalline lens (Preussner, Wahl, & Lahdo, 2002). With the refraction data and the corneal shape before and after surgery together with the anterior chamber depth and the vertex distance we calculate the meridional magnification change of the eye due to surgery. Even if our concept is not restricted to a stable vertex distance or anterior chamber depth, these values are normally not changed significantly during surgery and we assumed that both values remain unchanged. We found, that the optical system changes the magnification in two orthogonal meridians: in the one cardinal meridian the image is magnified by 2.63%, whereas in the other cardinal meridian the image is minified by 4.17%. In example 2, we assumed a more pronounced change of the corneal shape due to the surgical intervention. The axes of the corneal astigmatism and refractive cylinder were not properly aligned before and after surgery (5° difference) and thus we did not get orthogonal meridians for the change of ocular magnification. We found, that in an orientation of 170.1° the image is minified by 10.7% and in an orientation of 78.7° the image is minified by 6.1%. For completeness, we included all relevant data for determining the total magnification of the eye: axial length, curvature of the front and back surface of the crystalline lens as well as the central thickness of the lens. Applying the same strategy as in example 1 we derived the magnification change by comparing the slope angle of a ray entering the system and the respective slope angle passing through the centre of the pupil. In a second step, we determined the system matrix of the entire optical system and extracted the blurred image magnification matrices before and after the surgical intervention. Comparing both matrices, we could verify the results of our concept.

In conclusion, we presented a mathematical straight-forward matrix-based strategy for calculation of the meridional magnification changes due to a change of corneal shape and spectacle correction during a surgical intervention. This methodology can be applied for estimating the image size disparities of different meridians of one eye or between both eyes of an individual and may be of clinical relevance for the assessment of aniseikonia after corneal surgery in case of significant change of corneal shape, especially in high corneal astigmatism.

Appendix A. Supplementary data

Supplementary data associated with this article can be found, in the online version, at doi:10.1016/j.visres.2007.05.015.

References

- Arfken, G. (1985). Eigenvectors, eigenvalues. §4.7 in *Mathematical methods for physicists* (3rd ed.). Orlando, FL: Academic Press (pp. 229–237).
- Gierrard, A., & Burch, J. M. (1975). *Introduction to matrix methods in optics*. London: Wiley, p. 287.
- Harris, W. F. (1994). Paraxial ray tracing through noncoaxial astigmatic optical systems, and 5x5 augmented system matrix. *Optometry and Vision Science*, 71, 282–285.
- Harris, W. F. (1999). A unified paraxial approach to astigmatic optics. *Optometry and Vision Science*, 76, 480–499.
- Harris, W. F. (2000). Interconverting the matrix and principal-meridional representations of dioptric power and reduced vergence. *Ophthalmic & Physiological Optics*, 20, 494–500.
- Harris, W. F. (2001a). Magnification, blur, and ray state at the retina for the general eye with and without a general optical instrument in front of it. 1. Distant objects. *Optometry and Vision Science*, 78, 888–900.
- Harris, W. F. (2001b). Magnification, blur, and ray state at the retina for the general eye with and without a general optical instrument in front of it. 2. Near objects. *Optometry and Vision Science*, 78, 901–905.
- Keating, P. K. (1980). An easier method to obtain the sphere, cylinder and axis from an off-axis dioptric power matrix. *American Journal of Optometry and Physiological Optics*, 57, 734–737.
- Keating, P. K. (1981a). A system matrix for astigmatic optical systems: I. Introduction and dioptric power relations. *American Journal of Optometry and Physiological Optics*, 58, 810–819.
- Keating, P. K. (1981b). A system matrix for astigmatic optical systems: II. Corrected systems including an astigmatic eye. *American Journal of Optometry and Physiological Optics*, 58, 919–929.
- Kramer, P. W., Lubkin, V., Pavlica, M., & Covin, R. (1999). Symptomatic aniseikonia in unilateral and bilateral pseudophakia. A projection space eikonometer study. *Binocular Vision & Strabismus Quarterly*, 14, 183–190.
- Krzizok, T., Kaufmann, H., & Schwerdtfeger, G. (1996). Binocular problems caused by aniseikonia and anisophoria after cataract operation. *Klinische Monatsblätter für Augenheilkunde*, 208, 477–480.
- Langenbacher, A., Huber, S., Nguyen, N. X., Seitz, B., & Küchle, M. (2003). Cardinal points and object-image magnification with an accommodative lens implant (1 CU). *Ophthalmic & Physiological Optics*, 23, 61–70.
- Langenbacher, A., Reese, S., Huber, S., & Seitz, B. (2005). Compensation of aniseikonia with toric intraocular lenses and spherocylindrical spectacles. *Ophthalmic & Physiological Optics*, 25, 35–44.
- Langenbacher, A., Reese, S., Sauer, T., & Seitz, B. (2004). Matrix-based calculation scheme for toric intraocular lenses. *Ophthalmic & Physiological Optics*, 24, 511–519.
- Langenbacher, A., & Seitz, B. (2003). Calculation scheme for bitoric eikonic intraocular lenses. *Ophthalmic & Physiological Optics*, 23, 213–220.
- Long, W. F. (1979). Matrix optics of catadioptric systems. *American Journal of Optometry and Physiological Optics*, 55, 760–764.
- MacKenzie, G. E., & Harris, W. F. (2002). Determining the power of a thin toric intraocular lens in an astigmatic eye. *Optometry and Vision Science*, 79(10), 667–671.
- Preussner, P. R., Wahl, J., & Lahdo, H. (2002). Raytracing for intraocular lens calculation. *Journal of Cataract and Refractive Surgery*, 28, 1412–1419.
- Rosenblum, W. M., & Christensen, J. L. (1974). Optical matrix method: Optometric applications. *American Journal of Optometry and Physiological Optics*, 51, 961–968.
- Scarpattetti, A. (1983). Binocular vision after lens implantation. *Acta Ophthalmologica Scandinavica*, 61, 844–850.

Faint, illegible text on the left page, likely bleed-through from the reverse side of the document.

Faint, illegible text on the right page, likely bleed-through from the reverse side of the document.

Magnification and accommodation with phakic intraocular lenses

Achim Langenbacher¹, Nóra Szentmáry² and Berthold Seitz³

¹Department of Medical Physics, University of Erlangen-Nürnberg, Erlangen, Germany, ²Department of Ophthalmology, Semmelweis University Budapest, Budapest, Hungary and ³Department of Ophthalmology, University of Saarland, Homburg (Saar), Germany

Abstract

Background and Purpose: The calculation of phakic lenses (PL) was described by van der Heijde *et al.* [*Klin. Monatsbl. Augenheilkd* (1988) Vol. 193, pp. 99–102], but a formalism for estimating relative magnification compared with spectacle correction and accommodation effects are not yet published. The purpose of this study was to describe a mathematical strategy for calculating PL and relative magnification as a function of object vergence (phakic accommodation).

Methods: Parameters used for the calculations are the spectacle refraction before and after (target refraction) surgery, the vertex distance, corneal refraction, and the predicted position of the phakic intraocular lens. The lens power is determined as the difference in vergences between the spectacle-corrected eye and the uncorrected eye at the reference plane of the predicted lens position. If we simplify the crystalline lens to a single refracting surface located at the principal plane of the crystalline lens, the vergence of the eye with spectacle correction and with PL is determined as a function of object distance [object vergence 0 D (infinity) to 10 D (object at a distance of 10 cm)] to evaluate accommodation effects of the crystalline lens.

Results: The method was applied to two clinical examples. In example 1 we calculated the power of a PL for correction of a 10-D myopia and determined the relative magnification and the vergence at the principal plane of the crystalline lens as a function of object vergence. Magnification gain increases with objects at near from 17% to 26%, whereas the vergence at the principal plane of the crystalline lens changes by 3.04 D less than in the spectacle-corrected eye. In example 2, a 20-D myopia was corrected with a PL. The gain in magnification changed from 33% to 58% with nearer objects. The change in vergence at the principal plane of the crystalline lens with objects at near was much higher with the PL compared with the spectacle correction, which implies that the refractive change necessary for focusing objects at near distance is much higher in the PL correction.

Conclusions: Even if the predictability of postoperative refraction with PL is comparable or better than in other methods of correcting high or excessive ametropia, the effects of lateral magnification change and accommodation have to be considered to avoid image-size disparities (aniseikonia) and to maintain binocular vision, especially with monocular PL implantation and anisometropia.

Keywords: intraocular lens power calculation, lateral magnification, object vergence, phakic intraocular lenses, retinal image size, vergence transformation

Received: 17 July 2006

Revised form: 28 September 2006

Accepted: 24 October 2006

Correspondence and reprint requests to: Achim Langenbacher.
Tel.: 49-9131-8525557; Fax: 49-9131-8522824.
E-mail address: achim.langenbacher@imp.uni-erlangen.de

The authors have no proprietary interest in the development or marketing of this or any competing instrument or piece of equipment.

Introduction

The association of spectacle-corrected high ametropia with poor visual quality caused by inherent optical aberrations and frequent contact lens intolerance, justifies the search for and investigation of new technologies in the correction of high ametropia. However, the surgical correction of high ametropia is controversial in the literature (Scarpattetti, 1983; Lackner *et al.*, 2003; Saxena *et al.*, 2003).

The implantation of phakic lenses (PL) is a highly effective and predictable procedure to correct high ametropia such as myopia, hyperopia, or astigmatism (van der Heijde *et al.*, 1988). In contrast to corneo-refractive surgery with excimer laser or radial keratotomy, the potential range of correction is much greater, the optical zone is much wider which enhances vision performance especially in dim light and there is no risk of keratectasia (Güell *et al.*, 2003).

Intraocular procedures capable of correcting ametropia include PL implantation, which permits optical correction of the refractive error while maintaining accommodation, and clear lens extraction, which must be done with caution especially in myopic eyes because of the potentially higher risk of retinal detachment (Colin *et al.*, 1999; Lopez, 2001; Fernandez-Vega *et al.*, 2003) and the loss of accommodation in young patients. Similar to corneo-refractive laser surgery, phakic intraocular lenses (IOL) use a smaller optical zone to treat higher ametropia (Güell *et al.*, 2003).

The implantation of anterior chamber intraocular lenses in phakic eyes has proved to be an effective and predictable technique. However, the risk of damage to anterior chamber structures, in particular the endothelium (Menezo *et al.*, 1998) initiated the development of a new concept of posterior chamber lens implantation. In 1986, Fechner and Worst modified the iris claw lens for correcting aphakia introduced by Fyodorov into a biconcave lens for correction of high myopia (Worst *et al.*, 1990). To increase the safety of this lens, the design of the lens optics was changed in 1991 to a concave-convex shape. This lens design was reported to cause less alteration to the corneal endothelium. With the introduction of the toric phakic IOL (Güell *et al.*, 2003) there are completely new options for correcting corneal or lenticular astigmatism whilst preserving the physiological accommodation of the eye. Especially in high or excessive astigmatism, where corneo-refractive laser surgery may fail because of potential complications such as flap striae, haze, reduced contrast sensitivity or glare, toric phakic IOL may be an appropriate surgical option.

In clinical practice, phakic IOL are normally calculated using the so-called van der Heijde formula (van der Heijde *et al.*, 1988). In this seminal paper, the authors described a calculation strategy for phakic intraocular Worst-Fechner lenses for correction of myopia using classical vergence transformation. With a prediction of the cardinal point of the PL at 3 mm behind the corneal vertex, the dioptric power of such a lens implant can be calculated from the pre-existing myopia, the vertex distance of the spectacle correction and the corneal power. In their paper, they displayed some examples illustrating how the lateral magnification of an aphakic and a myopic eye may change with the position of the

plane of correction in comparison to an emmetropic eye (aniseikonia). In the aphakic eye, the magnification decreases when the correction moves closer to the eye (i.e. from a spectacle correction to a contact lens correction to a pseudophakic eye). In contrast, in the myopic eye the magnification increases when the correction comes closer to the eye.

The purpose of the present study was to generalise the van der Heijde formula for calculation of phakic intraocular lenses to non-emmetropising lenses and to present a vergence-based formalism for calculating relative magnification changes by moving the position of correction from the spectacle plane to an IOL plane. This formalism is presented for phakic anterior and posterior chamber lenses, which partially or fully correct pre-existing ametropia (myopia or hyperopia). The applicability of this calculation scheme is demonstrated in two worked examples.

Methods

Vergence transformation and prediction of the power of the PL implant

For our calculations, the spectacle lens, the cornea, the phakic IOL and the crystalline lens are considered as thin refractive elements. The simplified schematic drawing of the optical system of the myopic spectacle-corrected eye and the eye with a PL implant (and spectacle correction) is given in *Figure 1*.

Before implantation of the PL, the optical system of the eye consists of the spectacle correction P_{Spr} , the interspace between the spectacle and the cornea (vertex distance, d_s), the cornea P_C , the interspace between the cornea and the crystalline lens (anterior chamber, d_{ac}),

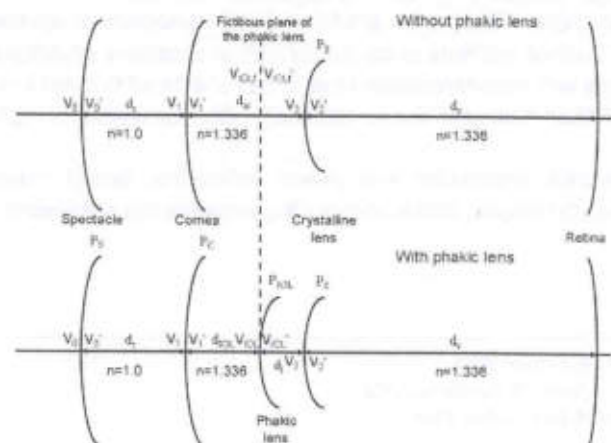


Figure 1. Schematic drawing of the simplified optical system of a myopic phakic eye with spectacle correction (upper part) or with a phakic lens correction (lower part). For partial correction with a phakic lens implant, a spectacle correction is applied for correcting the residual refraction error of the eye.

the crystalline lens P_L , and the interspace between the crystalline lens and the retina (vitreous, d_v). A bundle of rays entering the system at the spectacle plane with an object vergence V_{0pr} is refracted (spectacle refraction, vergence V_{0pr}') and transferred to the corneal plane (vergence V_{1pr}). After being refracted by the cornea (vergence V_{1pr}') and passing the anterior chamber of the eye (vergence V_{2pr}), it is refracted by the crystalline lens (vergence V_{2pr}').

With n as the refractive index of aqueous humour and d_{obj} as the object distance, the respective vergences are described by

$$\begin{aligned} V_{0pr} &= -\frac{1}{d_{obj}} \\ V_{0pr}' &= V_{0pr} + P_{Spr} \\ V_{1pr} &= \frac{1}{\frac{1}{V_{0pr}'} - d_s} \\ V_{1pr}' &= V_{1pr} + P_C \\ V_{2pr} &= \frac{1}{\frac{1}{V_{1pr}'} - \frac{d_{am}}{n}} \\ V_{2pr}' &= V_{2pr} + P_L \end{aligned} \quad (1)$$

After implantation of the PL, the optical system of the eye consists of the spectacle correction (= target refraction) P_{SPO} , the interspace between the spectacle and the cornea (vertex distance, d_s), the cornea P_C , the interspace between the cornea and the PL implant d_{IOL} , the phakic IOL P_{IOL} , the interspace between the IOL and the crystalline lens d_l , the crystalline lens P_L , and the interspace between the crystalline lens and the retina (vitreous, d_v). A bundle of rays entering the system at the spectacle plane with an object vergence V_{0po} is refracted (spectacle refraction, vergence V_{0po}') and transferred to the corneal plane (vergence V_{1po}). After being refracted by the cornea (vergence V_{1po}') and passing the aqueous humour to the PL (vergence V_{IOL}) it is refracted by the phakic intraocular lens (vergence V_{IOL}'). Then, the bundle of rays passes through the aqueous humour again to the crystalline lens (vergence V_{2po}) and is refracted by the crystalline lens (vergence V_{2po}').

The respective vergences are described by

$$\begin{aligned} V_{0po} &= -\frac{1}{d_{obj}} \\ V_{0po}' &= V_{0po} + P_{SPO} \\ V_{1po} &= \frac{1}{\frac{1}{V_{0po}'} - d_s} \end{aligned}$$

$$V_{1po}' = V_{1po} + P_C$$

$$V_{IOL} = \frac{1}{\frac{1}{V_{1po}'} - \frac{d_{IOL}}{n}}$$

$$V_{IOL}' = V_{IOL} + P_{IOL}$$

$$V_{2po} = \frac{1}{\frac{1}{V_{IOL}'} - \frac{d_l}{n}}$$

$$V_{2po}' = V_{2po} + P_L \quad (2)$$

At the (fictitious) position of the phakic intraocular lens (d_{IOL} behind the cornea), the vergence V_{IOL}' yields

$$V_{IOL} = \frac{1}{\frac{1}{V_{IOL}'} - \frac{d_{IOL}}{n}} \quad (3)$$

For a specific object distance d_{obj} , the vergences V_{IOL}' of the untreated eye and V_{IOL} of the eye after implantation of the phakic intraocular lens must be equal. After re-organisation of equations (1) and (3) and equation (2), this implies that

$$V_{IOL}' = \frac{1}{\frac{1}{\frac{1}{\frac{1}{V_{0po}'} + P_C} - d_s} - \frac{d_{IOL}}{n}} + P_{IOL} = V_{IOL} \quad (4)$$

As the power of an intraocular lens implant is normally calculated for far distance ($1/d_{obj}$ equals zero), equation (4) reads

$$\frac{1}{\frac{1}{\frac{1}{P_{Spr}} + P_C} - d_s} - \frac{d_{IOL}}{n} = \frac{1}{\frac{1}{\frac{1}{P_{SPO}} + P_C} - d_s} + P_{IOL} \quad (5)$$

or

$$P_{IOL} = \frac{1}{\frac{1}{\frac{1}{P_{Spr}} + P_C} - d_s} - \frac{1}{\frac{1}{\frac{1}{P_{SPO}} + P_C} - d_s} \quad (6)$$

Object-image magnification and aniseikonia

The total image-object magnification of the eye before treatment is given by

$$M_{pr} = \frac{V_{0pr} \cdot V_{1pr} \cdot V_{2pr}}{V_{0pr}' \cdot V_{1pr}' \cdot V_{2pr}'} \quad (7)$$

and after implantation of the phakic IOL, it is

$$M_{po} = \frac{V_{0po} \cdot V_{1po} \cdot V_{IOL} \cdot V_{2po}}{V_{0po}' \cdot V_{1po}' \cdot V_{IOL}' \cdot V_{2po}'} \quad (8)$$

As the vergences of the untreated and the treated eye must be equal at the spectacle plane and again at the

(fictitious) position of the PL implant, the relative magnification M_{po}/M_{pr} yields

$$\frac{M_{po}}{M_{pr}} = \frac{V_{0po} \cdot V_{1po} \cdot V_{IOL} \cdot V_{2po}}{V_{0po'} \cdot V_{1po'} \cdot V_{IOL'} \cdot V_{2po'}} \cdot \frac{V_{0pr'} \cdot V_{1pr'} \cdot V_{2pr'}}{V_{0pr} \cdot V_{1pr} \cdot V_{2pr}} = \frac{V_{1po} \cdot V_{IOL} \cdot V_{0pr'} \cdot V_{1pr'}}{V_{0po'} \cdot V_{1po'} \cdot V_{IOL'} \cdot V_{1pr'}} \quad (9)$$

In equation (9), if both $V_{0po'}$ and V_{1po} are zero, or both $V_{0pr'}$ and V_{1pr} are zero, their quotients should be treated as unity. Using equation (9) together with equations (1) to (3) the gain or loss in magnification due to implantation of a phakic intraocular lens in comparison with a spectacle-corrected eye can be derived.

Results

Example 1

For the first example we assume a spherical equivalent of refraction P_{Spr} of -10 D at a vertex distance d_v of 14 mm before the surgical intervention. Keratometric corneal power P_C is 43 D, the cardinal plane of the phakic posterior chamber lens (intraocular contact lens) d_{IOL} is assumed to be located 3.5 mm behind the corneal vertex and the refractive index of aqueous humour n is 1.336.

For postoperative emmetropia, the power P_{IOL} of the PL implant is determined using equation (6) to be $D_{IOL} = -10.86$ D (vergence $V_{IOLr} = 37.60$ D and $V_{IOL} = 48.46$ D).

Calculating the vergences $V_{0pr'}$, V_{1pr} and $V_{1pr'}$ with equation (1) and $V_{0po'}$, V_{1po} , $V_{1po'}$, V_{IOL} and $V_{IOL'}$ using equation (2), the relative magnification yields $M_{po}/M_{pr} = 1.17$, which means that the image size after implantation of a fully correcting phakic intraocular lens is 17% larger compared to the myopic eye with the respective spectacle correction.

If we assume that the object is approaching the eye from far distance to 10 cm (object vergence of 10 D, V_{0pr} and V_{0po} are both changing from 0 to -10 D), the magnification ratio M_{po}/M_{pr} comparing the eye with a phakic intraocular lens and the spectacle-corrected eye is a function of the object vergence as displayed in *Figure 2a*. The figure shows that the relative magnification M_{po}/M_{pr} increases to 1.26 if the object is moved from far distance to near distance (10 cm).

To estimate the required change in the geometry of the crystalline lens for adapting to near distances we determined the vergence at the principal plane of the crystalline lens as a function of the object vergence and compared that value with the respective vergence for far

distant objects (*Figure 2b*). For that purpose, the crystalline lens is simplified to a single-surface lens posi-

tioned at the principal plane of the crystalline lens. The data for the principal plane of the crystalline lens were extracted from the Gullstrand model eye (5.85 mm behind the corneal vertex) (Langenbuecher *et al.*, 2003). The vergence of the eye with the phakic intraocular lens at the principal plane of the crystalline lens changes from 40.26 D for far distant objects to 28.06 D for objects at 10 cm (object vergence 10 D) (change of -12.20 D), whereas the vergence of the spectacle corrected eye changes from 40.26 D to 31.10 D (change of -9.16 D). This implies that in the eye with the phakic intraocular lens, the crystalline lens has to change its power by 3.04 D more than in the spectacle-corrected eye.

Example 2

For the second example we assume a spherical equivalent of refraction P_{Spr} of -20 D at a vertex distance d_s of 14 mm before the surgical intervention. Keratometric corneal power P_C is 43 D, the cardinal plane of the phakic anterior chamber lens (iris claw lens) d_{IOL} is assumed to be located 3.0 mm behind the corneal vertex and the refractive index of aqueous humour n is 1.336.

In a *first step*, we determine the power P_{IOL} of the PL implant for postoperative emmetropia using equation (6) to $D_{IOL} = -18.43$ D (vergence $V_{IOLr} = 29.17$ D and $V_{IOL} = 47.60$ D). In a *second step*, we calculate the respective lens power for a PL implant, which partially corrects preoperative myopia, where the residual myopia (-10 D to 0 D in steps of 1 D) is corrected by spectacles. The respective lens powers are given in *Table 1*. In a *third step*, we calculate the vergences $V_{0pr'}$, V_{1pr} and $V_{1pr'}$ with equation (1) and $V_{0po'}$, V_{1po} , $V_{1po'}$, V_{IOL} and $V_{IOL'}$ using equation (2) for postoperative emmetropia and for partially correcting lens implants. The relative magnification for the fully correcting phakic IOL for far distant objects yields $M_{po}/M_{pr} = 1.33$, which means that the image size after implantation of a fully correcting phakic intraocular lens is 33% larger compared with the myopic eye with the respective spectacle correction. The respective values for partially correcting phakic intraocular lenses are provided in *Table 1*. In a *fourth step*, if we assume that the object is approaching the eye from far distance to 10 cm (object

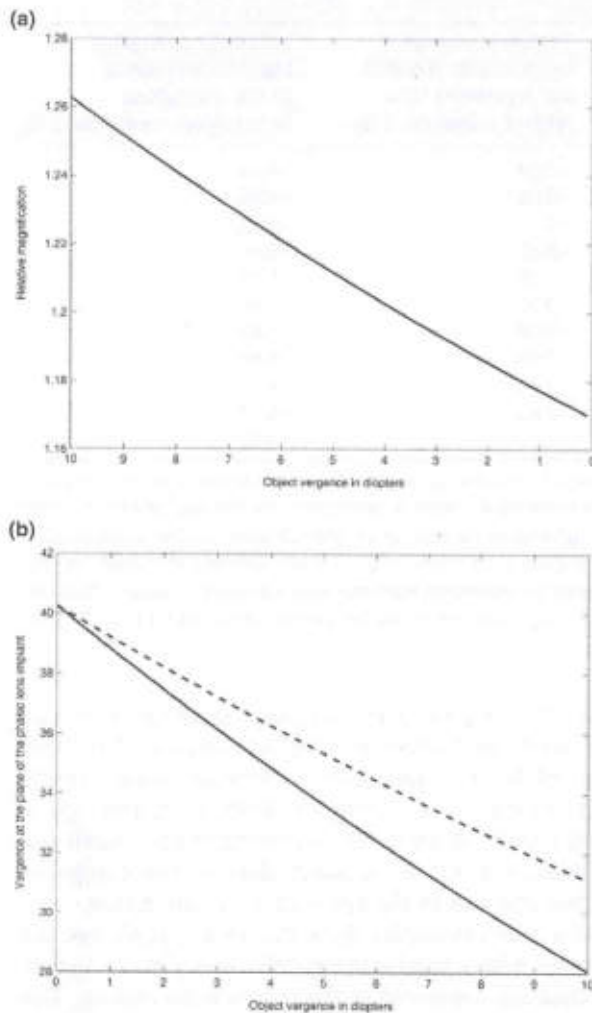


Figure 2. Myopic eye with a refraction of -10 D, vertex distance of the spectacle correction 14 mm, corneal power 43 D, phakic lens position 3.5 mm behind the corneal vertex, object vergence ranges from 0 to 10 D (object distances: infinity to 10 cm). (a) Relative magnification of an eye as a function of object vergence. Relative magnification refers to the gain in lateral magnification (retinal image size) due to correcting ametropia with a phakic intraocular lens implant instead of a spectacle correction. The lens power was determined for far distant objects and the relative magnification was calculated as a function of object distance. (b) Vergence at the spectacle-corrected eye and the eye with a phakic lens correction at the principal plane of the crystalline lens as a function of object vergence. The location of the principal plane of the crystalline lens (5.85 mm behind the corneal vertex) was taken from the Gullstrand model eye. The graph shows, that the change in vergence of the spectacle correction (broken line) is much less than the respective value of the phakic lens correction (solid line), which implies that the refractive change of the crystalline lens necessary for focusing on near objects is much higher with a phakic lens implant.

vergence of 10 D, both V_{opr} and V_{opo} change from 0 to -10 D), the magnification ratio M_{po}/M_{pr} comparing the eye with a phakic intraocular lens to the spectacle corrected eye is displayed as a function of object vergence in Figure 3a for the fully correcting as well as

for the partially correcting lens implants. The figure shows that the relative magnification M_{po}/M_{pr} is increasing from the far distant object to a near object at 10 cm distance. In a *fifth step*, we estimate the required change in power of the crystalline lens (simplification to a single surface lens positioned at the principal plane) to accommodate for near objects. For that purpose, we determine the vergence of the spectacle corrected eye preoperatively as well as the vergence of the eye with the PL (in case of a full correction) or with a PL and a spectacle correction (in case of a partial phakic lens correction) at the principal plane of the crystalline lens as a function of the object vergence. The changes in vergences due to a change in object vergence are displayed in Figure 3b for the fully correcting PL and for PL, which partially correct for myopia (residual refraction -10 D to 0 D in steps of 1 D). The respective change in vergence for the eye with spectacle correction only (preoperative state) is included as a reference in the plot.

Discussion

In a case of high or excessive ametropia the implantation of phakic anterior or posterior chamber intraocular lenses is an appropriate strategy for correcting the refractive error of the eye. In contrast to clear lens extraction for correction of excessive myopia, phakic intraocular lenses are beneficial especially in young patients due to maintenance of phakic accommodation. In the range of low or medium ametropia, other surgical interventions such as LASIK or LASEK are more popular, because the risk of endothelial damage because of contact with the PL is not accepted (Lackner *et al.*, 2003). In the last decade a series of different phakic intraocular lenses were launched to the market for correction of myopia, hyperopia (Saxena *et al.*, 2003) and – especially in the last 5 years – for correction of astigmatism (toric lenses) (Güell *et al.*, 2003; Langenbacher and Seitz, 2003).

The first to describe the calculation of dioptric power of phakic intraocular lenses were van der Heijde *et al.* (1988). They presented a vergence-based strategy to determine the lens power from preoperative spectacle refraction, vertex distance, corneal power and the predicted position of the lens implant within the eye. They transferred the vergence both through the spectacle-corrected eye and the ametropic (uncorrected) eye to the plane of the predicted PL position. The power of the PL implant was determined as the difference of these vergences at the predicted position of the PL implant. For the difference in magnification between the eye with spectacle correction and PL correction the authors demonstrated their results with some figures, but they did not show the theory behind the determination of ocular magnification.

Table 1. The parameters of an eye which was preoperatively myopic and corrected with spectacles at a vertex distance of 14 mm

Residual refraction at spectacle plane in D	Dioptic power of the phakic lens in D	Relative magnification M_{po}/M_{pr} for far distant objects	Vergence change at the principal plane of the crystalline lens (object vergence: 3 D)	Vergence change at the principal plane of the crystalline lens (object vergence: 5 D)
-10	-7.91	1.14	-2.94	-4.75
-9	-8.83	1.16	-3.02	-4.88
-8	-9.77	1.17	-3.11	-5.02
-7	-10.74	1.19	-3.20	-5.16
-6	-11.74	1.21	-3.29	-5.31
-5	-12.77	1.23	-3.39	-5.46
-4	-13.83	1.25	-3.49	-5.63
-3	-14.93	1.27	-3.60	-5.80
-2	-16.06	1.29	-3.71	-5.97
-1	-17.22	1.31	-3.83	-6.16
0 = Full correction with phakic lens	-18.43	1.33	-3.95	-6.35

Postoperatively it is emmetropic (fully corrected with a phakic intraocular lens (residual refraction 0)) or partially corrected with a phakic lens with a residual spectacle refraction of -10 D to -1 D in steps of 1 D. The dioptric power of the lens located 3 mm behind the corneal vertex is given in the 2nd column. The relative magnification M_{po}/M_{pr} refers to the ratio of lateral magnification comparing the preoperative and the postoperative state. The vergence change at the principal plane of the crystalline lens (from the Gullstrand model eye, 5.85 mm behind the corneal vertex) (negative values in columns 4 and 5) has to be compensated by a refractive change of the crystalline lens (respective positive values) to focus on near targets at 33 cm (3 D object vergence) or 20 cm (5 D object vergence). The respective values for the preoperative state are -2.27 D or -3.68 D.

In general, if an optical system consists of refracting surfaces subdivided by interspaces with a homogeneous refractive index, lateral magnification is given by the product of the vergences in front of the surfaces divided by the product of the vergences behind the surfaces. However, if we do not have any information about the geometry and refraction of the crystalline lens, the absolute lateral magnification of the eye cannot be determined (Keating, 1982; Harris, 2001a,b, 2003). Instead of that, as we have information about the optical pathway from the object position, the position and refractive power of the spectacle correction, the corneal refraction, as well as the predicted position and the refraction of the implanted PL, the lateral magnification of that part of the optical pathway can be separated and estimated for the spectacle-corrected eye and for the eye with a PL correction. As the optical pathway through the residual eye is the same for both corrections, we can calculate the quotient of both magnifications to determine relative magnification. This relative magnification refers to the gain or loss in magnification, if in a spectacle-corrected eye the spectacle correction is substituted by an adequate correction with a PL implant.

In the present paper, we address an additional functionality of the presented strategy. If we calculate the PL power for objects at infinity (objective vergence equals zero) and consider the relative magnification of objects at near distance, we are able to determine the vergences at the principal plane of the crystalline lens as a function of object distance or vergence. This means that using the simplification of a thin crystalline lens

(single refracting surface) the change in vergence at that plane has to be compensated by an adequate refractive change of the crystalline lens to focus the object sharply on the retina. If we compare both vergences for a defined object distance, we can estimate how much the crystalline lens has to accommodate in the spectacle-corrected eye and in the eye with a PL correction.

Our worked examples show that in a myopic eye the correction with a phakic intraocular lens yields a higher magnification compared to the spectacle correction. The magnification gain can easily reach values up to 30% in high myopia, if such an eye is treated with a PL implantation. However, spectacle correction or clear lens extraction may be beneficial in patients where the range of phakic accommodation is limited. Myopic patients corrected with a PL require a much higher change in crystalline lens refraction in contrast to spectacle-corrected patients, if they focus on objects at near distance. This may be of special importance if one eye of an individual is corrected with spectacles and the fellow eye is corrected with a PL implant. In such cases, near point anisometropia may cause severe fusion problems to the patient. From the literature, fusion of disparate images can be achieved if the difference in magnification between the two eyes does not exceed 5% (Crone and Leuridan, 1973a,b; Kramer *et al.*, 1999; Langenbucher *et al.*, 2005; Wang and Pomeratzeff, 1983).

Many surgeons more or less ignore the effect of lateral magnification and focus on a full refractive correction of the eye (Scarpattetti, 1983; Kramer *et al.*, 1999). But an adequate correction of both eyes of an individual with spectacles, contact lenses or PL implants is not able to

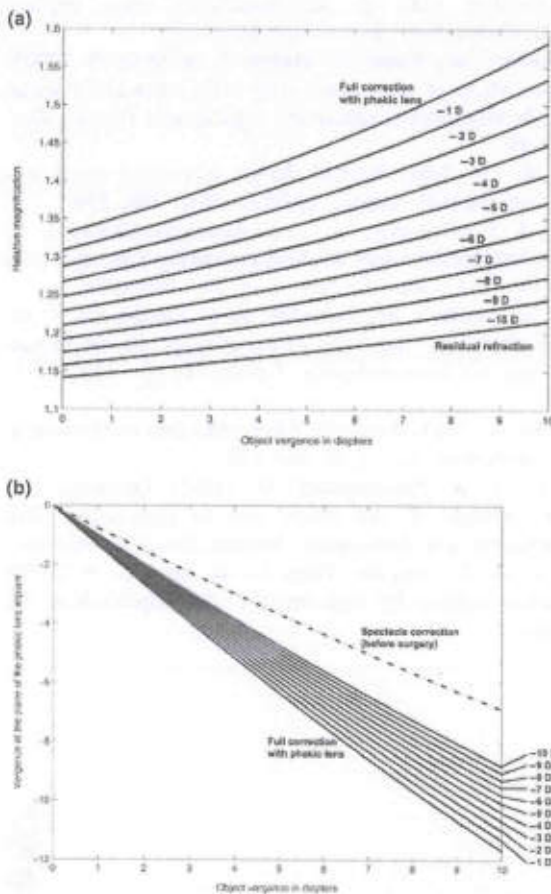


Figure 3. Myopic eye with a refraction of -20 D, vertex distance of the spectacle correction 14 mm, corneal power 43 D, phakic lens position 3.0 mm behind the corneal vertex, object vergence ranges from 0 to 10 D (object distances: infinity to 10 cm). (a) Relative magnification of an eye as a function of object vergence. Relative magnification refers to the gain in lateral magnification (retinal image size) due to correcting ametropia with a phakic intraocular lens implant instead of a spectacle correction. The set of graphs refer to a full correction (for emmetropia) or partial correction with a residual myopia of -1 to -10 D. The lens power was determined for far distant objects and the relative magnification was calculated as a function of object vergence. (b) Change in vergence at the principal plane of the crystalline lens in the spectacle-corrected eye, and the eye with fully or partially correcting phakic lens, as a function of object vergence. The location of the principal plane of the crystalline lens (5.85 mm behind the corneal vertex) was taken from the Gullstrand model eye. The graph shows that the change in vergence of the spectacle correction is much less than the respective value of the phakic lens correction, which implies that the refractive change of the crystalline lens necessary for focusing to near objects is much higher with a phakic lens implant.

compensate for magnification disparities (Krzizok *et al.*, 1996). It is generally accepted that minus lenses for correction of myopia minify the retinal image, whereas plus lenses for correction of hyperopia magnify the retinal image. It is also generally accepted that a correction of myopia at the corneal plane (using contact

lenses) or (phakic) intraocular lenses reduces the minification effect. But if the correction of ametropia in both eyes is not appropriate, discrepancies in retinal image sizes may be challenging for both the ophthalmologist and the patient (Krzizok *et al.*, 1996).

In conclusion, we presented a mathematical strategy for calculation of phakic anterior or posterior chamber lenses and a formalism to predict the gain or loss in lateral magnification, if a spectacle-corrected eye undergoes phakic intraocular lens implantation. As the change in magnification for high or excessive ametropia can produce levels of aniseikonia between 5 and 30% , the fusion of the two images, especially after monocular correction with a PL implant, may be impossible. Anterior segment surgeons should be aware of these image size disparities. As after implantation of phakic IOLs myopic patients require a much higher change in crystalline lens power compared to the spectacle-corrected eye if they focus on near objects, the supposed advantage of preserving accommodation is somewhat lost in higher myopic patients. An enhanced (aspherical) optical model including thick lenses for the spectacle, the cornea, the PL and the crystalline lens may enhance the precision of the calculation.

References

- Colin, J., Robinet, A. and Cochener, B. (1999) Retinal detachment after clear lens extraction for high myopia: seven-year follow-up. *Ophthalmology* **106**, 2281–2284.
- Crone, R. A. and Leuridan, O. M. A. (1973a) Tolerance for aniseikonia. I. Diplopia thresholds in the vertical and horizontal meridians of the visual field. *Albrecht v Graefes Archiv für Ophthalmologie* **31**, 1–16.
- Crone, R. A. & Leuridan, O. M. A. (1973b) Tolerance for aniseikonia. II. Determination based on the amplitude of cyclofusion. *Albrecht v Graefes Archiv für Ophthalmologie* **31**, 17–22.
- Fernandez-Vega, L., Alfonso, J. F. & Villacampa, T. (2003) Clear lens extraction for the correction of high myopia. *Ophthalmology* **110**, 2349–2354.
- Güell, J. L., Vázquez, M., Malecaze, F., Manero, F., Gris, O., Velasco, F., Hulin, H. & Pujol, J. (2003) Artisan toric phakic intraocular lens for the correction of high astigmatism. *Am. J. Ophthalmol.* **3**, 442–447.
- Harris, W. F. (2001a) Magnification, blur, and ray state at the retina for the general eye with and without a general optical instrument in front of it. 1. Distant objects. *Optom. Vis. Sci.* **78**, 888–900.
- Harris, W. F. (2001b) Magnification, blur, and ray state at the retina for the general eye with and without a general optical instrument in front of it. 2. Near objects. *Optom. Vis. Sci.* **78**, 901–905.
- Harris, W. F. (2003) Image size magnification and power and dilation factors for optical instruments in general. *Ophthalmic Physiol. Opt.* **23**, 251–261.

- van der Heijde, G. L., Fechner, P. U., Worst, J. G. F. (1988) Optische Konsequenzen der Implantation einer negativen Intraokularlinse bei myopen Patienten. *Klin. Monatsbl. Augenheilkd.* **193**, 99–102.
- Keating, P. K. (1982) A matrix formulation of spectacle magnification. *Ophthalmic Physiol. Opt.* **2**, 145–158.
- Kramer, P. W., Lubkin, V., Pavlica, M. & Covin, R. (1999) Symptomatic aniseikonia in unilateral and bilateral pseudophakia. A projection space eikonometer study. *Binocul. Vis. Strabismus Q* **14**, 183–190.
- Krzizok, T., Kaufmann, H. & Schwerdtfeger, G. (1996) Binokulare Probleme durch Aniseikonie und Anisophorie nach Katarakt-Operation. *Klin. Monatsbl. Augenheilkd.* **208**, 477–480.
- Lackner, B., Pieh, S., Schmidinger, G., Hanselmayer, G., Dejaco-Ruhswurm, I., Funovics, M. A. & Skorpik, C. (2003) Outcome after treatment of ametropia with implantable contact lenses. *Ophthalmology* **110**, 2153–2161.
- Langenbacher, A. & Seitz, B. (2003) Calculation scheme for bitoric eikonic intraocular lenses. *Ophthalmic Physiol. Opt.* **23**, 213–220.
- Langenbacher, A., Huber, S., Nguyen, N. X., Seitz, B. & Kühle, M. (2003) Cardinal points and object-image magnification with an accommodative lens implant (1 CU). *Ophthalmic Physiol. Opt.* **23**, 61–70.
- Langenbacher, A., Reese, S., Huber, S. & Seitz, B. (2005) Compensation of aniseikonia with toric intraocular lenses and spherocylindrical spectacles. *Ophthalmic Physiol. Opt.* **25**, 35–44.
- Lopez, M. O. (2001) Retinal detachment after clear lens extraction for high myopia. *Ophthalmology* **108**, 239.
- Menezo, J. L., Cisneros, A. L. & Rodriguez-Salvador, V. (1998) Endothelial study of iris-claw phakic lens: four year follow-up. *J. Cataract Refract. Surg.* **24**, 1039–1049.
- Saxena, R., Landes, M., Noordzij, B. & Luyten, G. P. M. (2003) Three-year follow-up of the Artisan phakic intraocular lens for hypermetropia. *Ophthalmology* **110**, 1391–1395.
- Scarpatici, A. (1983) Binocular vision after lens implantation. *Acta Ophthalmol. Scand.* **61**, 844–850.
- Wang, G. J. & Pomerantzeff, O. (1983) Iseikonia and accommodation in the fellow eye in monocular IOL implantation. *Am. Intra-ocular Implant Soc. J.* **9**, 441–444.
- Worst, J. G. F., van der Veen, G. & Los, L. I. (1990) Refractive surgery for high myopia. *Doc. Ophthalmol.* **75**, 335–341.

Compensation of aniseikonia with toric intraocular lenses and spherocylindrical spectacles

Achim Langenbacher, Sven Reese, Stefan Huber and Berthold Seitz

Department of Ophthalmology, University of Erlangen-Nürnberg, Schwabachanlage 6, D-91054 Erlangen, Germany

Abstract

Background and Purpose: Magnification disparity between the two eyes (aniseikonia) is one of the major unresolved problems in modern cataract surgery, potentially degrading binocular visual function or causing diplopia. The purpose of this study is to describe a paraxial computing scheme using 4×4 system matrices to simulate a corrected pseudophakic 'optical system eye' with a meridional magnification that matches the magnification of a given contralateral eye.

Methods: Based on the definition of a centred optical system in the paraxial Gaussian space containing astigmatic surfaces using 4×4 refraction and translation matrices, we derived a methodology for calculating the refractive power and axis of toric intraocular lenses and spherocylindrical spectacle corrections for (i) fully correcting the optical system eye and (ii) realizing an arbitrary meridional magnification by solving a linear equation system.

Results: The capabilities of this computing scheme are demonstrated with two examples. In example 1 we calculate a toric lens and a spherocylindrical spectacle correction for compensation of a corneal astigmatism to realize a predefined iso-meridional magnification. In example 2 we first determine the meridional magnification of the contralateral eye, which has been treated with cataract surgery and toric lens implantation, and then we compute the appropriate combination of a fully correcting toric lens and spherocylindrical spectacle refraction, which exactly matches the meridional magnification of the contralateral eye.

Conclusion: We presented an *en bloc* matrix based strategy for the calculation of an optical system eye containing an astigmatic cornea, a toric lens implant and a spherocylindrical spectacle correction, where the toric lens and the spherocylindrical spectacle correction are determined to fully correct the system and to realize an arbitrary meridional magnification i.e. to eliminate aniseikonia.

Keywords: astigmatism, lateral magnification, matrix formalism, paraxial optics

Introduction

Aniseikonia is a binocular condition in which left and right images differ in perceived size or shape. There are

two types of aniseikonia: static and dynamic aniseikonia. The first type is the classical aniseikonia, denoting a perceived image size difference with a fixed gaze direction. The second type of aniseikonia is also called induced anisophoria and denotes a perceived image size difference because of unequal prism effects when looking through different parts of the two (anisometric) spectacle lenses.

The incidence of aniseikonia is often underestimated. Beside the large patient group at risk with anisometropia with a prevalence of up to 10% (anisometropia > 1 diopter, age above 20 years), a second group of patients at risk for aniseikonia are the patients who have had cataract or refractive surgery. For example, Kramer

Received: 20 May 2004

Revised form: 15 July 2004

Accepted: 17 July 2004

The authors have no proprietary interest in the development or marketing of this or any competing instrument or piece of equipment.

Correspondence and reprint requests to:

Priv.-Doz. Dr Achim Langenbacher.

Tel.: 49 9131 853 4052; Fax: 49 9131 853 4436.

E-mail address: achim.langenbacher@augen.imed.uni-erlangen.de

et al. (1999) found that 40% of all pseudophakes had ophthalmic complaints referable to aniseikonia. Because these numbers are significant, testing for and managing aniseikonia is important.

The sensitivity to aniseikonia can vary a lot from person to person. Some patients are very grateful if 1% of aniseikonia is corrected, while others might not be bothered by as much as 3% of aniseikonia. Equivalent to a sphere and cylinder refractive error, there is an overall and a meridional aniseikonia. For some patients, correcting the overall aniseikonia is sufficient to eliminate potential determinants for headache and asthenopia. Meridional aniseikonia, on the contrary, gives rise to distorted space perception. The classical way to reduce or eliminate aniseikonia is to provide an iseikonic prescription. One cannot change the effective power at the cornea, because this would reduce the patient's visual acuity. However, one can change the accompanying spectacle magnifications of the corrective lenses by manipulating the base curve, centre thickness, index of refraction, and back vertex distance. For patients who have had cataract surgery with implantation of a spherical or toric lens in one eye in the past, and who develop ophthalmic complaints because of aniseikonia, it would be a logical consequence to correct aniseikonia with a combination of a (toric) lens implant compensated with a spectacle correction in the event that the contralateral eye is indicated for cataract surgery.

In the last decade, toric intraocular lenses have become more popular in clinical practice for the correction of corneal astigmatism during cataract surgery to improve the postoperative visual performance of the patient (Frohn *et al.*, 1999; Nguyen and Miller, 2000; Novis, 2000; Ruhswurm *et al.*, 2000; Sun *et al.*, 2000; Gerten *et al.*, 2001; Leyland *et al.*, 2001; Amm and Halberstadt, 2002; Gills and van der Karr, 2002; Tehrani and Dick, 2002; Till *et al.*, 2002; Gills, 2003). In the past, toric intraocular lenses have been determined using standard formulae initially designed for spherical lenses (SRK/T, Hoffer, Holladay, Haigis, SRK-2). Although these standard formulae are optimized for the prediction of spherical intraocular lenses, they yield correct results in the simple case, when the axes of all toric surfaces in the eye, as well as in the spectacle correction are aligned. In this case, we can predict the toric lens implant by separately calculating a spherical lens in both cardinal meridians. This will not, in general, be the case. Additionally, in classical second generation IOL calculation formulae the predicted lens position after cataract surgery is based on the keratometric reading (Retzlaff, 1980; Holladay *et al.*, 1988; Retzlaff *et al.*, 1990; Hoffer, 1993) and results in different predicted lens positions for each meridian.

The first IOL formula to fully treat the astigmatic eye using matrices has been provided by MacKenzie and

Harris (2002). In this paper, a step-along procedure is presented in a demonstration of the derivation of the traditional Gaussian theoretical formulae for the determination of intraocular lens power in a stigmatic eye. A raytracing scheme using paraxial approximations was first described by Bennett (1986a,b) to determine retinal image size by tracing an axial pencil of rays through the 'optical system eye' consisting of astigmatic surfaces with axes at random. It incorporates a method of summing up any number of astigmatic prescriptions at any axis by adding the respective components (Bennett, 1986a,b; Langenbucher *et al.*, 2003; Langenbucher and Seitz, 2003). This methodology using vergence transformation in the Gaussian space has been modified and rearranged for the calculation of toric lenses and the prediction of the residual refraction after implantation of toric lenses (Langenbucher and Seitz, 2003, 2004a,b).

A matrix-based description of spherical optical systems in ophthalmological applications was first described by Rosenblum and Christensen (1974) and later used by many other investigators. This formalism breaks down any spherical optical system into a product of 2×2 refraction and translation matrices and the resulting system matrix relates the slope and height of an incident ray to the respective slope and height of the exiting ray. Keating (1980, 1981a,b) was the first to introduce a generalization of these 2×2 matrices to astigmatic systems described by 4×4 system matrices. In accordance with the spherical case described with 2×2 matrices, the generalized formulation for an astigmatic optical system breaks down into 4×4 refraction and translation matrices. The system matrix relates the incident ray with slopes in x - and y -direction and intersection coordinates x and y at the first refractive surface to the respective slopes in x - and y -direction and the coordinates x and y of the exiting ray at the last refractive surface of the optical system.

As the entire optical system from the spectacle to the retina is represented with a 4×4 system matrix, a 2×2 submatrix of this 4×4 system matrix represents the lateral magnification of the spectacle corrected eye. Thus, the matrix formulation seems to be an adequate tool to calculate meridional magnification disparities and to match the magnification of the eye by combination of a toric intraocular lens implant and an adequate spherocylindrical spectacle correction.

The purpose of this paper was (i) to describe a matrix-based methodology to determine the meridional magnification of a spectacle corrected eye, (ii) to present a novel calculation strategy to realize an arbitrary meridional magnification by correcting an astigmatic eye with a toric intraocular lens implant and a spherocylindrical spectacle refraction, and (iii) to demonstrate the clinical applicability of the formalism by providing two examples.

Methods

Refraction and translation matrices and the system matrix

In any astigmatic optical system, the refraction matrix for a single refracting interface R and the translation matrix for a homogenous gap T can be written as

$$R = \begin{bmatrix} 1 & 0 & A & D \\ 0 & 1 & D & B \\ 0 & 0 & 1 & 0 \\ 0 & 0 & 0 & 1 \end{bmatrix} \quad T = \begin{bmatrix} 1 & 0 & 0 & 0 \\ 0 & 1 & 0 & 0 \\ \frac{d}{n} & 0 & 1 & 0 \\ 0 & \frac{d}{n} & 0 & 1 \end{bmatrix} \quad (1)$$

Elements A , B and D of the refraction matrix are given (Long, 1976) with

$$\begin{aligned} A &= -[S + C \cdot \sin^2(\varphi)] \\ B &= -[S + C \cdot \cos^2(\varphi)] \\ D &= C \cdot \sin(\varphi) \cdot \cos(\varphi). \end{aligned} \quad (2)$$

Parameters S , C and φ in matrix R refer to the spherical power, cylindrical power (positive cylinder form) each in diopters and the orientation of the cylinder and parameters d and n in matrix T refer to the interspace between surfaces in meters and the refractive index of the medium.

The system matrix of an optical system consisting of m spherocylindrical surfaces with interspaces in between can be written as

$$S = R_m \cdot T_{m-1,m} \cdot R_{m-1} \cdot T_{m-2,m-1} \cdot \dots \cdot R_2 \cdot T_{1,2} \cdot R_1, \quad (3)$$

and any incident ray from the left (surface 1) with slope angles α_{0x} and α_{0y} in x and y direction and intersection coordinates x_0 and y_0 with surface 1 will exit the system at surface m to the right with slope angles α_x and α_y at coordinates x and y (Figure 1) so that

$$\begin{pmatrix} \alpha_x \\ \alpha_y \\ x \\ y \end{pmatrix} = S \cdot \begin{pmatrix} \alpha_{0x} \\ \alpha_{0y} \\ x_0 \\ y_0 \end{pmatrix}. \quad (4)$$

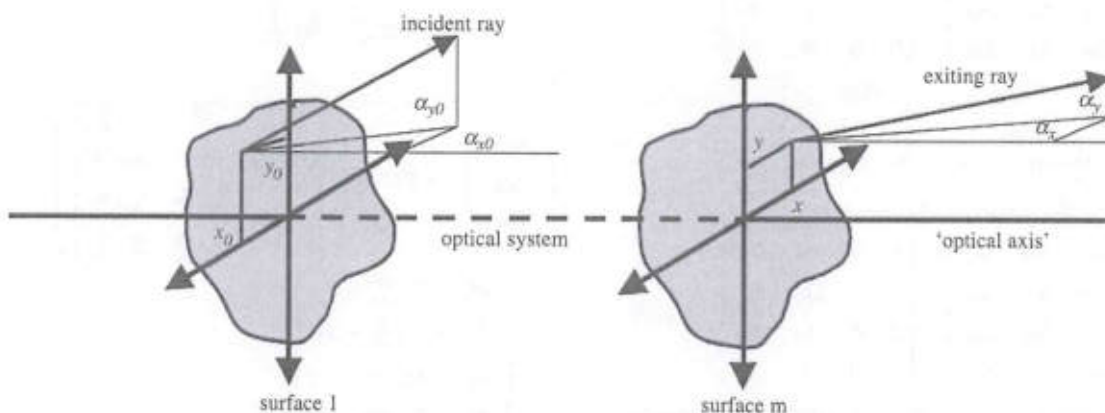


Figure 1. Optical system with an incident ray coming from left and exiting the system to right. The incident ray enters the system (surface 1) at co-ordinates x_0 and y_0 with slope angles α_{x0} and α_{y0} . The exiting ray leaves the system (surface m) at co-ordinates x and y with slope angles α_x and α_y .

The reverse calculation of the elements S , C and φ from the submatrix

$$K = \begin{bmatrix} A & D \\ D & B \end{bmatrix} \quad (5)$$

can easily be performed by deriving the trace $\text{tr}(K)$ (Keating, 1980) and the determinant $\det(K)$ with

$$\begin{aligned} \text{tr}(K) &= A + B \\ \det(K) &= A \cdot B - D^2 \\ C &= \sqrt{\text{tr}(K)^2 - 4 \cdot [\det(K)]^2} \end{aligned} \quad (6)$$

$$S = \left(\frac{\text{tr} - C}{2} \right)$$

$$\varphi = \tan^{-1} \left(\frac{S - A}{B} \right).$$

Matrix definition of the pseudophakic 'optical system eye' and meridional magnification

The optical system of a pseudophakic eye containing spherocylindrical surfaces is characterized in the simplest form with a spherocylindrical spectacle correction, a single surface cornea, and a thin toric lens implant. Thus, the matrix representation of the total system starting from the spectacle plane and ending at the retina is represented with a system matrix S with

$$S = T_V R_{IOL} \cdot T_{ACD} \cdot R_C \cdot T_S \cdot R_S, \quad (7)$$

where T_V refers to the (pseudophakic) vitreous space, R_{IOL} refers to the refraction matrix of the toric IOL implant, T_{ACD} refers to the (pseudophakic) anterior chamber of the eye (the humour bounded posteriorly by the intraocular lens and anteriorly by the cornea), R_C to the corneal surface, T_S to the vertex distance from the cornea to the spectacle plane and R_S to the intended target refraction at the spectacle plane after cataract

where PINV is the pseudo-inverse of a rectangular matrix (see Appendix).

The specific set of magnification parameters M_x , M_c and M_y can be directly derived with

$$\begin{aligned} M_x &= M_{\min} + (M_{\max} - M_{\min}) \cdot \sin^2(\varphi_{\max}) \\ M_y &= M_{\min} + (M_{\max} - M_{\min}) \cdot \sin^2(\varphi_{\max}) \\ M_c &= (M_{\max} - M_{\min}) \cdot \sin(\varphi_{\max}) \cdot \cos(\varphi_{\max}), \end{aligned} \tag{15}$$

where M_{\max} refers to the major magnification meridian, M_{\min} refers to the minor magnification meridian and φ_{\max} to the orientation of the major magnification meridian.

(ii) In a second step, the respective spectacle correction for viewing distant objects will be determined so that the entire optical system from the spectacle correction to the retina is corrected. For a fully corrected optical system, incident rays with a slope angle equal zero have to intersect the retina at coordinates $x = 0$ and $y = 0$ irrespective of their intersection with the first refractive surface (spectacle correction). This means, that a bundle of rays incident to the system parallel to the optical axis is imaged to $x = y = 0$ at the focal plane. In matrix notation this means

$$S \cdot \begin{pmatrix} \alpha_{0x} = 0 \\ \alpha_{0y} = 0 \\ \dots \\ \dots \end{pmatrix} = \begin{pmatrix} \dots \\ \dots \\ x = 0 \\ y = 0 \end{pmatrix}. \tag{16}$$

This condition can only be realized if each element of the lower right 2×2 submatrix (third to fourth row and third to fourth column) of the entire 4×4 system matrix equal zero or

$$\begin{aligned} \frac{d_V}{n_V} (S_{11}A_S + S_{12}D_S + S_{13}) + \left(\frac{d_V}{n_V}A_{IOL} + 1\right)(S_{31}A_S + S_{32}D_S \\ + S_{33}) + \frac{d_V}{n_V} D_{IOL} (S_{41}A_S + S_{42}D_S + S_{43}) &= 0 \\ \frac{d_V}{n_V} (S_{11}D_S + S_{12}B_S + S_{14}) + \left(\frac{d_V}{n_V}A_{IOL} + 1\right)(S_{31}D_S + S_{32}B_S \\ + S_{34}) + \frac{d_V}{n_V} D_{IOL} (S_{41}D_S + S_{42}B_S + S_{44}) &= 0 \\ \frac{d_V}{n_V} (S_{21}A_S + S_{22}D_S + S_{23}) + \frac{d_V}{n_V} D_{IOL} (S_{31}A_S + S_{32}D_S + S_{33}) \\ + \left(\frac{d_V}{n_V}B_{IOL} + 1\right)(S_{41}A_S + S_{42}D_S + S_{43}) &= 0 \\ \frac{d_V}{n_V} (S_{21}D_S + S_{22}B_S + S_{24}) + \frac{d_V}{n_V} D_{IOL} (S_{31}D_S + S_{32}B_S + S_{34}) \\ + \left(\frac{d_V}{n_V}B_{IOL} + 1\right)(S_{41}D_S + S_{42}B_S + S_{44}) &= 0. \end{aligned} \tag{17}$$

After rearrangement of this equation system, we get

$$K \cdot \begin{pmatrix} A_S \\ B_S \\ D_S \end{pmatrix} = \begin{pmatrix} -\frac{d_V}{n_V}S_{13} - \left(\frac{d_V}{n_V}A_{IOL} + 1\right)S_{33} - \frac{d_V}{n_V}D_{IOL}S_{43} \\ -\frac{d_V}{n_V}S_{14} - \left(\frac{d_V}{n_V}A_{IOL} + 1\right)S_{34} - \frac{d_V}{n_V}D_{IOL}S_{44} \\ -\frac{d_V}{n_V}S_{23} - \frac{d_V}{n_V}D_{IOL}S_{33} - \left(\frac{d_V}{n_V}B_{IOL} + 1\right)S_{43} \\ -\frac{d_V}{n_V}S_{24} - \frac{d_V}{n_V}D_{IOL}S_{34} - \left(\frac{d_V}{n_V}B_{IOL} + 1\right)S_{44} \end{pmatrix}, \tag{18}$$

with elements of the 4×4 matrix K defined by

$$\begin{aligned} K_{11} &= \frac{d_V}{n_V} s_{11} + \left(\frac{d_V}{n_V}A_{IOL} + 1\right)s_{31} + \frac{d_V}{n_V} D_{IOL}s_{11} \\ K_{22} &= \frac{d_V}{n_V} s_{12} + \left(\frac{d_V}{n_V}A_{IOL} + 1\right)s_{32} + \frac{d_V}{n_V} D_{IOL}s_{42} \\ K_{31} &= \frac{d_V}{n_V} s_{21} + \frac{d_V}{n_V} D_{IOL}s_{31} + \left(\frac{d_V}{n_V}B_{IOL} + 1\right)s_{41} \\ K_{42} &= \frac{d_V}{n_V} s_{22} + \frac{d_V}{n_V} D_{IOL}s_{32} + \left(\frac{d_V}{n_V}B_{IOL} + 1\right)s_{42} \\ K_{13} &= \frac{d_V}{n_V} s_{12} + \left(\frac{d_V}{n_V}A_{IOL} + 1\right)s_{32} + \frac{d_V}{n_V} D_{IOL}s_{41} \\ K_{23} &= \frac{d_V}{n_V} s_{11} + \left(\frac{d_V}{n_V}A_{IOL} + 1\right)s_{31} + \frac{d_V}{n_V} D_{IOL}s_{41} \\ K_{33} &= \frac{d_V}{n_V} s_{22} + \frac{d_V}{n_V} D_{IOL}s_{32} + \left(\frac{d_V}{n_V}B_{IOL} + 1\right)s_{42} \\ K_{34} &= \frac{d_V}{n_V} s_{21} + \frac{d_V}{n_V} D_{IOL}s_{31} + \left(\frac{d_V}{n_V}B_{IOL} + 1\right)s_{41} \\ K_{12} &= K_{21} = K_{32} = K_{41} = 0. \end{aligned} \tag{19}$$

The required parameters A_S , B_S and D_S for the spectacle refraction can be derived analogous to Equations 13 and 14 calculating the pseudo-inverse of K . In a last step, the elements A_S , B_S and D_S have to be re-converted from component notation into standard notation (sphere, cylinder and orientation) using Equations 6.

Results

For both examples we assume a vertex distance of 14 mm, an axial length of 23.6 mm, and a measured phakic anterior chamber depth of 3.5 mm. From the biometric data and the ACD constant of the lens (MS 6116TU, Dr Schmidt Intraocularlinsen, St Augustin, Germany, ACD = 4.7) we estimate a postoperative lens position of 4.79 mm [‘optical anterior chamber depth’ according to the Haigis formula (Haigis, 1995, 2001)] for a thin toric lens implant. The refractive index of air equals 1, that of the aqueous humour and the vitreous are set to $n_h = n_v = 1.336$. Corneal radius of curvature is assumed to be 7.8 mm at 22° and 7.2 mm at 112° . With an effective keratometer index of the Zeiss ophthalmometer ($n_c=1.3315$) corneal refraction reads $42.50/3.54 \times 22$.

Example 1

In this simple case we want to calculate a pseudophakic optical system with the existing cornea combined with a toric lens implant and a respective spectacle correction to get an iso-meridional magnification of 0.16 to match the magnification of the contralateral eye. The matrices read

$$T_S = \begin{bmatrix} 1 & 0 & 0 & 0 \\ 0 & 1 & 0 & 0 \\ 0.014 & 0 & 1 & 0 \\ 0 & 0.014 & 0 & 1 \end{bmatrix},$$

$$R_C = \begin{bmatrix} 1 & 0 & -42.9970 & 1.2301 \\ 0 & 1 & 1.2301 & -45.5447 \\ 0 & 0 & 1 & 0 \\ 0 & 0 & 0 & 1 \end{bmatrix},$$

$$T_{ACD} = \begin{bmatrix} 1 & 0 & 0 & 0 \\ 0 & 1 & 0 & 0 \\ 0.0035853 & 0 & 1 & 0 \\ 0 & 0.0035853 & 0 & 1 \end{bmatrix},$$

$$T_V = \begin{bmatrix} 1 & 0 & 0 & 0 \\ 0 & 1 & 0 & 0 \\ 0.0140793 & 0 & 1 & 0 \\ 0 & 0.0140793 & 0 & 1 \end{bmatrix},$$

After multiplication, S_A yields

$$S_A = \begin{bmatrix} 0.3980 & 0.0172 & -42.9970 & 1.2301 \\ 0.0172 & 0.3624 & 1.2301 & -45.5447 \\ 0.0154 & 0.0001 & 0.8458 & 0.0044 \\ 0.0001 & 0.0153 & 0.0044 & 0.8367 \end{bmatrix}$$

and with Equation 14, the required elements A_{IOL} , B_{IOL} , and D_{IOL} are determined as $A_{IOL} = -23.1586$, $B_{IOL} = -20.4272$ and $D_{IOL} = -1.3188$. Reconverted to standard notation, we get a dioptric power of the toric lens implant of $19.8944/3.7971 \times 112$. Inserting the parameters A_{IOL} , B_{IOL} , and D_{IOL} as well as the elements of matrix S_A into Equation 19 and solving for the spectacle refraction parameters yields $A_S = 2.2127$, $B_S = 2.8282$ and $D_S = -0.2972$. Reconverted to the standard notation, spectacle refraction reads $-2.0926/-0.8557 \times 22$. At a last step, we check for validity of the entire system matrix by multiplying all refraction and translation matrices together according to Equation 7 and we get

$$S = \begin{bmatrix} 0.0407 & -0.0044 & -62.5000 & 0.0000 \\ -0.0044 & 0.00498 & 0.0000 & -62.5000 \\ 0.0160 & 0.0000 & 0.0000 & 0.0000 \\ 0.0000 & 0.0160 & 0.0000 & 0.0000 \end{bmatrix}$$

The lower left 2×2 submatrix characterizing the lateral magnification of the system indicates an isometric magnification of $M_x = M_y = 0.016$ and the lower right 2×2 submatrix proves that the entire system is correctly compensated for in terms of refraction and image magnification (elements in the third and fourth row and column equal zero).

Example 2

In this example we intend to calculate a toric lens implant with a lateral magnification that matches the magnification of the pseudophakic contralateral eye. The contralateral eye with corneal radii of curvature 7.6 mm at 155° and 7.3 mm at 65° , a pseudophakic anterior chamber depth of 4.9 mm and an axial length of 23.8 mm has been treated by cataract extraction with toric lens implant. For a spherical target refraction of -1.0 diopters, a toric lens power $17.6158/2.5384 \times 65$ is required and a toric lens with $17.5/2.5 \times 60$ has been implanted revealing a residual refraction of $-0.7428/-0.3192 \times 15$. From the entire system matrix

$$S = \begin{bmatrix} 0.0862 & 0.0077 & -60.1287 & 0.2669 \\ 0.0077 & 0.0904 & 0.2659 & -60.1275 \\ 0.0166 & 0.0001 & 0.0000 & 0.0000 \\ 0.0001 & 0.0166 & 0.0000 & 0.0000 \end{bmatrix}$$

we derive the magnification parameters of the contralateral eye of $M_x = 0.0166313$, $M_c = 0.0000735$ and $M_y = 0.0166316$.

Matrices T_S , R_C , T_{ACD} , T_V and S_A are identical to the respective matrices in example 1. The required elements A_{IOL} , B_{IOL} , and D_{IOL} can be derived using Equation 14. With $A_{IOL} = -20.2534$, $B_{IOL} = -17.4964$ and $D_{IOL} = -0.9894$, reconverted to standard notation we get a dioptric power of the toric lens implant of $(17.1781/3.3937) \times 108$. Inserting the parameters A_{IOL} , B_{IOL} , and D_{IOL} as well as the elements of matrix S_A into Equation 19 and solving for the spectacle refraction parameters yields $A_S = 0.0496$, $B_S = 0.6460$ and $D_S = 0.5330$. Reconverted to the standard notation, spectacle refraction reads $(0.2629/-1.2215) \times 30$. At a last step, we check for validity of the entire system matrix by multiplying all refraction and translation matrices together according to Equation 7 and we get

$$S = \begin{bmatrix} 0.0855 & 0.0008 & -60.1288 & 0.2679 \\ 0.0009 & 0.0946 & 0.2657 & -60.1277 \\ 0.0166313 & 0.0000735 & 0.0000 & 0.0000 \\ 0.0000735 & 0.0166316 & 0.0000 & 0.0000 \end{bmatrix}$$

The lower left 2×2 submatrix characterizing the lateral magnification of the system indicates a magnification of $M_x = 0.0166313$, $M_y = 0.0166316$ and $M_c =$

0.0000735 ($M_{max} = 0.0167049$, $M_{min} = 0.0165580$) and the lower right 2×2 submatrix proves that the entire system is correctly compensated for in terms of refraction and image magnification (elements in the third and fourth row and column equal zero).

Discussion

In general, anisometropia is defined as a difference in the refractive power of the two eyes, whereas aniseikonia is defined as a visual defect in which the perceived shape and size of an ocular image differ in the two eyes. Many studies have been performed concerning magnification disparities between two eyes, but only a very limited number of investigations have been published concerning the meridional magnification properties of the eye (Harris, 2001a,b). Image size disparities of up to 5% are clinically accepted to be tolerable for patients (Crone and Leuridan, 1973a,b; Scarpatetti, 1983). Higher values of aniseikonia may cause diplopia, suppression or loss of binocular summation. For meridional magnification disparities the limits of tolerance are not yet known. Furthermore, aniseikonia is not only a problem of the optical system eye, but has a neural component probably because of differences in receptor spacing. In this context, several more or less empirical measurements are used in clinical practice for assessment of aniseikonia.

With the invention of toric lens implants, a compensation of an excessive congenital or surgically induced corneal astigmatism, especially after penetrating keratoplasty, is possible. The technique of manufacturing those toric intraocular lenses in polymethylmethacrylate (PMMA), acrylates or silicone has become standard, and calculation concepts have been provided for determination of the dioptric power of thin or thick toric intraocular lenses (MacKenzie and Harris, 2002, 2003; Harris and MacKenzie, 2003; Langenbacher and Seitz, 2004a,b). Some of these calculation schemes are based on successive vergence transformation from the retina to the predicted position of the lens implant in an anterior direction and through the intended spectacle correction (target refraction), the cornea and the anterior chamber backwards to the predicted lens position to subtract both vergences and to derive the desired lens power (Langenbacher and Seitz, 2003, 2004b). Other calculation schemes are based on a generalization of the classical 2×2 matrix notation introduced to visual optics by Rosenblum and Christensen (1974) to a 4×4 matrix terminology, which enables a characterization of astigmatic optical systems with an unlimited number of toric refractive surfaces with axes at random and interspaces in between (MacKenzie and Harris, 2002, 2003; Harris, 1994; Harris and MacKenzie, 2003; Langenbacher and Seitz, 2003). The system matrix of the eye breaks down into a product of 4×4 refraction matrices representing

the refracting surfaces in the optical system and 4×4 translation matrices representing the interspaces between surfaces. For the formulation of the refraction matrices, we follow the notation introduced by Keating (1981a,b). With the typical structure of the refraction and translation matrices, the required elements A , B , and D of the power matrix can be derived by calculating the pseudo-inverse of a 4×3 matrix (i.e. using singular value decomposition). Elements A , B , and D can be directly reconverted into standard notation by calculating the trace and the determinant of the upper right 2×2 submatrix. In contrast to the successive algorithms used for vergence transformation, matrix notation yields an *en bloc* calculation strategy for the power of toric intraocular lenses or residual refraction after implantation of a toric lens in any orientation.

In a previous paper we have presented an iterative calculation scheme for thick bitoric eikonic intraocular lenses (Langenbacher and Seitz, 2003). Starting from a spherical front surface and a toric back surface of the thick intraocular lens implant compensating the refractive error of the spectacle-corrected eye (target refraction), we added cylindrical lenses and spheres in small steps to the front surface of the lens implant compensated by the back surface of the lens in order to get an iso-meridional magnification of the entire optical system. The potential of this calculation scheme has been demonstrated with some clinical examples. The drawback of this idea is that because of the very limited thickness of the bitoric lens the toric power at both lens surfaces may differ extensively although with small meridional magnification disparities and the manufacture of these bitoric lenses may be challenging.

In the present study, we decided to realize a novel strategy for matching the meridional magnification of an eye to be treated with cataract extraction and toric lens implantation to the meridional magnification of the contralateral eye, which may have undergone cataract extraction and spherical or toric lens implantation before. This strategy considers the telescopic effect of an optical system, where the astigmatic corneal power is compensated for with a thin toric lens implant and a toric spectacle correction, so that the meridional magnification of the entire system exactly matches that of the contralateral eye. Because of the large distance between the spectacle plane and the predicted lens plane the toric power of both surfaces is tolerable. Mathematically, this concept is realized using generalized 4×4 matrix notation limited to paraxial optics (Gaussian space). In general, eight matrix elements of the 4×4 system matrix (rows 3 and 4) are predefined with the meridional magnification of the system (lower left 2×2 submatrix), and the property that the entire system from the spectacle to the retina is fully corrected (elements of the lower right 2×2 submatrix equal zero) to ensure

that a parallel bundle of rays entering the system parallel to the optical axis from left is imaged at the retina to $x = y = 0$. Unknown parameters are the components of the toric lens implant A_{IOL} , B_{IOL} , and D_{IOL} as well as the respective components of the toric spectacle correction A_S , B_S , and D_S . Normally, such a matrix problem is solved by rearrangement

$$[8 \times 6] \cdot \begin{pmatrix} A_S \\ B_S \\ D_S \\ A_{IOL} \\ B_{IOL} \\ D_{IOL} \end{pmatrix} = (8 \times 1).$$

and calculating the pseudo-inverse (left-inverse) of the 8×6 matrix. Fortunately, the 8×6 matrix has a special diagonal block structure and allows a separation of the calculation for the lens parameters A_{IOL} , B_{IOL} , and D_{IOL} and the parameters of the spectacle correction A_S , B_S , and D_S . Both sets of parameters can easily be re-converted to standard notation using Equations 6 to derive the sphere, cylinder and axis of the toric lens implant and the spectacle correction.

If the meridional magnification of the contralateral eye is known prior to the calculation (see example 1), we can directly start with the calculation scheme provided in the Methods section. If the meridional magnification of the contralateral eye (preferably after cataract surgery and implantation of an intraocular lens) is not known, we have to insert a step prior to the calculation scheme described in order to derive the meridional magnification of the contralateral eye. This procedure has been described in detail in example 2. As the methodology is, in principle, not limited to three refractive surfaces, it can easily be generalized to thick toric lenses or to a thick cornea with two refractive surfaces.

Several assumptions have been made for our optical model to limit the mathematical complexity. These assumptions cannot hold under general conditions: (i) limitation to linear Gaussian optics (paraxial space), (ii) all optical elements are centred to the 'optical axis' without tilt, (iii) the pseudophakic lens position (effective lens position) can be determined exactly from the preoperative biometric data, and (iv) the vertex distance of the spectacle correction after cataract surgery is known prior to surgery.

Assumption 1

The limitation to paraxial optics means that only paraxial rays with a small slope angle are considered for our calculations. For larger slope angles, or rays

which intersect the refractive surfaces in the optical system more peripherally, optical aberrations such as spherical aberration, coma or astigmatism of skew rays have to be considered.

Assumption 2

This means that the spectacle correction and the cornea as well as the lens implant are aligned to the 'optical axis' without any tilt. Decentration of optical elements may cause prismatic effects as well as asymmetric optical aberrations of higher order.

Assumptions 1 and 2 may be addressed by using numerical ray-tracing techniques instead of matrix formalism. Analytical solutions such as with the matrix formalism presented in the present paper are normally restricted to paraxial centred optical systems.

Assumption 3

For this purpose, we have to rely on the experience of the inventors of standard intraocular lens formulae such as the SRK/T (Retzlaff *et al.*, 1990), the Hoffer-Q (Hoffer, 1993), the Holladay I (Holladay *et al.*, 1988), the Haigis formula (Haigis, 1995, 2001) or the calculation scheme presented by Naeser (1997). All these theoretical-optical formulae provide an estimation of the postoperative lens position using multiple regression analysis, A- or ACD-constant, keratometric readings, surgeon factors etc. Naeser *et al.* (1990) developed a new methodology for prediction of the pseudophakic anterior chamber depth based on biometric measurements of the posterior lens capsule. Norrby developed a new concept (lens haptic plane concept) for estimation of the effective postoperative position of a thick intraocular lens implant (Norrby and Koranyi, 1997). The prediction of the postoperative effective position of a thin intraocular lens implant as described by Olsen (Olsen *et al.*, 1995) uses the form factor of the lens (in terms of an A-constant or an ACD-constant) and a number of biometric data, which may influence the lens position. In contrast to these estimations, if we are able to biometrically evaluate anterior chamber depth and thickness of the crystalline lens, we can extract the position of the lens equator of the crystalline lens from theoretical eye models such as Gullstrand's (Gullstrand, 1909), Navarro *et al.* (1985), or Kooijman's (1983) model eye. Assuming that the haptics of the lens implant are positioned at the lens equator and considering the shape of the lens and the angulation of the haptics, this may be an alternative concept to determine the pseudophakic lens position without using an A- or ACD-constant.

Assumption 4

Beside the prediction of the postoperative pseudophakic lens position, the vertex distance for the spectacle correction has to be predicted precisely before cataract surgery. For our examples, we used a fixed vertex distance of 14 mm, but in clinical cases this simplification is insufficient and may cause inaccuracies both in the IOL power and spectacle refraction, as well as in the calculation of the magnification of the entire optical system.

In conclusion, we presented an *en bloc* matrix based strategy for the calculation of an pseudophakic optical system with a thin toric intraocular lens and a compensating spherocylindrical spectacle correction in order to realize an arbitrary meridional magnification of the eye and to eliminate aniseikonia between the two eyes. In general this concept offers the flexibility of crossing an unlimited number of cylinders with the limitations to paraxial optics. The potential and practicability of the methodology as well as a step-by-step walk-through has been demonstrated in two clinical examples.

References

Amm, M. and Halberstadt, M. (2002) Implantation torischer intraokularlinsen zur Korrektur hoher postkeratoplastischer Astigmatismen. *Ophthalmologie* **99**, 464–469.

Bennett, A. G. (1986a) Two simple calculation schemes for use in ophthalmic optics. I: Tracing oblique rays through systems including astigmatic surfaces. *Ophthalmic Physiol. Opt.* **6**, 325–331.

Bennett, A. G. (1986b) Two simple calculation schemes for use in ophthalmic optics. II: Tracing axial pencils through systems including astigmatic surfaces at random axes. *Ophthalmic Physiol. Opt.* **6**, 419–429.

Crone, R. A. and Leuridan, O. M. A. (1973a) Tolerance for aniseikonia. I. Diplopia thresholds in the vertical and horizontal meridians of the visual field. *Albrecht v Graefes Archiv für Ophthalmologie* **31**, 1–16.

Crone, R. A. and Leuridan, O. M. A. (1973b) Tolerance for aniseikonia. II. Determination based on the amplitude of cyclofusion. *Albrecht v Graefes Archiv für Ophthalmologie* **31**, 17–22.

Frohn, A., Dick, H. B. and Thiel, H. J. (1999) Implantation of a toric poly(-methyl)-methacrylate intraocular lens to correct high astigmatism. *J. Cataract Refract. Surg.* **25**, 1675–1678.

Gerten, G., Michels, A. and Olmes, A. (2001) Torische Intraokularlinse. Klinische Ergebnisse und Rotationsstabilität. *Ophthalmologie* **98**, 715–720.

Gills, J. P. (2003) Sutured piggyback toric intraocular lenses to correct high astigmatism. *J. Cataract Refract. Surg.* **29**, 402–404.

Gills, J. P. and van der Karr, M. A. (2002) Correcting high astigmatism with piggyback toric intraocular lens implantation. *J. Cataract Refract. Surg.* **28**, 547–549.

Gullstrand, A. (1909) Anhang zu Teil I. In: *Physiologische Optik*, 3 (ed. H. von Helmholtz), Ausgabe, Band 1, Voss Hamburg, pp. 350–358.

Haigis, W. (1995) Biometrie. In: *Augenärztliche Untersuchungsmethoden* (eds W. Straub, P. Kroll and H. J. Kühle), Biermann, Köln, Germany, pp. 255–304.

Haigis, W. (2001) Pseudophakic correction factors for optical biometry. *Graefes Arch. Clin. Exp. Ophthalmol.* **239**, 589–598.

Harris, W. F. (1994) Paraxial ray tracing through noncoaxial astigmatic optical systems, and 5 × 5 augmented system matrix. *Optom. Vis. Sci.* **71**, 282–285.

Harris, W. F. (2001a) Magnification, blur, and ray state at the retina for the general eye with and without a general optical instrument in front of it. 1. Distant objects. *Optom. Vis. Sci.* **78**, 888–900.

Harris, W. F. (2001b) Magnification, blur, and ray state at the retina for the general eye with and without a general optical instrument in front of it. 2. Near objects. *Optom. Vis. Sci.* **78**, 901–905.

Harris, W. F. and MacKenzie, G. E. (2003) The thin intraocular lens required for a given target refraction. *S. Afr. Optom.* **62**, 3–7.

Hoffer, K. J. (1993) The Hoffer Q formula: a comparison of theoretic and regression formulas. *J. Cataract Refract. Surg.* **19**, 700–712, Erratum 1994, **20** 677.

Holladay, J. T., Prager, T. C., Chandler, T. Y., Musgrove, K. H., Lewis, J. W. and Ruiz, R. S. (1988) A three-part system for refining intraocular lens power calculations. *J. Cataract Refract. Surg.* **14**, 17–24.

Keating, M. P. (1980) An easier method to obtain the sphere, cylinder and axis from an off-axis dioptric power matrix. *Am. J. Optom. Physiol. Opt.* **57**, 734–737.

Keating, M. P. (1981a) A system matrix for astigmatic optical systems: I. Introduction and dioptric power relations. *Am. J. Optom. Physiol. Opt.* **58**, 810–819.

Keating, M. P. (1981b) A system matrix for astigmatic optical systems: II. Corrected systems including an astigmatic eye. *Am. J. Optom. Physiol. Opt.* **58**, 919–929.

Kooijman, A. C. (1983) Light distribution on the retina of a wide-angle theoretical eye. *J. Opt. Soc. Am.* **73**, 1544–1550.

Kramer, P.W., Lubkin, V., Pavlica, M. and Covin, R. (1999) Symptomatic aniseikonia in unilateral and bilateral pseudophakia. A projection space eikonometer study. *Binocul. Vis. Strabismus Q* **14**, 183–190.

Langenbacher, A. and Seitz, B. (2003) Calculation scheme for bitoric eikonic intraocular lenses. *Ophthalmic Physiol. Opt.* **23**, 213–220.

Langenbacher, A. and Seitz, B. (2004a) Difficult lens power calculations. *Curr. Opin. Ophthalmol.* **15**, 1–9.

Langenbacher, A. and Seitz, B. (2004b) Computerized calculation scheme for toric intraocular lenses. *Acta Ophthalmol. Scand.* **82**, 270–276.

Langenbacher, A., Huber, S., Nguyen, N. X., Seitz, B. and Kühle, M. (2003) Cardinal points and object-image magnification with an accommodative lens implant (1 CU). *Ophthalmic Physiol. Opt.* **23**, 61–70.

- Leyland, M., Zinicola, E., Bloom, P. and Lee, N. (2001) Prospective evaluation of a plate haptic toric intraocular lens. *Eye*, **15**, 202–205.
- Long, W. F. (1976) A matrix formalism for decentration problems. *Am. J. Optom. Physiol. Opt.* **53**, 27–33.
- MacKenzie, G. E. and Harris, W. F. (2002) Determining the power of a thin toric intraocular lens in an astigmatic eye. *Optom. Vis. Sci.* **79**, 667–671.
- MacKenzie, G. E. and Harris, W. F. (2003) The thick intraocular lens required for a given target refraction. *S. Afr. Optom.* **62**, 66–71.
- Naeser, K. (1997) Intraocular lens power formula based on vergence calculation and lens design. *J. Cataract Refract. Surg.* **23**, 1200–1207.
- Naeser, K., Boberg-Ans, J. and Bargum, R. (1990) Biometry of the posterior lens capsule: a new method to predict pseudophakic anterior chamber depth. *J. Cataract Refract. Surg.* **16**, 202–206.
- Navarro, R., Santamaria, J. and Bescos, J. (1985) Accommodation-dependent model of the human eye with aspherics. *J. Opt. Soc. Am.* **2**, 1273–1281.
- Nguyen, T. M. and Miller, K. M. (2000) Digital overlay technique for documenting toric intraocular lens axis orientation. *J. Cataract Refract. Surg.* **26**, 1496–1504.
- Norrby, N. E. and Koranyi, G. (1997) Prediction of intraocular lens power using the lens haptic plane concept. *J. Cataract Refract. Surg.* **23**, 254–259.
- Novis, C. (2000) Astigmatism and toric intraocular lenses. *Curr. Opin. Ophthalmol.* **11**, 47–50.
- Olsen, T., Corydon, L. and Gimbel, H. (1995) Intraocular lens power calculation with an improved anterior chamber depth prediction algorithm. *J. Cataract Refract. Surg.* **21**, 313–319.
- Retzlaff, J. (1980) A new intraocular lens calculation formula. *Am. Intra-Ocul. Implant Soc. J.* **6**, 148–152.
- Retzlaff, J. A., Sanders, D. R. and Kraff, M. C. (1990) Development of the SRK/T intraocular lens implant power calculation formula. *J. Cataract Refract. Surg.* **16**, 333–340. Erratum 16 528.
- Rosenblum, W. M. and Christensen, J. L. (1974) Optical matrix method: Optometric applications. *Am. J. Optom. Physiol. Opt.* **51**, 961–968.
- Ruhswurm, I., Scholz, U., Zehetmayer, M., Hanselmayer, G., Vass, C. and Skorpik, C. (2000) Astigmatism correction with foldable toric intraocular lens in cataract patients. *J. Cataract Refract. Surg.* **26**, 1022–1027.
- Scarpattetti, A. (1983) Binocular vision after lens implantation. *Acta Ophthalmol. Scand.* **61**, 844–850.
- Sun, X. Y., Vicary, D., Montgomery, P. and Griffiths, M. (2000) Toric intraocular lenses for correcting astigmatism in 130 eyes. *Ophthalmology* **107**, 1776–1781.
- Tehrani, M. and Dick, H. B. (2002) Implantation einer ARTISAN torischen Linse zur Korrektur eines hohen

Astigmatismus nach Keratoplastik. *Klin. Monatsbl. Augenheilkd.* **219**, 159–163.

- Till, J. S., Yoder, P. R. Jr, Wilcox, T. K. and Spielman, J. L. (2002) Toric intraocular lens implantation: 100 consecutive cases. *J. Cataract Refract. Surg.* **28**, 295–301.

Appendix

A square matrix A with dimension $n \times n$ and without rank deficiency (number of eigenvalues equals the dimension n) has an inverse $B = \text{inv}(A)$. That means that $A \cdot B = B \cdot A$ is the unit matrix with diagonal elements equal to 1 and other elements equal to zero. If a rectangular matrix with dimensions $m \times n$ (m rows and n columns) with $m > n$ has a rank equal to n (number of singular values), Moore-Penrose or pseudo-inverse of A [$B = \text{PINV}(A)$] with dimensions $n \times m$ also has a rank equal to n and $B \cdot A$ is the $n \times n$ unit matrix. If a rectangular matrix with dimensions $m \times n$ with $m < n$ has a rank equal to m , the (Moore-Penrose-) pseudo-inverse of A [$B = \text{PINV}(A)$] with dimensions $n \times m$ also has a rank equal to m and $A \cdot B$ is the $m \times m$ unit matrix. Furthermore,

$$A_{m \times n} \cdot B_{n \times m} \cdot A_{m \times n} = A_{m \times n}$$

and

$$B_{n \times m} \cdot A_{m \times n} \cdot B_{n \times m} = B_{n \times m}$$

and $A_{m \times n} \cdot B_{n \times m}$ and $B_{n \times m} \cdot A_{m \times n}$ are square matrices and Hermitians. The computation of the pseudo-inverse is normally based on the singular value decomposition and singular values less than a tolerance (for our calculations: 10^{-18}) are treated as zero. References to Moore-Penrose matrices or pseudo-inverse matrices as well as to the singular value decomposition is provided on the website, i.e. at

<http://www.uwlax.edu/faculty/will/svd/systems/>

<http://mathworld.wolfram.com/Moore-PenroseMatrixInverse.html>

http://www.cs.ut.ee/~toomas_l/linalg/lin2/node16.html#SECTION00014100000000000000

http://www.cs.ut.ee/~toomas_l/linalg/lin2/node17.html#SECTION00014200000000000000

<http://www.stat.uni-muenchen.de/~strimmer/genets/html/pseudoinverse.html>

<http://www.omatrix.com/manual/pinv.htm>

Computerized calculation scheme for bitoric eikonic intraocular lenses

Achim Langenbucher and Berthold Seitz

Department of Ophthalmology, University of Erlangen-Nürnberg, Schwabachanlage 6, D-91054 Erlangen, Germany

Abstract

Despite full correction of the corneal astigmatism with toric intraocular lenses, the retinal image is distorted and the lateral image-object magnification is different in different meridians. The purpose of this study is to describe an iteration strategy for tracing an axial pencil of rays through the 'optical system eye' containing astigmatic refractive surfaces with their axes at random to calculate a thick bitoric lens implant which eliminates image distortion. The capabilities of this computing scheme are demonstrated with two clinical examples. We present a mathematically straightforward computer-based strategy for the calculation of thick bitoric eikonic lens implants. The iteration algorithm is initialized with a spherical front and a toric back surface and stepwise decreases the image distortion by adding cylinder lenses to the front lens surface corrected by the toric lens back surface. Total magnification can be modulated by varying the front-to-back surface power of the thick lens.

Keywords: bitoric intraocular lens, calculation scheme, eikonic lens, optimization algorithm, paraxial ray-tracing

Introduction

In the last decade, toric intraocular lenses have become more popular for the correction of corneal astigmatism during cataract surgery to improve the post-operative visual performance of the patient (Frohn *et al.*, 1999; Novis, 2000).

Keating (1981a,b) developed a generalized 4×4 system matrix consisting of power and translation matrices to describe an optical system including astigmatic surfaces with non-orthogonal axes. From this system matrix, the conjugate image of any object as well as the magnification of the optical system can be directly derived. In contrast, a ray-tracing scheme using paraxial approximations has been described by Bennett (1986a,b) to trace an axial pencil of rays through the 'optical system eye' consisting of astigmatic surfaces at different axes: specifically the spectacle correction and the cornea, as well as the front and back surface of the intraocular

lens implant. It incorporates a method of summing up any number of spherocylindrical powers or the vergence at any specified point of an astigmatic pencil of rays traced through the eye at various (non-orthogonal) orientations by adding the respective components (Bennett, 1986a). Haigis (1991) described a method for tracing a pencil of rays through the spectacle correction and the refractive surfaces of the eye using paraxial geometrical optics for the special case of spherical surfaces. Preussner *et al.* (2002) developed a numerical ray-tracing calculation scheme for the pseudophakic eye, where individual rays are calculated and then undergo refractions on all surfaces on the cornea and intraocular lens using Snell's law without paraxial approximations.

In the majority of cases, toric intraocular lenses are used to compensate for corneal astigmatism. A less obvious application for these lenses lies in the enhancement of near vision: implantation of toric intraocular lenses may induce against the rule astigmatism which, some believe, lends itself to improved visual function at near (Novis, 2000). In most cases, toric intraocular lenses are designed with a spherical front surface and a toric back surface. This means that even with an adequate correction of the corneal astigmatism in the front or back principal plane of the lens, the

Received: 21 October 2002

Revised form: 22 January 2003

Accepted: 27 January 2003

Correspondence and reprint requests to: Achim Langenbucher.

Tel.: +49-9131-8534052; Fax: +49-9131-8534436,

E-mail address: achim.langenbucher@augen.imed.uni-erlangen.de

image-object magnification is not homogeneous in different meridians. If the lens implant has a sufficient central thickness, a bitoric intraocular lens has the potential to overcome this drawback and to normalize the magnification in all meridians.

Thus, one of the most important issues in the calculation procedure of toric lens implants is the derivation of the retinal image size in the uncorrected and (spectacle-)corrected eye (Good and Polasky, 1979; Keating, 1982; Wang and Pomerantzeff, 1983; Achiron *et al.*, 1997, 1998). In the uncorrected eye, the retinal image can be regarded as a complex of overlapping blurs from the individual pencils of rays, assumed to be circular or elliptical in shape and varying in size with the pupil diameter. The centre of each individual blur lies on the chief or principal ray directed towards the centre of the entrance pupil and is hence refracted through the centre of the actual pupil (Bennett, 1986b). In any given ocular meridian, the basic size of the blurred image is determined by such rays from the extremities of the given object. In effect, it is the retinal image size when the pupil diameter is made infinitely small, so that the individual blurs are reduced to points. In the corrected eye, the object is in sharp focus. Consequently, all the rays in the pencil from any one object point are directed at the same point at the retina. We may choose any convenient point of incidence for the start of the ray-trace.

All spherocylindrical surfaces of the eye and the spectacle lens are transformed from a standard notation (sphere, cylinder, axis) to a component notation. Starting with a spherical front surface of the thick lens implant, the toric back surface power required to achieve a specified target refraction was calculated. From two characteristic object points at a distance, the retinal image of a circular object (incident slope angle of 10 prism dioptres) was derived and an ellipse was fitted to this image. Based on the orientation of the image, a cylindrical component was added to the front surface increasing the magnification of the semi-minor meridian of the ellipse and reducing image distortion. In light of the change in front surface power, the power of the back surface was recalculated so as to maintain the desired refractive outcome. This process was iterated until the semi-major-to-semi-minor meridian ratio was minimized to eliminate image distortion.

The purpose of this paper is to describe an iteration strategy for the calculation of a thick bitoric intraocular lens implant that will eliminate retinal image distortion. This involves tracing a pencil of rays through the 'optical system eye' containing astigmatic refractive surfaces with non-orthogonal axes and the iterative calculation of front and back intraocular lens surface powers. The applicability of this calculation scheme is demonstrated in two examples.

Methods

Determination of the retinal image dimensions

The ray-tracing scheme has to be initialized by defining the horizontal (H) and vertical (V) components of the ray slope angle measured in prism dioptres (cm per m) and the x and y coordinates of the point where the incident ray intersects the first refractive surface. The distant object was assumed to be a circle with its centre O on the optical axis of the eye. C is an arbitrary point on this circle positioned at the meridian OC with an azimuthal angle ξ in the standard axis notation. Let the clockwise angle ω , for example, 10 prism dioptres, denote the angular slope of the radius OC at the vertex A of the eye. Resolved into horizontal and vertical components, the slope angle OCA becomes

$$H = \omega \cos \xi, \quad V = \omega \sin \xi. \quad (1)$$

Since all the rays from a given point on a distant object may be considered as parallel at incidence, the slope angle and its components do not vary with the point of incidence (e.g. x and y), but only with the angle defining the object point (e.g. ω).

Although the shape of the retinal image is mathematically found not to be an exact ellipse (Bennett, 1986a), we simplified our calculation scheme with the assumption that the retinal image is elliptical in shape. So, the aim is to find the dimensions and orientation of the ellipse that passes through or is closest to the two retinal image points yielded by the ray-trace. This simplification allows us to consider only two characteristic rays for our approach.

Calculation scheme

For each refracting surface we have to enter the refractive index of the media n in front of and n' behind the surface as well as the sphere S , the cylinder C (both in dioptres) and the axis Θ in degrees and the distance d of the space behind the surface in metres. From S , C and Θ we calculate the respective values A , B and D in component notation, which are independent from the sign of the cylinder (minus or plus cylinder is allowed) (Keating, 1981a,b)

$$A = S + C \sin^2 \Theta, \quad B = -C \sin \Theta \cos \Theta, \\ D = S + C \cos^2 \Theta. \quad (2)$$

Any ray incident on a refractive surface is then defined by the slope angles H and V (H : horizontal slope angle in prism dioptres and V : vertical slope angle in prism dioptres) as well as the position of intersection with the refractive surface x and y . From these data, the changes

in slope angle (ΔH and ΔV) as well as the absolute slope angles of the ray V' and H' and the intersection points with the subsequent refractive surface x' and y' at a distance d can be derived in terms of linear geometrical optics (Langenbacher and Seitz, submitted for publication):

$$\begin{aligned} \Delta H &= Ax + By, & \Delta V &= -Bx - Dy, \\ H' &= \frac{(nH + \Delta H)}{n'}, & V' &= \frac{(nV + \Delta V)}{n'}, \\ x' &= x - d \cdot H', & y' &= y - d \cdot V'. \end{aligned} \tag{3}$$

Image size in the corrected eye

Since the retinal image in the corrected eye is in sharp focus, all ray paths from a point on the object can be traced to a conjugate point on the retina. So we do not necessarily have to search for the specific rays that pass through the centre of the pupil. For convenience, both the rays traced through the eye are directed towards the vertex of the correcting lens (spectacle correction), so that x and y are both zero for the first refracting surface. Because the object is positioned at optical infinity, no change is needed in the slope angle. The calculations are in accordance with those of the uncorrected eye except for the additional refractive surfaces of the correcting lens.

From the coordinates (x', y') of the position of a ray traced through the eye to the retina, the size of the retinal image can be derived (Bennett, 1986a). For example, from the coordinates (x', y') of the point V' conjugate to the object point V in the vertical meridian, the magnitude p and orientation μ of the image is described by

$$p = (x'^2 + y'^2)^{1/2}, \quad \mu = -\tan^{-1}\left(\frac{x'}{y'}\right). \tag{4}$$

The magnitude q and orientation ν of the image H' at the retina corresponding to the object point H from a horizontal meridian is described by

$$q = (x'^2 + y'^2)^{1/2}, \quad \nu = \tan^{-1}\left(\frac{y'}{x'}\right). \tag{5}$$

Since the image points V' and H' are formed by cardinal rays from the vertical and horizontal extremities of the circular object at distance, the retinal image describes the scissors distortion, which is characteristic for astigmatic systems.

Fitting an ellipse to the retinal image

An ellipse can be derived from a circle in two different ways: First, a circle of radius r_s equal to the semi-minor axis of the ellipse could be elongated by

meridional magnification along the meridian Θ_1 coincident with the major axis of the ellipse. Alternatively, a larger circle of radius r_1 equal to the semi-major axis of the ellipse could be flattened by meridional minification along the meridian Θ_s coincident with the minor axis of the ellipse.

On this basis, the orientation of the cardinal meridians of the ellipse (Θ_1 and Θ_s) as well as both the semi-major and semi-minor axes of the ellipse (r_1 and r_s) have to be derived to fully describe the ellipse. In contrast to another paper, (Bennett, 1986b), in which these parameters are derived using trigonometric functions, we apply simple vector algebra to solve this problem. Since both conjugate points in the image plane V' (x'_V, y'_V) and H' (x'_H, y'_H) corresponding to the object points V and H are lying on the ellipse and can be assumed to be parallel translated from extremity points of a circle with radius r_1 or r_s this problem can be formulated by the basic equations

$$\begin{aligned} \begin{pmatrix} x'_V \\ y'_V \end{pmatrix} + k \cdot \begin{pmatrix} dx \\ dy \end{pmatrix} &= \begin{pmatrix} R \\ 0 \end{pmatrix} \\ \begin{pmatrix} x'_H \\ y'_H \end{pmatrix} + l \cdot \begin{pmatrix} dx \\ dy \end{pmatrix} &= \begin{pmatrix} 0 \\ R \end{pmatrix} \end{aligned} \tag{6}$$

with the translation vector (dx, dy) , R is the semi-major or semi-minor axis, r_1 or r_s and the magnifications k and l . From this equation system, k and l can be expressed as

$$k = -\frac{y'_V}{dy}, \quad l = -\frac{x'_H}{dx}. \tag{7}$$

Inserting these terms into Eqn (6)

$$\begin{aligned} x'_V + k \cdot dx &= x'_V - \frac{y'_V}{dy} \cdot dx = r_s, \\ y'_H + l \cdot dy &= y'_H - \frac{x'_H}{dx} \cdot dy = r_s \end{aligned} \tag{8}$$

yields

$$x'_V - \frac{dx}{dy} \cdot y'_V = y'_H - \frac{dy}{dx} \cdot x'_H \tag{9}$$

or after multiplication, for example, with dx/dy , a quadratic equation

$$\left(\frac{dx}{dy}\right)^2 \cdot y'_V + \left(\frac{dx}{dy}\right) \cdot (y'_H - x'_V) - x'_H = 0 \tag{10}$$

which can be solved using standard formulae. The two solutions for $(dx/dy)_{1,2}$ characterize the directions of meridional magnification along Θ_1 or meridional minification along Θ_s with $\Theta_{1,s} = \tan^{-1}[1/(dx/dy)_{1,2}]$. Together with Eqn (6) they yield the semi-major and semi-minor axes, r_1 and r_s of the ellipse, respectively.

the conjugate image points. The ellipse dimensions are 1.66 mm at an orientation of 105° and 1.63 mm in the orthogonal meridian (distortion 1.8%). After this we add cylinders in 0.25-D steps aligned to the semi-major axis of the ellipse to the front surface of the lens and correct the refractive changes by the toric back surface, until the image distortion is minimized and the retinal image is circular. This optimization yields a front surface of the toric lens of 0.0 D/+16.25 D × 105 and a toric back surface of 4.64 D/+13.10 D × 15, resulting in a total front vertex power (equivalent power of the thick bitoric lens implant referenced to the front lens surface) of the lens of 18.08 D/+2.83 D × 105 (column 3). With this thick bitoric eikonic lens, the retinal image size is determined to be 1.66 mm in radius in both cardinal meridians.

The same procedure was applied to an intraocular lens with front surface power +10.00 and +20.00 D. The results are shown in Table 1 (columns 4–7).

Example 2

In this example, we intend to calculate a thick bitoric eikonic lens implant to correct the patient for a distance refraction of -0.75 D/-0.50 D × 90 to enhance unaided near vision (Table 2). We start with a plano front surface (0.0 D, column 2) and calculate the respective back surface power of the lens (18.93 D/+5.90 D × 103.2), which fully corrects the corneal

astigmatism in light of the intended target refraction. Then we ray-trace an object point with an incident slope angle of 10 prism dioptres in the vertical and horizontal directions through the correcting spectacles (vertex distance 14 mm) and the eye and fit an ellipse to the conjugate image points. The ellipse measures 1.63 mm along orientation of 99.9 and 1.59 mm in the orthogonal meridian (distortion 2.7%). The image distortion with a ray-trace of the same object through the uncorrected eye (principal ray) yields an image distortion of 1.9%. After this, we add cylinders in 0.25-D steps aligned with the semi-major axis of the ellipse to the front surface of the lens, until the image distortion is minimized and the retinal image is circular. This optimization yields a front surface of the toric lens of 0.00 D/ +23.75 D × 100 and a toric back surface of -2.24 D/ +21.19 D × 9.1 resulting in a total front vertex power of the lens of 19.28 D/+2.29 D × 108.8 (column 3). With this thick bitoric eikonic lens, the retinal image size is determined to be 1.63 mm in radius.

The results of the same procedure applied to an intraocular lens with front surface power +10.00 and +20.00 D are shown in Table 2 (columns 4–7).

Discussion

A quantum leap in the world of cataract surgery was the introduction of toric lens implants for the correction of

Table 2. Calculation of a thick bitoric eikonic lens implant for a target refraction of -0.75-0.50 D/A = 90° starting with a spherical front surface of 0.0 D (column 2), +10.0 D (column 4) and +20.0 D (column 6). Rows 2–4 refer to the sphere, cylinder and axis of the lens front surface, respectively; rows 5–7 to the back surface sphere, cylinder and axis, respectively; and rows 8–10 to the sphere, cylinder and axis (front vertex power = equivalent power of the thick bitoric lens implant referenced to the front lens surface), respectively, of the thick lens implant. A circular object with an incident slope angle of 10 prism dioptres is ray-traced through the spectacle correction and the eye to the retina and an ellipse is fitted to the retinal image. Semi-major meridian (image size in row 11 and orientation in row 12); semi-minor meridian (image size in row 13, orientation in row 14); image distortion (row 15). Additional information is provided about the image distortion without spectacle correction in row 16. In order to condense the table, the cardinal meridians of the ellipse are not shown for the uncorrected eye. In an iteration procedure, the front surface cylinder is increased in steps of 0.25 D oriented in the semi-major meridian of the ellipse image, until the ellipse retinal image improves to a circular image (columns 3, 5 and 7)

	Initialized	Optimized bitoric	Initialized	Optimized bitoric	Initialized	Optimized bitoric
Front surface S (D)	0.00	0.00	10.00	10.00	20.00	20.00
C (D)	0.00	23.75	0.00	23.50	0.00	23.50
A (°)	0.0	100.0	0.0	100.0	0.0	100.0
Back surface S (D)	18.93	-2.24	7.59	-13.77	-4.02	-25.87
C (D)	5.90	21.19	6.03	21.38	6.17	21.88
A (°)	103.2	9.1	103.2	9.1	103.2	9.1
Front vertex power S (D)	19.32	19.28	17.65	17.61	16.00	15.97
C (D)	6.18	2.29	6.17	2.37	6.16	2.40
A (°)	103.2	108.8	103.2	108.5	103.2	108.3
Semi-major meridian L (mm)	1.63	1.63	1.65	1.65	1.67	1.67
Orientation [°]	99.9	71.6	99.9	83.7	99.9	13.0
Semi-minor meridian S (mm)	1.59	1.63	1.61	1.65	1.63	1.67
Orientation (°)	9.9	161.6	9.9	173.7	9.9	103.0
2(L-S)/(L+S)	2.7%	0.0%	2.7%	0.0%	2.7%	0.0%
2(L-S)/(L+S) (uncorrected)	1.9%	0.9%	1.9%	0.9%	1.9%	0.9%

1.67 mm. This range mostly depends on the central thickness of the thick lens implant: the thicker the lens the wider the range of variation.

The calculation concept for thick bitoric eikonic lenses has the potential to solve three different problems: (1) to calculate a lens implant which fully compensates for the refractive state of the eye [with or without (spherocylindrical) spectacles]; (2) to calculate a bitoric lens implant which normalizes the lateral magnification of the eye in different meridians; and (3) to calculate a lens implant which eliminates aniseikonia.

With this mathematical concept, the image size and the conjugate image points of an arbitrary object for an optical system consisting of an unlimited number of astigmatic surfaces of non-orthogonal orientation with interspaces between the surfaces can be assessed (Bennett, 1986b) and the residual refraction at the corneal or spectacle plane can be derived by tracing backward through the eye (Dunne *et al.*, 1994, 1997). If the refraction of both corneal surfaces is known, the optical system can be enhanced using the thick lens model of the cornea. This modification may have the potential to offer a suitable concept for determination of lens implant power and aniseikonia after refractive surgery (Applegate and Howland, 1993; Seitz and Langenbacher, 2000), especially in cases where only one refractive surface of the cornea has been selectively changed in geometric shape by excimer laser ablation.

The examples assumed a model eye with known values for ACD, axial length and vitreous length. In the real world, in the preoperative situation, the clinician has to guess or predict the position of the implant and the subsequent length of the vitreous. However, these predictions are not very accurate. We addressed this problem with a model calculation to show how 1 mm of error in the prediction of ACD

and/or vitreous length will affect the magnitudes of the bitoric elements.

Table 3 shows the results for the example 2 (Table 2) and a spherical front surface power of 10.0 D for initialization of the iteration process. This table demonstrates the effect of an incorrectly predicted ACD on the bitoric lens implant (3.27 and 5.27 mm instead of 4.27 mm). An underestimation of the post-operative lens position by 1 mm (column 2 of Table 3) will result, in this example, in a significant miscalculation of both lens surface powers and the front vertex power (1.7 D in sphere, 0.28 D in cylinder), whereas with an overestimation of the lens position by 1 mm (column 4 of Table 3) the miscalculation is less pronounced (0.75 D in sphere, 0.12 D in cylinder). We feel, however, that 1 mm is an extreme error for the prediction of the effective lens position.

An additional problem may occur when it is not possible to construct useful bitoric intraocular lenses with the required magnitudes of accuracy. The manufacturing of such a bitoric lens with crossed cylinders presents a high tech challenge. At the moment it is possible to create bitoric lenses only in PMMA with a defined thickness and a precision of ± 0.125 D of sphere and cylinder and $\pm 2^\circ$ of rotation range between the orientation of the front and back surface. The manufacturers must invest much effort in creating foldable customized implants to high precision.

In conclusion, we presented a computer-based iteration strategy for the calculation of a thick bitoric eikonic lens implant which compensates for the refractive state of the eye, eliminates image distortion in the case of an astigmatic cornea and is able to correct disparate image sizes between both eyes of a patient. This may be of clinical relevance for treatment of aniseikonia and for compensation of corneal astigmatism.

Table 3. This table refers to example 2 (Table 2) and demonstrates the effect of an incorrectly predicted ACD on the bitoric lens implant (3.27 and 5.27 mm instead of 4.27 mm). We initialized the iteration process with a spherical front surface power of 10.0 D (Table 2, columns 4 and 5)

Optimized bitoric	Lens position 3.27 mm	Lens position 4.27 mm	Lens position 5.27 mm
Front surface S (D)	10.00	10.00	10.00
C (D)	20.00	23.50	25.00
A (°)	99.0	100.0	100.0
Back surface S (D)	-11.68	-13.77	-14.68
C (D)	17.61	21.38	23.03
A (°)	7.6	9.1	9.1
Front vertex power S (D)	15.91	17.61	18.36
C (D)	2.65	2.37	2.25
A (°)	108.2	108.5	109.3
Semi-major meridian L (mm)	1.68	1.65	1.64
Orientation (°)	145.6	83.7	120.8
Semi-minor meridian S (mm)	1.68	1.65	1.64
Orientation (°)	55.6	173.7	30.8
$2(L-S)/(L+S)$	0.0%	0.0%	0.0%
$2(L-S)/(L+S)$ (uncorrected)	0.8%	0.9%	0.9%

References

Achiron, L. R., Witkin, N., Primo, S. and Brooker, G. (1997) Contemporary management of aniseikonia. *Surv. Ophthalmol.* **41**, 321–330.

Achiron, L. R., Witkin, N. S., Ervin, A. M. and Brooker, G. (1998) The effect of relative spectacle magnification on aniseikonia. *J. Am. Optom. Assoc.* **69**, 591–599.

Applegate, R. A. and Howland H. C. (1993) Magnification and visual acuity in refractive surgery. *Arch. Ophthalmol.* **111**, 1335–1342.

Bennett, A. G. (1986a) Two simple calculation schemes for use in ophthalmic optics. I. Tracing oblique rays through systems including astigmatic surfaces. *Ophthal. Physiol. Opt.* **6**, 325–331.

Bennett, A. G. (1986b) Two simple calculation schemes for use in ophthalmic optics. II. Tracing axial pencils through systems including astigmatic surfaces at random axes. *Ophthal. Physiol. Opt.* **6**, 419–429.

Dunne, M. C., Elawad, M. E. and Barnes, D. A. (1994) A study of the axis of orientation of residual astigmatism. *Acta Ophthalmol. (Copenh)* **72**, 483–489.

Dunne, M. C., Elawad, M. E. and Barnes, D. A. (1997) Determination of the influence of effectivity upon residual astigmatism. *Acta Ophthalmol.* **75**, 170–173.

Frohn, A., Dick, H. B. and Thiel, H. J. (1999) Implantation of a toric poly(methyl methacrylate) intraocular lens to correct high astigmatism. *J. Cataract Refract. Surg.* **25**, 1675–1678.

Good, G. W. and Polasky, M. (1979) Eikonic lens design for minus prescriptions. *Am. J. Ophthalmol.* **56**, 345–349.

Haigis, W. (1991). Strahldurchrechnung in Gaußscher Optik. In: *4. DGII-Kongress* (eds Schott K., Jacobi K. W. and Freyler H.) Springer, Berlin, pp. 233–246.

Keating, M. P. (1981a) A system matrix for astigmatic optical systems: I. Introduction and dioptric power relations. *Am. J. Optom. Physiol. Opt.* **58**, 810–819.

Keating, M. P. (1981b) A system matrix for astigmatic optical systems: II. Corrected systems including an astigmatic eye. *Am. J. Optom. Physiol. Opt.* **58**, 919–929.

Keating, M. P. (1982) A matrix formulation of spectacle magnification. *Ophthal. Physiol. Opt.* **2**, 145–158.

Naeser, K. (1997) Intraocular lens power formula based on vergence calculation and lens design. *J. Cataract Refract. Surg.* **23**, 1200–1207.

Novis, C. (2000) Astigmatism and toric intraocular lenses. *Curr. Opin. Ophthalmol.* **11**, 47–50.

Preussner, P. R., Wahl, J., Lahdo, H., Dick, B. and Findl, O. (2002) Raytracing for intraocular lens calculation. *J. Cataract Refract. Surg.* **28**, 1412–1419.

Seitz, B. and Langenbacher, A. (2000) IOL power calculation in eyes after corneal refractive surgery. *J. Refract. Surg.* **16**, 349–361.

Wang, G. J. and Pomerantzeff, O. (1983) Iseikonia and accommodation in the fellow eye in monocular IOL implantation. *Am. Intra-Ocular Implant Soc. J.* **9**, 441–444.

Cardinal points and image–object magnification with an accommodative lens implant (1 CU)

Achim Langenbacher, Stefan Huber, Nhung X. Nguyen, Berthold Seitz and Michael Kühle

Department of Ophthalmology, University of Erlangen-Nürnberg, Schwabachanlage 6, D-91054 Erlangen, Germany

Abstract

A simple mathematical method for the determination of the cardinal points of pseudophakic eyes after implantation of an accommodative intraocular lens [posterior chamber intraocular lenses (PCIOL)] is presented. The purpose of this study was to explore the changes during pseudophakic accommodation (PAC) in (1) the positions of the cardinal points, (2) the distance of the object conjugate with the retina, and (3) the image–object magnification. These theoretical accommodation data are compared with clinical measurements.

Methods and Patients: Using biometrical measurements of the axial length, equivalent power of the cornea and the anterior chamber depth (ACD) in the non-accommodated state we used linear geometric optics for determination of the cardinal points and object distance as well as lateral magnification (the ratio of image to object size). With the measurement of ACD decrease (following pharmacological stimulation of the ciliary muscle with 2% pilocarpine eye drops) we determined the changes of the cardinal points and magnification to assess PAC amplitude from the shortening of the object distance. Calculated values of PAC amplitude were compared with the respective measured values derived from amplitude measures by accommodometer, defocusing and streak retinoscopy. We analysed the results of a prospective study on 35 eyes of 28 patients after cataract surgery (target refraction: -0.2 D) and accommodative PCIOL implantation (1 CU, HumanOptics AG, Erlangen, Germany) 3 months after surgery.

Results: After pilocarpine eye drops, ACD (mean \pm S.D., range; median) decreased by 0.88 ± 0.48 mm (0.51–1.91; 0.66). Distance of the in-focus object decreased from the non-accommodated state (-5.62 ± 1.83 m, -25 to -1.1 ; -4.83 m) to the accommodated state (ACD decrease) (-0.81 ± 0.21 , -2.11 to -0.65 ; -0.79 m). For a theoretical ACD decrease of 1.0 mm (the intrinsic limitation of the PCIOL design) it was -0.59 ± 0.28 , -1.31 to -0.51 ; -0.63 m and resulted in an objective accommodative response of 1.49 ± 0.16 , 1.21–1.81; 1.46 D, depending on the actual geometry of the individual eye. On average, magnification as induced by PAC in contrast to that induced by adequate spectacle addition differed by only about 1%. Accommodation measured with defocusing and the accommodometer correlated significantly with the theoretical value based on IOLMaster measurement of ACD decrease ($r = 0.752$, $p = 0.005$ and $r = 0.676$, $p = 0.02$). Likewise, accommodation measured with streak retinoscopy correlated weakly with the theoretical value based on IOLMaster ACD decrease ($r = 0.465$, $p = 0.05$).

Received: 10 June 2002

Revised form: 2 October 2002

Accepted: 28 October 2002

Correspondence and reprint requests to: Achim Langenbacher.

Tel.: +49 9131 853 4052; fax: +49 9131 853 4436.

E-mail address: achim.langenbacher@augen.imed.uni-erlangen.de

The authors have no proprietary interest in the development or marketing of this or any competing instrument or piece of equipment.

For the Erlangen Study Group 'Accommodative Intraocular Lens' additional members: G. C. Gusek-Schneider, A. Hafner, T. Riedel and A. Viestenz.

Conclusions: Using geometrical optics, PAC can be derived from the biometric data of the eye and the measured ACD decrease. This approach may be an additional indicator for the accommodative response in pseudophakic patients and may allow a subdivision of the measured accommodation into true PAC and pseudoaccommodation, for example, because of increased depth of focus induced by pupillary constriction.

Keywords: accommodative IOL, cardinal points, geometrical optics, intraocular lens, magnification

Introduction

Despite excellent restoration of visual acuity and good biocompatibility of presently used posterior chamber intraocular lenses (PCIOLs), there is very little accommodation in pseudophakic eyes with monofocal lens optics, so that patients usually remain presbyopic after cataract surgery. This problem has only partly been solved by the introduction of diffractive and bifocal PCIOLs (Gray and Lyall, 1992; Allen *et al.*, 1996; Knorz and Seiberth, 1996; Steinert *et al.*, 1999). Thus, efforts are being undertaken to develop a new PCIOL that restores accommodation. One of the new PCIOLs that have been developed is the 1 CU (HumanOptics AG, Erlangen, Germany). This intraocular lens (IOL) does not change its form or power but rather moves forward in near vision when the ciliary body changes in form and the pupil constricts. This increases the overall power of the eye and hence allows nearer objects to be focused (focus-shift principle). *Figure 1* illustrates the conditions of the eye, when the ciliary muscle is relaxed and when it is contracted. Whereas the crystalline lens is known to increase its rigidity during life, the ciliary muscle retains its strength in later life (Swegmark, 1969; Saladin and Stark, 1975; Fisher, 1977; Fisher, 1986; Strenk *et al.*, 1999).

If the action of this type of PCIOL is to be properly understood, we need to know the position of the cardinal

points of the eye both when the ciliary muscle is relaxed and when it is accommodated. The calculation schemes of IOLs are well-established in clinical practice (Gernet *et al.*, 1970; Hoffer, 1975; Holladay *et al.*, 1988; Retzlaff *et al.*, 1990; Haigis, 1995), but the determination of the image-object magnification is normally ignored, thus making aniseikonia a still unsolved problem (Wang and Pomerantzeff, 1983; Snead *et al.*, 1991; Rubin, 1997). The differences between these optically based formulas lie in the predictions of different 'effective lens positions' after cataract surgery, because they use different regression models including individualization of the calculation and are optimized on a more or less large and representative number of patient data (Holladay, 1997).

The positions of the cardinal points such as the object-side and image-side focal points, the object distance to the focus on the retina, both principal points and especially the object-side and image-side nodal points are crucial factors which influence the magnification of the eye and may predict anisometropia between the left and the right eye (Wang and Pomerantzeff, 1983; Snead *et al.*, 1991; Garcia *et al.*, 1996; Rubin, 1997). The nodal points may be defined as two points on the principal axis of a lens system such that an incident ray of light directed towards one of them emerges from the system as if from the other, in a direction parallel to that of the incident ray (Rosenblum and Christensen, 1974; Keating, 1981).

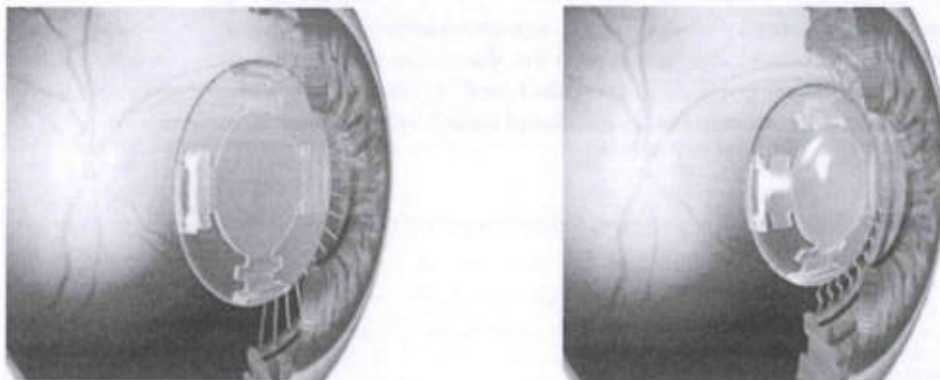


Figure 1. Principle of the focus-shift design. The 1 CU lens does not change its form or power but rather moves forward in near vision when the ciliary body changes in form and the pupil constricts. On the left side the lens is shown in the non-accommodated state, whereas on the right side it is in the accommodated state.

These cardinal points can be easily deduced using linear geometrical optics with simple matrix operations (Rosenblum and Christensen, 1974). After defining power matrices for each refractive surface and translation matrices for each space between the surfaces, the total optical system can be described with the resulting 2×2 matrix. The purpose of this study was to check for changes in (1) the cardinal points, (2) distance of the in-focus object, and (3) image-object magnification during pseudophakic accommodation (PAC). In addition, the theoretical accommodation results were compared with clinical measurements on patients with the 1 CU PCIOL.

Methods

Study design and population

Of a total of 50 consecutive patients with senile or presenile cataract who underwent phacoemulsification and implantation of the new accommodative PCIOL between June 2000 and April 2002, 35 eyes of 28 patients (15 males, 13 females) were included in the study.

In addition to a complete ophthalmological examination, post-operative examinations included slit-lamp evaluation, laser flare-cell photometry, applanation tonometry, keratometry, corneal videokeratography with the TMS-1 topography analysis system (Tomey, Nagoya, Japan), corneal specular microscopy (EM 1100; Tomey), subjective refraction, retinoscopy, auto-refraction (Canon, Tokyo, Japan), and measurement of anterior chamber depth (ACD) before and after application of 2% pilocarpine eye drops using the Zeiss IOLMaster® (Zeiss, Jena, Germany) and ultrasound (Schwind, Aschaffenburg, Germany), and photodocumentation.

Surgical intervention was standardized and has been described in detail in previous papers (Küchle *et al.*, 2000, 2001, 2002; Langenbacher *et al.*, 2002; Nguyen *et al.*, 2002).

Post-operative examinations were performed 1 day, 1 and 4 weeks, 3, 6, 12 and 18 months following surgery. In the present study we consider the 3-month results.

Determination of the cardinal points and system magnification

Any optical system can be subdivided into refracting surfaces and their interspaces. An incident ray of light intersects a refractive surface with a certain angular direction and exits the surface in a different angular direction. Refraction can, therefore, be interpreted as a coordinate transformation specified as a matrix problem using a 'refraction matrix'. A second type of matrix is necessary to specify the change in distance from the optical axis which arises during the passage of the ray

through the lens or through an interspace between lenses (Rosenblum and Christensen, 1974). This type of matrix is called a 'translation matrix'. Both the refraction and the translation matrices are 2×2 matrices. In order to determine the effect of an optical system on an incident ray of light, it is necessary to calculate the refractive effect of each interface and the translation of the ray through the interspaces. This is performed by specifying the refraction and translation matrices of all refracting surfaces and interspaces, and then multiplying them together to get the specification of the total optical system.

The refraction matrix P has the following form:

$$P = \begin{pmatrix} 1 & -R \\ 0 & 1 \end{pmatrix}$$

where R describes the refractive power of the surface. The translation matrix T has the characteristic format:

$$T = \begin{pmatrix} 1 & 0 \\ t/n' & 1 \end{pmatrix}$$

where t means the distance between two refractive surfaces and n' is the refractive index of the optical medium (t/n' means the 'reduced distance' between sequential surfaces). Distances are described in meters (m) and refractive powers in dioptres (D).

The system matrix P_{system} of an optical system consisting of the refractive elements R_1, R_2, \dots, R_n from left to right and interspaces $t_{1;2}, t_{2;3}, \dots, t_{n-1;n}$ is defined as

$$P_{\text{system}} = P_n \cdot T_{n-1;n} \cdots P_2 \cdot T_{1;2} P_1 = \begin{pmatrix} a & b \\ c & d \end{pmatrix}$$

with the definition of the refraction matrix P and the translation matrix T as shown above.

The cardinal points, i.e. the primary (F_1) and secondary (F_2) focal point, the primary (H_1) and secondary (H_2) principal point and the primary (N_1) and secondary (N_2) nodal point can be extracted from the elements of the system matrix P as follows:

$$F_1 = n \frac{a}{b}$$

$$F_2 = n'' \frac{-d}{b}$$

where n is the refractive index of the medium before the lens and n'' is the refractive index behind it. Following the common convention in geometrical optics, light is considered to enter from the left passing through the optical system and exiting to the right and the cardinal points are referenced from the respective vertices of the lens surface. Distances with a negative value mean that

the respective cardinal point is located on the left-hand side of the reference, whereas positive values indicate that the cardinal point is located on the right-hand side of the reference. The distances between the lens vertices and the principal points are:

$$H_1 = n \frac{a-1}{b}$$

$$H_2 = n'' \frac{1-d}{b}$$

The position of the nodal points relative to the lens surfaces are given by

$$N_1 = n \frac{(a-n'')/n}{b}$$

$$N_2 = n'' \frac{n/(n' - d)}{b}$$

For a symmetrical lens, the primary and secondary focal lengths are equal and the nodal points coincide with the principal points, because the optical medium on both sides of the lens has the same refractive index. In the Appendix, we demonstrate in an example the calculation of the cardinal points with a thick lens in air.

The lateral magnification of the optical system as the ratio of the image to the object size can be calculated as:

$$M = \frac{\text{image size}}{\text{object size}} = \frac{b}{V'} - d$$

$$\frac{1}{M} = a - \frac{b}{V}$$

$$\frac{b}{V'} - d = \frac{1}{a - \frac{1}{V}}$$

where V is the vergence of the light ray in dioptres before the front surface of the optical system and V' characterizes the vergence of the ray exiting the back surface of the optical system given in dioptres (Keating, 1981; Snead *et al.*, 1991). With this formulation, the object vergence can be transformed into image vergence and vice versa.

The optical system eye can be assessed by generalization of this formula to a system with more than one lens (Figure 2). From the left, the spectacle correction (equivalent power R_s) is followed by the single surface cornea (equivalent power R_c at a distance t_s behind the spectacle plane). The lens implant is predicted to lie at distance t_1 behind the corneal plane, which shortens during PAC based on the focus shift principle (dashed lines in Figure 2). The total axial length of the eye is assumed to be t_{al} and the residual distance from the lens to the retina (vitreous) is $t_v = t_{al} - t_1$.

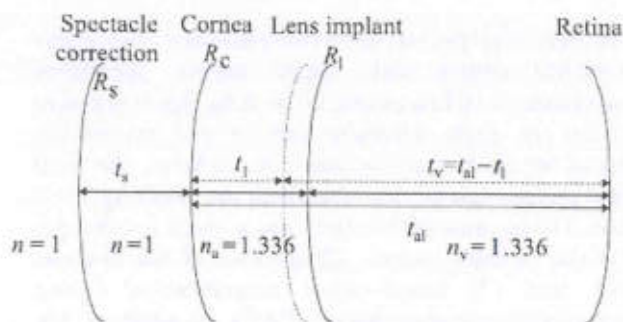


Figure 2. Schematic drawing of a simplified eye model with a single surface cornea and intraocular lens implant used in the example for calculation of the cardinal points of the (1) pseudophakic eye in the relaxed (non-accommodated) state (target refraction -0.2 D in the spectacle plane) (solid line), (2) in the accommodated state after forward movement of the lens optics (dashed lines), and (3) in the non-accommodated state of the lens implant (solid line) with a spherical near spectacle correction to remodel the decrease in object distance derived from the forward shift of the lens optics.

As an example, we predict an accommodative PCIOL power (21.39 D) using the Haigis formula (Haigis, 1995) ($a_0 = 1.487$, $a_1 = 0.195$, $a_2 = 0.112$, target refraction -0.2 D at 14 mm spectacle distance) with 43.81 D as the equivalent power of the cornea, an axial length of $t_{al} = 23.5$ mm and a preoperatively measured ACD of 3.1 mm. The predicted lens position according to the Haigis formula is $d_l = 4.723$ mm. The resulting cardinal points and the lateral magnification of the eye are given in Table 1 (second column). Assuming a forward shift of the lens optics of 1.0 mm (this being an intrinsic limitation of the 1 CU PCIOL design), the cardinal points (third column) result in a shortening of the in-focus object distance from -5.0 m (target refraction -0.2 D) to -0.61 m. This is equivalent to a PAC amplitude of 1.45 D. To remodel this object distance with the same PCIOL in the non-accommodated state with spectacle correction, the cardinal points of the optical system (including a near addition of 1.45 D at a spectacle distance of 14 mm) result in cardinal points shown in the fourth column of Table 1. Note that the lateral magnification with the spectacle correction for near distance (-2.722×10^{-2}) differs very little from the value derived with PAC because of a forward shift of the PCIOL optics (-2.696×10^{-2}) (Table 1).

Clinical assessment of accommodation and main outcome measures

Anterior chamber depth was measured with the IOL-Master and by non-contact (immersion with balanced salt solution) ultrasonic biometry (Schwind A-Scan, Aschaffenburg, Germany). Five consecutive measurements were taken and averaged. First, measurements were taken from PCIOL eyes without any pharmacolo-

Table 1. An example of the calculation of the cardinal points of the pseudophakic eye with an axial length of 23.5 mm, a measured anterior chamber depth of 3.1 mm (predicted PCIOL position 4.723 mm, predicted power of the PCIOL according to Haigis: 21.39 D) and an equivalent power of the cornea of 43.81 D. Column 2 describes the non-accommodated state, column 3 the conditions following a forward shift of the lens optics by 1.0 mm (the theoretical maximum, limited by the current 1 CU lens design) (PCIOL position 3.723 mm) and column 4 the non-accommodative state of the PCIOL (lens position 4.723 mm), but with a near spectacle correction of +1.45 D to move the object-side focal distance from -5.0 m to the respective value calculated from a forward shift of the PCIOL by 1.0 mm (-0.61 m). The negative magnification values indicate the inverted image on the retina

Distances relative to the corneal apex	Non-accommodated state	Pseudophakic accommodation due to forward shift of the lens	Simulation of the object-side focal distance with glasses
Object-side focal distance (mm)	-14.94	-15.03	-14.94
Image-side focal distance (mm)	22.93	22.43	22.41
Object-side principal point (mm)	1.20	0.93	1.18
Image-side principal point (mm)	1.36	1.10	0.87
Object-side nodal point (mm)	6.63	6.30	6.60
Image-side nodal point (mm)	6.79	6.46	6.29
Lateral magnification (image/object × 10E-2)	-0.323	-2.696	-2.722
Object distance (m)	-5.01	-0.61	-0.61
Equivalent power of the total optical system (D)	61.94	62.64	62.02

gical influence on pupil size or the state of the ciliary muscle. Secondly, measurements were taken 30 min after application of two pilocarpine 2% eye drops (Langenbacher *et al.*, 2002).

The cardinal points and the lateral magnification were calculated for each individual eye:

1. in the non-accommodated state,
2. in the state of PAC with the maximum of the forward shift of the lens optics as measured with the IOLMaster and ultrasound,
3. in the state of PAC with a standardized forward shift of the lens optics of 1.0 mm (the intrinsic limitation of the 1 CU PCIOL design) and
4. for the spectacle near correction necessary to image the same object distance as in 3.

The theoretical amplitude of PAC derived from the forward shift of the lens optics as a result of ciliary muscle contraction as measured with the IOLMaster and with ultrasound was compared with the corresponding measurements derived from (a) the subjective near point (Küchle *et al.*, 2002; Langenbacher *et al.*, 2002) (accommodometer), (b) the defocusing technique (Langenbacher *et al.*, 2002), and (c) dynamic streak retinoscopy (Kommerell, 1993).

Statistical analysis

All data were recorded on specifically designed data sheets and stored in a relational database (Access Office 2000, Microsoft). For statistical analysis, SPSS/PC 9.0 (Windows NT; SPSS, Inc., Chicago, IL, USA) was used. Measurement values of variables were described with mean, S.D., median, minimum and maximum values. Comparisons between variables were performed using non-parametric tests (Mann-Whitney *U*-test for

unpaired samples, Wilcoxon test for paired samples). For bivariate correlation analysis, Spearman's rank correlation coefficient *r* was used. A *p*-value of less than 0.05 was considered statistically significant.

Results

Anterior chamber depth 3 months after cataract extraction and implantation of the 1 CU posterior chamber lens decreased after instillation of 2% pilocarpine eye drops by 0.51–1.91 mm (mean 0.88 ± 0.48, median 0.66 mm), as measured using the IOLMaster, and by 0.46–1.23 mm (mean 0.63 ± 0.15, median 0.66 mm) as assessed by ultrasonic biometry.

Mean accommodation amplitude measured with an accommodometer (subjective near point) was 1.87 ± 0.42 D (median: 1.85 D, range: 1.00–2.78 D). The corresponding values were 1.10 ± 0.56 D (median: 1.12 D, range: 0.38–1.88 D) when assessed with streak retinoscopy and 1.66 ± 0.48 D (median: 1.75 D, range: 1.50–2.50 D) with the defocusing technique.

The positions of the cardinal points of the eye calculated with geometrical optics as described above are presented in *Table 2*. The mean equivalent power of the total optical system eye in the non-accommodated state (61.66 D) did not differ significantly from powers for the simulation of the object distance with glasses (61.75 D, *p* = 0.25), the PAC state calculated from the forward shift measured with ultrasound (62.11 D, *p* = 0.12) and with the IOLMaster (62.16 D, *p* = 0.10). The mean equivalent power was maximal with a fixed forward shift of the lens optics of 1.0 mm (theoretical maximum shift as limited by the current PCIOL design) (62.37 D).

Table 2. Calculation of the cardinal points in pseudophakic eyes after implantation of an accommodative posterior chamber IOL ($n = 35$). Lens power was predicted using the Haigis formula considering the equivalent power of the cornea, axial length of the eye and preoperatively measured anterior chamber depth. Column 2 describes the non-accommodated state, columns 3, 4 and 5 the conditions with forward shift of the lens optics by the value derived with the IOLMaster, ultrasound or a forward shift of 1.0 mm (theoretical maximum limited by the current lens design), and column 6 the non-accommodative state of the lens with individual spectacle correction necessary to remodel the change in object-side focal distance equivalent to a forward shift of the lens optics by 1.0 mm. The negative magnification values indicate the inverted image at the retina. In each row the figures give the mean and its S.D., the median, and the range

	N = 35 Mean ± S.D.; Median; Range				
	Non-accommodated state	PAC due to forward shift of the lens optics			Simulation of the object-side focal distance with glasses
		IOLMaster	Ultrasound	1.0 mm	
Object-side focal distance (mm)	-14.93 ± 0.82 -14.99 -15.90 to -13.96	-14.99 ± 0.99 -14.95 -15.50 to -14.05	-14.99 ± 0.88 -14.91 -15.95 to -14.04	-15.02 ± 1.12 -15.05 -15.98 to -14.08	-14.93 ± 0.93 -15.21 13.96-15.90
Image-side focal distance (mm)	23.13 ± 0.8 23.21 22.08-24.12	22.76 ± 1.02 22.88 21.74-23.81	22.80 ± 1.01 22.95 21.87-24.01	22.60 ± 1.06 22.71 21.53-23.65	22.59 ± 0.89 22.93 21.73-23.79
Object-side principal point (mm)	1.29 ± 0.09 1.26 1.17-1.41	1.09 ± 0.10 1.06 0.99-1.24	1.11 ± 0.12 1.08 1.04-1.29	1.01 ± 0.10 1.03 0.92-1.09	1.27 ± 0.93 1.25 1.14-1.41
Image-side principal point (mm)	1.46 ± 0.10 1.41 1.32-1.60	1.27 ± 0.11 1.26 1.15-1.42	1.29 ± 0.13 1.31 1.19-1.49	1.19 ± 0.11 1.20 0.93-1.22	0.96 ± 0.12 1.10 1.02-1.19
Object-side nodal point (mm)	6.74 ± 0.15 6.78 6.57-6.90	6.50 ± 0.19 6.55 6.31-6.74	6.52 ± 0.21 6.58 6.39-6.88	6.40 ± 0.18 6.42 6.19-6.78	6.71 ± 0.21 6.69 6.57-6.87
Image-side nodal point (mm)	6.91 ± 0.11 6.95 6.77-7.05	6.68 ± 0.18 6.71 6.50-6.87	6.70 ± 0.22 6.72 6.55-6.91	6.57 ± 0.19 6.56 5.39-6.75	6.40 ± 0.22 6.59 6.36-6.74
Lateral magnification (Image/object × 10E-2)	-0.324 ± 0.012 0.328 -0.307 to -0.342	-2.031 ± 0.23 -1.984 -1.423 to -22.78	-1.858 ± 0.20 -1.769 -1.653 to -2.078	-2.778 ± 0.27 -2.813 -2.439 to -3.141	-2.806 ± 0.25 -1.933 -1.810 to -2.298
Object distance (m)	-5.62 ± 1.83 -4.83 -25 to -1.1	-0.81 ± 0.21 -0.79 -2.11 to -0.65	-0.88 ± 0.25 -0.93 -2.82 to -0.63	-0.59 ± 0.28 -0.63 -1.314 to -0.510	-0.59 ± 0.28 -0.63 -1.314 to -0.510
Equivalent power of the total optical system (D)	61.66 ± 2.84 61.02 58.58-65.06	62.16 ± 3.53 61.99 58.95-65.64	62.11 ± 3.38 62.03 58.89-65.60	62.37 ± 3.26 62.17 59.18-65.89	61.75 ± 2.93 62.02 58.72-65.05

The forward shift of the lens optics by 1.0 mm effected a decrease in median in-focus object distance from -4.83 to -0.63 m, indicating a median PAC amplitude of 1.49 D (range: 1.21-1.81 D depending on the individual axial length, the equivalent power of the cornea, the effective lens position and the power of the inserted PCIOL). In contrast, the accommodation amplitude calculated from the real forward shift of the lens optics as measured with the IOLMaster (1.13 D) and ultrasound (0.98 D) yielded somewhat lower values.

The lateral magnification of the optical system evaluated from the position of the nodal points, the object distance and the distance between the PCIOL and the image plane (retina) was -0.00324 on average in the non-accommodated state (object distance in median

-4.83 m) and increased significantly to the accommodated states (IOLMaster: -0.02031; ultrasound: -0.01858; 1.0 mm forward shift: -0.02778; same object distance corrected with glasses: -0.02045) because of the shortening of the in-focus object distance. The difference in lateral magnification comparing PAC and spectacle correction (-0.02778/-0.02806 = 0.9900) seems to be of minor clinical relevance.

The calculated accommodation amplitude based on the forward shift measured with the IOLMaster did not differ significantly from the corresponding value as measured with the defocusing technique ($p = 0.08$), the accommodometer ($p = 0.13$) or streak retinoscopy ($p = 0.06$). It correlated significantly with the accommodation amplitude evaluated with the defocusing tech-

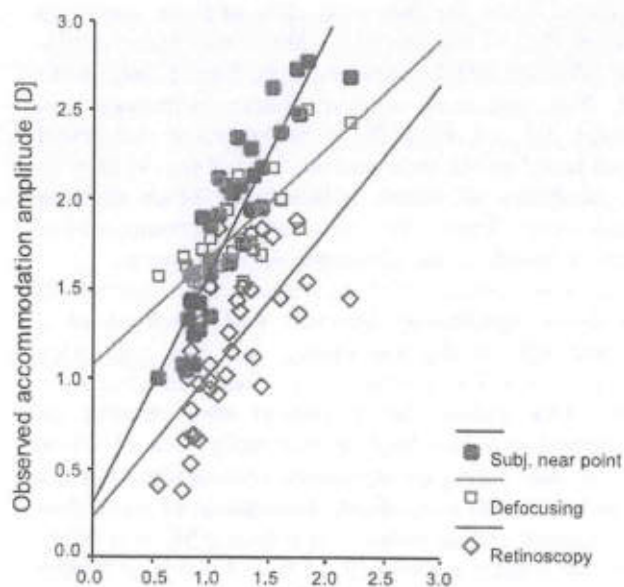


Figure 3. Correlation between the theoretical accommodation amplitude based on the model calculation and the change of anterior chamber depth measured with the IOLMaster (x-axis) and the accommodation amplitude measured with the subjective near point (accommodometer), defocusing technique and streak retinoscopy (y-axis) in diopters. The presented data are based on 35 eyes 3 months after cataract surgery and implantation of the new accommodative posterior chamber lens 1 CU.

nique ($r = 0.752, p = 0.005$) and the accommodometer (subjective near point) ($r = 0.676, p = 0.02$), but only to a borderline extent with the accommodation amplitude evaluated with streak retinoscopy ($r = 0.465, p = 0.05$) (Figure 3).

The calculated accommodation amplitude based on the forward shift measured with ultrasound did not differ significantly in our limited number of patients from the corresponding value measured with the defocusing technique ($p = 0.15$) and the accommodometer ($p = 0.08$), but was significantly larger than the corresponding value as assessed by streak retinoscopy ($p = 0.02$). It correlated significantly with the accommodation amplitude evaluated with the defocusing technique ($r = 0.522, p = 0.01$) and to a borderline extent with the accommodometer (subjective near point) ($r = 0.414, p = 0.05$), but did not correlate with the accommodation amplitude evaluated with streak retinoscopy ($r = 0.421, p = 0.08$).

Discussion

A ray of light from the height of any given object passing undeviated through the nodal point of the eye will determine the height of its image on the retina. The lateral magnification of the pseudophakic eye is defined

by the ratio between the second nodal point to retina distance, to the object to first nodal point distance. For a rough estimate, it is not necessary to consider the cornea and the lens implant as a 'thick' lens (Wang and Pomerantzeff, 1983; Garcia et al., 1996; Rubin, 1997). In most cases, the curvature or equivalent power of the cornea is known, but not the equivalent power of both refractive surfaces and the pachymetry. The same problem occurs for the PCIOL, where normally the total power is given, but not the curvature of the front and back surface, the central thickness and the refractive index of the medium. The form factor of the lens is considered in the A-constant or ACD-constant or in the Haigis formula with a_0, a_1 and a_2 , which affects the predicted post-operative lens position provided by the PCIOL calculation scheme (Gernet et al., 1970; Hoffer, 1975; Holladay et al., 1988; Retzlaff et al., 1990; Holladay, 1993; Haigis, 1995). The 1 CU accommodative implant used in our study has an equi-convex shape and can be modelled by a single refracting surface positioned exactly at the predicted lens position given from the PCIOL calculation scheme (Küchle et al., 2002).

One possible problem following cataract surgery is anisometropia or aniseikonia. If the difference in lateral magnification from one eye to the contralateral eye exceeds a value of 4–5%, both images cannot be fused or processed in the brain together as a single image (Wang and Pomerantzeff, 1983; Garcia et al., 1996; Rubin, 1997). In an experimental setup with trained patients, lateral magnification disparities up to 25% may be tolerated. Linear geometry offers a straightforward method to evaluate the position of the cardinal points of the eye and to predict the lateral magnification after implantation of a PCIOL. It was not the aim of our study to compare the magnification between both eyes of one patient, but rather to demonstrate how easy it is to calculate the magnification from the matrix representation. However, in the case of an accommodative lens implant such as the 1 CU that works according to the focus shift principle (Küchle et al., 2000, 2001, 2002; Nguyen et al., 2002), this methodology provides the option of predicting the amount of PAC from the measurement of the forward shift of the lens optics. This option further allows a subdivision of the total accommodation response into true PAC because of ciliary muscle contraction and that due to increased depth of focus following pupillary constriction (Nakazawa and Ohtsuki, 1984; Hardman et al., 1990; Fukuyama et al., 1999; Leyland and Bloom, 1999).

One of the unsolved problems in measuring accommodation amplitude in patients with subjective clinical methods is the lack of reproducibility and repeatability (Langenbacher et al., 2002; Krueger, 1980; Rosenfield

and Cohen, 1996). Pharmacologically stimulated accommodation using pilocarpine 2% normally creates much greater miosis and contraction of the ciliary body than with normal physiological accommodation. Accommodation is dependent on the general condition of the patient as well as external measuring conditions. Small variations in parameters may result in markedly different accommodative results. In contrast, the measurement of the ACD using the IOLMaster or ultrasound seems to be more reproducible and reliable. With geometrical optics, the lens positions in the non-accommodated and in the accommodated state were used in our study to derive the amplitude of PAC. This value is independent of any pseudoaccommodation, which may also be observed in pseudophakic patients with a non-accommodative lens implant (Nakazawa and Ohtsuki, 1984; Hardman *et al.*, 1990). Thus, the indirect method of measuring the change in ACD for the prediction of the accommodative response may be the first step towards objectively evaluating the true PAC, in the case where the PCIOL is working according to the focus shift principle.

Our data demonstrate that the accommodative response because of a forward shift of the lens optics ranges between 1.21 and 1.81 D mm⁻¹, with a mean of 1.49 D. This value depends on the individual biometric conditions, such as the axial length, the equivalent power of the cornea, the equivalent power of the lens implant and the post-operative lens position, all of which are included in the PCIOL calculation scheme. Because of space limitations in the capsular bag and technical limitations associated with the distance between the inner and outer transmission zones of the lens haptics, the focus shift principle can only be a first step to overcome presbyopia after cataract surgery and implantation of an artificial lens. The accommodative amplitude is limited to values of about 0.75–2.00 D and therefore cannot fully restore phakic accommodation. To ensure an accommodative response, the target refraction should be handled with care and should be slightly myopic between 0 and –0.50 D. If the target refraction is >0 D, the patient has to accommodate for far distance vision and even more so for near vision. In contrast, if the target refraction is more than –0.50 D of myopia, the patient requires additional far distance correction.

A previous study demonstrated that the subjective near point measured with an accommodometer and defocusing technique yielded superior reproducibility and stability of the accommodation results, as compared with streak retinoscopy and videorefractometry, which showed the lowest repeatability and the largest variation (Langenbacher *et al.*, 2002). The results of the current study confirm that defocusing and the accommodometer correlated best with the accommodation response

calculated from the biometric data and the measured forward shift of the lens optics because of accommodation, whereas streak retinoscopy correlated only partially. The measured accommodative amplitudes on average did not differ from the respective calculated values based on the measured decrease of the ACD, with the exception of streak retinoscopy, which differed significantly from the calculated accommodative response based on the ultrasonic ACD decrease.

Our results indicate that the lateral magnification does not differ significantly between PAC because of a forward shift of the lens optics, and near correction with glasses to focus objects at the same distance as in PAC. This means that a patient who receives an accommodative lens implant bilaterally, one of which fails to shift during ciliary muscle contraction, will not be bothered with a significant aniseikonia of more than 1% (lateral magnification spectacle/PAC = 0.9900), when we assume a maximum shift of 1.0 mm as limited by the current design of the I CU.

The drawback of the present study is that the actual measurement of the ACD cannot be performed dynamically in clinical routine up to now and a pharmacological stimulation with pilocarpine eye drops is necessary. Dr Haigis from the Department of Ophthalmology in Würzburg/Germany together with the Zeiss company are working on solutions to overcome this problem by coaxially presenting a fixation target in far and near distance to measure the decrease in ACD dynamically with the IOLMaster. The first clinical measurements have been made and the results are very promising. But these measurements are made under experimental conditions and may be only integrated into clinical practice in the future after a validation period and an optimization of the hardware and software of the IOLMaster (unpublished data). If valid data from a separate measurement of the anterior and posterior corneal surface as well as detailed data from the PCIOL manufacturer are available, our model can be enhanced by these data.

In conclusion, we have presented a straightforward mathematical computer-based strategy for calculation of the cardinal points and the lateral magnification of the pseudophakic eye using linear geometrical optics applied to a study group after cataract surgery and implantation of the I CU accommodative lens working on the focus shift principle. We have demonstrated that with the measured shift of the lens optics and the biometrical data of the eye the PAC can be derived directly. This technique may be an additional indicator for the accommodative response in pseudophakic patients and may allow a subdivision of the measured accommodation into true PAC and pseudoaccommodation, for example, because of depth of focus increase induced by pupillary constriction.

Appendix

As an example, the system matrix P_{system} of a 'thick' IOL in air with a front surface of 9.00 D and a back surface of 12.00 D separated by a space of $t = 1.0$ mm and a material-specific refractive index of $n' = 1.42$ can be expressed in matrix notation as

$$\begin{aligned}
 P_{\text{system}} &= \begin{pmatrix} 1 & -12 \\ 0 & 1 \end{pmatrix} \begin{pmatrix} 1 & 0 \\ 0.001/1.42 & 1 \end{pmatrix} \begin{pmatrix} 1 & -9 \\ 0 & 1 \end{pmatrix} \\
 &= \begin{pmatrix} 1 & -12 \\ 0 & 1 \end{pmatrix} \begin{pmatrix} 1 & -9 \\ 0.0007042 & 0.9937 \end{pmatrix} \\
 &= \begin{pmatrix} 0.9915 & -20.9239 \\ 0.0007042 & 0.9937 \end{pmatrix}
 \end{aligned}$$

The validity of the resulting matrix can be checked with its determinant, which must be equal $\det(P) = 0.9915 \times 0.9937 - (-20.9239) \times 0.0007042 = 1$. The cardinal points (primary and secondary focal point F_1 and F_2 , primary and secondary principal point H_1 and H_2 and primary and secondary nodal point N_1 and N_2) of the thick lens in air are

$$\begin{aligned}
 F_1 &= 1.0 \frac{0.9915}{-20.9239} = -47.4 \text{ mm} \\
 F_2 &= 1.0 \frac{-0.9937}{-20.9239} = 47.5 \text{ mm} \\
 H_1 &= 1.0 \frac{0.9915 - 1}{-20.9239} = 0.406 \text{ mm} \\
 H_2 &= 1.0 \frac{1 - 0.9937}{-20.9239} = -0.301 \text{ mm} \\
 N_1 &= 1.0 \frac{0.9915 - 1.0/1.0}{-20.9239} = 0.406 \text{ mm} \\
 N_2 &= 1.0 \frac{1.0/1.0 - 0.9937}{-20.9239} = -0.301 \text{ mm}
 \end{aligned}$$

In a generalized form, P_{system} can be written as

$$P_{\text{system}} = \begin{pmatrix} 1 - R_2 t/n' & -R_1 - R_2 + R_1 R_2 t/n' \\ t/n' & 1 - R_1 t/n' \end{pmatrix} = \begin{pmatrix} a & b \\ c & d \end{pmatrix}$$

where R_2 is the refractive power of the back surface, R_1 the refractive power of the front surface and t/n' the reduced thickness of the interspace. The upper right element of the system matrix is well known as the negative value of the equivalent power of a 'thick' lens.

References

Allen, E. D., Burton, R. L., Webber, S. K., Haaskjold, E., Sandvig, K., Jyrkkio, H., Leite, E., Nystrom, A. and Wollensak, J. (1996) Comparison of a diffractive and a monofocal intraocular lens. *J. Cataract Refract. Surg.* **22**, 446-451.
 Fisher, R. F. (1977) The force of contraction of the ciliary muscle during accommodation. *J. Physiol. (London)* **270**, 51-74.

Fisher, R. F. (1986) The ciliary body in accommodation. *Trans. Ophthalmol. Soc. UK* **105**, 208-219.
 Fukuyama, M., Oshika, T., Amano, S. and Yoshitomi, F. (1999) Relationship between apparent accommodation and corneal multifocality in pseudophakic eyes. *Ophthalmology* **106**, 1178-1181.
 Garcia, M., Conzaes, C., Pascual, I. and Fimia, A. (1996) Magnification and visual acuity in highly myopic phakic eyes corrected with an anterior chamber intraocular lens versus by other methods. *J. Cataract Refract. Surg.* **22**, 1416-1422.
 Gernet, H., Ostholt, H. and Werner, H. (1970) Die präoperative Berechnung intraokularer Binkhorst-Linsen. In: *122. Versammlung der Rheinisch-Westfälischen Augenärzte* (ed. Balve), Zimmermann-Verlag, Frankfurt, Germany, pp. 54-55.
 Gray, P. J. and Lyall, M. G. (1992) Diffractive multifocal intraocular lens implants for unilateral cataracts in presbyopic patients. *Br. J. Ophthalmol.* **76**, 336-337.
 Haigis, W. (1995) Biometrie. In: *Augenärztliche Untersuchungsmethoden* (eds W. Straub, P. Kroll and H. J. Kühle), Biermann, Köln, Germany, pp. 255-304.
 Hardman Lea, S. J., Rubinstein, P. M., Snead, M. P. and Haworth, S. M. (1990) Pseudophakic accommodation? A study of the stability of capsular bag supported, one piece, rigid tripod, or soft flexible implants. *Br. J. Ophthalmol.* **74**, 22-25.
 Hoffer, K. J. (1975) Mathematics and computers in intraocular lens calculation. *Am. Intra-Ocul. Implant Soc. J.* **1**, 4-5.
 Holladay, J. T. (1993) Refractive power calculations for intraocular lenses in the phakic eye. *Am. J. Ophthalmol.* **116**, 63-66.
 Holladay, J. T. (1997) Standardizing constants for ultrasonic biometry, keratometry and intraocular lens power calculations. *J. Cataract Refract. Surg.* **23**, 1356-1370.
 Holladay, J. T., Prager, T. C. and Chandler, T. Y. (1988) A three-part system for refining intraocular lens power calculations. *J. Cataract Refract. Surg.* **14**, 17-24.
 Keating, M. P. (1981) Lens effectivity in terms of dioptric power matrices. *Am. J. Optom. Physiol. Optics* **58**, 1154-1160.
 Knorz, M. C. and Seiberth, V. (1996) Die True-Vista-Bifokal-IOL. *Ophthalmologie* **93**, 17-21.
 Kommerell, G. (1993) Strichskioskopie: Optische Prinzipien und praktische Empfehlungen. *Klin. Monatsbl. Augenheilkd.* **203**, 10-18.
 Krueger, P. B. (1980) The effect of cognitive demand on accommodation. *Am. J. Ophthalmol.* **57**, 440-445.
 Kühle, M., Gusek-Schneider, G. C., Langenbacher, A., Seitz, B. and Hanna, K. H. (2001) Erste Ergebnisse der Implantation einer neuen, potentiell akkommodierbaren Hinterkammerlinse. *Klin. Monatsbl. Augenheilkd.* **218**, 603-608.
 Kühle, M., Langenbacher, A., Gusek-Schneider, G. C. and Seitz, B. (2000) First and preliminary results of a new posterior chamber intraocular lens. *Online Journal of Ophthalmology*, (<http://www.onjoph.com/deutsch/artikel/pciol.html>).
 Kühle, M., Nguyen, N. X., Langenbacher, A., Gusek-Schneider, G. C., Seitz, B. and Hanna, K. D. (2002)

- Implantation of a new accommodative posterior chamber intraocular lens (1 CU). *J. Refract. Surg.* **8**, 208–217.
- Langenbucher, A., Huber, S., Nguyen, N. X., Seitz, B. and Kühle, M. (2002) Measurement of accommodation after implantation of a new accommodative posterior chamber lens (1 CU). *J. Cataract Refract. Surg.* (in press).
- Leyland, M. and Bloom, P. (1999) Intraocular lens design for pseudoaccommodation (letter). *J. Cataract Refract. Surg.* **25**, 1038–1039.
- Nakazawa, M. and Ohtsuki, K. (1984) Apparent accommodation in pseudophakic eyes after implantation of posterior chamber intraocular lenses: optical analysis. *Invest. Ophthalmol. Vis. Sci.* **25**, 1458–1460.
- Nguyen, N. X., Langenbucher, A., Huber, S., Seitz, B. and Kühle, M. (2002) Short-term blood–aqueous barrier breakdown after implantation of a new accommodative posterior chamber intraocular lens (1 CU). *J. Cataract Refract. Surg.* **28**, 1189–1194.
- Retzlaff, J. A., Sanders, D. R. and Kraff, M. C. (1990) Development of the SRK/T intraocular lens implant power calculation formula. *J. Cataract Refract. Surg.* **16**, 333–340.
- Rosenblum, W. M. and Christensen, J. L. (1974) Optical matrix method: optometric applications. *Am. J. Optom. Physiol. Opt.* **51**, 961–968.
- Rosenfield, M. and Cohen, A. S. (1996) Repeatability of clinical measurements of the amplitude of accommodation. *Ophthalmic. Physiol. Opt.* **16**, 247–249.
- Rubin, M. L. (1997) Contemporary management of aniseikonia. *Surv. Ophthalmol.* **41**, 321–330.
- Saladin, J. J. and Stark, L. (1975) Presbyopia: new evidence from impedance cyclography supporting the Hess-Gullstrand theory. *Vision Res.* **15**, 537–541.
- Snead, M. P., Harman, S., Rubinstein, M. P., Reynolds, K. and Haworth, S. M. (1991) Determination of the nodal point position in the pseudophakic eye. *Ophthalm. Physiol. Opt.* **11**, 105–108.
- Steinert, R. F., Aker, B. L., Trentacost, D. J., Smith, P. J. and Tarantino, N. (1999) A prospective comparative study of the AMO ARRAY zonal-progressive multifocal silicone intraocular lens and a monofocal intraocular lens. *Ophthalmology* **106**, 1243–1255.
- Strenk, S., Semmlow, J. L., Strenk, L. M., Munoz, P., Gronland-Jacob, J. and deMarco, J. K. (1999) Age-related changes in human ciliary muscle and lens: a magnetic resonance imaging study. *Invest. Ophthalmol. Vis. Sci.* **40**, 1162–1169.
- Swegmark, G. (1969) Studies with impedance cyclography on human accommodation at different ages. *Acta Ophthalmol.* **47**, 1186–1206.
- Wang, G. J. and Pomerantzeff, O. (1983) Iseikonia and accommodation in the fellow eye in monocular IOL implantation. *Am. Intra-Ocul. Implant Soc. J.* **9**, 441–444.

Pseudophakic accommodation with translation lenses – dual optic vs mono optic

Achim Langenbucher, Sven Reese, Christina Jakob and Berthold Seitz

Department of Ophthalmology, University of Erlangen-Nürnberg, Schwabachanlage 6, D-91054 Erlangen, Germany

Abstract

Purpose: To investigate the pseudophakic accommodation effect in dual and mono optic translation accommodative intraocular lenses (AIOL) using linear matrix methods in the paraxial space.

Methods: Dual (anterior optic of power +32 D linked to a compensatory posterior optic of negative power) and mono lens power was determined in the non-accommodated state using linear geometric optics based on the Gullstrand model eye. The position of the AIOL was calculated from a regression formula. Pseudophakic accommodation was assessed with three systems: (1) forward shift of the mono optic lens, (2) anterior translation of the anterior optic in the dual optic lens system with an unchanged position of the posterior minus lens and (3) symmetrical anterior and posterior translation of the anterior and posterior lens. The Gullstrand model eye was modified by changing the axial length (and proportionally changing the phakic anterior chamber depth) to investigate the accommodative effect in myopic and hyperopic eyes.

Results: The dual optic lens system (2) yields a nearly constant accommodation amplitude of 2.4–2.5 D mm⁻¹ movement over the total range of axial lengths. The mono optic lens (1) provides a higher accommodative effect only in extremely short eyes (high refractive power of the lens), whereas for normal eyes (1.4–1.5 D mm⁻¹ movement) and for long (myopic) eyes the accommodative effect is much less than the dual optic lens. The dual optic lens system under condition (3) yields less accommodation amplitude compared with the dual optic system under condition (2) over the total range of axial length but provides higher accommodation amplitude compared with the mono optic lens system (1) with axial lengths greater than 22.3 mm (lens power 25.5 D). In the accommodated state, with lens translation of 1 mm, the absolute value of the lateral magnification increases with the refractive power of the mono optic lens (1) and decreases in both dual optic lens systems (under conditions 2 and 3).

Conclusions: A mathematical strategy is presented for calculation of the accommodative effect of mono-optic and dual optic AIOL. The dual optic lens yielded a nearly constant accommodation amplitude of about 2.4–2.5 D mm⁻¹ translation, whereas the mono optic lens yielded an accommodative response of <2 D mm⁻¹ translation in long myopic or normal eyes. Only in extremely short eyes is the accommodative amplitude of the mono-optic lens higher than the dual optic lens.

Keywords: accommodative intraocular lenses, cardinal points, dual optic intraocular lens, geometrical optics, pseudophakic accommodation

Introduction

Accommodation in the phakic human eye is accomplished by ciliary body contraction and subsequent

release in the resting tension of the zonular fibres by which the crystalline lens is suspended, resulting in increased lens curvature (Fisher, 1973, 1977, 1986). In contrast, Schachar's theory, which has not been validated by other study groups, suggests that increased lens curvature is a result of increased zonular tension (Schachar, 1994).

Presbyopia is defined by the progressive loss of accommodative amplitude compromising near function and has been attributed to mechanical changes in the lens and capsule including changes in the elastic

Received: 12 January 2004
Revised form: 25 March 2004
Accepted: 2 April 2004

Correspondence and reprint requests to: Achim Langenbucher PhD.
Tel.: 49 9131 853 4052; Fax: 49 9131 853 4436.
E-mail address: achim.langenbucher@augen.imed.uni-erlangen.de

property and progressive circumferential enlargement of the crystalline lens, weakening of the ciliary muscle and loss of zonular and ciliary body effectiveness and elasticity (Saladin and Stark, 1975; Strenk *et al.*, 1999).

Despite excellent restoration of visual acuity and good biocompatibility of posterior chamber intraocular lenses, there is very little accommodation in pseudophakic eyes with monofocal lens optics, so that patients usually remain presbyopic after cataract surgery. This problem has only partly been solved by the introduction of diffractive and bifocal intraocular lenses (Gray and Lyall, 1992; Allen *et al.*, 1996; Knorz and Seiberth, 1996; Steinert *et al.*, 1999). Thus, efforts are being undertaken to develop new concepts that restore accommodation. Attempts have been made to replace the crystalline lens by refilling the capsular bag with appropriately deformable gels (Nishi and Nishi, 1998). However, this approach is limited by the intrinsic mechanical instability of such materials that cannot be expected to retain a specific shape over time while sustaining a rapid, constant, and predictable response to radial zonular tension as required for the dynamics of accommodation.

The principle of axial lens movement has been adopted by more recent accommodating lens designs, such as the AT-45 developed by Cumming *et al.* (2001) or the accommodative I CU developed by Hanna *et al.* (Küchle *et al.*, 2001, 2002). In preliminary clinical studies, the anterior movement of the lens optics is shown to be in a range up to 0.7 mm corresponding to a pseudophakic accommodation response of about 1.1 D. This pseudophakic accommodation effect may be enhanced by pseudoaccommodation because of asphericity of the refractive surfaces and the enlargement of the focus depth because of a pinhole effect (Nakazawa and Ohtsuki, 1984; Leyland and Bloom, 1999; Langenbucher *et al.*, 2003b).

McLeod recently presented a dual optic accommodating lens, where the dual lens complex is designed such that anterior optic, of positive power (32 D), is linked to an optic of negative power by means of an articulated haptic. The power of the posterior optic is such that it is intended to produce emmetropia or, alternatively, some pre-determined ametropia at the plane of the cornea (McLeod *et al.*, 2003). With this design, anterior translation of the anterior optic produces significantly greater change in object distance than translation of a similar magnitude for a single optic lens.

Linear geometric optics using matrix conventions provides a simple mathematical tool for prediction of the pseudophakic accommodative amplitude because of a translation of the lens optics. The purpose of the present study was to provide a simple mathematical concept for deriving accommodative amplitude on account of the translation accommodative lenses and

to apply this model to both mono- and dual optic accommodative lenses placed in Gullstrand's model eye. Variations of this eye model can be used to simulate the pseudophakic accommodative effect in myopes and hyperopes.

Methods

Description of the optical system with a system matrix

Any optical system can be subdivided into refracting surfaces and their interspaces. An incident ray of light intersects a refractive surface with a certain angular direction and may exit the surface with a different angular direction. Refraction can, therefore, be interpreted as a coordinate transformation specified as a matrix problem using a 'refraction matrix'. A second type of matrix is necessary to specify the change in distance from the optical axis, which arises during the passage of the ray through the lens or through an interspace between lenses (Rosenblum and Christensen, 1974). This type of matrix is called a 'translation matrix'. For spherical surfaces, both the refraction and the translation matrix are 2×2 -matrices. In order to determine the effect of an optical system on an incident ray of light, it is necessary to calculate the refractive effect of each interface and the translation of the ray through the interspaces. This is carried out by specifying the refraction and translation matrices of all refracting surfaces and interspaces and then multiplying them together in reverse order to get the specification of the total optical system.

The refraction matrix P has the following form:

$$P = \begin{bmatrix} 1 & -R \\ 0 & 1 \end{bmatrix}, \quad (1)$$

where R describes the refractive power of the surface. The translation matrix T has the characteristic format:

$$T = \begin{bmatrix} 1 & 0 \\ t/n' & 1 \end{bmatrix}, \quad (2)$$

where t is the distance between two refractive surfaces and n' is the refractive index of the optical medium (t/n' means the 'reduced distance' between sequential surfaces). Distances are described in meters (m) and refractive powers in diopters (D).

The system matrix P_{system} of an optical system consisting of the refractive elements R_1, R_2, \dots, R_n from left to right and interspaces $t_{1,2}, t_{2,3}, \dots, t_{n-1,n}$ is defined as

$$P_{\text{system}} = P_n \cdot T_{n-1,n} \cdots P_2 \cdot T_{1,2} P_1 = \begin{bmatrix} a & b \\ c & d \end{bmatrix}, \quad (3)$$

with the definition of the refraction matrix P and the translation matrix T as shown above.

The cardinal points, i.e. the primary (F_1) and secondary (F_2) focal point, the primary (H_1) and secondary (H_2) principal point and the primary (N_1) and secondary (N_2) nodal point can be extracted from the elements of the system matrix P as follows (Rosenblum and Christensen, 1974; Langenbucher *et al.*, 2003a):

$$F_1 = n \frac{a}{b}$$

$$F_2 = n'' \frac{-d}{b}, \tag{4}$$

where n is the refractive index of the medium before the lens and n'' is the refractive index behind it. Following the common convention in geometrical optics, light is considered to enter from the left passing through the optical system and exiting to the right and the cardinal points are referenced from the respective vertices of the lens surface. Distances with a negative value mean that the respective cardinal point is located on the left hand side of the reference, whereas positive values indicate that the cardinal point is located on the right hand side of the reference. The distances between the lens vertices and the principal points are:

$$H_1 = n \frac{a-1}{b}$$

$$H_2 = n'' \frac{1-d}{b}. \tag{5}$$

The position of the nodal points relative to the lens surfaces are given by

$$N_1 = n \frac{a - \frac{a''}{n}}{b}$$

$$N_2 = n'' \frac{\frac{n}{a''} - d}{b}. \tag{6}$$

For a symmetrical lens, the primary and secondary focal lengths are equal and the nodal points coincide with the principal points if the optical medium on both sides of the lens has the same refractive index.

In the case of a finite object distance, the lateral magnification of the optical system is the ratio of the image to the object size and yields:

$$M = \frac{\text{Image size}}{\text{Object size}} = \frac{b}{V'} - d$$

$$\frac{1}{M} = a - \frac{b}{V'}$$

$$\frac{b}{V'} - d = \frac{1}{a - \frac{1}{V'}} \tag{7}$$

where V is the vergence of the light ray in diopters before the front surface of the optical system and V' characterizes the vergence of the ray exiting the back surface of the optical system given in diopters (Keating, 1981; Snead *et al.*, 1991). With this formulation, the object

vergence can be transformed into image vergence and vice versa.

Calculation of the mono and dual optic lens for the Gullstrand model eye

First, we predict the position of the mono-optic thin lens from the data of the Gullstrand model eye provided in *Table 1*. From the IOL-specific anterior chamber depth (ACD) constant of the manufacturer (i.e. $ACD_{\text{Constant}} = 5.1$ for the HumanOptics 1 CU lens) the postoperative lens position according to the Haigis regression formula (Haigis, 1995) reads

$$d_{\text{IOL}} = 1.08 \cdot ACD_{\text{Constant}} + 0.1 \cdot (AL - 23.39) + 0.4 \cdot (ACD + CT - 3.37) - CT = 5.647 \text{ mm}$$

The system matrix S_M for the Gullstrand model eye (data from *Table 1*) with a mono-optic artificial lens implant with refractive power P_M at position d_{IOL} is defined as

$$S_M = \begin{bmatrix} 1 & -P_M \\ 0 & 1 \end{bmatrix} \cdot \begin{bmatrix} 1 & 0 \\ -\frac{d_{\text{IOL}}}{n_a} & 1 \end{bmatrix} \cdot \begin{bmatrix} 1 & -\frac{n_a - n_c}{R_{CP}} \\ 0 & 1 \end{bmatrix} \cdot \begin{bmatrix} 1 & 0 \\ -\frac{d_{CT}}{n_c} & 1 \end{bmatrix} \cdot \begin{bmatrix} 1 & -\frac{n_c - 1}{R_{CA}} \\ 0 & 1 \end{bmatrix}$$

$$= \begin{bmatrix} 1 - P_M & [1.0024 - 42.3564] \\ 0 & 1 \end{bmatrix} \cdot \begin{bmatrix} 1.0024 - 42.3564 & [0.0046 \quad 0.8018] \\ 0.0046 & 0.8018 \end{bmatrix} \tag{8}$$

As the secondary focal point F_2 (equation 4) of the above described system should coincide with the retina,

$$F_2 = n_v \frac{0.8018}{42.3564 + 0.8018 \cdot P_M} = AL - d_{CT} - d_{\text{IOL}} = 0.017663 \tag{9}$$

or

$$P_M = 22.8148 \text{ D}$$

The equivalent refractive power of the eye as the upper right element of S_M equals 60.6503 D.

Let us assume a dual optic lens system as described by McLeod *et al.* (2003) with a refractive power of 32 D for the anterior optic and a compensating lens of

Table 1. Biometric data of the Gullstrand model eye

Corneal anterior vertex radius (R_{CA})	0.0078 m
Corneal posterior vertex radius (R_{CP})	0.0065 m
Cornea index of refraction (n_c)	1.3771
Aqueous index of refraction (n_a)	1.3374
Vitreous index of refraction (n_v)	1.336
Cornea thickness (CT)	0.00055 m
Axial length (AL)	0.02386 m
Phakic anterior chamber depth (ACD) (endothelium to anterior lens surface)	0.00305 m

negative power separated by $d_{D12} = 3$ mm interspace in the non-accommodated state. The equator of the lens system is assumed to coincide with the position of the mono lens system described earlier. The anterior plus lens and the posterior minus lens are positioned relative to the equator of the lens system in a symmetrical fashion, so that the anterior plus lens is located 4.147 mm and the posterior compensating minus lens is positioned 7.147 mm from the back surface of the cornea.

The system matrix S_D for the Gullstrand model eye with an dual optic artificial lens implant with refractive power P_{DA} equal 32 D and a compensating posterior lens P_{DP} is defined as

$$S_D = \begin{bmatrix} 1 & -P_{DP} \\ 0 & 1 \end{bmatrix} \cdot \begin{bmatrix} 1 & 0 \\ d_{D12} & 1 \end{bmatrix} \cdot \begin{bmatrix} 1 & -P_{DA} \\ 0 & 1 \end{bmatrix} \cdot \begin{bmatrix} 1 & 0 \\ d_{OL} & 1 \end{bmatrix} \cdot \begin{bmatrix} 1 & -\frac{n_s - n_c}{R_{CP}} \\ 0 & 1 \end{bmatrix} \cdot \begin{bmatrix} 1 & 0 \\ -\frac{d_{CT}}{n_c} & 1 \end{bmatrix} \cdot \begin{bmatrix} 1 & -\frac{n_s - 1}{R_{CA}} \\ 0 & 1 \end{bmatrix} \\ = \begin{bmatrix} 1 & -P_{DP} \\ 0 & 1 \end{bmatrix} \cdot \begin{bmatrix} 0.8902 & -69.5357 \\ 0.0055 & 0.6934 \end{bmatrix} \\ = \begin{bmatrix} 0.8902 - 0.0055 \cdot P_{DP} & -69.5357 - 0.6934 \cdot P_{DP} \\ 0.0055 & 0.6934 \end{bmatrix} \quad (10)$$

As the secondary focal point F_2 (equation 4) of the above described system should coincide with the retina,

$$F_2 = n_v \frac{0.6934}{69.5357 + 0.6934 \cdot P_{DP}} \\ = AL - d_{CT} - d_{OL} - \frac{d_{D12}}{2} \\ = 0.016163 \quad (11)$$

or

$$P_{DP} = -17.6282D$$

The equivalent refractive power of the eye as the upper right element of S_M equals 57.3128 D.

Prediction of the pseudophakic accommodation because of lens translation

The optical system in the accommodated state can be described in an analogous way. In the mono optic pseudophakic eye, the lens moves forward reducing the distance to the cornea and enlarging the interspace to the retina. The system matrix S_{MA} for a forward movement of the lens $\Delta = 1.0$ mm, calculated for emmetropia (in the non-accommodated state) reads

$$S_{MA} = \begin{bmatrix} 1 & -P_M \\ 0 & 1 \end{bmatrix} \cdot \begin{bmatrix} 1 & 0 \\ -\frac{d_{OL} - \Delta}{n_s} & 1 \end{bmatrix} \cdot \begin{bmatrix} 1 & -\frac{n_s - n_c}{R_{CP}} \\ 0 & 1 \end{bmatrix} \cdot \begin{bmatrix} 1 & 0 \\ -\frac{d_{CT}}{n_c} & 1 \end{bmatrix} \cdot \begin{bmatrix} 1 & -\frac{n_s - 1}{R_{CA}} \\ 0 & 1 \end{bmatrix} \\ = \begin{bmatrix} 0.9139 & -61.3729 \\ 0.0039 & 0.8335 \end{bmatrix} \quad (12)$$

with an equivalent refractive power of 61.3729 D. The lateral magnification of the optical system can be determined using equation 7 to be $M_M = -0.0238$. The object distance/accommodation amplitude in the accommodated state is found from equation 7 to be -0.6989 m/1.4308 D.

In the dual optic pseudophakic eye, the anterior plus lens moves forward reducing the distance to the cornea and enlarging the interspace to the posterior minus lens. The system matrix S_{DA} for a forward movement of the lens $\Delta = 1.0$ mm calculated for emmetropia in the non-accommodated state reads

$$S_{DA} = \begin{bmatrix} 1 & -P_{DP} \\ 0 & 1 \end{bmatrix} \cdot \begin{bmatrix} 1 & 0 \\ d_{D12} + \Delta & 1 \end{bmatrix} \cdot \begin{bmatrix} 1 & -P_{DA} \\ 0 & 1 \end{bmatrix} \cdot \begin{bmatrix} 1 & 0 \\ d_{OL} - \frac{\Delta}{n_s} & 1 \end{bmatrix} \cdot \begin{bmatrix} 1 & -\frac{n_s - n_c}{R_{CP}} \\ 0 & 1 \end{bmatrix} \cdot \begin{bmatrix} 1 & 0 \\ -\frac{d_{CT}}{n_c} & 1 \end{bmatrix} \cdot \begin{bmatrix} 1 & -\frac{n_s - 1}{R_{CA}} \\ 0 & 1 \end{bmatrix} \\ = \begin{bmatrix} 1.0110 & -58.7379 \\ 0.0055 & 0.6700 \end{bmatrix} \quad (13)$$

with an equivalent refractive power of 58.7379 D. The lateral magnification of the optical system can be determined using equation 7 to be $M_D = -0.0406$. The object distance/accommodation amplitude in the accommodated state is determined from equation 7 to be -0.4366 m/2.2904 D.

If, in contrast to a forward shift of the anterior lens by 1.0 mm, the anterior lens is now moving 0.5 mm towards the cornea and the posterior compensating minus lens is moving 0.5 mm towards the retina, the respective lateral magnification of the optical system yields 0.0300 and the object distance/accommodation amplitude in the accommodated state is -0.5581 m/1.7918 D.

Results

For a generalized evaluation of the accommodation amplitude and object-image magnification we varied the Gullstrand model eye by changing the axial length of the eye AL from 18 to 28 mm in steps of 0.1 mm and linear scaling of the phakic anterior chamber depth (interspace

Printed by Universitätsbibliothek Der Universität Des Saarlandes - 134 096 155 212 - (doi:10.14753/SE.2021.2503) at 15/11/2020

between the posterior surface of the cornea and the anterior pole of the lens):

$$ACD = AL \cdot \frac{3.05}{23.86}$$

The corneal parameters such as the anterior and posterior radii of curvature and corneal thickness were used directly from the data of the model eye. For a comparison of the accommodation effects, we defined three different systems of artificial intraocular lenses: (1) a mono optic accommodating intraocular lens implant with an axial shift of $\Delta = 1.0$ mm from the non-accommodated state towards the cornea, (2) a dual optic accommodating intraocular lens implant comprising a 32 D anterior lens and a compensating lens of negative power intended to produce emmetropia in the non-accommodated state, where the distance between both lenses is 3.0 mm (McLeod *et al.*, 2003) and where only the anterior lens shifts $\Delta = 1.0$ mm towards the cornea during accommodation, and (3) a dual optic accommodating intraocular lens implant with a plus 32 D anterior lens and a compensating lens for emmetropia in the non-accommodated state, where the distance between both lenses is 3.0 mm (McLeod *et al.*, 2003) and the anterior lens shifts $\Delta/2$ mm towards the cornea and the posterior lens shifts $\Delta/2$ mm towards the retina. The predicted pseudophakic lens positions for both the mono-optic lens implant and the equator of the dual optic lens complex are calculated from the linear regression provided by the Haigis formula:

$$d_{IOL} = 1.08 \cdot ACD_{Constant} + 0.1 \cdot (AL - 23.39) + 0.4 \cdot (ACD + CT - 3.37) - CT$$

Figure 1a gives the accommodative amplitude of the three optical systems described earlier relative to the refractive lens power of the mono optic (1). The dual optic lens (2) shows nearly constant accommodation amplitude, whereas the accommodation amplitude of the mono optic lens system (1) increases and the

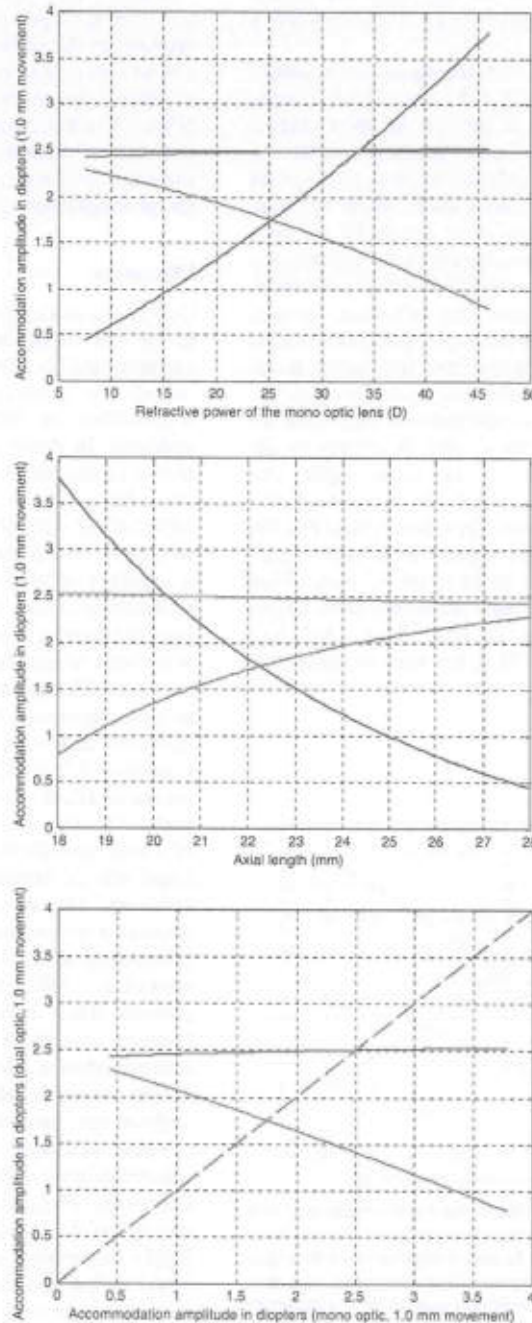


Figure 1. Accommodation amplitude in diopters of the mono optic lens system (blue) and the dual optic lens systems (McLeod *et al.*, 2003) (systems 2 and 3) calculated for an axial movement of the lens optic of 1 mm and variations of the Gullstrand model eye (axial length from 18 to 28 mm in steps of 0.1 mm). The dual lens systems consist of a +32 D anterior lens and a compensating posterior lens. In dual optic system 2 (green) the posterior lens is fixed and the anterior lens moves 1 mm towards the cornea, whereas in system 3 (red) the anterior lens moves 0.5 mm towards the cornea and the posterior lens 0.5 mm towards the retina. (a) Accommodation amplitude vs the refractive power of the mono optic lens system. (b) Accommodation amplitude vs the axial length. (c) Accommodation amplitude of both dual optic lens systems vs the accommodation amplitude of the mono optic lens system.

Printed by Universitätsbibliothek Der Universität Der Saarlandes - 134 096 155 212 - (doi:10.1111/j.1475-1313.2004.00222.x) at [15/11/2020]

accommodation amplitude of the dual optic lens system (3) decreases with the refractive power of the mono optic system (1).

Figure 1b demonstrates the accommodative amplitude of the mono optic and both dual optic systems related to the axial length of the eye. In short (hyperopic) eyes the mono optic lens system (1) yields the highest accommodation amplitude, whereas dual system (3) yields the lowest accommodation. With an axial length of 23–24 mm, the dual optic system (2) provides the highest amplitude of accommodation, whereas the mono optic lens system (1) yields the lowest accommodation. In long (myopic) eyes, the difference between both dual optic lens systems (2 and 3) decreases, whereas the accommodation of the mono optic lens system is less than one quarter of that of the dual optic lens systems.

Figure 1c displays the accommodative amplitude of both dual optic lens systems (2 and 3) relative to the accommodative amplitude of the mono optic lens system (1). In those eyes where the accommodative amplitude is low with a mono optic lens system (1), the dual optic lens system (2) especially reveals higher accommodative amplitude. In contrast, in eyes where the mono-optic provides a high accommodative amplitude, the accommodation of both dual optic lens systems [especially system (3)] is less than in the mono-optic system.

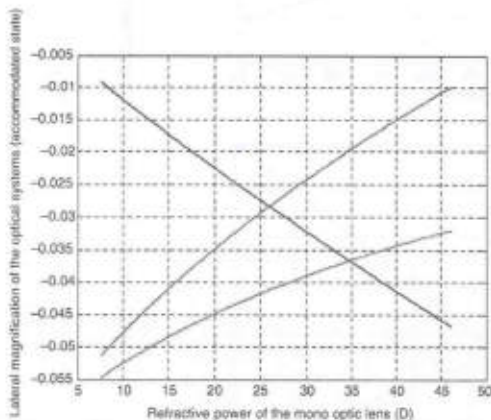


Figure 2. Lateral object-image magnification of the mono optic lens system (blue) and both dual optic lens systems (green and red) in the accommodated state because of an axial movement of the lens optic of 1 mm as a function of the refractive power of the mono optic lens. For the analysis the Gullstrand model eye was varied in axial length from 18 to 28 mm to cover the total range of intraocular lens powers. The dual optic lens systems consist of a +32 D anterior lens and a compensating posterior lens. In dual optic system 2 (green) the posterior lens is fixed and the anterior lens moves 1 mm towards the cornea, whereas in system 3 (red) the anterior lens moves 0.5 mm towards the cornea and the posterior lens 0.5 mm towards the retina.

Figure 2 gives the lateral object-image magnification of the mono optic and both dual optic lens systems in relation to the refractive power of the mono optic lens system. For low and 'normal' refractive power lens implants, the mono optic lens system (1) yields the highest lateral magnification, whereas for high refractive power lens implants (for hyperopic patients) especially the dual optic lens system (2) reveals the highest object-image magnification.

Discussion

One of the still unresolved problems of cataract surgery is the loss of accommodation. In the quest to restore accommodation after cataract surgery, possible options include the extension of the depth of focus, such as in monovision or bifocal/ multifocal intraocular lens implants. In recent years, different types of accommodative intraocular lenses (AIOL) have been developed, in the hope of restoring accommodation to some degree. Most of the clinically proven concepts work according to the so-called focus shift principle, where the lens optic is axially translated because of the forces exerted by the contracting ciliary muscle and subsequent release of capsular tension according to the Helmholtz theory. The magnitude of such lens translation is mainly constrained by the inefficient translation of ciliary body movement to lens movement. With a normal mono optic accommodative lens such as the HumanOptics I CU or the Cumming AT-45 (Cumming *et al.*, 2001), pseudophakic accommodation has been shown to range between 0.2 and 1.4 D. For a 'normal' eye, a shift of the lens optics of 1 mm towards the cornea affects an accommodation amplitude of around 1.4–1.6 D (Langenbacher *et al.*, 2003a–c). This pseudophakic accommodation may be facilitated by pseudoaccommodation because of optical aberrations of the refractive surfaces of the eye (Hardman *et al.*, 1990; Fukuyama *et al.*, 1999) and lens, the pinhole effect because of pupil constriction and a forward movement of the total ciliary plane during accommodation. However, in most cases the accommodation after cataract surgery is insufficient for reading without near correction.

Some attempts have been made to enlarge the accommodative effect of focus shift intraocular lenses. Currently, McLeod *et al.* (2003) described the novel concept of dual optic AIOL. These systems consist of a highly converging plus lens as an anterior optic combined with a compensating diverging lens. Only one of these lenses or both may shift axially because of ciliary muscle activity. Two different types of movement are possible during accommodation: only the anterior plus lens moves towards the cornea, or, the anterior plus lens moves towards the cornea and the compensating minus lens moves towards the retina. The dimensions of the

new dual optic accommodative lens are described extensively by McLeod *et al.* (2003) in their paper. McLeod *et al.* used a commercially available paraxial raytracing software package to predict the accommodative effect of the lens. But, especially in the Gaussian space, much simpler calculation algorithms may be used for calculation of the cardinal points, accommodation amplitude or object image magnification of such a lens system inserted into a (modified) model eye. Using linear geometrical optics with matrix notation, this problem may be resolved in a straightforward fashion without using raytracing software. The entire optical system is described by a system matrix, which is a product of refractive power matrices as a representation of the optical refractive surfaces and translation matrices, which represent the transformation of the vergence between subsequential refractive surfaces. From the system matrix, the cardinal points such as the primary and secondary nodal, principal and focal points can be derived directly. The upper right element of the system matrix represents the negative value of the equivalent power of the total system. The position of the intraocular lens implant may be predicted using classical lens calculation schemes such as the Gernet formula (Gernet *et al.*, 1970), the Haigis formula (Haigis, 1995), the SRK/T (Retzlaff *et al.*, 1990), Hoffer-Q (Hoffer, 1975) or Holladay formula (Holladay *et al.*, 1988; Holladay, 1993, 1997).

In our study, we provided a simple calculation scheme for calculation of the refractive power of mono- or dual optic intraocular lenses. For the calculation, we used biometric data including axial length, anterior and posterior corneal radius of curvature, corneal thickness and the predicted pseudophakic lens position derived from the Haigis formula. The calculation scheme may easily be generalized to some given ametropia not equal to zero by multiplying the system matrix of the spectacle correction (as a product of a translation matrix from the cornea to the spectacle plane and a refractive power matrix as the spectacle correction itself) to the right of the system matrix (equations 8 and 10) of the eye. Our data demonstrate that the accommodation amplitude of the dual optic lens system described by McLeod *et al.* (2003) with an anterior lens of 32 D and a compensating posterior lens 3 mm behind the front lens provides a nearly constant accommodation amplitude by anteriorly translating the anterior lens by 1 mm. Especially in low power intraocular lenses for myopic patients, this dual optic lens system allows an accommodation amplitude of about 2.4 D mm⁻¹ shift, whereas the mono-lens system provides an accommodative change of less than 1 diopter. Even in normal eyes with an axial length of 23–24 mm, this new dual optic lens concept (2) provides much more pseudophakic accommodation compared with the dual optic system (3) or the mono optic

system (1). Only in extremely short (hyperopic) eyes (<20.4 mm, *Figure 1b*), does the classical mono optic accommodative lens such as the HumanOptics 1 CU (Küchle *et al.*, 2001, 2002; Langenbacher *et al.*, 2003a,c) develop a higher accommodative effect compared with the dual optic lens system. For the model data given in the McLeod *et al.* (2003) paper, we calculated an accommodation amplitude of about 2.4 D (*Figure 1b*) for a forward shift of the anterior optic by 1 mm in comparison to 2.2 D mm⁻¹ as described in that paper. The exact value depends on the predicted position of the dual lens system from the preoperative biometrical data and the exact geometrical shape of the lens. If the exact geometry of the 'thick' lens implant is given by the manufacturer, the calculation may be generalized in order to optimize the description of the total optical system. However, for clinical purposes, the approximation made with a thin lens implant may be sufficient.

One additional problem to be resolved with linear geometrical optics is the calculation of the lateral object-image magnification. As the lateral magnification is zero for an emmetropic eye, we provided the lateral magnification in the accommodated state with an axial translation of the lens optics of 1 mm. Although this lateral magnification is calculated for a fixed axial translation of the lens optics of 1 mm, it may be indicative for implanting one or the other intraocular lens model in cases where the patient has anisometropia before cataract surgery.

In conclusion, we have presented a simple mathematical strategy for calculation of the accommodative effect of mono optic and dual optic AIOL. The dual optic lens recently published by McLeod *et al.* (2003) yielded a nearly constant accommodation amplitude of about 2.4–2.5 D mm⁻¹ movement, where the mono optic lens provided an accommodative response of <2 D mm⁻¹ movement in long (myopic) or normal eyes. Only in extremely short eyes, is the accommodative amplitude of the mono optic lens higher than the dual optic lens.

References

- Allen, E. D., Burton, R. L., Webber, S. K., Haaskjold, E., Sandvig, K., Jyrkkio, H., Leite, E., Nystrom, A. and Wollensak, J. (1996) Comparison of a diffractive bifocal and a monofocal intraocular lens. *J. Cataract Refract. Surg.* **22**, 446–451.
- Cumming, J. S., Slade, S. G., Chayet, A. and AT-45 Study Group (2001) Clinical evaluation of the model AT-45 silicone accommodating intraocular lens: results of feasibility and the initial phase of a Food and Drug Administration clinical trial. *Ophthalmology* **108**, 2005–2009.
- Fisher, R. F. (1973) Presbyopia and the changes with age in the human crystalline lens. *J. Physiol.* **228**, 765–779.
- Fisher, R. F. (1977) The force of contraction of the ciliary muscle during accommodation. *J. Physiol.* **270**, 51–74.

- Fisher, R. F. (1986) The ciliary body in accommodation. *Trans. Ophthalmol. Soc. UK* **105**, 208–219.
- Fukuyama, M., Oshika, T., Amano, S. and Yoshitomi, F. (1999) Relationship between apparent accommodation and corneal multifocality in pseudophakic eyes. *Ophthalmology* **106**, 1178–1181.
- Gernet, H., Ostholt, H. and Werner, H. (1970) Die präoperative Berechnung intraokularer Binkhorst-Linsen. In: *Versammlung der Rheinisch-Westfälischen Augenärzte*, Vol. **122**, Zimmermann, Balve, pp. 54–55.
- Gray, P. J. and Lyall, M. G. (1992) Diffractive multifocal intraocular lens implants for unilateral cataracts in prepresbyopic patients. *Br. J. Ophthalmol.* **76**, 336–337.
- Halgis, W. (1995) Biometry. In: *Augenärztliche Untersuchungsmethoden* (eds W. Straub, P. Kroll and H. J. Kühle), Biermann, Köln, pp. 255–304.
- Hardman, S. J., Rubinstein, M. P., Snead, M. P. and Haworth, S. M. (1990) Pseudophakic accommodation? A study of the stability of capsular bag supported, one piece, rigid tripod, or soft flexible implants. *Br. J. Ophthalmol.* **74**, 22–25.
- Hoffer, K. J. (1975) Mathematics and computers in intraocular lens calculation. *Am. Intra. Ocul. Implant. Soc. J.* **1**, 4–5.
- Holladay, J. T. (1993) Refractive power calculations for intraocular lenses in the phakic eye. *Am. J. Ophthalmol.* **116**, 63–66.
- Holladay, J. T. (1997) Standardizing constants for ultrasonic biometry, keratometry and intraocular lens power calculations. *J. Cataract Refract. Surg.* **23**, 1356–1370.
- Holladay, J. T., Prager, T. C. and Chandler, T. Y. (1988) A three-part system for refining intraocular lens power calculations. *J. Cataract Refract. Surg.* **14**, 17–24.
- Keating, M. P. (1981) Lens effectivity in terms of dioptric power matrices. *Am. J. Optom. Physiol. Opt.* **58**, 1154–1160.
- Knorz, M. C. and Seiberth, V. (1996) Die True-Vista-Bifokal-IOL. *Ophthalmology* **93**, 17–21.
- Kühle, M., Gusek-Schneider, G. C., Langenbacher, A., Seitz, B. and Hanna, K. H. (2001) Erste Ergebnisse der Implantation einer neuen, potentiell akkommodierbaren Hinterkammerlinse. *Klin. Monatsbl. Augenheilkd.* **218**, 603–608.
- Kühle, M., Nguyen, N. X., Langenbacher, A., Gusek-Schneider, G. C., Seitz, B. and Hanna, K. D. (2002) Implantation of a new accommodative posterior chamber intraocular lens (1 CU). *J. Refract. Surg.* **8**, 208–217.
- Langenbacher, A., Huber, S., Nguyen, N. X., Seitz, B. and Kühle, M. (2003a) Cardinal points and object-image magnification with an accommodative lens implant (1 CU). *Ophthalm. Physiol. Opt.* **23**, 61–70.
- Langenbacher, A., Huber, S., Nguyen, N. X., Seitz, B. and Kühle, M. (2003b) Measurement of accommodation after implantation of a new accommodative posterior chamber lens (1 CU). *J. Cataract Refract. Surg.* **29**, 677–685.
- Langenbacher, A., Seitz, B., Huber, S., Nguyen, N. X. and Kühle, M. (2003c) Theoretical and measured pseudophakic accommodation after implantation of a new accommodative posterior chamber intraocular lens. *Arch. Ophthalmol.* **121**, 1722–1727.
- Leyland, M. and Bloom, P. (1999) Intraocular lens design for pseudoaccommodation [letter]. *J. Cataract Refract. Surg.* **25**, 1038–1039.
- McLeod, S. D., Portney, V. and Ting, A. (2003) A dual optic accommodating foldable intraocular lens. *Br. J. Ophthalmol.* **87**, 1083–1085.
- Nakazawa, M. and Ohtsuki, K. (1984) Apparent accommodation in pseudophakic eyes after implantation of posterior chamber intraocular lenses: optical analysis. *Invest. Ophthalmol. Vis. Sci.* **25**, 1458–1460.
- Nishi, O. and Nishi, K. (1998) Accommodation amplitude after lens refilling with injectable silicone by sealing the capsule with a plug in primates. *Arch. Ophthalmol.* **116**, 1358–1361.
- Retzlaff, J. A., Sanders, D. R. and Kraff, M. C. (1990) Development of the SRK/T intraocular lens implant power calculation formula. *J. Cataract Refract. Surg.* **16**, 333–340.
- Rosenblum, W. M. and Christensen, J. L. (1974) Optical matrix method: optometric applications. *Am. J. Optom. Physiol. Opt.* **51**, 961–968.
- Saladin, J. J. and Stark, L. (1975) Presbyopia: new evidence from impedance cyclography supporting the Hess-Gullstrand theory. *Vision Res.* **15**, 537–541.
- Schachar, R. A. (1994) Zonular function: a new model with clinical implications. *Ann. Ophthalmol.* **26**, 36–38.
- Snead, M. P., Harman, S., Rubinstein, M. P., Reynolds, K. and Haworth, S. M. (1991) Determination of the nodal point position in the pseudophakic eye. *Ophthalm. Physiol. Opt.* **11**, 105–108.
- Steinert, R. F., Aker, B. L., Trentacost, D. J., Smith, P. J. and Tarantino, N. (1999) A prospective comparative study of the AMO ARRAY zonal-progressive multifocal silicone intraocular lens and a monofocal intraocular lens. *Ophthalmology* **106**, 1243–1255.
- Strenk, S., Semmlow, J. L., Strenk, L. M., Munoz, P., Gronland-Jacob, J. and deMarco, J. K. (1999) Age-related changes in human ciliary muscle and lens: a magnetic resonance imaging study. *Invest. Ophthalmol. Vis. Sci.* **40**, 1162–1169.